UNIVERSITY OF SOUTHAMPTON

FACULTY OF MEDICINE

ACADEMIC UNIT OF HUMAN DEVELOPMENT AND HEALTH

A STUDY OF REPOLARISATION CHARACTERISTICS IN HIGHLY ARRHYTHMOGENIC ADULT HUMAN VENTRICLES USING NONCONTACT MAPPING

by

Nadia S. Sunni

MBBCh, MRCP (UK)

Thesis for the degree of Doctor of Medicine

April 2013

Abstract

UNIVERSITY OF SOUTHAMPTON
ABSTRACT
FACULTY OF MEDICINE
ACADEMIC UNIT OF HUMAN DEVELOPMENT AND HEALTH
Doctor of Medicine
A STUDY OF REPOLARISATION CHARACTERISTICS IN HIGHLY ARRHYTHMOGENIC ADULT HUMAN VENTRICLES USING NONCONTACT MAPPING
By Nadia Senussi Sunni

Global and dynamic dispersion of cardiac repolarisation has been linked to arrhythmogenesis and fibrillation. The use of noncontact mapping allows simultaneous study of the whole cardiac chamber over a limited number of beats. This technology has emerged as a validated clinical tool in the assessment of patients with structurally normal hearts and low arrhythmic risk; however, limited knowledge is available in those with high arrhythmic risk. To enhance understanding of the underlying pathophysiology of arrhythmogenesis, I investigated dispersion of repolarisation and electrical and conduction velocity restitution in patients with high arrhythmia burden using noncontact mapping.

Patients who suffered ventricular arrhythmias or those deemed high risk of sudden cardiac death were separated into two groups with structurally normal or abnormal hearts. Electrical and conduction velocity restitution, activation and repolarisation coupling and T wave morphology were assessed globally and regionally in the right or left ventricles using virtual unipolar electrograms and their first derivative from reconstructed three dimensional endocardial maps produced by the Ensite system. Restitution characteristics, T wave maps and activation- repolarisation relationships were compared between the two groups.

Both patient groups had similar electrical and conduction velocity restitution characteristics and responded similarly to decremental pacing. Steep restitution slopes were regionalised and corresponded to segments of arrhythmia ablation. Uncoupling of activation and repolarisation occurred during induction of ventricular tachycardia in structurally abnormal hearts and following spontaneous ectopic beats and with increased prematurity of extrastimuli in the structurally normal hearts. T waves were mainly positive in the structural heart disease group notably around areas of scar but were mainly negative in the normal hearts. Complex fractionated electrograms were found in both populations. Flecainide suppressed ventricular ectopy and prolonged conduction velocity but had minimal effect on electrical restitution and activation repolarisation coupling. Over one third of all participants suffered an arrhythmia over the next four years.

Similarity of the repolarisation characteristics in patients of high arrhythmic risk regardless of underlying cardiac structure supports the concept that arrhythmia substrates are likely to be parts of the functioning myocardium and suggests a common pathophysiology underlying arrhythmogenesis.

Global and regional variations in ventricular repolarisation can be appropriately assessed in high-risk groups using the Ensite system. Incorporating these techniques into a real-time functioning algorithm could potentially be used for risk stratification purposes.

Table of contents

List of figures

List of tables

Glossary of abbreviations

ARI (ARIs) = activation recovery interval

ARVC= arrhythmogenic right ventricular cardiomyopathy

AT= activation time

CABG= coronary artery bypass graft

CAD= coronary artery disease

CL= cycle length

CMR= cardiac magnetic resonance scan

CV= conduction velocity

CI= coupling interval

DCM= dilated cardiomyopathy

DI (DIs) = diastolic interval/ intervals

ERC = electrical restitution curve

ERP= effective refractory period

GUCH= 'grown up' congenital heart disease

ICD= internal cardiac defibrillator

IHD= ischaemic heart disease

LQTs= long QT syndrome

LV= left ventricle

MAP= monophasic action potential

MEA= multielectrode array

NCM= noncontact mapping

NSVT= nonsustained ventricular tachycardia

PES= programmed electrical stimulation

RT= repolarisation time

RVA= right ventricular apex

RVOT= right ventricular outflow tract

SCD= sudden cardiac death

SHD= structural heart disease

S_{max}= maximum restitution slope

SNH= structurally normal heart

SR= sinus rhythm

TdP= torsades de pointes

TDR= transmural dispersion of repolarisation

TGA transposition of great arteries

TOF tetralogy of Fallot

UE= unipolar electrogram

VE= ventricular ectopic

VF= ventricular fibrillation

VT= ventricular tachycardia

Declaration of authorship

I, Nadia S. Sunni declare that the thesis entitled:

A Study of Repolarisation Characteristics in Highly Arrhythmogenic Adult Human Ventricles Using Noncontact Mapping

and the work presented in the thesis are both my own, and have been generated by me as the result of my own original research. I confirm that:

- this work was done wholly or mainly while in candidature for a research degree at this University;
- where any part of this thesis has previously been submitted for a degree or any other qualification at this University or any other institution, this has been clearly stated;
- where I have consulted the published work of others, this is always clearly attributed;
- where I have quoted from the work of others, the source is always given. With the exception of such quotations, this thesis is entirely my own work;
- I have acknowledged all main sources of help;
- where the thesis is based on work done by myself jointly with others, I have made clear exactly what was done by others and what I have contributed myself;
- none of this work has been published before submission,
- parts of this work have been presented as posters and oral presentations at conferences including:

Sunni N, Yue A, Michael K, Allen S, Roberts P, Morgan J **:** *Regionalisation of Steep Restitution Slopes and Ventricular Tachycardia Circuits.* Heart (92) Supplement (2) May 2006, A 57. Oral presentation at BCS annual conference Glasgow, April 24-27, 2006.

Sunni N, Yue A, Michael K, Robinson S, Roberts P, Morgan J **:** *Comparison of Global Restitution Characteristics between Normal and Diseased Hearts Using Noncontact Mapping.* A poster workshop presentation (PW 19/7) for Cardiostim June 2006. Europace vol. 8 supplement 1 June 2006.

Sunni, N, Yue A, Paisey J, Morgan D, Clothier H, Michael K, Roberts P, Morgan J *Noncontact Mapping of Human Cardiac Restitution is Accurate and Reproducible.* A poster workshop presentation (PW 19/8) for Cardiostim June 2006. Europace vol. 8 supplement 1 June 2006.

Sunni N, Yue A, Michael K, Allen S, Roberts P, Morgan J **:** Regionalization of Steep Restitution Slopes and Ventricular Tachycardia Circuits in Pathological Human Hearts. A poster (178P/16) for Cardiostim June 2006. Europace vol. 8 supplement 1 June 2006.

Sunni, N, Yue A, Paisey J, Morgan D, Clothier H, Michael K, Roberts P, Morgan J**:** *Noncontact Mapping of Human Cardiac Restitution is Accurate and Reproducible.* A poster presentation for the World Congress of Cardiology, Sept. 2006, Session Info: Poster session 4.Citation**:** Eur Heart J 2006, 27(Abstract Suppl), 470

Signed: Nadia S. Sunni……

Date: April 26, 2013

Dedication

I dedicate this work to my parents, who have supported me through many troubled times and to whom I shall be forever indebted, and to my son Adam, who has shown patience despite my long working hours, referring to me as “not a real mummy”.

Acknowledgements

To my supervisors; Professors John Morgan and Mark Hanson, I give my thanks for their enormous support and patience, for giving me that one more chance and for their inspiration, time, effort and enthusiasm.

I extend my thanks to Dr Arthur Yue who taught me the nuts and bolts of using the Ensite system and introduced me to this research with enthusiasm, and to Dr John Paisey and Dr Paul Roberts for their overall support during my time at Southampton.

I thank the electrophysiology research team at Southampton General Hospital for always finding the time to smile and say hello especially Sarah, Bibi and Dr Kevin Michael.

I acknowledge Boston Scientific (Guidant, at the time) for funding my salary during the two-year research period. I also thank and acknowledge Mr Shah Fahedur Rahman, independent software engineer, for his assistance in writing the software for the purpose built windows application (Heat map generator version1) that allowed the display of a colour-coded polar map of the distribution and density of the T wave morphology in the studied ventricle.

My thanks go to; my friend Prof Frank Vella for proof reading my work and his valuable suggestions, Dr Michael Coupe for inspiring me to do cardiology training and research and Dr Rudulph Canepa- Anson, for his support and encouragement and for believing in me.

Finally, I thank my family, particularly my parents Senussi and Naama, without their encouragement, sacrifices and spirit-lifting nature; I could not have produced this thesis.

.

Chapter 1 Historical review

1.1 Sudden cardiac death

1.1.1 Definition and epidemiology

Sudden cardiac death (SCD) ,defined as a natural unexpected death from cardiac causes heralded by abrupt loss of consciousness within one hour of the onset of acute symptoms in a person without any prior condition that would appear fatal, continues to be a major health issue worldwide (Engelstein ED and Zipes DP 1998) (Myerburg RJ and Castellanos A 2008) A witnessed sudden cardiac death attributed to coronary atherosclerosis was described by Da Vinci in the 15th century related to a “parched and shrunk and withered artery….that feeds the heart” (MacCurdy E 1954). Eighty per cent of individuals who die suddenly have coronary artery disease (CAD), the rest have cardiomyopathy, other structural heart disease eg congenital heart disease, channelopathy or bradyarrythmia. Five per cent of SCD is attributed to primary ventricular fibrillation. Thus, the epidemiology of SCD parallels that of CAD. the incidence of SCD rising 2-4 fold in the presence of CAD and 6- 10 fold in the presence of structural heart disease (Myerburg RJ & Castellanos A 2008;Myerburg and Junttila 2012). SCD is a worldwide phenomenon. Approximately 50,000- 70,000 people experience SCD annually in the UK, 85-90% of these constitute the index presentation with a ventricular arrhythmic event while the rest are attributed to recurrent events (NICE 2006). In the USA, SCD accounts for 1-2/1000 population with an estimated 300,000- 400,000 deaths annually mainly from degeneration of ventricular tachycardia (VT) into ventricular fibrillation (VF) (Jimenez and Myerburg 1993;Myerburg et al. 1993) in which CAD and its sequelae are the culprits in 80% of cases. The second major cause is ventricular arrhythmia arising in nonischaemic dilated and hypertrophic cardiomyopathy, whereas congenital heart disease and genetically based channelopathies account for 5-10% of cases.

Event rates in Europe are similar to those in the USA but with significant geographic variations being reported (Priori et al. 2002;Priori et al. 2003a). However, in less developed countries SCD rates follow those of IHD and thus are generally lower.

The number of SCDs differs according to the definition used to determine suddenness. Variations in the definition used, from 1 hour to 24 hours, may falsely reduce the fraction of recorded sudden deaths from cardiac causes as in the Maastricht community- wide

study where it rises to 18.5% compared to 13% of all natural deaths in the 1-hour statistic.(de Vreede-Swagemakers et al. 1998)

Unfortunately, the true incidence of SCD remains unclear given the variation in definition of the event, its timing and whether it was witnessed or not. It has been estimated to range between 180,000- 450,000 per year for the past three decades indicating the degree of discrepancy (Kong et al. 2011). The overall incidence of SCD in the general population in Europe has improved to 0.8 per 1000/ year. However, SCD in the below 35 -year olds remains at a plateau level between 0.8-2.8 /100,000/year (Corrado et al. 2006;Margey et al. 2011;Winkel et al. 2011).

Disease states at risk of SCD

A. **CAD** is the leading cause that predisposes to ventricular arrhythmias with hereditary cardiomyopathies and channelopathies following but far behind (NICE 2006). Recent implantable cardioverter defibrillator trials (ICD) have shown that roughly 50% of deaths in patients with CAD and impaired left ventricular (LV) function are sudden or arrhythmic in nature (Cleland et al. 2002). At least 80% of patients who die suddenly have coronary atherosclerosis as an underlying arrhythmia substrate with autopsy studies showing a recent coronary thrombosis in 15-64% of victims (Roberts et al. 1994).

B. **Cardiomyopathy** is the second largest cause of SCD. This comprises idiopathic dilated cardiomyopathy (DCM), hypertrophic cardiomyopathy (HCM), and arrhythmogenic right ventricular cardiomyopathy (ARVC).

Dilated cardiomyopathy (DCM)

DCM is the basis for ~ 10% of SCD in the adult population. Annual mortality in patients with idiopathic DCM ranges from 10-50% and is highly dependent on disease severity, particularly LV dysfunction. In a meta-analysis of 14 studies that contained 1432 patients with DCM, mean mortality during a 4 -year follow up was 42%, with 28% of deaths being sudden (Tamburro and Wilber 1992). Sudden deaths in this group can be attributed to fatal ventricular arrhythmias, to asystole or to pump failure especially in advanced LV dysfunction (Taliercio et al. 1985;Maire et al. 1985;Juilliere et al. 1988). Familial forms have been described in 25% of cases (Michels et al. 1992) including Lamin A/C cardiomyopathy which has been linked to conduction disease, atrial and

ventricular arrhythmias and SCD and genetic mutations in LMNA and *SCN5A* genes however only a few genes associated with inherited forms of this condition have been identified (Hershberger et al. 2002;Serio et al. 2012).

Factors linked to increased incidence of SCD in this population, which are:

- Poor LV function
- Nonsustained VT
- Syncope
- Bundle branch reentry

Hypertrophic cardiomyopathy (HCM)

Prevalence of this condition is 2/1000 young adults in the USA from multiple centres (Maron et al. 1995;Maron 2002). The incidence of SCD in this group is 2-4 %per year in adults and 4-6% per year in children and adolescents. This is the commonest cause of SCD in people below the age of 35 years particularly in competitive athletes (Maron et al. 1986). Markers of increased risk of SCD in HCM patients include: recurrent syncope, previous cardiac arrest , episodes of sustained VT or symptomatic episodes of non-sustained VT, family history of SCD and the presence of specific genotypes: e.g mutations in α- tropomyosin or in ß- myosin heavy chain gene. The degree of left ventricular hypertrophy (LVH) and LV mass is a strong independent risk factor for SCD even in hypertensive patients or those with valvular heart disease. This may relate to their susceptibility to triggered activity resulting from prolonged repolarisation (QT) from the increased muscle mass, local myocardial ischaemia, or interstitial fibrosis.

Arrhythmogenic right ventricular cardiomyopathy (ARVC)

This is a fibro or fibro-fatty infiltration of the myocardium and is familial in nearly 30% of cases from autosomal dominant inheritance that affects mainly the right ventricle and has a propensity to result in ventricular arrhythmias, cardiac failure and SCD. It is attributed to a genetic defect on chromosome 1 and 14 q23-q24.(Corrado et al. 1997) and is of significant importance in the young adult population and in athletes in whom exercise is a well-documented trigger for ventricular arrhythmias. It is estimated that it accounts for nearly 2% of SCD per year. ARVC is characterised by T wave inversion in the right and septal precordial leads V1-V3 with RBBB and evidence of intraventricular slow conduction manifested as terminal notching or inscription of QRS in V1-V3 (this is called the epsilon wave). Characteristically VTs in this condition have a left bundle branch morphology arising usually from the RV outflow tract, inflow area or apex.

C. Grown up congenital heart disease (GUCH)

Cardiac defects are the most common of birth defects and have an incidence of 1-2% of all live births. Thanks to early intervention especially corrective surgery, this subset of patients are living longer and thus the alteration in age distribution, arrhythmia and heart failure prevalence of survivors of these conditions over the years. The majority of sudden deaths are arrhythmic in nature and related to VT (30%). The estimated annual incidence of sudden arrhythmic death in the GUCH population is 0.09% with the

majority having moderate or severe lesions e.g tetralogy of Fallot (TOF) and transposition of great arteries (TGA) (Koyak et al. 2012b). Increased arrhythmic SCD has been associated mainly with the repaired cyanotic and left-sided obstructive lesions including:

- Tetralogy of Fallot
- Transposition of great arteries
- Univentricular defects
- Aortic stenosis
- Pulmonary vascular obstruction

Their morbidity burden is substantial and commonly underestimated with arrhythmias being the leading cause for functional decompensation, disability and hospitalisation. The risk of SCD is an additive phenomenon that encompasses the influences of anatomy with congenitally malformed or eccentric conduction systems, abnormal genetics, previous surgical and catheter interventions- their timing, residual defects and postoperative sequelae. The presence of altered haemodynamics with mechanical and hypoxic stress resulting in chamber dilatation and fibrosis serves a prerequisite for conduction delay and re-entry arrhythmias. SCD also occurs as a late complication after corrective surgery for these malformations.

D. Valvular heart disease

This accounts for 3-5% of SCD the most common cause being aortic stenosis, especially bicuspid valve, which when symptomatic has a SCD incidence of 1% per annum and remains to a degree even after operative valve replacement. SCD in patients with aortic stenosis has been reported to be the second most common mode of death after valve surgery accounting for 20% of postoperative deaths, with an incidence of 2-4% over a 7 year follow up period (Engelstein ED & Zipes DP 1998).

Floppy mitral valve disease, a spectrum of mitral valve prolapse has been found in 3% of autopsies in SCD victims (Loire and Tabib 1996). Because of its high prevalence, it remains unclear whether this is a coincidental finding or causally linked. However, malignant subsets of the condition have been described (Sriram et al. 2013) (Duren et

al. 1988) with myxomatous degeneration of the mitral valve and LV dysfunction increase the risk of valvular endocarditis, thromboembolism and SCD.

E. Primary electrophysiological abnormality (Channelopathy)

These patients have normal mechanical structure and function of the myocardium associated with an electrophysiological derangement that is the primary cause of arrhythmia or death. They include long QT (LQT), Brugada, catecholaminergic polymorphic ventricular tachycardia (CPVT), Wolff-Parkinson White, early repolarisation and short QT syndromes.

The Long QT syndromes

These were first described in association with sensorineural deafness (Jervell and Lange-Nielsen 1957). The congenital LQTs are marked by prolongation of repolarisation, abnormal T waves, syncope and the occurrence of SCD mainly due to torsade de pointes (TdP) from the development of after depolarisations or the occurrence of dispersion of repolarisation (Surawicz 1989;Kirchhof et al. 2003b) . The cellular and ionic basis of the ECG manifestations of the normal T wave and that in LQTs have been attributed to voltage gradients across the ventricular wall with the duration of the M cell action potential determining the duration of the QT interval both under baseline conditions and under a variety of circumstances (van Dam and Durrer 1964;Yan and Antzelevitch 1998). Yan and Antzelevitch on the basis of their LV wedge prepared canine model formulated an index of transmural dispersion of repolarisation from the T_{peak}- T_{end} interval which was dependent on the point of repolarisation of the epicardium and M cell region. This was probably useful in assessment of arrhythmic risk. Various mechanisms of arrhythmogenesis in LQTs have been studied in wedge preparations and in intact canine hearts in vivo. Similarly, T wave alternans in LQTs in-vitro canine perfused cardiac wedges relied on repolarisation of the M cell region and TdP occurred as a result of exaggeration of the transmural dispersion of repolarisation during alternans which relied on beat to beat changes in intracellular calcium (Ca^{+2}) (Shimizu and Antzelevitch 1999). This results in early after depolarisations which may lead to initiation of re-entry resulting in TdP and VT (Huffaker et al. 2004). Earlier studies in LQT3 model performed with three-dimensional isochronal mapping of intact dog hearts using 64 needle electrodes produced by infusing the sodium channel -inactivation slowing agent anthropleurin A, illustrated two different arrhythmia mechanisms in this group with the initiation of polymorphic VT dependent on focal subendocardial activation and perpetuation of the arrhythmia reliant on re-entry of

excitation from dispersion of repolarisation and functional conduction blocks with circulating wave fronts (el-Sherif et al. 1996). In a LQT2 model in canine hearts, Yamauchi et al that made use of a pure potassium rectifier channel blocker (I Kr), demonstrated steepness of the ARI restitution slope compared to normal (Yamauchi et al. 2002).

These channelopathies are due to increased positivity in the cardiac myocytes either because of impaired sodium ion channel inflow or potassium channel outflow. Thirteen genetic variants of congenital LQTs have been identified. However, the most common – those due to mutations in the genes KCNQ1 (LQT1), KCNH2, HERG (LQT2), and SCN5A (LQT3). LQT3 along with Brugada and progressive cardiac conduction disease-seem to be an overlap syndrome because of their association with mutations in the sodium channel gene (Bezzina et al. 1999).

Brugada Syndrome

This is a channelopathy first described (Brugada and Brugada 1992) in 8 patients with right bundle branch block, ST segment elevation in the precordial leads V1-V3, with T wave inversion, normal QT interval, recurrent syncope and aborted sudden arrhythmic death. Although the presence of a structurally normal heart is a requirement for the diagnosis recently studies have demonstrated fibrosis in the area of the RV outflow tract (RVOT) and dilatation of the RVOT (Catalano et al. 2009). This fibrosis may be due to degeneration or inflammation resulting from premature ageing of myocytes arising from abnormal ion channel kinetics and cell destruction causing a localised myocardial disorder. Although there are three main types of Brugada syndrome based on the appearance of ST segment and T wave morphology on surface ECG, the finding of localised structural abnormality with fibrous degeneration, particularly in the RVOT epicardium and the ablation of the Brugada phenotype, raises the question of whether this is a form localised cardiomyopathy with overlap between the 2 conditions. No genetic links between ARVC and Brugada syndrome have been demonstrated (Letsas et al. 2011;Nademanee et al. 2011). Nevertheless, Brugada syndrome appears to be an inherited form of channelopathy related predominantly to the sodium channels with heterogeneous genetics that affect not only sodium but also L-calcium channel kinetics and outward potassium current (I_{TO}). There is variable penetrance with the main gene defect related to SNC5A and its arrhythmogenic mechanism probably related to both repolarisation and depolarisation phases 2, 1 and 0 of the action potential and phase 2 re-entry. The effects of autonomic modulation and intracellular Ca^{+2} handling are being investigated in their role for promoting arrhythmogenesis in this cohort (Stockner and

Koschak 2012;Fukuyama et al. 2013) (Miyazaki et al. 1996;Wichter et al. 2002;Krittayaphong et al. 2003). However, not only is there a role for functional conduction slowing and thus functional block but also tissue heterogeneity and non-uniform dispersion of repolarisation particularly related to alteration of restitution kinetics (Lambiase et al. 2009) and the disparity and transventricular gradients contribute to re-entry and arrhythmogenesis in this population (Yan and Antzelevitch 1999).

Catecholaminergic polymorphic ventricular tachycardia (CPVT)

This is the result of an abnormal ryanodine receptor that regulates calcium release from the sarcoplasmic reticulum. It occurs in structurally normal hearts associated with an inherited or spontaneous missense mutation in the RyR2 gene (Priori et al. 2001). The arrhythmogenic mechanism is delayed after depolarisations, which result from calcium overload following exertion or emotion. However, the occurrence of alternans dissociated from changes in mean action potential durations, ventricular effective refractory periods or restitution curve characteristics in a murine model of CPVT has been demonstrated (Sabir et al. 2010). Despite the prerequisite of normal cardiac structure, the same ryanodine receptor mutation has been reported in some forms of ARVC (Tiso et al. 2001).

Short QT syndrome (SQTs)

This is a very rare condition related to repolarisation abnormalities, caused by gain of function mutations in the genes that control the outward K^+ current channels (KCNH2, KCNJ2, and KCNQ1 genes). It manifests as a corrected QT of less than 320ms and tall peaked T waves from an increased efflux of K^+ thus shortening repolarisation and APD. These are usually of autosomal dominant inheritance and are associated with palpitations due to atrial fibrillation or SCD due to VF. Unlike LQTs, no triggers have been reported that predispose to arrhythmias in SQTs. Experimental models in canine ventricular wedge tissue with potassium channel activator- pinacidil- increased transmural dispersion of repolarisation from endocardium to epicardium and shortening the APD which with the introduction of a single extra-stimulus caused polymorphic VT in 9 of the 12 arterially perfused LV wedges. This suggested that the disparity of the APD shortening across the ventricular wall was the substrate for genesis of ventricular arrhythmias (Extramiana and Antzelevitch 2004). Other studies support that reduction in VERP and dispersion of repolarisation are the main mechanisms of arrhythmogenesis in these populations which can be improved with quinidine therapy (Schimpf et al. 2008).

Idiopathic VF

This condition usually affects young adults with structurally normal hearts and manifests as syncope and sudden cardiac death from polymorphic VT or VF which is not triggered by emotion or exertion and can be initiated by narrow complex ventricular extrasystoles. It accounts for 5-10% of survivors of out-of -hospital cardiac arrests (Belhassen and Viskin 1993;Meissner et al. 1993;Priori and Maugeri F S 1997). The first published case of idiopathic VF also involved an arrhythmic storm that responded to quinidine (Dock W 1929). The condition includes a spectrum of conditions with normal ECGs to those with early repolarisation syndromes and J point elevation (Haissaguerre et al. 2008). The arrhythmogenic mechanism may be related to the abnormally short ventricular refractory period and prominent transient outward potassium current (I_{To}) plays a major role (Yan and Antzelevitch 1996). There are similarities between the idiopathic VF and Brugada syndrome groups regarding their characteristic VF storms. Both isoprenaline and quinidine have been effective in preventing VF in these patients by reducing the dispersion of repolarisation by the former and beneficial effects of I_{To} blockade by the latter (Belhassen et al. 1999;Yamauchi, Yamaki, Watanabe, Yuuki, Kubota, & Tomoike 2002;Mok et al. 2004;Belhassen et al. 2004;Shimizu et al. 2005).

1.1.2 Risk stratification

Risk stratification is a challenging concept particularly as most arrhythmic events occur in individuals without previously known cardiac disease, or in those who are considered low risk, and SCD could be the first presentation of the disease (Sanders et al. 2007) (Adabag et al. 2010). An ideal risk stratification strategy would identify patients who may suffer SCD due to a reversible arrhythmia within a foreseeable time and would exclude those who would not. Given the magnitude of SCD more specific markers are required to facilitate screening of the general population especially since the risk of SCD is not equal to that of developing SHD. Despite advances in ICD technology and on-going research for the last 25 years there are still major limitations in preventing sudden arrhythmic death with the current risk stratification strategies (Sanders, Al-Khatib, Berliner, Bigger, Buxton, Califf, Carlson, Curtis, Curtis, Domanski, Fain, Gersh, Gold, Goldberger, Haghighi-Mood, Hammill, Harder, Healey, Hlatky, Hohnloser, Lee, Mark, Mitchell, Phurrough, Prystowsky, Smith, Stockbridge, & Temple 2007).

Risk stratification of the population and provision of therapy related to risk in clinical scenarios are usually separated despite the demonstration that risk, including that of SCD, results from multiple dynamic factors. This necessitates the development of a reliable continuous risk function for a population so as to enable appropriate risk assessment that would warrant an intervention based on risk/ benefit and cost effectiveness considerations. Importantly this risk is not constant and shows temporal variations (Arntz et al. 2000; 2001;Page et al. 2004;Zipes 2005;Savopoulos et al. 2006)

Death due to ventricular arrhythmias remains a major public health problem, patients with history of myocardial infarction being the largest identifiable group who warrant prophylactic interventions and risk stratification. Several major landmark studies (MADIT, MADIT II, MUSTT, SCD-HeFT) have shown correlations between several known risk factors for fatal ventricular arrhythmias and SCD (Buxton et al. 1993;Moss et al. 1996;Moss et al. 2002;Bardy et al. 2005). In all of these, the strongest predictor for adverse outcome and arrhythmic death was impaired LV function. Regardless of changes in the absolute numbers of the SCD burden, it remains generally accepted that the proportion of all SCDs resulting from CAD is approximately 80% and that SCD accounts for nearly 50% of all CAD related deaths. The magnitude of this burden is highlighted by the fact that approximately two thirds of all SCDs caused by CAD occur either as a first clinical manifestation of the underlying disease or in subjects in whom disease has been identified but their risk prediction is considered low, based on current strategies for risk profiling.

Risk stratification markers

Apart from age and male gender, conventional known risk factors for SCD (Table 1) are non-specific, non-sensitive and do not provide an understanding of the mechanisms of SCD. None of these markers, individually or as a group, dominates for individual risk prediction. Individuals in whom CAD is not known, the risk factors of SCD are those of developing CAD; however, the magnitude of arrhythmia-associated risk is greater in those who have established predisposing conditions usually when substantial myocardial damage has occurred. Thus conventional markers depend on the degree of LV dysfunction, NYHA functional class, the degree of LV hypertrophy and LV myocardial mass, ECG variables demonstrating late potentials, fractionated QRS and QRS duration (>120 ms), positive signal average ECG (SAECG), dispersion of repolarisation (QT dispersion) and T wave alternans. There has been extensive interest in the role of autonomics including resting and exercise heart rate, baroreflex sensitivity, heart rate turbulence, deceleration capacity and heart rate variability on sudden

arrhythmic death, and the occurrence of sustained or nonsustained VT on ambulatory recordings. Acquired, functional and structural changes such as scar size and characteristics and specific genetic factors including mutations of ion channels, myocardial heavy chain proteins, polymorphism of coagulation factors or β adrenergic receptors are new risk factors.(Watkins et al. 1995;Priori et al. 2004).

The nature of the immediate precipitating event that triggers the cascade that leads to a fatal arrhythmia (VT/VF) in an otherwise stable individual remains very vague and a major unanswered question. Many ICD trials (especially MADIT II) have emphasized the need for developing novel tools in order to identify patients at the highest risk of ventricular arrhythmias and SCD and investigators have suggested a cumulative arrhythmia risk score given the intertwining nature of multiple risk factors of SCD in precipitating an event (Buxton et al. 2002;Maron et al. 2003;Priori et al. 2003b;Zipes et al. 2006).

Table 1 Electrophysiologic and functional surrogate high risk markers

Electrophysiology Surrogates	Functional Contractile Surrogates
Measures of myocardial conduction disorders (non-specific intraventricular conduction delay, degrees of AV block, LBBB)	NYHA Class
	LVEF %
	LV mass
SAECG, EPS	LVH- independent marker for SCD
Measures of dispersion of repolarization	Peak O_2 consumption
QT dispersion, T wave alternans	BNP
Measures of autonomic imbalance	
Resting HR, heart rate variability, baroreflexes.	

Conventional Risk Stratifiers of SCD *modified* (el-Sherif and Turitto G 2003)

LV dysfunction and ejection fraction

This is considered to be a major independent predictor of total and sudden cardiac mortality in patients with ischaemic and nonischaemic cardiomyopathy (Stevenson et al. 1993). The inverse relationship between impaired LV function and the occurrence of

sudden death and ventricular arrhythmias is well established (Goldman et al. 1993). This is more so with evidence of symptomatic heart failure a manifestation of impaired functional class especially that the correlation between symptomatic heart failure and EF is relatively poor and studies including MADIT-CRT demonstrated that despite poor EF (<30%) patients with minimal or no heart failure symptoms had low risk of SCD (3% per year) (Moss et al. 2009). The sensitivity of EF for predicting SCD using a cut-off of ≤ 30% is in fact quite low. The Maastricht Circulatory Arrest Registry (Gorgels et al. 2003) found that only about a third of patients who died suddenly of cardiac causes had an EF ≤ 30%. In a prior report from the same registry over half of the patients who had previously documented myocardial infarction and EF > 30 % suffered a cardiac arrest. Analysis of the mode of deaths in the 1791 patients from the MUSTT trial revealed no statistically significant difference in the arrhythmic deaths in patients whose EF was < 30% compared to those with ejection fractions of 30-40% (Buxton, Lee, Hafley, Wyse, Fisher, Lehmann, Pires, Gold, Packer, Josephson, Prystowsky, & Talajic 2002) The analysis of the 674 control patients in this trial suggested that relative risk of death depended largely on the presence of multiple risk factors rather than on LV EF% alone and that those with EF < 30% with no other defined risk factors had a low risk of 2 year sudden death (<5%) (Buxton et al. 2007). Similarly, the CABG-PATCH trial, ICD implantation did not reduce all-cause mortality significantly compared to controls because 71% of deaths were due to non-arrhythmic causes in this group of patients with LV EF< 36% (Bigger, Jr. et al. 1999). In the ATRAMI study, which enrolled 1284 recently post myocardial infarction patients, La Rouvere et al observed that heart rate variability and disturbed vagal reflexes had an effect on prognosis independent to LV EF (La Rovere et al. 1998). While not all sudden deaths are due to VT or VF, the vast majority are, especially in those who have had a previous myocardial infarction and were otherwise stable prior to the event.

Hereditary cardiomyopathies (including HCM and ARVC), unlike ischaemic and dilated cardiomyopathies display poor overall correlation between arrhythmic events and LV dysfunction and similarly ventricular arrhythmias and SCD in patients with channelopathies usually have good LV function and structurally normal hearts.

The electrophysiology study (EPS)

The EPS is important in the assessment of monomorphic re-entry VT especially in CAD with EF of 35-40% (Marchlinski et al. 1983). However, its prognostic value in inducible ventricular flutter and fibrillation is still controversial. Limited data suggest that it may be an important end point and, although formally popular, the EPS has not been found to provide positive predictive information of future arrhythmic events in the channelopathy populations. Nevertheless, its role in positive prediction of arrhythmic events in ischaemic cardiomyopathy is established (Buxton, Fisher, Josephson, Lee, Pryor, Prystowsky, Simson, DiCarlo, Echt, & Packer 1993;Moss, Hall, Cannom, Daubert, Higgins, Klein, Levine, Saksena, Waldo, Wilber, Brown, & Heo 1996). Its role remains controversial in Brugada syndrome where some studies (Priori et al. 2012) showed no predictive value in identifying future events related to inducibility of ventricular arrhythmias whereas others (Brugada et al. 2011) suggested a role. Recently, Makimoto et al proposed a role in the ease with which ventricular arrhythmias were induced during the EPS (Makimoto et al. 2012) Nevertheless, its negative predictive value is thought to be beneficial (Imaki et al. 2006). There is now a consensus that programmed electrical stimulation (PES) has no role in predicting fatal ventricular arrhythmias in DCM, HCM and LQT patients (Bhandari et al. 1985;Behr et al. 2002;Brilakis et al. 2005).

1.1.3 Substrate risk factor interaction

The paradigm for the pathophysiology of SCD is an abnormal myocardial substrate and transient triggering factors although these are very difficult to demonstrate. These are displayed in the modified Venn diagram below (Figure 1).

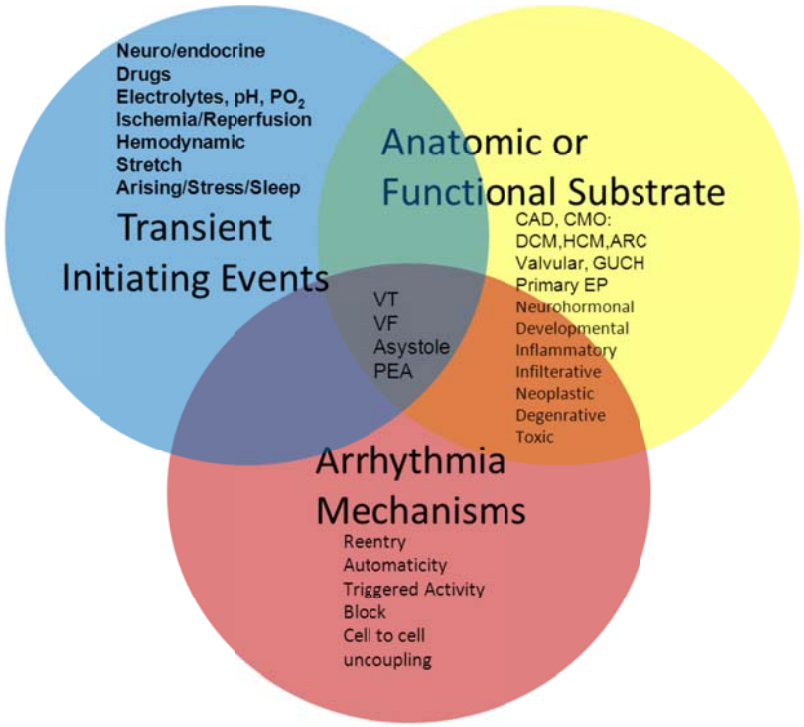

Figure 1 Multifactorial interaction of contributors to SCD Venn diagram showing the multifactorial interaction of causes and events contributing to the cardiac arrest. *Modified from Zipes and Wellens (Sudden cardiac death, Circulation ,Nov 24, 1998).*

Mechanisms underlying SCD are multiple and depend on many factors. Following myocardial infarction. important factors that determine the occurrence of SCD and its timing, include : the time from infarction, presence of potential ischaemia, extent of compensatory hypertrophy, adverse ventricular remodelling and functional NYHA class with the development of symptomatic heart failure.

The observation that VF and VT initiation is multifactorial and probabilistic suggests that no single test will be sufficient to identify patients at risk from SCD. Add to this complexity, the evolutionary nature of much cardiac pathology including coronary artery disease implies that the results and prognostic significance of tests used for risk stratification are likely to change over the course of the disease with the change of the underlying substrate and its triggers. Thus, dynamic measures or periodical testing for reassessment will be required. Structural factors may create a substrate in those conditions associated with the presence of transient factors eg ischaemia, reperfusion, haemodynamic alterations, drugs, metabolic and electrolyte changes. These may require clinically identifiable, genetically predisposed individuals and differences in the response of membrane channels, receptors and exchangers in susceptible individuals

similar to the effects of exercise in LQT1, sleep and rest in LQT3, startle and sudden awaking in LQT2.(Myerburg RJ & Castellanos A 2008)

Further analysis of the MUSST data (Buxton, Lee, Hafley, Pires, Fisher, Gold, Josephson, Lehmann, & Prystowsky 2007) led to the construction of a predictive model for total mortality in the CAD population with increased arrhythmic risk. These predictive factors included digitalis therapy, EF %, age (> 65 years), intraventricular conduction delay, LBBB, NSVT (>10 days post CABG or without revascularisation), AF, number of diseased vessels in the patient, CABG, beta blockers, inducible VT at EPS, spontaneous polymorphic NSVT and duration of longest episode of NSVT.

The most dramatic ICD survival benefits have been demonstrated in trials that assessed cumulative mortality risk using markers other than a reduced EF, for example the presence of spontaneous and inducible ventricular arrhythmias. The survival benefits (demonstrated in both MADIT II substudy and the MUSTT trial) appear to be limited to patients with remote myocardial infarction at least more than forty days.

1.2 Arrhythmia mechanisms

Over the last century, academics, clinicians and scientists have strived to understand the electrophysiological mechanisms responsible for the initiation and maintenance of cardiac arrhythmias in the hope of preventing their occurrence or at least terminating them should they occur. Broadly speaking mechanisms responsible for cardiac arrhythmias at basic electrophysiology level are divided into 2 categories: those related to impulse formation and those related to impulse conduction (Figure 2).

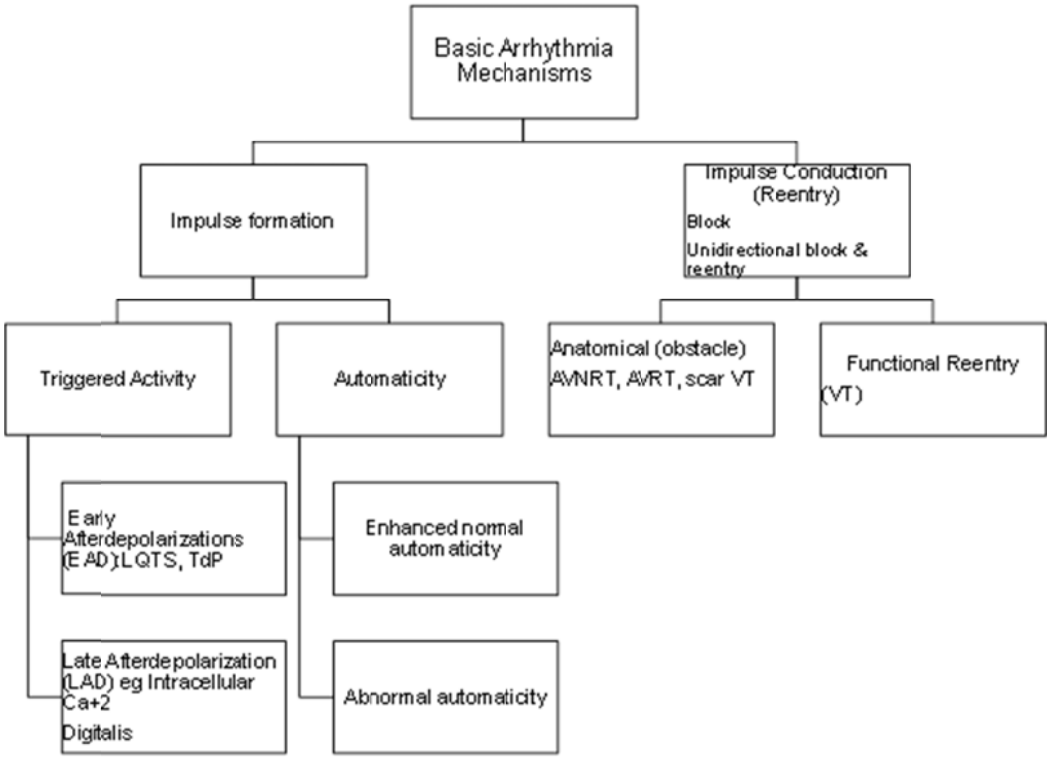

Figure 2 Flow chart of basic arrhythmia mechanisms

Proposed mechanisms of arrhythmogenesis include:

- Re-entry
- Automaticity
- Triggered activity

At the cellular level, conditions like:

Cell to cell coupling

Unidirectional conduction block

- Adrenergic stimulation
- ↑ extracellular Ca^{+2}
- ↑ extracellular digitalis

- intracellular Ca^{+2} overload (oscillatory release from sarcoplasmic reticulum)

These factors could activate an inward current via Na^{+}- Ca^{+2}exchange, non-selective cation exchange or chloride channels.

1.2.1 Triggered activity

Triggered activity is caused by after depolarisations. These are second depolarisations that occur either during repolarisation and referred to as early afterdepolarisations (EAD) or after repolarisation is nearly over or complete and referred to as delayed after depolarisations (DAD). They result in prolongation of repolarisation and may occur during phase 2 or 3 of the action potential in EAD or phase 4 in DAD. After depolarisations may be single or multiple oscillations that result in further depolarisation before repolarisation is complete and the resting membrane potential is reached. EAD have been linked to LQTs and the occurrence of TdP as a result of increased inward positive currents; of sodium or calcium (L type or T type Ca^{+2}) ions or reduction of outward flow of potassium or both.

In the 1970's much work was done on afterdepolarisations to clarify their role in arrhythmogenesis (Cranefield 1977) especially as they have been linked to bradycardia-induced tachycardias and those related to congenital and acquired LQTs (Surawicz 1989). EAD was studied mainly in animal models and in vivo using microelectrodes that assessed the effects of cesium salts (which prolong the action potential and the QT interval), ischaemia and reperfusion, isoprenaline infusion, pacing, stellate ganglion stimulation, increased vagal stimulation and drugs including sotalol and procainamide with an emphasis on the effect of the metabolic milieu particularly hypokalemia and hypomagnesemia (Sano and Sawanobori 1972;Katzung and Morgenstern 1977;Damiano and Rosen 1984). By using different pacing techniques at different levels of transmembrane potentials Damiano and Rosen were able to differentiate EAD-sustained arrhythmias from those with DAD, re-entry and automaticity at high membrane potentials (Damiano & Rosen 1984).

DAD occur in phase 4 of repolarisation and were described and extensively investigated in animal studies related to digitalis toxicity and pacing (Rosen et al. 1973). They have been produced following ischaemia and by injection of catecholamines into the canine coronary sinus which produced a triggered atrial tachycardia (Johnson et al. 1986). The hallmark is their response to pacing where they tend to occur with faster pacing rates and they result in a shorter post pacing coupling interval compared to the drive.

The mechanism common to the diverse triggered arrhythmias appears to be intracellular calcium overload, which induces an oscillatory transmembrane current carried by sodium and referred to as *Iti* (transient inward current) through the sodium-calcium exchange (Matsuda et al. 1982). This has been proposed as the mechanism and studies in the human heart of exercise induced VT -mainly of RVOT origin- which characteristically follow the sinus rate and do not show features of re-entry (Belhassen et al. 1984).

1.2.2 Enhanced automaticity

This can occur in normal tissue as a response to physiologic conditions, alterations in autonomic nervous system tone, electrolyte disturbances or drugs, or may occur in abnormal tissue within the myocardium. It refers to the accelerated generation of an action potential. Enhanced normal automaticity accounts for the occurrence of sinus tachycardia, while abnormal automaticity may result in various atrial or ventricular arrhythmias, for example, an accelerated idioventricular rhythm that occurs in ischaemic tissue (Scherlag et al. 1983). Abnormal automaticity can occur in atrial, ventricular and Purkinje fibres resulting from hyperpolarisation-activated inward calcium current and decay of outward potassium currents causing an increased intracellular positivity (Imanishi and Surawicz 1976) and this can be enhanced by increased sympathetic tone and catecholamines post myocardial infarction and heart failure and can be reduced by calcium channel blockers rather than sodium channel blockers (Katzung 1975;Grant and Katzung 1976).

1.2.3 Re-entry

This is deemed to be the primary mechanism responsible for arrhythmogenesis especially for fatal ventricular arrhythmias. Re-entrant excitation occurs when the propagating impulse does not die out after complete activation of the heart, but persists to re-excite the atria or ventricles after the end of the refractory period. Discovered as a mechanism of arrhythmia by Mines who described the basis of re-entry in frogs and electric rays, termed the resultant arrhythmia “ the reciprocating rhythm” and established that it occurred after a blocked impulse (Mines 1913).

Re-entry arises from discrepancy in the properties of the tissue, thus non-uniform dispersion of repolarisation initiates functional conduction delay or block and provides a

suitable medium for the occurrence of re-entry if two suitable adjacent conducting tissues which differ in their electrical properties are in place.

Re-entry due to abnormal impulse propagation has 3 main prerequisites:

- Slowed conduction: due to altered intercellular coupling, from non-uniform anisotropic conduction properties of adjacent cells or both.
- Unidirectional block, an essential requirement for both anatomical and functional re-entry. This can be associated with changes in the anisotropic properties of the myocardium and heterogeneity of refractoriness, which is suggested to initiate functional conduction block and re-entry and use dependency.
- Obstacle to conduction

Re-entry in the ventricle predisposes to VT and VF. This could be anatomical being mainly caused by scar tissue as an obstacle or functional being caused by alterations in local tissue characteristics which produce a suitable functional barrier and conduction block from ischaemia, metabolic and electrolyte derangements and the effect of drugs or toxins including antiarrhythmic agents. Several models have been suggested for functional re-entry including the leading circle, figure of 8, anisotropic and spiral wave models, which result from:

1) Sudden alterations in cardiac geometry.
2) Propagation failure due to decremental conduction.
3) Dispersion of refractoriness.
4) Differences in conduction properties relative to fibre orientation and tissue anisotropy.

Re-entry in ventricular arrhythmias

Re-entry is the main mechanism of arrhythmogenesis in the ventricle. From the concept of re-entry of Mines (Mines 1913) clinically significant findings were established in the late twentieth century from electrophysiology studies initially in the atria, AV node and accessory pathways (Durrer et al. 1967;Janse et al. 1971;Wellens et al. 1971;Allessie et al. 1972;Allessie et al. 1973). In chronic ischaemic hearts and those that have undergone remodelling from previous infarcts, re-entry has been postulated as the mechanism for monomorphic VT particularly identifying the circuit at the

ischaemia, infarction border zone (Josephson et al. 1982). Earlier studies suggested the possibility of re-entry or focal activity as the probable mechanism on the basis of results from the EP study (Wellens 1975) and from the ability to induce VT with PES (Marchlinski, Buxton, Waxman, & Josephson 1983). Tissue heterogeneity is marked in these infract border zones. They have been investigated extensively because of their association with re-entry (Dillon et al. 1988). Surviving re-entrant layers that follow a myocardial infarction are usually those in the subepicardium. In addition to tissue anisotropy and fibre disorientation the border zone of healed infarcts is characterised by reduction in the number and density of gap junctions in hearts with inducible VT (Peters et al. 1997;Peters and Wit 1998). In infarcted human hearts ventricular pacing and PES, which induces VF, is related to re-entry from the occurrence of multiple arcs of functional conduction block and slowed conduction demonstrated by NCM (Chow et al. 2004). Similarly in the canine model NCM using the Ensite system demonstrated that acute ischaemic VF was initiated at a focal point which transitioned into re-entry with subsequent induced VF in the same animals (Everett et al. 2005).

1.2.4 The nature of ventricular fibrillation (VF)

VF, the most common cause and end result of SCD, has been defined as a chaotic, random, asynchronous electrical activity of the ventricles due to repetitive re-entrant excitation and/ or rapid focal discharge (Zipes 1975).

This definition has been challenged by the suggestion that VF is not a random and chaotic phenomenon but an organised deterministic phenomenon that may even be re-entrant (Garfinkel et al. 1997) (Walcott et al. 2002;Weiss et al. 2004;Nanthakumar et al. 2004). This was demonstrated over half a century ago in studies in which fibrillation was found to consist of propagating wavefronts that meandered through the myocardium in complex patterns (Wiggers CJ et al. 1930;Wiggers CJ 1940;Moe et al. 1964). Similarly, Mc William was able to induce and study VF in various animals. He suggested that it was constituted by a rapid succession of uncoordinated peristaltic contractions which assumes the form of a wave along the complexly arranged and intercommunicating muscular bundles and that it differed from AF in the lack of its response to vagal stimulation (McWilliam 1887). But Garrey in 1914 described the relationship between VF and the heart size and demonstrated that by cutting the fibrillating tissue into a ring, a circus movement was established similar to the re-entry phenomenon described previously by Mines (Mines 1913;Garrey WE 1914). Various computer simulation studies and advanced mapping techniques have facilitated our understanding of VF.

However, treatment and prevention of VF has advanced little since the development of the electrical defibrillator in the 1950's given the poor performance of pharmacologic agents in the treatment and prevention of VF (CAST and SWORD trials) where post MI patients treated with class I and III antiarrhythmic drugs to suppress VEs were at increased risk of mortality (Echt DS et al. 1989;Waldo et al. 1995;Waldo et al. 1996).

Types of ventricular fibrillation:

High speed cinematography studies in the canine model demonstrated 4 stages to an uninterrupted VF: undulation lasting a few seconds, convulsion lasting 15- 40 s, tremulous incoordination lasting 2-3 minutes and atonic fibrillation (Wiggers CJ, Bell JR, & Paine M 1930). This set the stage for the conclusion that limited circuits and re-entry occur throughout the evolution of the arrhythmia (Wiggers CJ 1940). VF has been classified into two types (Table 2) on the basis of different electrical and conduction properties that account for the discrepant findings reported by Garfinkel's and Jalife's groups (Gray et al. 1995;Weiss et al. 1999;Garfinkel et al. 2000;Chen et al. 2003). Studies in isolated rabbit hearts using optical mapping techniques (Wu et al. 2002) revealed that two types of VF can occur at different times and different situations in the normal heart or they may coexist in the same heart under differing conditions. Type I VF was present in nonischaemic zones of the studied rabbit heart whilst type II VF occurred simultaneously in the ischaemic zone (Liu et al. 2004). Many factors, including antiarrhythmic and channel blocker drugs, may facilitate the conversion of one VF type to another. Experimentally Wu et al (2002) demonstrated that conversion of type I to type II VF was possible with the addition of increasing concentrations of D600 (methoxyverapamil)- an excitation contraction uncoupler- albeit after a transient period of reorganisation of the arrhythmia to VT. This resulted from the slowing of conduction from inhibition of inward slow Ca^{2+-} and fast Na^{+} currents at low and high concentrations respectively and from flattening of the APD restitution curve (Garfinkel, Kim, Voroshilovsky, Qu, Kil, Lee, Karagueuzian, Weiss, & Chen 2000;Wu, Lin, Weiss, Ting, & Chen 2002). Once the fast Na^{+} channels were blocked, there was low excitability with broad CV restitution, which initiated type II VF. At the electrical level, VF I may be due to multiple wandering wavelets; if the activation rate slows and the APD restitution curve flattens, further spiral wave break up would be hindered (Banville and Gray 2002;Wu, Lin, Weiss, Ting, & Chen 2002) so that any tissue heterogeneity would allow the faster spiral waves to become the mother rotors by overdriving the slower spiral waves and result in a focal source which initiates type II VF. Similarly, changes in tissue heterogeneity between ischaemic and nonischaemic zones (Rankovic et al. 1999) and impaired cell coupling, synergistically act to cause conduction block that maintains VF either by causing wave breaks or reducing excitability .

Table 2 Types of VF and their characteristics

VF Type I- Fast type	VF Type II-Slow type
• Rapid activation rate • Reentry is uncommon • Steep APD restitution slope- which is thought to be responsible for the conduction block • Flat CV restitution-Inverse conduction time restitution curve is flat (representing CV & excitability) • Found to be in nonischemic zone- with normal or lengthened APD • Proposed: VF maintained by multiple wandering wavelets	• Slow activation rate • Decreased excitability • Flat APD restitution curve • Broad CV restitution curve- thought to be the cause of the conduction block • Found in ischaemic zone • Spatiotemporal periodicity in activation maps • Maintained by mother rotors (dominant rotors)

Mapping of VF

Wiggers high speed cinematography studies served as a stepping stone for mapping VF (Wiggers CJ, Bell JR, & Paine M 1930). In 1981, Ideker et al were able to map VF, which degenerated from VT following the acute occlusion of a coronary artery in open chest dogs. Using an electrode array for epicardial mapping they noticed organised ventricular activity occurred in the ischaemic border zone which suggested that VF was not a totally random chaotic arrhythmia (Ideker et al. 1981). Further information following VF induction was obtained from optical mapping with fluorescein dyes suggested the presence of rotors, vortices and wave breaks as mechanisms of VF (Gray, Jalife, Panfilov, Baxter, Cabo, Davidenko, & Pertsov 1995;Bourgeois et al. 2012). Clinically, mapping of VF or its triggers has become a method of treating VF storm and minimising shocks in patients with idiopathic VF, LQT and Brugada syndromes (Haissaguerre et al. 2002;Haissaguerre et al. 2003;Nademanee, Veerakul, Chandanamattha, Chaothawee, Ariyachaipanich, Jirasirirojanakorn, Likittanasombat,

Bhuripanyo, & Ngarmukos 2011;Sunsaneewitayakul et al. 2012). Promising results with the possible cure of Brugada syndrome and abolition of the phenotype has been described with RVOT epicardial ablation (Nademanee, Veerakul, Chandanamattha, Chaothawee, Ariyachaipanich, Jirasirirojanakorn, Likittanasombat, Bhuripanyo, & Ngarmukos 2011). RF ablation of idiopathic VF largely relies on the targeting of triggers (namely from the specialised intraventricular conduction system and Purkinje fibres) by mapping and ablation of repetitive VEs, the precursors of VF or targeting the specialised conduction fibres during sinus rhythm (Haissaguerre, Shoda, Jais, Nogami, Shah, Kautzner, Arentz, Kalushe, Lamaison, Griffith, Cruz, de, Gaita, Hocini, Garrigue, Macle, Weerasooriya, & Clementy 2002). These potentials, which precede ventricular activation during premature beats, indicated that the VE originated from the Purkinje system whereas its absence at the site of earliest activation indicates that they originate from ventricular muscle.

1.3 Hypotheses regarding fibrillation

Wave break is the hallmark of fibrillation and is critically important in both AF and VF. It has not been established yet whether this is cause or effect. It has long been debated whether VF consists of multiple wandering wavelets or a single stable mother rotor that gives rise to daughter rotors. However, there seems to be a consensus that re-entry plays a major role in driving fibrillation (Davidenko et al. 1992;Lee et al. 1996;Valderrabano et al. 2001).

1.3.1 Multiple wavelet hypothesis

A computer model of atrial fibrillation led to the hypothesis that anatomic (tissue) and electrical heterogeneities in refractoriness, which are present in normal hearts but exacerbated by pathology, result in nonuniform dispersion of recovery which initiates wave breaks or wave splitting that lead to formation of multiple wandering wavelets with random re-entry that eventually leads to and maintains fibrillation (Moe 1962;Moe , Rheinboldt , & Abildskov 1964;Moe and Abildskov 1964) This proposed that dispersion of refractoriness promoted wavebreak. Experimental validation of this wavelet hypothesis in the atrium appeared soon thereafter and showed that cardiac re-entry could occur in the absence of anatomical obstacles. This updated version of the hypothesis emphasised that functional re-entry could cause wave breaks and fibrillation (Allessie, Bonke, & Schopman 1973). Spiral wave re-entry was then demonstrated to be the underlying mechanism for VF on the basis of computer simulation of sheets of

tissue, that established a connection between spiral waves and functional scroll wave re-entry in VF and polymorphic VT (Davidenko, Pertsov, Salomonsz, Baxter, & Jalife 1992;Pertsov et al. 1993). Similar findings of complex random appearance and termination waves were described in open chest dogs (Lee, Kamjoo, Hough, Hwang, Fan, Fishbein, Bonometti, Ikeda, Karagueuzian, & Chen 1996).

Recently, studies on the atrium vagal nerve stimulation in canine and computer models revealed that multiple foci mainly from the pulmonary veins and the coronary sinus drove the atria, and produced and maintained AF. In contrast with the prediction of the multiple wavelet hypothesis of Moe, no random re-entry was witnessed and there was limited ordered re-entry with head to tail interactions (Lee et al. 2012).

1.3.2 Focal source hypothesis

That a rapidly firing focus (mother focus) is the driver of the wave formation and fibrillation, this was suggested by Gray et al (Gray, Jalife, Panfilov, Baxter, Cabo, Davidenko, & Pertsov 1995). Stationary rapidly-firing foci generate single scroll waves (mother rotors), and wavebreak occurs as a secondary phenomenon. This single firing focus causes the formation of a re-entrant scroll wave which maintains VF, was quickly suggested (Jalife 2000). Studies of fibrillation in the guinea pig hearts showed an anatomic predilection for persistent rotor activity with the highest frequency waves always located at the anterior left ventricular wall (Samie and Jalife 2001). This implied that not all regions were important for VF maintenance. Further studies suggested that VF results from interaction between re-entry, possibly intramural, and local tissue heterogeneities (Valderrabano, Lee, Ohara, Lai, Fishbein, Lin, Karagueuzian, & Chen 2001). These mechanisms of VF induction and maintenance suggest therapy through ablation of the mother rotor responsible for the VF. This has been demonstrated in patients with idiopathic VF originating from foci in the Purkinje system (Haissaguerre, Shoda, Jais, Nogami, Shah, Kautzner, Arentz, Kalushe, Lamaison, Griffith, Cruz, de, Gaita, Hocini, Garrigue, Macle, Weerasooriya, & Clementy 2002).

Not all studies support the focal source or mother rotor hypothesis, In particular those conducted in larger mammalian hearts where rotors were observed for brief periods, but did not appear to be the driving force of VF. It has been proposed that continual formation of new rotors is necessary to maintain VF (Rogers et al. 2003;Kay and Rogers 2006;Kay et al. 2006). These discrepancies suggests that there is more than one type of VF and its manifestations are species- and tissue- dependent (Wu et al. 1998;Walcott, Kay, Plumb, Smith, Rogers, Epstein, & Ideker 2002;Chen, Wu, Ting, Karagueuzian,

Garfinkel, Lin, & Weiss 2003;Nanthakumar, Walcott, Melnick, Rogers, Kay, Smith, Ideker, & Holman 2004;Liu, Pak, Lamp, Okuyama, Hayashi, Wu, Weiss, Chen, & Lin 2004;Everett, Wilson, Foreman, & Olgin 2005). And that these are not mutually exclusive but can be converted from one type to another. Thus the finding that human hearts fibrillated whilst undergoing surgery, demonstrated that both mother rotors and multiple wavelets take part in maintaining VF and are not mutually exclusive (Kay & Rogers 2006;Kay, Walcott, Gladden, Melnick, & Rogers 2006;Nash et al. 2006).

Wavebreaks

Wavebreak is the hallmark of fibrillation in both AF and VF, but it is still unknown whether wavebreak is cause or effect in VF.

Wave length (λ) cm= APD (s) x CV (cm/s)

Cardiac excitation is an electrical wave with a wave front, that corresponds to action potential upstroke (phase 0) and a wave back, that corresponds to rapid repolarisation (phase 3). Wavelength is the distance between the wave front and the wave back. Thus, changes in wavelength are dependent on changes in APD, CV or both. Wavelength has been shown to be an important determinant of susceptibility to fibrillation and a good predictor of arrhythmia inducibility in the atrium (Rensma et al. 1988).

Alterations in wavelength could be proarrhythmic since shortening of the wavelength exhibits that the initiation of a circuit would require a small area of functional conduction block. Weiss et al hypothesized that spiral wave breakup is a result of wavelength oscillations. Theoretically, wavebreaks will occur if the wavelength is zero. In reality, this can only occur if either the APD or the CV is zero and, as these are governed and controlled by their preceding Dis and, electrical restitution is a principal determinant of wavebreak (Weiss et al. 2000;Weiss et al. 2002;Weiss, Chen, Wu, Siegerman, & Garfinkel 2004).

In the multiple wavelet hypothesis: wavebreak depends on pre-existing electrophysiological heterogeneity usually dispersion of refractoriness. For a wave to break its wavelength must be zero at a discrete point somewhere along the wave. This can happen if the wave blocks locally are due to local heterogeneity, so that although the wave is blocked locally it propagates elsewhere.

Wavebreak leads to 2 broken ends which lead to tips of potential re-entry (spiral waves or scroll waves), if they propagate or circulate around a functional or anatomical

obstacle they may result in re-entry triggering: monomorphic VT, polymorphic VT or VF. Wave breakage leading to spiral wave re-entry is a generic property of excitable media (also known as reaction- diffusion or activator inhibitor).

It has been believed that pre-existing heterogeneity of refractoriness or conduction, whether it was caused by anatomical (stationary) or functional factors was necessary for the initiation of re-entry. However, Omichi et al (2002) using optical mapping in guinea pig hearts showed that wavebreak- and thus the initiation of VF- may occur in completely homogeneous tissue and amiodarone was able to terminate VF by dramatically reducing the spontaneous wavebreaks, prolonging the VF cycle lengths from 83 ms to 118 ms and increasing the wave front in addition to flattening the APD restitution slope (Omichi et al. 2002).

Weiss et al (2000) connected the initiation of VF with the initiation of wavebreak, which was increasingly dependent on pre-existing heterogeneity and the response to dynamically induced heterogeneity. They suggested that understanding the complex relationship between dynamic heterogeneity and the initiation of VF is likely to be promising in the quest for effective pharmacological therapy for VF especially with drugs targeting the initial VT re-entry phase of VF. They elaborated on the clinical observation that diseased hearts fibrillate more easily than normal hearts and attributed this to their increase in susceptibility to wavebreak because of increased anatomical and electrophysiological heterogeneity, from the disease process.(Weiss, Chen, Qu, Karagueuzian, & Garfinkel 2000).

Model studies have shown that pre-existing heterogeneity is not necessary for wavebreak because wavebreak can be induced from rapid pacing or a large premature stimulus that results in dynamic heterogeneity (Karma 1994;Qu et al. 1999;Qu et al. 2000b). This may explain the occurrence of VF in structurally normal hearts, notwithstanding the contributory role of ionic channels in facilitating tissue heterogeneity**.** This causes the first wavebreak, which is then sustained spontaneously. This type of wavebreak depends on electrical (APD and CV) restitution properties.

1.3.3 The restitution hypothesis

This describes dynamic instabilities in APD and its relation to the preceding DI and results in a relationship whereby small abrupt changes in the DI result in large changes in the APD and cause unstable dynamics and wavebreaks which may predispose to fibrillation. In its original form it stated that a maximum APD restitution slope greater

than 1 predisposes to APD alternans (Nolasco 1968). Previous studies had shown that wavebreaks could occur even in totally homogeneous tissue (Karma 1994;Weiss, Garfinkel, Karagueuzian, Qu, & Chen 1999). As wavebreaks are the hallmark of fibrillation, they result in instability which precipitates further heterogeneity by perpetuating VF. APD restitution has been proposed as the primary cause for instability that results in unstable wave propagation and alternans due to spiral wave breakage when the slope of the restitution curve is steep and exceeds unity (Weiss, Chen, Qu, Karagueuzian, Lin, & Garfinkel 2002). However, diseased hearts fibrillate more commonly than normal hearts given their propensity to increased wavebreak because of increased anatomical and electrophysiological heterogeneity from the pathological process. This hypothesis gives support to development of antiarrhythmic therapy to convert VF to VT by flattening the restitution slope (Garfinkel, Kim, Voroshilovsky, Qu, Kil, Lee, Karagueuzian, Weiss, & Chen 2000).

1.4 Dynamic factors and fibrillation

Dynamic factors which, experiments suggest, initiate electrical alternans and VF, include APD restitution, CV restitution, short-term cardiac memory, calcium cycling and electrotonic currents.

1.4.1 Electrical restitution

In everyday language restitution means the restoration of something to its original state (The Oxford Dictionary; (Simpson J and Weiner E 1989) but in cardiac electrophysiology it means the dynamic dependence of action potential duration (APD) or conduction velocity (CV) on the previous diastolic interval (DI). The electrical restitution curve (ERC) typically describes the recovery of APD as a function of the DI. Its importance is that it allows the APD to adapt to changes in heart rate. It is also believed to manifest the incomplete recovery of all ion channels during fast heart rates from inactivation before the next action potential can occur. First described by Nalasco and Dahlen (Nolasco 1968) who showed that APD restitution slopes in excess of 1 produced alternans, which they described as oscillations but which were characterised by experiments on cat Purkinje fibres (Bass 1975). Thus, small changes in the DI amplified the changes in the APD, which may result in cardiac instability from multiple factors (Figure 4) including increased dispersion of tissue refractoriness and formation of a substrate for functional block, re-entry and VF (Pastore and Rosenbaum 2000). In fast heart rates and constant cycle lengths, this may result in discordant alternans with repeated long short cycles that predispose to wavebreaks especially in heterogeneous tissue (Garfinkel, Chen, Walter, Karagueuzian, Kogan, Evans, Karpoukhin, Hwang, Uchida, Gotoh, Nwasokwa, Sager, & Weiss 1997;Weiss, Chen, Qu, Karagueuzian, & Garfinkel 2000;Weiss, Chen, Qu, Karagueuzian, Lin, & Garfinkel 2002). Discordant alternans occurs more readily in the presence of tissue heterogeneity mainly because of pre-existing structural heart disease. Thus Koller et al, assessed dynamic restitution kinetics in patients with structural heart disease and found that while dynamic alternans occurred in six patients, VT was induced only in the three that had steep electrical restitution slopes. Similar results have been reported by other groups (Pak et al. 2004;Koller et al. 2005). However, tissue heterogeneity is not essential for induction of discordant alternans in simulation models but rather rapid pacing or VEs were sufficient to produce discordant alternans in spatial homogeneous tissue as a result of slowing of CV (Watanabe et al. 2001).

Steepness of APD restitution slope

The APD (or ARI) and DI pairs for a given S2 beat obtained at different coupling intervals form the standard restitution curve.
APD restitution is a critical requirement for spiral wave stability. When the slope of the APD curve is> 1, a small change in DI is magnified into a larger change in APD, which is translated into a larger change in wavelength. This causes a later larger change in DI.

Construction of the ERC required the assessment of local refractory periods and transmembrane action potentials, which have been represented and validated by the use of unipolar electrogram measurements on the endocardial surface. This has been true using a contact catheter for validation in animals (in dog- Haws, Lux 1990, Millar Kvalios 1985, in pig- Gepstein 1997) and in humans (Chen 1999, Chinushi 2002).

Factors that affect restitution

Electrical restitution describes the relationship between the APD and the preceding DI. However, there is a significant effect not only from the preceding beat but also from the history of the earlier beats which is called cardiac memory (page 55). Temporal and spatial heterogeneities affect restitution dynamics and include pacing site and pacing rates. Factors which may affect not only the steepness but also the shape of the restitution curve since increasing drive pacing rates shift the restitution curves in the human RV down and leftward and vary the size of the supernormal “hump” of the ERC (Morgan et al. 1992b). RV apical pacing has greater global restitution slopes compared to right atrial and RV septal pacing, which support theories of the arrhythmogenicity of RV apical pacing (Ahlberg et al. 2008). Ischaemia has a marked effect on the ERC slope both by flattening it or making it steeper. Despite flattening of the ERC slope within 5 minutes of induced acute ischaemia in rabbit hearts this resulted in APD alternans and easily inducible tachyarrhythmias (Kurz et al. 1993;Kurz et al. 1994). During on-going ischaemia the ERC slope continued to flatten into a horizontal line following irreversible ischaemic damage. On the contrary, in the anterior LV of chronically ischaemic dogs, regional ARI restitution slopes constructed from 60 unipolar electrodes in a nylon stocking in the ischaemic region showed significantly steeper restitution slopes in VF-inducible dogs (0.75) compared to the noninducible group (0.41, $p<0.05$) (Yuuki et al. 2004).

Certain drugs particularly antiarrhythmics that affect sodium, potassium and calcium channels, influence restitution and especially the steepness or flatness of the APD restitution slope. Garfinkel et al demonstrated the antifibrillatory effects of breytlium in

swine heart on electrical restitution due to its potassium blocking -properties (Garfinkel, Kim, Voroshilovsky, Qu, Kil, Lee, Karagueuzian, Weiss, & Chen 2000). These effects were purely related to bretylium's effect on flattening the APD restitution curve slope than to its APD-prolonging effect as shown by the same results being obtained with addition of cromakalim and the dynamic rapid pacing method. In a model of isolated rabbit hearts Wu et al converted VF to VT with the infusion of methoxyverapamil (D600), by flattening the ERC slope acting as a calcium channel blocker (at low doses) and a sodium channel blocker (at high doses) (Wu, Lin, Weiss, Ting, & Chen 2002). Amiodarone and propafenone have antifibrillatory effects by inducing postrepolarisation refractoriness (PRR), which delays the onset of electrical restitution beyond full repolarisation (Kirchhof et al. 1998;Kirchhof et al. 2003a). The effects of sotalol, procainamide and their combination on electrical restitution have been studied in a pig model. This supported the combined usage of both agents given their synergistic ability to alter the electrical restitution properties and prevent the induction of VF (Jin et al. 2008). The antianginal sodium channel blocker ronolazine has been studied in isolated rat hearts in both re-entrant and EAD induced VF. It has showed promise from its effect on both; flattening of the maximum restitution slope in re-entrant VF rendering pacing induced sustained VF to nonsustained VF which terminated spontaneously after 24 ± 8 s. And from blocking the late sodium channels in EAD mediated VF leading to its suppression (Morita et al. 2011). Quinidine has shown very good results in Brugada syndrome and VF by inhibiting the transient outward current (I_{to}) and flattening of the slope of the ARI restitution curve in 5 of 6 patients (Ashino et al. 2011). This should have a prominent role in future antiarrhytmic drug therapy.

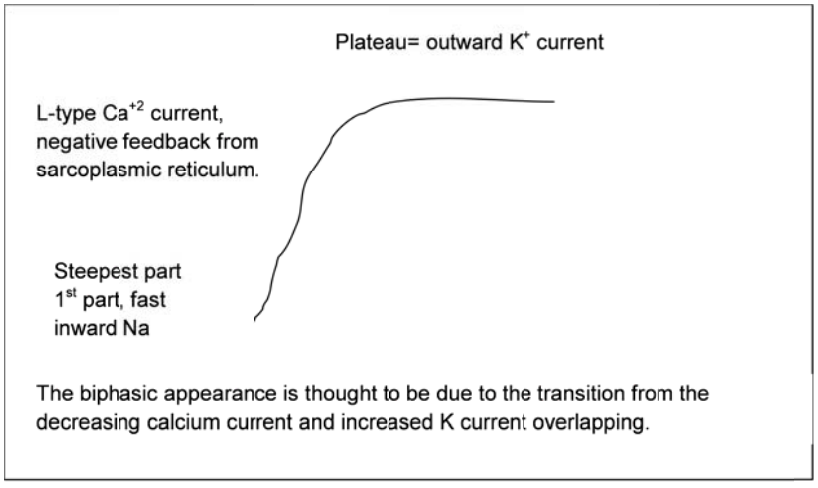

Figure 3 Ionic basis of electrical restitution in a biphasic curve

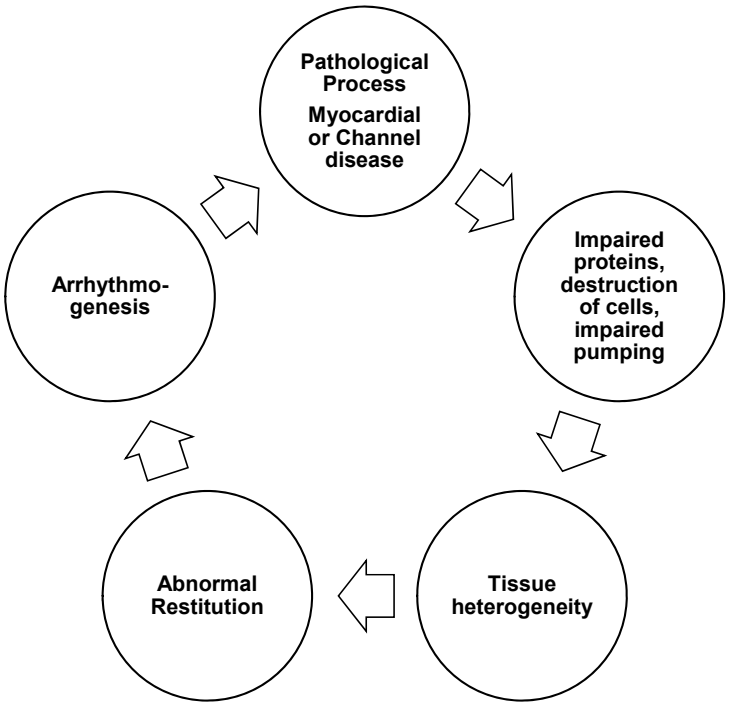

Figure 4 Flow diagram of the proposed effects of pathology on arrhythmogenesis

1.4.2 Conduction velocity

Like APD, CV is affected by the preceding DI. CV restitution influences the stability of spiral wave re-entry and the dynamics of impulse propagation by producing spatial variations in DI and thus influencing the occurrence of discordant alternans even in spatially homogeneous tissue following rapid pacing or even an ectopic beat (Cao et al. 1999;Qu, Weiss, & Garfinkel 1999;Qu et al. 2000a;Watanabe, Fenton, Evans, Hastings, & Karma 2001). Stimulation and optical mapping studies mainly from animal tissue, have demonstrated the central role of CV to produce QRS and T wave alternans. Watanabe et al (2001) showed that reducing the CV at longer pacing intervals and decreasing the slope of the CV restitution slope promoted APD instabilities. Banville and Gray were able to quantify APD and CV restitution and their dispersion in the rabbit heart during rapid ventricular pacing under control conditions and with an electromechanical uncoupling drug (diacetyl monxime DAM) which slowed propagating waves by slowing CV and prevented the induction and maintenance of VF (Banville & Gray 2002). The shape of the CV restitution curve determines the ease by which discordant alternans arises. The broader the CV restitution curve, the more likely wave

front breakages occur that result in alternans without the need for a steep APD restitution curve. This has been linked to type II VF induced by selective L type calcium channel blocker D600 (Wu, Lin, Weiss, Ting, & Chen 2002).

Wu et al adapted the inverse of the conduction time (CT^{-1}) between two epicardial points to estimate CV and excitability (Wu, Lin, Weiss, Ting, & Chen 2002). Using optical mapping the conduction time at the ventricular walls was inhomogeneous during S1 pacing so they used the mean value of the inverse conduction time from four readings. Global CV restitution properties in low arrhythmic risk human hearts displayed a relatively homogeneous pattern with overall broad flat CV restitution curves over a vast range of DIs which steepened only at very short DI when assessed in vivo using the Ensite NCM technology (Yue et al. 2005b). In their study, CV restitution magnitude was steeper than ARI restitution at the same endocardial points in all their patients (25 ± 10% vs 18 ± 9 %) respectively. Although the range of CV during steady state pacing in that study was in keeping with the results from optical mapping studies in rabbit hearts (Banville & Gray 2002;Wu, Lin, Weiss, Ting, & Chen 2002), the magnitude of CV restitution slopes in the human hearts was nearly five times that of the rabbit (Banville & Gray 2002;Yue, Franz, Roberts, & Morgan 2005b). This species- dependent phenomenon may be related to tissue heterogeneity and difference in the heart size, which in its interaction with APD restitution may serve to promote electrical stability.

1.4.3 Cardiac memory

Short- term cardiac memory is the phenomenon in which APD is influenced not solely by the immediately preceding DI but also by previous DIs and APDs, thus incorporating previous cycles. Because of the short term cardiac memory, ERCs and their slopes differ according to the pacing history and protocols used; from S1-S2 static protocols to dynamic pacing as demonstrated in studies by Koller et al initially in canine Purkinje fibres (Koller et al. 1998) and later in both structurally normal human hearts (0.97 ± 0.18 vs 0.83 ± 0.15) and those with structural heart disease (1.05 ± 0.09 vs 0.91 ±0.06) (Koller, Maier, Gelzer, Bauer, Meesmann, & Gilmour, Jr. 2005). Given the effect of this memory, the steepness of the APD curve even when exceeding 1, does not always predict the occurrence of alternans and VF (Banville et al. 2004;Cherry and Fenton 2004) .More important than the isolated proarrhythmic effect of the steepness of the APD restitution slope is the rate of adaptation of APD change to sudden rate change or a premature beat, which is inherently dependent on APD memory. Along the same lines, Franz et al demonstrated that approximately 40% of final APD rate adaptation is

achieved within 5 seconds (10-15 beats), which promotes DI lengthening and causes a leftward shift of the ERC with each DI increment and shifts the curve away from the vulnerable hump toward the plateau phase and away from the threshold of alternans (Franz et al. 1988;Franz 2003).

1.4.4 Electrotonic currents

Electrotonic currents may develop from the voltage difference between adjacent sites and gap junction conductance between cells, influence APD, CV and the propagated excitation wavelength. These currents may result in wavebreaks by enhancing the twisting of scroll waves or they may reduce the meandering of a scroll and thus suppress arrhythmias. The latter is due to the effect of the electrotonic currents on flattening of the restitution slope or altering the shape of the action potential by enhancing or reducing the wave back or front and its effect on the phase 0 and 3 of the action potential and the wavelength. Electrotonic effects from depolarised or normally polarised cells may cause the development of abnormal automaticity. Additional dynamic effects of elecrotonicity on APD and CV restitution may provide an explanation for lack of alternans despite APD restitution curves greater than 1 in a study in rabbit hearts (Banville & Gray 2002).

1.4.5 Intracellular calcium

Intracellular calcium haemostasis plays a major role in both electrical and mechanical restitution. Calcium can influence wave stability by multiple mechanisms. The cardiac myocyte has evolved to allow autoregulation of sarcoplasmic reticulum (SR) calcium content and sarcolemmal fluxes. Ca^{+2} is released from the SR by the process of calcium -induced calcium release via an exchange system through the ryanodine receptors and the L-type calcium channels. In normal conditions, the intracellular calcium level is tightly controlled by the voltage membrane channels. Intracellular calcium increases following tachycardia or rapid ventricular pacing and thus VT results in increased intracellular calcium and may predispose to VF after spiral wave breakup and alternans (Chudin et al. 1999). Ca^{+2} alternans is thought to be the most common cause of APD alternans in intact tissue (Chudin, Goldhaber, Garfinkel, Weiss, & Kogan 1999). Experimental studies using optical mapping and Ca^{+2} chelating agents have shown that APD discordant alternans can occur primarily from Ca^{+2} alternans without rapid pacing or tachycardia even if the heart rate is slowed (Walker et al. 2003).

1.4.6 Miscellaneous factors

The complexity of cardiac tissue and the intertwined nature of multiple dynamic factors and their roles in development of fatal ventricular arrhythmias should have become obvious from the above discussed points and the multiple studies included there. Those studies agree on the fact that no single explanation or mechanism can account for sudden occurrence of ventricular arrhythmias in all hearts. There is also agreement that the likelihood of SCD or of development of ventricular arrhythmias is greater in structurally damaged hearts, that VF can occur in structurally normal hearts which contain anatomical heterogeneity in the cardiac tissue and that APD restitution slopes >1 occur even in morphologically normal hearts. However, the probabilistic nature of VF, which is usually preceded by ectopic beats which may appear at a critical time, labelled the “vulnerable window”, can be found in all hearts and reflects the ability of VF to be induced in all hearts. This vulnerable period coincides with the initial steep portion of ERC, which is caused by the rapid recovery of APD (Bass 1975) and is associated with recovery from inactivation of the fast sodium channels (Franz 2003) with the spatial dispersion of tissue repolarisation from asynchrony in APD shortening and with electrical conduction and dispersion in sodium channel recovery playing major arrhythmogenic roles in initiation of discordant alternans.(Garfinkel, Kim, Voroshilovsky, Qu, Kil, Lee, Karagueuzian, Weiss, & Chen 2000;Watanabe, Fenton, Evans, Hastings, & Karma 2001;Weiss, Chen, Qu, Karagueuzian, Lin, & Garfinkel 2002).

Sympathetic stimulation by isoprenaline and adrenaline of the APD curve in the human heart at a single endocardial point (on the septum) showed steepening of the ERC slope possibly due to the accelerated recovery of electrical current channels, mainly calcium transit and accelerated deactivation of inward potassium channels (Taggart et al. 2003). However, despite the uniform increase in the restitution slope in that study to>1, no ventricular arrhythmias were induced during the construction of the ERC with the different drive train CL 400, 500 and 600 ms. The role of the autonomic nervous system in SCD has received a large amount of attention particularly because of the establishment of the diurnal variations in the occurrence of SCD (Arntz et al. 2001;Savopoulos, Ziakas, Hatzitolios, Delivoria, Kounanis, Mylonas, Tsougas, & Psaroulis 2006). VEs post MI may be related to sympathetic stimulation and given the circadian and diurnal nature of SCD and the protective effect of beta blockade, it may be that the sympathetic nervous system plays an inherent but not well defined role (Schwartz 1998). The nerve-sprouting hypothesis of SCD proposes that in chronic post MI patients cardiac nerve sprouting and hyperinnervation occur in the infarcted zones and may contribute to the occurrence of ventricular arrhythmias and SCD. Chen and

colleagues (Cao et al. 2000) conducted immunocytochemical studies in native hearts following previous MI of cardiac transplant recipients, which showed a positive correlation between the density of nerve endings in the removed hearts and the clinical history of ventricular arrhythmias. A study on the hearts of dogs with AV node blockade and chronic MI who received nerve growth factor infusion to the stellate ganglia and experienced repeated episodes of spontaneous ventricular arrhythmias found that 44% of them suffered SCD, whereas the control group of dogs which did not receive the nerve growth factor infusion did not suffer SCD or experience frequent ventricular arrhythmias (Chen et al. 2001). This supports the existence of a causal link between SCD and enhanced sympathetic sprouting. Autonomic nerve modulation has been studied in isolated intact rabbit heart by assessing through direct stimulation of sympathetic and vagus nerves on the restitution kinetics and establishment of alternans using suction epicardial MAP recordings (Ng et al. 2007). This showed that sympathetic stimulation steepens the APD restitution curve, lowers the VF threshold and causes greater degrees of alternans even at longer pacing CL, whereas vagal stimulation had an opposite and protective effect by flattening the ERC and raising VF threshold.

To summarise, wavebreaks and the development of ventricular arrhythmias and specifically VF depend on multiple intertwined factors (Figure 5) including the effects of underlying substrate or tissue heterogeneity and triggering dynamic factors most of which effect repolarisation.

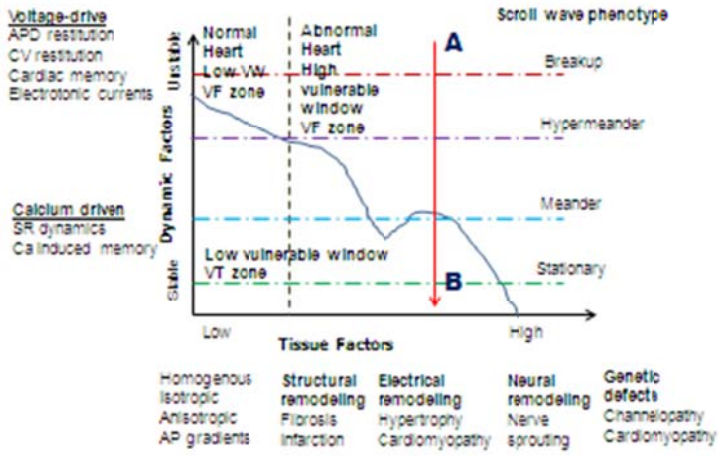

Figure 5 Hypothetical interaction between dynamic and tissue factors for risk stratifying VF

Dynamic factors (y axis) and the tissue factors (x axis) SR indicates sarcoplasmic reticulum, VW indicates vulnerable window. Modified from The dynamics of cardiac fibrillation; Weiss JN et al, 2005; Circ. 112:1232-1240).

1.5 Ventricular repolarisation

The focus of clinical cardiac electrophysiology and arrhythmology has shifted slightly from abnormalities in activation to those of repolarisation. However, our ability to map accurately and routinely, the repolarisation phase continues to be hindered by time restraints and repolarisation mapping still being considered a research tool. The overall direction of the of repolarisation in the heart is from apex to base and from epicardium to endocardium and supports the existence of a ventricular and transmural electrical gradient (Wilson et al. 1931).

1.5.1 Ventricular myocyte action potential

There are five phases to the action potential of the cardiac muscle cell, ranging from phase 0-4 that occur in response of a trigger or stimulus to the cell or from intrinsic automaticity which triggers a cascade of channel openings and closings with influx and efflux of ions across the cell membrane which result in its depolarisation and repolarisation.

Phase 0 represents the action potential upstroke or rapid depolarisation phase that occurs as a result of rapid influx of Na^+ into the cell through the voltage-gated Na^+ channels and alters the resting membrane potential from -95 mV to roughly +47 mV. Subsequently, the gated Na^+ channels shut in < 5 seconds as a function of voltage and time. This is the phase where class I antiarrhythmics generally function to block I_{Na} , prolong action potential and slow CV.

Phase 1 represents the early repolarisation phase during which activation of inward Ca^{+2} currents and outward K^+ currents occur. Because the Ca^{+2} currents are smaller than the fast Na^+ the upstroke terminates at +47 mV and is followed by a phase of rapid repolarisation to +10 mV, through rapid voltage- dependent inactivation of the I_{Na} and the activation of Ca^{+2} -independent transient outward and K^+ current (I_{TO}) (Oudit et al. 2001). Two variants of I_{TO} have been identified, a fast and a slow variant, with differing kinetic properties. These show regional variations in distribution with predominately greater expression of the fast variant in the epicardial cells, RV and the basal segments which when associated with K^+ channel defects may increase dispersion of repolarisation by increasing the transmural gradient potentially becoming arrhythmogenic as demonstrated in negatively transgenic mice (Baker et al. 2000) and the prominent phase 1 notch resulting in the spike and dome morphology which is exaggerated in Brugada syndrome occurs due to the high epicardial density of I_{TO} and

increased transmural dispersion. Relatively little is known about the transient outward chloride current, which is responsible for only a small current.

Phase 2 represents the plateau repolarisation process, which is complex because of the multitude of currents even though only a few channels are open during this phase. This phase is maintained by a fine balance between Ca^{+2} and K^{+}channels. Slow Ca^{+2} influx, occurs predominately through L-type Ca^{+2} channels, but there is a minor role for both T-type Ca^{+2} channels– which in normal hearts are found mainly in the specialised conduction system, in atrial pacemaker cells and Purkinje fibres- and Ca^{+2} –Na^{+} exchange pump which plays a minor role towards the end of the plateau phase. K^{+} efflux occurs through the slow delayed rectifier K^{+} channels (Ik_s) which are of three types with only the rapidly (Ikr) and slowly (Iks) activated variants being present in the ventricular myocardium and the ultrarapid delayed rectifier (Ikur) activating only being located in atrial tissue (Li et al. 1996).

Phase 3 represents the final rapid repolarisation process and occurs at the end of the plateau phase when the L-type Ca^{+2} channels are closed but the delayed rectifier K^{+} currents that were activated during the plateau phase remain open, thus reducing the membrane potential near to the K^{+} equilibrium and repolarising the cell. These potassium rectifier currents deactivate once membrane potential drops below -40 mV.

Phase 4 represents establishment of the resting membrane potential and diastolic depolarisation. Once the Ik repolarise the membrane to -40 mV they become inactive. However, the cell remains in the absolute refractory period and is unable to respond to a stimulus until the Na^{+} channels can be reactivated once the membrane potential drops below -70mV. Inward K^{+} rectifier current (I_{K1}) conducts small K^{+} currents in an inward direction and closes during depolarisation. Increased positivity of the cardiac myocyte from abnormal Ca^{+2} influx or abnormal K^{+} channels can result in EAD that occur with prolonged repolarisation, are seen in LQTs and are enhanced by sympathetic stimulation to provoke tachyarrhythmias. Diastolic depolarisation is a feature of automatic depolarising cells, which gradually self-depolarise even if not stimulated by an external trigger.

1.5.2 Genesis of the T wave

On a normal ECG, T wave polarity is the same as that of the QRS complex. This is thought to be due to progressive recovery of excitability from the epicardium to the endocardium. T waves are caused by the temporal and spatial sequence of rapid

repolarisation indicated by phase 3 of the membrane action potential and QRS,T wave ECG concordance is thought to occur because the repolarisation occurring in the opposite direction to that of depolarisation (Wilson, MacLeod, & Barker 1931). The use of intramural electrodes established that the wave of recovery progresses from the site of earliest depolarisation with endo/ epicardial antagonism and epicardial T wave morphology was generally found to be slightly negative (van and Durrer 1961). The polarity of the epicardial T wave is dictated by the sequence of recovery across the ventricular wall and on the distance from the recording sites. If the entire heart were synchronously activated and repolarised in phase the net electromotive force would be zero and no ECG deflections would occur. Spach and Barr suggested the presence of a transventricular gradient in the dog heart during ectopic beats was dictated by the progression of repolarisation rather than transmural gradients during normal beats (Spach and Barr 1975). Human endocardial and epicardial MAP recordings showed that regions with shorter ATs had longer APDs and vice versa regardless of whether they were measured from the endocardium or epicardium (inverse correlation, regression analysis -1.32) (Franz et al. 1987). Overall the epicardium was activated later but repolarised earlier than the endocardium. Unlike in earlier animal studies a transventricular gradient of APD (apico-basal) was not detected although there was significant regional variability in repolarisation time and T wave was thought to be the reflection of the repolarisation time its concordance a reflection of the repolarisation gradient from epicardium to endocardium (Autenrieth et al. 1975;Franz, Bargheer, Rafflenbeul, Haverich, & Lichtlen 1987). Although, in vitro studies on perfused canine ventricular wedge supported the concept of a transmural gradient being responsible for the cellular generation of the T wave, however they demonstrated that the epicardium always repolarised first and the M cell layer repolarised last. (Yan & Antzelevitch 1998) They also showed that the peak of the T wave coincided with epicardial APD_{90} and the end of the T wave with M cell repolarisation, thus establishing the index of transmural dispersion (T_{peak}-T_{end}), that the M cell APD established the QT interval and that marked transmural dispersion of repolarisation was associated with TdP. Accordingly, epicardial repolarisation gradients were demonstrated in human hearts and they corresponded to the morphology of the T wave. Spatial distribution of the morphology of the T wave has been studied with both experimental and computational simulation studies during sinus rhythm, ventricular pacing and VEs with positive T waves found in 44% of sinus rhythm and 85% of ventricular paced UE complexes. The positive T waves were related to early repolarisation and the negative ones to late repolarisation (Potse et al. 2009), where Chen at al using MAP recording in chronic pulmonary thromboembolism, RV

hypertrophy and raised RV pressure models found that the T waves were predominantly positive over the LV epicardium and anterior RV and negative or biphasic over the remainder of the RV epicardium. With the most predominant T wave morphology overall being positive (44%) (Chen et al. 1991). Visual spatial T wave representation was conducted globally in human hearts using the Ensite NCM system where by positive T waves were found at earliest endocardial activation sites, negative T waves at latest activation sites and biphasic in between during differing spontaneous and paced beats. However temporal maps of repolarisation were not produced (Yue et al. 2005a).

Definition of the T wave and its resulting dV/dt:

Arbitrarily, the T wave has been divided into 3 morphologies (Figure 6):

- Positive, which starts at the baseline then rises above the isoelectric line in a dome-type fashion then descends.
- Biphasic, which has a positive and negative component and could start either positively or negatively thus demonstrating two distinct turning points, one on each side of the baseline.
- Negative, which starts at the baseline but then descends below the isoelectric line.

Defining T waves is not clear-cut, the relationship of the deflection to the isoelectric line is an accustomed method of defining them however; there are waves that are asymmetrical displaying features of being more positive than biphasic or more negative than biphasic (Figure 7).

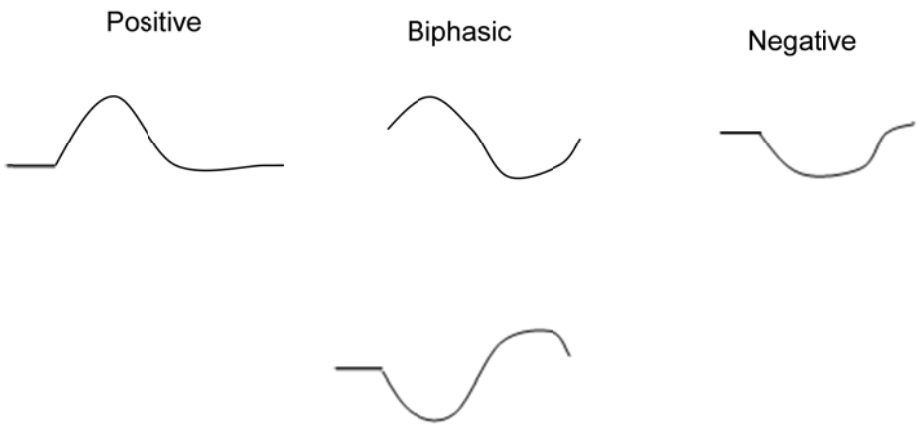

Figure 6 Basic T wave morphologies.

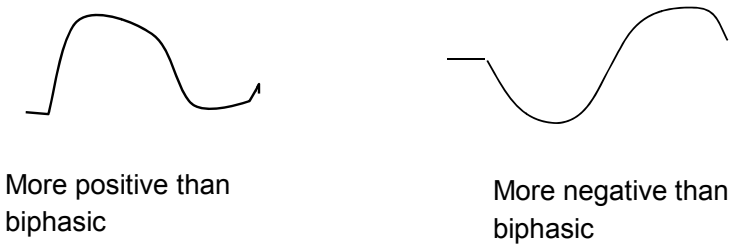

Figure 7 Schematic showing the different varieties of biphasic T waves

Defining the end of repolarisation depends largely on T wave morphology as demonstrated by when the positive waves were measured from the minimum dV/dt of the T, whereas in negative and biphasic T waves the end of repolarisation was taken to correspond to the maximum dV/dt of the T wave. Because of these difficulties, some have defined the end of repolarisation as the peak of the T wave (Nicolson et al. 2012). Especially in structurally diseased hearts, it can occasionally prove very difficult to classify the T wave into one of the three morphologies. It may also be difficult to define this morphology as there may be transitions from one morphology to another and ambiguity arises. These transitions may result in identifiable biphasic T waves, or in a wave, which is mainly negative or positive where only a fraction of it is biphasic. Herein lies the difficulty in determining the end of the T wave and thus the end of repolarisation. There are also situations where the T wave is ambiguous or produces double or triple humps (deflections).

1.5.3 Normal repolarisation sequence

The repolarisation phase starts during phase 1 of the membrane action potential. It is not a uniformly propagated phenomenon being caused mainly by spatial and temporal electrical gradients. The repolarisation sequence differs depending on the morphology of the T wave on the surface ECG (Cowan et al. 1988). These authors showed that during assessment of epicardial repolarisation in humans with IHD and aortic stenosis using MAP that in patients with upright T waves, there was a clear linear inverse relation between the APD and AT, whereas in patients with negative T waves the repolarisation sequence resembled the activation sequence. Experimental and simulation studies have shown a sequence and a global ventricular gradient of repolarisation which progressed from apex to base (Autenrieth, Surawicz, & Kuo 1975;Potse, Vinet, Opthof, & Coronel 2009). However Cohen et al in sheep experiments demonstrated a base to apex gradient of repolarisation (Cohen et al. 1976), but in human MAP studies Franz et al could not demonstrate a consistent transventricular gradient or sequence but noted marked APD disparity even within the same region, and longer APDs on average in the septal and diaphragmatic areas but shortest intervals at anteroapical and posterolateral sites (Franz, Bargheer, Rafflenbeul, Haverich, & Lichtlen 1987). Global mapping studies in swine and human ventricles using MAP recordings and a 3D electroanatomical mapping system (CARTO, Biosense Webster) suggested that the endocardial sequence of repolarisation was dictated by that of activation thus supporting the presence of endocardial ventricular repolarisation gradients (Yuan et al. 2001).

1.5.4 The relationship between repolarisation and refractoriness

A fairly constant relationship between the recovery of excitability and repolarisation has been demonstrated (Hoffman et al. 1957). Recovery of excitability from a stimulus usually outlasts a return to resting membrane potential and thus exceeds repolarisation, because recovery and the return of excitability are not merely voltage dependent but also time dependent. This phenomenon has been called *postrepolarisation refractoriness.* It remains unclear whether arrhythmogenesis is governed by repolarisation or refractoriness especially since under baseline conditions, APD and ARI are considered to be reliable estimates for local tissue refractoriness and they have the advantage of easy measurement.

There is a close relationship between the level of repolarisation and the return of excitability as shortening of the APD also results in shortening of the ERP and favours arrhythmogenesis (Wellens et al 1984, Mitchell et al 1986) as ERP is directly

proportional to shortening of the APD in response to various pacing rates (Davidenko and Antzelevitch 1986;Franz and Costard 1988;Koller et al. 1995) and as at a given site the ERP/APD ratio during steady state pacing is constant and not dependent on CL. Return of excitability has been related to repolarisation levels between 75-85% in different animal models and humans (Franz and Cosatrd1988, 1990, Lee et al 1992). The relationship between repolarisation and refractoriness is altered during ischaemia, rapid repetitive extrastimulus pacing and drugs. The return of excitability is delayed following ischaemia and certain antiarrhythmic drugs including amiodarone and bretylim due to the occurrence of PRR, which has been shown to have a protective antiarrhythmic effect with some drugs but is markedly proarrhythmic in the ischaemic heart (Coronel et al. 2012). MAP 90% has been taken as a cut-off for repolarisation because of the difficulty in measuring the asymptomatic end of repolarisation (Franz 1999).

Wyatt et al assessed the relationship between ARIs and APD in a few animal studies and established the Wyatt measurement where the ARIs in UE measurements were correlated with the minimum derivative of the QRS and the maximum derivative of the T wave regardless of T wave morphology. The maximum rate of rise of repolarisation – dV/dt max of the T wave- correlated with local refractoriness (Wyatt et al. 1981).

Haws and Lux (1990) emphasised the conclusions of Millar et al who correlated the end of repolarisation with ARI using measurements from UE first derivatives (Millar et al. 1985). They demonstrated good correlations between ARIs and transmembrane APD (correlation coefficients of 0.96 to 0.99) in the canine ventricle under a variety of conditions including changes in T wave polarity, drive site, steep gradients of repolarisation and myocardial ischaemia. (Haws and Lux 1990).

Chen et al in 1991 were the first to utilise ARI instead of APD for repolarisation measurements in humans. They also noticed an inverse relationship between ARI and AT. They correlated ARI with APD in the epicardium of human RV where the correlation ranged between 0.84- 0.94 (Chen, Moser, Dembitsky, Auger, Daily, Calisi, Jamieson, & Feld 1991).

Lee et al (1992) demonstrated that the APD, ERP relationship was a near constant linear one independent of changes in CL. This fixed relationship was less evident in the presence of sodium channel blockers (procainamide) at short CLs (Lee et al. 1992).

Similarly, the introduction of repetitive premature beats whilst shortening coupling intervals during VT stimulation tests was arrhythmogenic from progressively shortening the local repolarisation time of the subsequent beats that progressively encroached onto the preceding beat during the repolarisation phase, which further decreased the coupling interval, shortened the APD and delayed conduction all of which are arrhythmogenic. The mechanism was probably a facilitation of excitability prompted by earlier recovery of sodium channels or a tissue phenomenon (Koller, Karasik, Solomon, & Franz 1995).

The refractory period is the interval from depolarisation to the return of excitability. The effective refractory period (ERP): defined as the longest (S_1-S_2) coupling interval for an extrastimulus that did not trigger a propagating impulse. Gepstein et al using 3D contact mapping (CARTO, Biosense Webster) defined the refractory period at each measured site in the LV as the shortest S_1-S_2 interval that induced a propagated response minus the activation time at that site (Gepstein et al. 1997b). Measurement of the ERP of tissue is usually performed by pacing with a train of paced 8-10 beats at basic cycle length (S1) and progressively introducing an extrastimulus (S2) at progressively shorter coupling intervals until failure of impulse propagation occurs (Han and Moe G 1964). Although both repolarisation and refractoriness are influential in the development of arrhythmias, refractoriness plays a more substantial role as nonuniformity of recovery is key in promoting wavebreak and fractionation of impulses which results in the cascade of delayed conduction, re-entry and finally ventricular arrhythmias.

1.5.5 Postrepolarisation refractoriness (PRR)

This is defined as a delay in the onset of electrical restitution beyond full repolarisation of the previous steady state response and occurs when the recovery of excitability is delayed beyond the completion of repolarisation. It has been associated with increasing rather than flattening the speed of recovery of APD and CV (Kirchhof, Degen, Franz, Eckardt, Fabritz, Milberg, Laer, Neumann, Breithardt, & Haverkamp 2003a). It is due to delayed reactivation of the Na^+ channels that start at membrane potentials of -70 and -60 mv. Amiodarone induced PRR suppresses induction of VF and it is one of the few remaining drugs that prevent recurrent ventricular tachyarrhythmia and does not increase mortality or SCD rates. It acts by blocking multiple ion currents in the heart and may produce PRR without slowing of conduction, which modifies the induction of ventricular arrhythmias. Antiarrhythmic drugs which have sodium channel blocking and APD prolonging properties e.g amiodarone, propafenone and bretylium result in PRR

which plays a role in their properties mainly by narrowing the period of partial refractoriness (Garfinkel, Kim, Voroshilovsky, Qu, Kil, Lee, Karagueuzian, Weiss, & Chen 2000). Kirchof et al in experiments on chronically amiodarone treated rabbits showed that sodium channel blockers can prevent progressive encroachment by prolonging refractoriness beyond repolarisation, (Kirchhof, Degen, Franz, Eckardt, Fabritz, Milberg, Laer, Neumann, Breithardt, & Haverkamp 2003a). Amiodarone, unlike other sodium channel blockers has the additional desirable antiarrhythmic feature of inducing PRR with little conduction slowing. Slowing of CV is considered proarrhythmic and is a predictor of inducibility of ventricular arrhythmias (Koller, Karasik, Solomon, & Franz 1995;Kirchhof, Fabritz, & Franz 1998). When PRR occurs the disparity of refractoriness is much greater than the dispersion of ARIs (Haws & Lux 1990). PRR is proarrhythmic in particular during ischaemia.

1.5.6 Activation recovery interval

The ARI has been used as a surrogate for the APD, local refractory period and a useful measure of local repolarisation duration (Millar, Kralios, & Lux 1985;Haws & Lux 1990). The former demonstrated that ARIs from UE correlated closely with ventricular refractory periods under conditions of varying cycle length and adrenergic stimulation (infusion of norepinephrine and sympathetic nerve stimulation). In 1987 Blanchard demonstrated that that ARIs were suitable to measure local events as they were not significantly affected by changes in timing of distant electrical events (Blanchard et al. 1987).

Controversy and on-going debate regarding the appropriate method to measure repolarisation, particularly ARIs from UE in positive T waves remain (Wyatt, Burgess, Evans, Lux, Abildskov, & Tsutsumi 1981;Haws & Lux 1990;Chen, Moser, Dembitsky, Auger, Daily, Calisi, Jamieson, & Feld 1991;Yue et al. 2004;Coronel et al. 2006;Potse, Vinet, Opthof, & Coronel 2009). The Wyatt method measures ARI from the minimum derivative (dV/dt_{min}) of the QRS to the maximum derivative (dV/dt_{max}) of the T wave regardless of T wave morphology- thus using the instant of the steepest upstroke of the T wave. Correlation between APD and ARIs has been good under varying states including continuous pacing, during cathecholamine infusion, sympathetic nerve stimulation, hypothermia and graded ischaemia with alteration in T wave polarity (Millar, Kralios, & Lux 1985;Haws & Lux 1990). The overall correlations were less close in the ischaemic group, probably given the induced changes in morphology of the complexes particularly in relation to ST-T wave changes and decreased amplitude and triangulation

of the transmural MAP. ARIs have been applied given the ease with which repolarisation information and measurements are obtained especially from multiple sites simultaneously on a beat to beat basis that allows the assessment of temporal and spatial alterations adding to their advantage over MAPs. This enabled the global assessment of ventricular repolarisation in structurally normal human hearts (Yue, Paisey, Robinson, Betts, Roberts, & Morgan 2004;Yue, Betts, Roberts, & Morgan 2005a;Yue, Franz, Roberts, & Morgan 2005b). Yue et al (2005a) validated the use of NCM for assessment of repolarisation in the human ventricle compared to MAP. They demonstrated that ARIs determined by UEs correlated closely with MAP recordings during sinus rhythm, constant ventricular pacing and abrupt changes in the preceding diastolic interval, with all three T wave morphologies. However, ARIs continue to have some limitations especially with complexes that have ambiguous T wave morphologies.

1.5.7 Activation repolarisation coupling

The activation sequence and excitation of the heart, animal and human, has been extensively and thoroughly studied (Scher 1964;Durrer et al. 1970). Whereas activation proceeds from endocardium to epicardium, repolarisation proceeds in the reverse direction (Wilson, MacLeod, & Barker 1931) mainly due to transmural electrical gradients between endocardium and epicardium with the inner wall being more negative (Spach & Barr 1975). Franz et al found a marked negative correlation between AT and APD in human hearts using contact MAP recordings from 5-11 LV sites, with sites that were activated early having longer APD than those activated later and independent of where in the heart the measurements were taken (Franz, Bargheer, Rafflenbeul, Haverich, & Lichtlen 1987). In that study, the inverse relationship between activation and repolarisation was also demonstrated during sinus rhythm. Cowan et al in epicardial studies of the human LV (8-10 sites) revealed similar findings with reduced dispersion of epicardial repolarisation in patients with normal upright T waves (IHD and aortic stenosis patients). However this relationship was totally lacking in those hearts with baseline negative T waves (aortic stenosis patients) where the APD was independent of the AT and the dispersion of epicardial APD was greater (Cowan, Hilton, Griffiths, Tansuphaswadikul, Bourke, Murray, & Campbell 1988). Similar findings were reported from global endocardial MAP recordings from swine and human recordings using CARTO to establish sites of earliest activation, but the linear regression slopes were < 1 (Yuan, Kongstad, Hertervig, Holm, Grins, & Olsson 2001). That study found a positive correlation between the end of repolarisation- which they defined as the time from the

earliest ventricular activation to the point of intersection between the baseline and tangent to the steepest slope of phase 3 of the MAP- and the AT. This they suggested was due to insufficient progressive shortening of the MAP duration in relation to the AT that failed to compensate adequately for the progressive delay (Yuan, Kongstad, Hertervig, Holm, Grins, & Olsson 2001). That resulted in a loss of the inverse relationship between the activation sequence and repolarisation sequence. This was also described in a third of the patients in Franz et al (1987) and 50% of those in Cowan et al (1988).

The inverse correlation between activation and repolarisation has been proposed as a protective mechanism against arrhythmias, especially the effect of reducing the dispersion of repolarisation both regional and global, while loss of this coupling may be arrhythmogenic. In normal swine heart, the same tight coupling of activation and repolarisation was seen with electroanatomical mapping during sinus rhythm and atrial and ventricular pacing, the longest ARIs being recoded at sites of shortest AT and also the opposite and dispersion of repolarisation being functionally dependent on the location of the earliest activation and on the direction of the propagated wave (Gepstein, Hayam, & Ben-Haim 1997b). On the contrary Yuan et al found that repolarisation followed the same sequence of activation and refuted the presence of a reverse repolarisation gradient across the ventricular endocardium (Yuan, Kongstad, Hertervig, Holm, Grins, & Olsson 2001), These results are similar to those of Toyoshima et al in their study of 32-43 epicardial sites using suction electrodes in dogs (Toyoshima et al. 1981). They concluded that the activation sequence is an important determinant of the sequence of repolarisation.

Yue et al using NCM in structurally normal hearts whilst studying right and left ventricles, have also shown an inverse correlation of activation and repolarisation in sinus rhythm, following a spontaneous VE, constant ventricular pacing and increasing premature stimulation (Yue, Betts, Roberts, & Morgan 2005a). With increased premature stimulation, a reduction in negativity of the regression slope between activation and repolarisation has been shown and suggests a possible instantaneous adaptation effect possibly by electromodulation or cardiac memory (Rosenbaum et al. 1982;Laurita et al. 1996).

1.6 Dispersion of repolarisation and arrhythmogenesis

Dispersion of repolarisation has been linked to arrhythmogenesis, particularly fibrillation (Moe 1962;Han & Moe G 1964;Kuo et al. 1983). It is a measure of the heterogeneous recovery of excitability in a given mass of cardiac tissue. Dispersion is

defined as the difference between the longest and the shortest repolarisation times or refractory periods within a set of measurements.

1.6.1 Physiologic dispersion of repolarisation

Some non-uniformity in the refractory period and conduction is physiological being caused by tissue anisotropy. This is seen with LV and RV interventricular dispersion, transmural or transepicardial gradients and regional base to apex APD dispersion. In normal healthy hearts, the right and left ventricles are structurally heterogeneous with regional differences occurring in shape, wall thickness and fibre array. Intercellular coupling and electrotonic interactions between cells that are mediated by gap junctions act to attenuate the differences between cells in the cardiac syncytium in physiological and pathological states. However, the density of gap junctions is reduced following ischaemia and myocardial infarction, which alter their effect on anisotropy and CV and reduce intercellular coupling and enhance arrhythmogenesis (Peters 1996;Peters, Coromilas, Severs, & Wit 1997;Peters & Wit 1998).

Marked transventricular gradients have been described by Yuan et al in swine and human hearts where these gradients were located between the septum and the lateral/posterolateral and basal areas during sinus rhythm (Yuan, Kongstad, Hertervig, Holm, Grins, & Olsson 2001).

Transmural dispersion is also a product of heterogeneity of cell types. Cells that have been recognised in ventricular myocardium of mammals include epicardial, endocardial, midmyocardial (M cells) and Purkinje fibres. Relative differences in their ion channel densities dictate their differences in response to various agents and drugs and explains the presence of transepicardial gradients. These were demonstrated in optical mapping of the guinea pig heart where oblique gradients of APD were found from epicardium of the LV apex to the right atrio-ventricular groove (Laurita, Girouard, & Rosenbaum 1996). Franz et al in assessment of AT,APD and RT using contact MAP catheters from endocardial and epicardial LV sites, showed regional or geographic dispersion in the LV with the diaphragmatic and apicoseptal regions having the longest average and the anteroapical and posterolateral walls having the shortest average APD (Franz, Bargheer, Rafflenbeul, Haverich, & Lichtlen 1987). However, controversy over the existence of the M cell layer continues (Anyukhovsky et al. 1999).

The autonomic nervous system also plays a role in physiologic dispersion as sympathetic stimulation shortened the refractory period in LV free wall endocardium and

epicardium while vagal stimulation had minimal effects (Martins and Zipes 1980;Haws & Lux 1990).

As described in section1.3 (pages 46-50) dispersion of refractoriness has been viewed as the major drive for wavebreak during fibrillation in the multiple wavelet and the focal source hypotheses and although spontaneous sustained re-entrant ventricular arrhythmias should not occur in normal hearts, fibrillation can be induced by delivering electrical stimuli in the vulnerable period of any heart and anisotropy plays a part in that (Han et al. 1966). On the other hand, tissue anisotropy and heterogeneity can also promote stability by anchoring meandering spiral waves rather than cause destabilisation- a common misconception.

1.6.2 Spatial dispersion of repolarisation

This has received extensive attention in the past two decades because of its possible contribution to the mechanism of arrhythmogenesis which was first investigated by Han and Moe in the 60's (Han & Moe G 1964). Global, regional and local dispersions have been assessed with a variety of techniques and technologies. Dispersion has long been defined as the difference between the longest and shortest refractory periods or repolarisation times within a set of measurements, when assessed globally within a chamber from multiple sites. Global dispersion has been expressed as the range or standard deviation of the measured values or derived from them and expressed as the coefficient of variation. However, global measurements mask regional and local variations which may play a significant role of nonuniform recovery and arrhythmogenesis that is associated with local and regional changes (Burton et al. 2000). Local dispersion relates to the difference between the maximum and minimum values between 2 adjacent sites 1-2 cm apart. In normal hearts without a history of previous ventricular arrhythmias the mean dispersion of LV refractoriness was 40 ± 14 ms and the recovery time 52 ± 14 ms (Vassallo et al. 1988). These authors assessed the spatial dispersion of activation and recovery of excitability in 12 LV sites from normal controls and patients with IHD with induced monomorphic VT during PES and with cLQTs with VF arrest, and found that patients with IHD or LQTs had a significant increase in dispersion of refractoriness over the controls albeit the greater degree of dispersion of activation was the culprit in the IHD group whereas in LQTs group dispersion of repolarisation was determinant of the nonuniform recovery of excitability (Vassallo, Cassidy, Kindwall, Marchlinski, & Josephson 1988). Morgan et al reported from sequential assessment of 10-14 sites in human RV studies that geographic

dispersion of repolarisation from MAP recordings was similar in the control group of patients with normal hearts compared to patients with a variety of pathologies and VT. However, regional and adjacent variations in APD between these groups showed significant differences (Morgan et al. 1992a).

A spatial dispersion of repolarisation between the RVOT and RVA in patients with previous MI was found to influence electrical re-entry and the occurrence of T wave shock induced VF during defibrillation threshold testing and also failure of successful defibrillation (Moubarak et al. 2000).

Over the past decade, intense research on the role of electrical and mechanical dyssynchrony in arrhythmias has been conducted. LBBB and dyssynchrony produce heterogeneous stress and strain mainly on the lateral wall of the LV (Vernooy et al. 2005). In dog hearts optical action potentials from arterially perfused ventricular wedges were measured in controls and in dogs with chronic LBBB. Significant shortening of the APD, CV and refractoriness in the lateral wall of the dyssynchronous hearts was noticed. However, despite the intraventricular dispersion of repolarisation the induction of ventricular arrhythmias with a single paced extrastimulus in the dyssynchronous nonfailing ventricle was not significant (Spragg et al. 2005).

1.6.3 Temporal dispersion of repolarisation

The relationship between the response of the APD or ARI and the previous DI is an assessment of temporal dispersion which is signified by electrical restitution. This is a dynamic measure of dispersion, which I have alluded to on page 51.

Under normal conditions, refractory periods shorten in parallel with APD, however this relationship changes during ischaemia when the APD shortens, the refractory period lengthens and the recovery of excitability lags behind and leads to PRR. The effects of hypothermia, regional ischaemia and reperfusion were studied by Kuo et al in open chest dogs using suction MAP electrodes. They induced ventricular arrhythmias using a single VE at a critical level of APD dispersion under experimental but not under control conditions. Similarly, atrial over drive pacing prevented the induction of VT by reducing dispersion from the arrhythmogenic level of 103 ± 5 ms to a nonarrhythmogenic level of 86 ± 9 ms ($p < 0.05$) (Kuo, Munakata, Reddy, & Surawicz 1983).

MAP recordings in isolated rabbit hearts from RV and LV epicardial sites demonstrated that global ischaemia produced marked slowing of electrical restitution and flattening of the ERC slope with interventricular nonuniformity of dispersion, development of APD

alternans and deviation of the ERC between the two ventricles (Kurz, Mohabir, Ren, & Franz 1993;Kurz, Ren, & Franz 1994).

Spatial dispersion of repolarisation and steep ERC slopes were linked to induction of ventricular arrhythmias in human hearts when restitution kinetics were assessed at two points in the RV (RVOT and RVA). The restitution slopes were significantly steeper in the VT/VF induced groups 3.7 ± 2.1 and 2.3 ± 2.7 compared to the noniducible control group 1.9 ± 0.8 (RVOT) and 1.7 ± 1.1 (RVA) and with RVOT being the site of sustained arrhythmia induction in the majority of cases. (Pak, Hong, Hwang, Lee, Park, Ahn, Moo, & Kim 2004).

1.6.4 Transmural dispersion of repolarisation

Transmural dispersion of repolarisation (TDR) was defined as the difference between the longest and shortest repolarisation times (AT + APD_{90}) of transmembrane action potential recorded across the wall. This may be due to the cell types of the ventricular wall in most mammalian species including humans, i.e. endocardial, epicardial, midmyocardial (M cells) and Purkinje fibres (Antzelevitch et al. 1991). On the ECG this corresponded to the difference between the peak and the end of the T wave (APD_{90} of the epicardial layer and APD_{90} of the M cell layer respectively) (Shimizu & Antzelevitch 1999). This may be primarily related to the differences in the densities of such cells and the relative differences in their ion channel densities eg the I_{ks} and I_{Na}, their sensitivities to various agents including drugs, particularly anti-arrhythmic or alterations in the electrolyte milieu similar to potassium which contributes to heterogeneity in the APD across the wall between the subepicardium and subendocardium. *Shimizu and Antzelevitch* worked on arterially perfused wedges of canine LV models of LQT1, LQT2 and LQT3. In contrast, Shimizu and Antzelevitch (Shimizu and Antzelevitch 1998) using in vitro LQT1 (chromanol 293B to block I_{Ks} and mimic *Kv*LQT1) and LQT3 models demonstrated that APD was prolonged in the M cells and this increased TDR and caused ventricular arrhythmias under adrenergic influence. As there was a general prolongation of QT interval and APD in all cell layers, including the M cells, therefore under control conditions there was no increase in TDR. They assessed cellular basis of catecholamine stimulation and its effect on T wave morphology, TDR and the initiation of TdP by using rapid pacing, ß adrenergic stimulation with isoproterenol and sodium channel blockade with mexiletine on shortening the QT interval and diminishing the TDR and preventing TdP.

However, they demonstrated through their experimental model of LQT1 that deficiency of the I_{Ks} does not induce TdP but adrenergic influence predisposes the myocardium to the development of TdP by increasing TDR. Similarly, in their LQT2 model using d-sotalol as I_{Kr} blocker showed that independently it did not increase TDR, but the cumulative effects of d-sotalol, hypokalemia and bradycardia were required to induce TdP (Shimizu and Antzelevitch 1997).

Yamanchi et al used K^+ rectifier channel blocker (I_{kr}) E4031. In their LQT2 model of dog LV, and showed that prolongation of ARI was uniform in the four myocardial layers including the M cell region and the TDR did not increase (Yamauchi, Yamaki, Watanabe, Yuuki, Kubota, & Tomoike 2002).

This suggests that, a mechanism other than mere TDR may be involved in the occurrence of ventricular arrhythmias in the LQT2 model. It is interesting that the discrepancy of repolarisation across the ventricular wall described above was less evident in the intact heart. This was probably due to the presence of electrotonic interactions (Bryant et al. 1998;Nabauer 1998)

1.7 Cardiac mapping

Global cardiac chamber mapping has been fundamental in the evolution of activation and repolarisation assessments and of mapping. Activation mapping of the intact human heart was first performed on the hearts of brain dead trauma victims (Durrer, van Dam, Freud, Janse, Meijler, & Arzbaecher 1970). The initial assessments of global repolarisation mapping were performed in experimental studies in isolated animal hearts and involved the effect of alterations such as ischaemia, metabolic derangements, reperfusion, hypothermia, pacing and drugs. These were performed in hearts of dogs, sheep, pigs and rabbits with MAP recordings either endocardially or epicardially (Toyoshima, Lux, Wyatt, Burgess, & Abildskov 1981;Kuo, Munakata, Reddy, & Surawicz 1983;Kurz, Mohabir, Ren, & Franz 1993;Spragg, Akar, Helm, Tunin, Tomaselli, & Kass 2005). With the advent of 3D electroanatomical mapping, CARTO (Biosense Webster) was utilised in repolarisation assessments and ARI recordings from UE demonstrated tight coupling of activation and repolarisation in vivo in swine hearts (Gepstein, Hayam, & Ben-Haim 1997b). Endocardial MAPs (Yuan, Kongstad, Hertervig, Holm, Grins, & Olsson 2001) from sites in the LV and RV in swine and human hearts were measured with results in keeping with the dependence of activation on repolarisation and suggestive of the presence of repolarisation gradients over ventricular endocardium.

1.7.1 Contact mapping

Cardiac mapping is fundamental for identification of mechanisms of arrhythmias and for guiding ablation therapy. Since the early twentieth century contact endocardial mapping has been available. It has evolved from intracellular glass electrodes (Burdon-Sanderson J and Page FJM 1882) for measurement of transmemebrane action potentials in vitro to suction electrodes (Korsgren et al. 1966) and refined extensively to present-day contact MAP catheters.

Clinically contact mapping provides good spatial information and is ideal for mapping stable constant arrhythmias. However, it is frequently inadequate for activation mapping of complex haemodynamically unstable arrhythmias particularly compromising VT or infrequent arrhythmias such as VEs. Attempts at clinically useful ventricular endocardial mapping originated with single catheters used to sequentially map point by point and early on provided ample information to guide surgical ablations (Josephson et al. 1978b).

Monophasic Action Potentials

These are contact extracellularly recorded waveforms that under optimal conditions reproduce the repolarisation time course of the transmembrane action potential with high fidelity (Franz et al. 1986) (Ino et al. 1988). However, they are generally of lower amplitude than intracellular recordings from needle electrodes but their duration is similar (Hoffman et al. 1959;Franz, Burkhoff, Spurgeon, Weisfeldt, & Lakatta 1986).

MAP faithfully reflects the duration and the configuration of the repolarisation phases. They were initially obtained after causing traumatic tissue injury(Burdon-Sanderson J & Page FJM 1882;Franz 1983) but later recorded with suction electrodes (Korsgren, Leskinen, Sjostrand, & Varnauskas 1966) and subsequently using nondepolarisable substances mainly silver- silver chloride tip electrodes (Franz et al. 1980) were previously considered the method of choice for measuring repolarisation in vivo in the intact heart (Franz 1999). Initially utilised to study one or two simultaneous recordings (Koller, Karasik, Solomon, & Franz 1995;Pak, Hong, Hwang, Lee, Park, Ahn, Moo, & Kim 2004) but evolved to allow studying sequential recordings from 5-12 sites (Franz, Bargheer, Rafflenbeul, Haverich, & Lichtlen 1987;Cowan, Hilton, Griffiths, Tansuphaswadikul, Bourke, Murray, & Campbell 1988;Yuan, Kongstad, Hertervig, Holm, Grins, & Olsson 2001) (Franz 1983;Morgan, Cunningham, & Rowland

1992a;Morgan, Cunningham, & Rowland 1992b). Standard conventional platinum electrode catheters have been validated to produce good quality MAP recordings to allow MAP targeted ablations (Yuan et al. 2000). MAP recordings were extensively studied becoming an integral part of basic electrophysiology but allowing the integration with clinical cardiac electrophysiology and understanding of arrhythmia mechanisms from dispersion of repolarisation, the effects of ischaemia, drugs and RF ablation of myocardium and differentiating scar from viable hibernating myocardial tissue (Franz 1983;Franz et al. 1984;Franz & Costard 1988;Franz, Swerdlow, Liem, & Schaefer 1988;Morgan et al. 1991;Kurz, Mohabir, Ren, & Franz 1993;Kurz, Ren, & Franz 1994;Kirchhof, Fabritz, & Franz 1998;Kirchhof, Degen, Franz, Eckardt, Fabritz, Milberg, Laer, Neumann, Breithardt, & Haverkamp 2003a).

The drawbacks of MAP recordings include: the time needed and limited coverage area due to the small electrode tip of 1-2mm, distortion of recordings from movement artefacts during in vivo studies, constraints on simultaneous recording sites and limited spatial resolution and the reliance of the MAP morphology on the use of closed bipole and on contact pressure. Although some of these disadvantages have been rectified by the use of conventional platinum ablation catheters the technical difficulties of obtaining appropriate point-by-point contact, remain challenging. Hence, the development of techniques to allow rapid multisite global measurements which commenced with the use of MAP catheters incorporating three dimensional electroanatomical mapping (CARTO, Biosense Webster) to assess endocardial repolarisation in swine and humans which provided comprehensive spatial repolarisation data but were limited in its temporal data because of the need for sequential measurements (Yuan, Kongstad, Hertervig, Holm, Grins, & Olsson 2001).

The validation of MAP recordings against ARIs first with contact studies (Chen, Moser, Dembitsky, Auger, Daily, Calisi, Jamieson, & Feld 1991) and later with noncontact UE was a milestone in that they provided global spatial and temporal repolarisation data in human hearts (Yue, Paisey, Robinson, Betts, Roberts, & Morgan 2004).

CARTO

This is largely a nonfluoroscopic mapping and navigation system which allows the construction of three dimensional electroanatomic, activation, isochronal, propagation and voltage maps of the studied cardiac chamber. It relies on a locatable catheter connected to an endocardial mapping and navigation system which uses an ultra-low magnetic field emitted from the three coils within the locator pad below the patient's operating table. The subject's torso is covered by three magnetic fields of different frequencies and the mapping catheter (Navistar, Biosense Webster) navigates within the cardiac chamber. The location of the mapping catheter is determined by the interaction between the magnetic sensors in the mapping catheter tip (tip and ring electrodes with an embedded sensor) and the location reference in the three magnetic fields. The accuracy of the spatial localisation of this technology was validated by studies in vitro and vivo in swine heart with an accuracy of 0.7 mm (Gepstein et al. 1997a). Cardiac chamber access depends on the chamber of interest and two catheters are inserted percutaneously one the mapping navigating catheter and the other a catheter of reference (coronary sinus or RV catheter). The mapping catheter is dragged over the endocardium, sequentially acquiring its tip location and its electrogram while the catheter was in stable contact with the endocardium. UE or MAP can be used for mapping utilizing this system. The system has been used in experimental models to study repolarisation employing APD and ARI (Gepstein, Hayam, & Ben-Haim 1997b;Yuan, Kongstad, Hertervig, Holm, Grins, & Olsson 2001). When the catheter is moved within the magnetic field, the currents generated represent movement in three dimensions enabling tracking of the tip of the mapping catheter within the heart and navigation of the catheter independent of fluoroscopy.

The sequential point-by-point nature of the mapping system during activation and voltage mapping effectively limits its use to map short-lived tachyarrhythmias, polymorphic or heamodynamically unstable arrhythmias except in terms of anatomical mapping and catheter navigation. As opposed to the Ensite system, CARTO acquires sequential data whereas NCM acquires simultaneous data.

1.7.2 Optical mapping

This is a technique that involves the use of high-resolution mapping and voltage sensitive dyes to simultaneously map APD in excitable cells in the experimental setting. Unfortunately its use is limited to the surface of beating hearts and thus has only been

feasible in small mammalian hearts eg guinea pig and rabbit hearts. However, it shows promise in assessing the role of repolarisation in re-entry. Because of the ability of optical mapping to allow simultaneous measurements of APD from hundreds to thousands of sites using phototdiode arrays and special cameras. Its high spatial and temporal resolution and its ability to effect measurements during VF has led to its use in repolarisation studies (Laurita, Girouard, & Rosenbaum 1996;Choi et al. 2001;Banville & Gray 2002). Movement artefacts and noise are major drawbacks as they may affect the validity of repolarisation measurements. But have been reduced by the use of electromechanical uncoupling agents such as diacetyl monoxime or cytochalasin-D.

1.7.3 Non-contact Mapping

Over the past decade the Ensite 3000 NCM technology (St Jude) has been developed to allow three-dimensional simultaneous acquisition of endocardial electrogram data in any chamber of the human heart. This is a valuable tool for diagnostics and a guide for ablation in complex arrhythmias especially in structural heart disease. Global activation and repolarisation maps may allow a better understanding of the critical elements necessary to initiate and maintain a tachycardia. The idea of NCM arose from the necessity to increase the number of simultaneous mapped sites, which previously involved increasing the number of catheters introduced into the cardiac chamber (Davis et al. 1994), increasing the number of electrodes per catheter (Eldar et al. 1996) or using different shaped multielectrode catheters e.g basket electrodes, to improve spatial recordings (Triedman et al. 1997;Greenspon et al. 1997).

Historical aspects

The concept of NCM was introduced by Taccardi et al 1987, who used an olive shaped cylindrical probe to measure intracavitary potentials from ventricular ectopic beats in the LV of animal hearts (Taccardi et al. 1987). This probe provided poor spatial data and low amplitude EGMs but the authors could localise the site of origin of the ectopics to within 20 mm and calculated virtual UE within 10 ms of the contact electrograms. Multi-electrode catheter baskets were soon introduced which allowed the simultaneous measurement of a fixed number of contact recording sites but these proved difficult to use and were associated with unwanted myocardial irritation (Jenkins et al. 1993).
Khoury et al were able to reconstruct accurately intracavitary unipolar endocardial potentials with a 128 electrode probe in perfused canine LVs utilising the boundary-element inverse solution with the assistance of 2-D epicardial echocardiography during

SR, LV pacing and spontaneous VEs to display isopotential and isochronal maps of the LV endocardium (Khoury et al. 1995;Khoury et al. 1998). Their computed endocardial EGMs correlated well with direct contact EGMs (correlation coefficient r= 0.88) with agreement in activation times and an error of 4.7 ms.

NCM using the Ensite system is based on computing the endocardial potentials using the inverse solution to Laplace's equation:

$$\mathbf{V_p = A \times V_e}$$

Where V_p are the recorded potentials on the probe surface, A is the matrix coefficient between the two surfaces and V_e the endocardial potentials.

Endocardial potentials are stabilised by the Tikhonov numeric regularisation technique, which depends on bicubic spiline model instead of linear spikes.

Systems based on balloon catheters (Ensite NCM and basket catheters) allow simultaneous acquisition of data from multiple sites in a cardiac chamber. However, the resolution of maps derived from expandable basket catheters is limited as a result of inferior endocardial contact, difficulty of catheter localisation and wide spacing of the electrodes despite the simultaneous activation mapping and reconstruction of maps of the chamber (Eldar, Fitzpatrick, Ohad, Smith, Hsu, Whayne, Vered, Rotstein, Kordis, Swanson, Chin, Scheinman, Lesh, & Greenspon 1996). Thus, generally the maps derived from basket catheters offer inferior resolution and quality to those from other systems.

Ensite 3000 noncontact mapping system (Previously Endocardial Solutions Inc, St Paul, Mn, now St Jude Medical)

This is a three-dimensional mapping tool that allows simultaneous acquisition of electrogram data from the whole cardiac chamber.

It is composed of (Figures 8 and 9):

- A multielectrode array (MEA)
- Proprietary recorder and amplifier system
- Catheter locator system
- Silicon graphics workstation

Figure 8 The Ensite 3000 noncontact mapping system

The Ensite system used for the studies and offline analysis utilising versions 4.2- 6.0 of the software.

Multielectrode array (MEA):

The MEA is a mesh of polyimide-coated stainless steel wires of 0.003 inch in diameter braided on an inflatable 7.5 ml ellipsoid balloon -which should be filled with half strength contrast -and mounted at the distal end of a 9 F pig-tail catheter. Sixty four electrodes are distributed on the array at specific locations by using laser etching to remove 0.025 inch spots of insulation at these sites. Ring electrodes are positioned at either end of the array. Another electrode positioned ~ 16 cm back on the shaft of the catheter acts as a reference electrode for recording intracavitary UEs.

The MEA is introduced percutaneously over a 0.035-inch guide wire into the cardiac chamber of interest. The balloon is inflated to deploy the array once the catheter position is stable. (Figure 9 and 11).

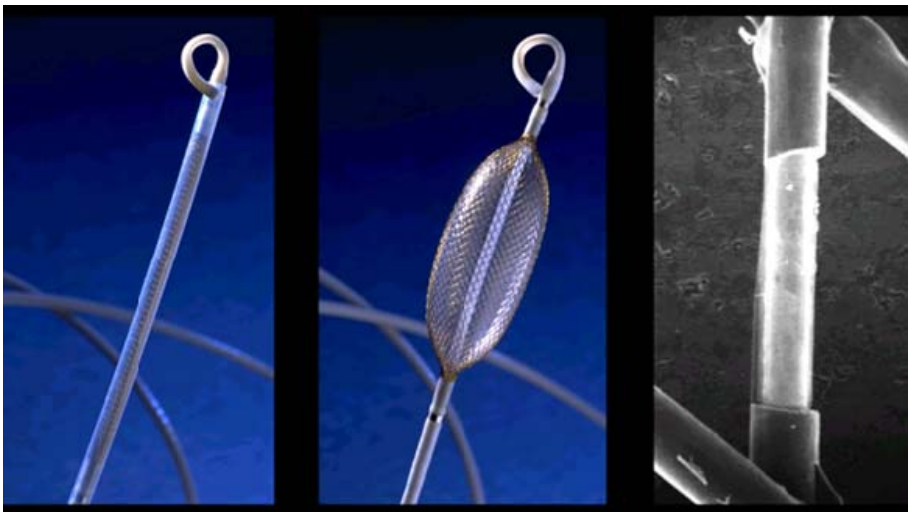

Figure 9 The Ensite multielectrode array before and after balloon inflation

Multielectrode array on the noncontact mapping balloon used by the Ensite 3000 system. (St Jude Medical).

Proprietary recorder and amplifier system:

The amplifier has 16 implants for electrograms for contact catheters , 12 for surface ECGs and 64 from the multielectrode array. Far field signals are fed into the amplifier system sampled at 1.3 KHz and filtered.

The MEA detects far field low amplitude and low frequency signals, which it enhances mathematically and resolves. An inverse solution to La Place's law is used to simulate how a remote signal would have appeared at the source. Then the boundary element method applies the inverse solution to resolve a matrix of such signals at the blood-endocardial boundary.

Catheter locator system:

A standard electrode catheter connected to the Ensite system is introduced into the same cardiac chamber to emit a 5.68 KHz low current locator signal. This signal is alternately detected by 2 ring electrodes at the tips of the MEA at 100 times per second allowing the system to compute the location of the mapping catheter.

By gliding the mapping catheter along the endocardial surface an anatomical geometry is gradually constructed. The resultant geometry represents the cardiac chamber in diastole, thus only the most remote locations of the roving catheter from the array are recorded.

The locator method relies on ambient conducting and solves a point source- sink model using a standard nonlinear least squares algorithm (Levenberg- Marquardt method).

The conventional mapping catheter is located by a 5.6KHz locator signal, this is a low current which is emitted from the roving catheter and passed alternately between it and two ring electrodes (current sink electrodes) one proximal and the other distal- on the shaft of the catheter and below the MEA. A custom algorithm can determine the location of the roving source in relation to the array electrodes and the 2 current sink electrodes by demo dilating the 5.68 KHz potentials on the MEA.

The 3D model of the endocardium is then constructed by moving the mapping catheter along the contour of the endocardium of the intended cardiac chamber. This results in a computer model of virtual endocardium, which is gradually built up from a series of coordinates for the endocardium. The result is a patient specific anatomically contoured model of its endocardial geometry. The system automatically stores the most distal points obtained by the roving catheter, and ignores those points when the catheter is not in contact with the endocardial wall. As the process continues and more points (coordinates) are collected, the geometry becomes a polygonal representation of the chamber surface, which is later completed, and smoothed to present a computer model of virtual endocardium.

The system allows reconstruction of 3360 UEs which are detected by the 64 electrodes of the MEA and allows the production of isopotential, isochronal, voltage and scar maps.

Silicon graphics workstation

Sophisticated software allows data analysis of activation both in real time and review mode using high resolution screens and precision software.

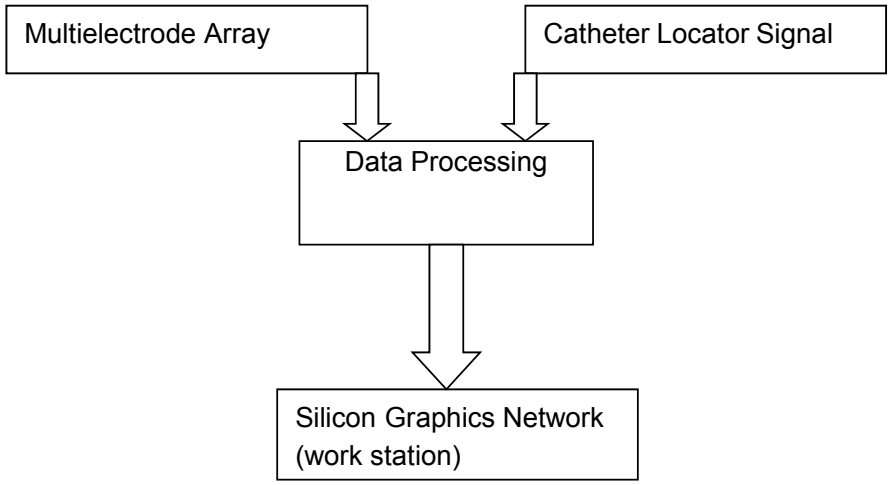

Figure 10 Flow diagram of the steps of data acquisition from the Ensite system

The main advantage of this system is that it requires only one beat to reconstruct a complete activation map, which potentially allows mapping of haemodynamically unstable arrhythmias. However, the distance between the endocardial wall and the balloon centre and the spatial complexity of the activation patterns has an adverse influence on the accuracy of the reconstructed electrograms. This is likely to affect the reliability of the data obtained when mapping markedly dilated or distorted cardiac chambers or complex reentrant circuits.

Validation of the Ensite NCM for activation mapping:

The Ensite NCM system, which allows simultaneous reconstruction of over 3000 virtual electrograms, that can be distributed globally in the cardiac chamber, was thought to be the turning point in overcoming the previously identified obstacles to contact mapping and MAP.

Landmark studies have validated the use of NCM over contact UEs by comparing the morphology and timing of reconstructed electrograms with contact electrograms from the same endocardial location (as indicated by the catheter location system).

Gornick et al validated the Ensite NCM array system in experimental in vitro settings using a tank filled with 0.45% saline in a hollow ellipsoid chamber with surrounding foam and in vivo in canine LV. Measurements were taken at distances of 10-58 mm from the MEA centre horizontally. In this idealised environment, reconstructed UEs using the Ensite's MEA were comparable to contact recordings from transmural plunge needles in respect to morphology and derivative timing with excellent correlation at distances < 50 mm but the accuracy dropped at > 50 mm (Gornick et al. 1999). Subsequently the Ensite NCM virtual UE was also assessed against contact electrograms for use in the right atrium for activation mapping of atrial arrhythmias including repeatedly induced atrial flutter and fibrillation in 12 mongrel dogs. A cross correlation was found between the noncontact and contact system data during SR, atrial flutter and AF, (correlation coefficient of 0.80, 0.85 and 0.81 respectively). This was distance related as evident by the reduction in correlation when the measured sites were farther away from the centre of the MEA. Thus a reduction in correlation was demonstrated between points that were </= 40 mm from the MEA centre (0.82) to those that were placed further (> 40 mm from MEA centre, 0.72) (Kadish et al. 1999). The first studies of the Ensite system in human hearts came from St Mary's hospital in London, UK where Schilling et al (1998) validated its use in the LV of thirteen human subjects who underwent ablation of well tolerated VT. They established a very accurate electrogram reconstruction between contact and noncontact measurements during SR but as reported by Gornick et al (1999) this decreases with increase in the radial distance between the electrode array and the endocardium which becomes significant for distances >34 mm (Schilling et al. 1998). Further they demonstrated feasibility in using the NCM technology for VT ablations and identification of the diastolic pathways in re-entry VT in cases with haemodynamic compromise (Schilling et al. 1999a;Schilling et al. 1999b;Strickberger et al. 2000). In ovine hearts Thiagalingam et al compared intramural, epicardial and endocardial contact electrograms from 50-60 plunge needles with the virtual UEs obtained from the Ensite NCM system and found equally good correlation in hearts without scarring during SR, endocardial and epicardial pacing provided the recordings were within 40 mm of the MEA centre and they suggested that the net virtual UE probably represented the summation of the transmural activation (Thiagalingam et al. 2004a).

The previous studies assessed activation patterns and utilised filter bandwidths ranging from 0.1-300 Hz, whereas repolarisation studies conducted by Yue et al (2004, 2005) validated the use of the Ensite system as a research tool to assess repolarisation in a single ventricular study in patients with structurally normal hearts. This made use of filter bandwidths of 0.1-25 Hz to assess accurately and to quantify repolarisation and T wave characteristics. They also demonstrated a close correlation between ARIs measured from virtual UE from the Ensite system and APD from MAP_{90} in patients with structurally normal hearts by utilising an alternative method to the Wyatt method to define the end of repolarisation depending on T wave morphology (Yue, Paisey, Robinson, Betts, Roberts, & Morgan 2004). Their findings agreed with those obtained from experimental contact studies from endo and epicardium (Haws & Lux 1990;Chen, Moser, Dembitsky, Auger, Daily, Calisi, Jamieson, & Feld 1991).

Defining scar substrate

Endocardial contact mapping has revealed that the normal human LV bipolar electrogram amplitude is > 3 mV with a duration of< 70 ms and an amplitude duration ratio of > 0.045 with no split, fractionation or double electrogram potentials (Cassidy et al. 1984). However, data on endocardial UE characteristics are scarce. In the isolated human heart studies of Durrer et al, activation of the epicardium of the LV rarely exceeds 80 ms (Durrer, van Dam, Freud, Janse, Meijler, & Arzbaecher 1970). Klein et al used tripolar and bipolar epicardial and endocardial measurements during SR from exposed human hearts at the time of bypass surgery and noted that patients who suffered ventricular arrhythmias had marked delay of activation in their ventricles i.e > 100 ms after QRS onset with a mean of 137 ms compared to 74 ms in those without arrhythmias. This was in addition to fractionated and double potential electrograms which they proposed to be the underlying substrate (Klein et al. 1982). Complex fractionated electrograms have been linked to scarring and arrhythmias both atrial and ventricular. Josephson et al proposed that fractionation and prolonged ATs in patients with prior myocardial infarction is the substrate for re-entry VT and occurs in over 80% of patients with significant prior myocardial infarction (Josephson et al. 1978a). Using contact electrograms, scar is characterised by relatively unexcitable tissue that displays low voltage electrograms of <0.5 mV and in some classifications <0.2 mv with border zone generally at 0.5- 1.8 mV (Marchlinski, Buxton, Waxman, & Josephson 1983). However, validation of NCM use for scar assessments was performed by Reek et al who studied chronically infarcted sheep hearts and showed a good correlation between scar localised using peak to peak voltage < 5.3mV via virtual UE from the Ensite system and MRI scan which were matched with the site and size of transmural infarction. They derived their cut off for normal endocardial voltage readings for virtual UE from a control population of normal sheep and found it to be > 5.3 mV (Reek et al. 2003).

Callans' group characterised VT circuits using NCM UEs in a porcine model. Chronically ischaemic pigs were studied using the dynamic substrate mapping function of the Ensite system which they defined at peak negative voltages <50% maximum unipolar deflection –using filters of 2-150 Hz- corresponding to surface QRS in a common location. Areas of low voltage were identified in SR and during LV pacing. The ventricle was mapped from 2-4 sites and the common intersected area displaying low voltage was described as scar material. Pacing exit sites were used to identify preferential conduction pathways within the substrate that may participate in VT circuits (Jacobson et al. 2006).

The findings of Jacobson et al (2006) were contrary to those of Thiagalingam et al who were not successful in defining scar using the dynamic scar mapping protocol (filters 0.5-300 Hz) and concluded in their ovine model that there was poor correlation between the virtual UE from the NCM system and histopathologic scar, thus suggesting that the Ensite system was not reliable for scar detection (Thiagalingam et al. 2004b). Newer versions of the Ensite system which allow the importation of various imaging modalities, sectioning the site of interest and imposing the created map onto the virtual endocardium will provide more detailed and highly accurate maps.

1.7.4 Unipolar and bipolar electrograms

UE are measured between two electrodes- one at the recording site of interest and the other at a distant reference point creating a potentially large circuit. Wave fronts that approach the recording electrode produce a positive deflection and those travelling away a negative deflection.

UE could permit the study of instantaneous cardiac repolarisation sequences and spatial distribution since they maximise spatial resolution and are not affected by the direction of the wave front propagation, but are not suitable for recording local progress of depolarisation (van Dam & Durrer 1964). UE morphology gives valuable information on the site of origin of focal tachycardias displaying a QS morphology at their site of origin but distant from the site, an RS morphology. UE require good contact with the endocardium (in contact mapping) and minimum high pass filtering. Unfortunately, they are susceptible to electrical noise and far field signals, because of their large circuit area but distant activity is inversely related to the square of the distance from the unipolar recordings.

Haws and Lux in 1990 validated the use of ARI measured from UE with transmembrane action potential under conditions that include atrial and ventricular pacing, sympathetic nerve stimulation, ischaemia and warming. The ARI was measured as the interval between the minimum derivative of the QRS (V_{min}) and the maximum derivative of the T wave (V_{max}) regardless of T wave polarity and morphology using the Wyatt method (Haws & Lux 1990) (Wyatt, Burgess, Evans, Lux, Abildskov, & Tsutsumi 1981). Their data were consistent to that from Millar et al from canine epicardium that showed that ARIs from UE were closely correlated to refractory periods over a range of CLs, drug infusion of norepinephrine and cardiac sympathetic stimulation (Millar,

Kralios, & Lux 1985). To establish human ventricular epicardial activation and repolarisation and the applicability of the Wyatt method of measuring repolarisation to humans, the epicardium of the LV and RV in patients with chronic pulmonary hypertension and RV hypertrophy undergoing operative pulmonary thromboendarterectomy were studied by Chen et al (1991). During SR they used a 56 electrode sock to measure UE filtered from 0.05- 300 Hz and 8 MAPs recorded with Ag-AgCl tip catheters at positions adjacent to button UE in patients before and after establishing cardiopulmonary bypass. In their validation of the use of ARI versus MAP_{90} to assess the end of repolarisation, using the Wyatt method of measuring the maximum dV/dt of positive T waves marked discrepancy was found between ARI and APD measurements of positive T waves although there was good correlation between them with negative and biphasic T waves. This was resolved when the end of repolarisation was measured at dV/dt minimum or on the downslope of the positive T waves which resulted in good correlation. This suggested that the Wyatt method markedly underestimated the end of repolarisation in positive T waves recordings so that an alternative measurement strategy for positive T waves was advocated (Chen, Moser, Dembitsky, Auger, Daily, Calisi, Jamieson, & Feld 1991).

Bipolar signals are the difference between two closely spaced electrodes of a multipolar catheter, which are in contact with the tissue, this results in near field signals and little far field sensing. However, less information on spatial resolution is provided and the direction of wave propagation affects the results. Most useful MAP studies have been conducted with bipolar or tripolar MAP catheters. The use of MAP catheters for the measurement of ARIs with the use of CARTO from both RV and LV in swine and human studies showed that repolarisation followed the sequence of activation and that ventricular gradients exist in the heart (Yuan, Kongstad, Hertervig, Holm, Grins, & Olsson 2001).

1.7.5 Body surface mapping

This concept was revealed in an introductory address at St Mary's Hospital Medical School with a torso map that showed isopotential lines of an electrical field of the heart which had a negative and positive pole (Waller 1888). Given its noninvasive nature it would be ideal as a screening test and to assess dispersion of depolarisation and repolarisation. The 12 lead ECG is inadequate for dispersion measurements and is insensitive to underlying myocardial changes for example QT dispersion (which refers to the different projections of the heart vector and is not a reliable indicator of intrinsic

regional patterns of repolarisation dispersion especially when measured from surface ECG alone at a standard paper speed of 25 mm/s), however some experimental studies in isolated small mammalian hearts have correlated between the QT, JT intervals and the MAP_{90} albeit weakly ($r= 0.58$ and 0.64 respectively, $p< 0.01$) (Zabel et al. 1995).

Because of advances in digital technology body surface mapping has evolved and staged a comeback. At first it relied on the use of tape recorders to store analog data from hundreds of body surface electrodes. Later, digitalisation reduced the number of electrodes. Its comparison with endocardial and epicardial mapping in in-vitro studies have varied from useful to useless (Flowers and Horan 1990;Nash et al. 2003). Its original dependence on the ECG to assess recovery time dispersion and QT dispersion, results in inadequate spatial resolution and marked observer measurement variability (Kautzner et al. 1994;Savelieva et al. 1998). Nash et al compared dispersion of depolarisation and repolarisation between ARI measurements from the epicardium and 256 vest ECG leads to the torso to assess QRST integrals; the upstroke of the QT and RT intervals which are dependent on their dV/dt slopes and the end of the T wave showed significant regional dispersion in ischaemic pigs with LAD ligation similar to the epicardial activation and recovery time responses to ischaemia (Nash, Bradley, & Paterson 2003). Body surface mapping has recently been used in the assessment of dispersion of repolarisation from surface ECGs in a retrospective study in patients with ischaemia and later assessed prospectively in non-ischaemic cardiomyopathies who underwent EP studies. The high resolution ECGs taken during the EP studies were analysed and electrical heterogeneity was assessed with surrogate measures for the APD and preceding DI in the form of T peak (surrogate for the end of repolarisation) of the last S_1 of the drive to QRS onset of the S_2 (TpQ) and the APD from the QRS onset to T peak (QTp) producing the restitution curves using the 40 ms linear least square segment method described by Taggart et al (2003) . The outcome was a potential prognostic index called the regional restitution instability index (R2I2) being the mean of the standard deviation of the recordings from all leads. Patients who developed ventricular arrhythmias or died had higher R2I2 measurements than those who did not (1.3 vs 1.03, $p=0.037$(Nicolson, McCann, Brown, Sandilands, Stafford, Schlindwein, Samani, & Ng 2012). This was replicated in nonischaemic cardiac conditions at risk of SCD undergoing risk stratification EP studies, in a retrospective study of 61 patients with a combination of DCM, Brugada syndrome and other miscellaneous disorders compared to controls and showed a higher R2I2 in the patients than in controls (0.97 vs 0.63, $p<0.01$) (Smith et al. 2012). Use of body-surface potential mapping has also been

reported in out of hospital VF arrest survivors to aid detection of acute coronary artery occlusion. Post-resuscitation, body surface potential mapping identified acute coronary occlusion with sensitivity 88% and specificity 100% (Daly et al. 2013).

1.7.6 An ideal cardiac mapping system

Such a system would be non- or minimally invasive, capable of rapid global real-time assessments of the chamber being studied with quick automated data processing, continuous data acquisition and simultaneous data display on large coloured or holographic screens; reliable, user friendly and non-fluoroscopic. Has large capacity for data storage and retrieval, able to differentiate tissue characteristics such as scar, ischaemic, hibernating and stunned myocardium; use topographic data to detect the arrhythmia site of origin. Be resistant to respiratory and electromagnetic interference from other electrical equipment in the vicinity or from devices such as pacemakers and defibrillators. Permits the use of inter-changeable catheters; able to calculate inter-, intra- chamber and transmural gradients and to measure currents at the cellular level including ion concentrations, local nonelectrophysiologic variables e.g. sodium, potassium, calcium concentrations, pH and O_2 levels.

Such a system, ideal in the clinical context, is very likely not to be ideal for experimental purposes. The universally ideal mapping system would establish a diagnosis, facilitate therapy, allow testing of experimental hypotheses and produce useful results. Although it seems to result from wishful thinking; inexpensive, self-calibrating, innovative technology is already striving for its achievement. There have been significant biomedical engineering advances with the conversion of 3D mapping systems to 4D systems. A high priority is the development of automated high-resolution real time analysis and minimising the use of x-rays. The additional functions in the present-day major clinical mapping systems have evolved to minimal or non-fluoroscopic mapping and respiratory gating to minimise movement artefact and geometry alteration during the different phases of respiration.

1.8 Summary

The heterogeneous appearance of ARI and CV restitution curves in pathologic human hearts may reflect the diversity of their underlying pathology. Their importance stems from its link to arrhythmogenesis as a determinant of cardiac electrical instability. The restitution hypothesis suggests that ERCs with steeper slopes predispose to wavebreaks and discordant alternans which are considered the basis for ventricular arrhythmias particularly VF. NCM technology has been successfully validated against MAP recordings and employed in the assessment and characterisation of global endocardial repolarisation in structurally normal hearts (Yue, Paisey, Robinson, Betts, Roberts, & Morgan 2004). Marked differences exist in electrical restitution dynamics between normal and pathological hearts and although there is a vast wealth of animal data and simulation models the global electrical restitution characteristics in pathological human hearts considered to be at highest risk, remains undefined. Over the last decade, efforts have been made to study various moderate to high-risk groups of patients (Koller, Maier, Gelzer, Bauer, Meesmann, & Gilmour, Jr. 2005;Lambiase, Ahmed, Ciaccio, Brugada, Lizotte, Chaubey, Ben-Simon, Chow, Lowe, & McKenna 2009). However, most of the information produced relies on data from a single or only a few points of the ventricle. Progressive evolution of mapping technologies has been a central driving force in the production of knowledge namely because of the haemodynamic instability in these dangerous arrhythmias and the need for techniques that allow global assessments of the cardiac chamber in a minimal number of beats. Successful validation of the Ensite MEA versus contact mapping catheters (MAP) to study repolarisation and the ability of the MEA to obtain global data from reconstructed UEs from a few beats, make it an ideal choice for investigation of these high-risk groups.

This thesis relied on the use of the Ensite NCM system, to determine the spatial and temporal characteristics of endocardial repolarisation in highly arrhythmogenic pathological human ventricles, with a focus on sufferers of compromising ventricular arrhythmias and survivors of SCD.

It examines the hypotheses that:

1- The maximum electrical restitution slope (S_{max}) in ventricular endocardium of high-risk structurally normal hearts is similar to that of high risk structural heart disease.

2- Conduction velocity restitution of the ventricular endocardium of highly arrhythmogenic structurally normal hearts is similar to that of high-risk structural heart disease conditions.
3- There is loss of activation repolarisation coupling in ventricular endocardium in these high risk ventricles in response to premature ventricular stimulation.

Chapter 2: General Methodology

2.1 Introduction to noncontact mapping

The concept of NCM was introduced by Taccardi et al in 1987 (Taccardi, Arisi, Macchi, Baruffi, & Spaggiari 1987) when they used olive shaped and cylindrical multi-electrode probes to assess the location and depth of paced extra-stimuli in normal dog hearts by measuring intracavitary potentials. In 1998 a cylindrical electrode probe with 128 electrodes that did not come in contact with the endocardium was used to locate the activation sequence of endocardial pacing sites and construct a three dimensional endocardial image in perfused canine LV (Khoury, Berrier, Badruddin, & Zoghbi 1998). This was superior to the then available basket multi-electrode catheters which were available and allowed contact mapping of the endocardium but were limited by their fixed electrode number and induced irritation (Josephson, Horowitz, Spielman, Waxman, & Greenspan 1982) (Jenkins, Walsh, Colan, Bergau, Saul, & Lock 1993) (Eldar, Fitzpatrick, Ohad, Smith, Hsu, Whayne, Vered, Rotstein, Kordis, Swanson, Chin, Scheinman, Lesh, & Greenspon 1996). Thus, establishment of NCM allowed the mapping of heamodynamically unstable ventricular arrhythmias and nonsustained arrhythmias from global assessments of isolated arrhythmia beats.

2.2 The Ensite system

The Ensite 3000 (St Jude Medical Inc.- USA) NCM technology is capable of three-dimensional, simultaneous acquisition of endocardial electrogram data in any chamber of the human heart without electrode contact to the endocardium, and is a valuable clinical tool for guiding ablation of complex and haemodynamically unstable arrhythmias. It consists of the MEA, a custom-built amplifier system and an electrophysiologic recording system that runs on specially designed software (Silicon Graphics, Mountain View, Ca, USA). The MEA has a woven braid of 64 polyimide insulated 0.003 inch stainless steel wires with electrodes made by laser etching off 0.025 inches of insulation in known locations over a 7.5 ml balloon which is mounted on a 9F catheter with a pigtail tip, ring electrode, two intra chamber ring electrodes and a fourth proximal system reference-ring electrode 16 cm on the shaft of the catheter.

The recording system has 100 analog inputs consisting of 64 from the MEA catheter, 16 unipolar or bipolar electrophysiologic catheter inputs, 12 from channels for surface

ECG leads and 8 user defined analog signal inputs that enable it to create 3360 virtual electrograms in unipolar or bipolar format. The recording system is connected to a breakout box. The raw far field electrographic data from the MEA are acquired and fed into a multichannel recorder and amplifier system sampled at 1.2 KHz and filtered through programmable bandwidth of 0.1-300 Hz. The signals are processed via an interface unit that enables the creation of electroanatomic, isopotential and isochronal maps and the display of unipolar and bipolar waveforms.

All patients were studied in the post-absorptive state with conscious sedation given for ablation. The MEA was introduced percutaneously over a 0.035 inch J tipped guidewire under fluoroscopy guidance and full haemodynamic monitoring in the cardiac catheterisation laboratory. The vascular access of introduction depends on the chamber to be studied, this was the femoral artery for retrograde trans-aortic LV studies or the common femoral vein for RV studies. The guidewire was withdrawn upon access to the chamber of interest and contrast saline mixture was injected to inflate the 7.5ml balloon upon which the MEA is woven (Figure 11). In patients with no documented arrhythmia, the LV was mapped and studied, with anticoagulation affected by incremental boluses of intravenous heparin to maintain an activated clotting time above 300 seconds. A 7-French, 4-mm tip conventional catheter (commonly a deflectable ablation catheter - Stinger, Bard, Lowell, MA, USA) was introduced into the same chamber as the MEA to enable the system to locate that catheter in space through a low current locator signal of 5.68 KHz between the standard catheter and the ring electrodes on the MEA, which allowed it to determine and locate the source through a custom algorithm. The locator signal was required to allow the construction of the 3D endocardial geometry by locating the conventional roving catheter whilst it was dragged around the chamber to build up a series of coordinates for the endocardium which could then be used to display and determine the position of any catheter on the created map.

NCM is central to the methodology of this research thesis, its use in human hearts has been validated against both contact EGM data in activation studies (Schilling, Peters, & Davies 1998) (Thiagalingam, Wallace, Boyd, Eipper, Campbell, Byth, Ross, & Kovoor 2004a) and against the use of MAP in repolarisation studies (Yue, Paisey, Robinson, Betts, Roberts, & Morgan 2004) .

2.3 Study design

This was a prospective observational study that assessed two high-risk patient groups for fatal ventricular arrhythmias and SCD. It had an experimental arm whereby one of

the groups (structurally normal heart patients) underwent baseline studies followed by repeat studies with flecainide challenge. The repolarisation characteristics of the control patients with structurally normal hearts with low arrhythmic risk were studied by Dr Yue from Professor Morgan's group and formed the basis of a previous DM thesis (Yue, Paisey, Robinson, Betts, Roberts, & Morgan 2004;Yue, Franz, Roberts, & Morgan 2005b;Yue 2006).

Validation of the use of the Ensite system for inter and intraobserver reproducibility was performed as a blinded prospective study.

2.3.1 Patient Selection

Patients at risk of SCD due to repolarisation abnormalities from either a previously aborted SCD or fatal ventricular arrhythmia or those with gross repolarisation abnormalities on resting 12 lead surface ECG with risk factors of SCD related to family history or depressed EF% were enrolled consecutively into the study. They had already fulfilled criteria for a ventricular stimulation study or VT ablation and the majority required coronary angiography.

The Ensite 3000 NCM system was used. This was a univentricular study requiring introduction of the MEA into the ventricle concerned related to the underlying diagnosis as described on page 93. The exception was one patient in whom we studied both ventricles sequentially because the point of the VT re-entry was in the common bundle of the conduction system across the interventricular septum resulting in acquisition of data sequentially from both RV and LV. This study was granted ethical approval by Southampton & Southwest Hampshire Research Ethics Committee. All patients provided written informed consent to participate. Enrolment was made between 2005-2007 at Wessex Cardiac Unit, Southampton General Hospital, UK. For patients who required VT ablation on clinical grounds the restitution data were obtained after the ablation was performed.

I assessed the repolarisation characteristics including ARIs, RTs and ERP in patients with diseased hearts and arrhythmogenic potential, which included cardiomyopathies: ischaemic, dilated and ARVC, corrected congenital heart disease, primary electrical disorders and macroscopically normal hearts classified as channelopathies or idiopathic VF. Transventricular repolarisation gradients were not assessed because of ethical and practical restraints.

Inclusion Criteria:

Patients 18 years of age or older with any of the following were eligible for enrolment.

- History of aborted SCD (from ventricular arrhythmias)
- Repolarisation syndromes with risk factors for ventricular arrhythmia.
- Hereditary cardiomyopathies with increased risk for SCD undergoing electrophysiology studies including ventricular (VT) stimulation study.
- Repolarisation abnormality on ECG, manifested as abnormal ST segment or T wave morphology with history of ventricular arrhythmia or significant family history of arrhythmias and /or SCD.
- Ventricular arrhythmias and structural heart disease.
- Structural heart disease or channelopathy awaiting ventricular tachycardia ablation.

The majority of patients in this study were clinically unstable and had suffered a failed SCD or repeated ventricular arrhythmias. This made it practically and ethically impossible to withhold their antiarrhythmic drug therapy for the well-established and practiced five half-lives of each drug. Many were receiving multiple antiarrhythmic drugs at the time of their study.

Exclusion Criteria

Patients with any of the following were excluded from participation.

- Myocardial infarction or acute coronary syndrome within the past 6 weeks
- Pregnancy.
- Concurrent participation in any other research trial.
- Inability to give informed consent.
- Contraindications to having an electrophysiology study eg: LV thrombus, high risk of thromboembolism, sepsis, and contraindication to anticoagulation bleeding dyscrasias

Patients with structural heart disease

These were adults over eighteen years of age with coronary artery disease, dilated non-ischaemic cardiomyopathy, adult congenital heart disease, hypertrophic cardiomyopathy and arrhythmogenic right ventricular cardiomyopathy.

In these patients a steady state was achieved after two minutes of constant pacing (S_1) from the right ventricular apex (RVA) at a cycle length of 400 ms via a bipolar woven catheter. An extra stimulus S_2 was introduced after a 10 beat train (S_1) at decrements of 20 ms until 300 ms and further down in 10 ms decrements at twice diastolic threshold

and 2 ms duration until the ERP was reached. In those patients with poor ventricular function and in those who were intolerant and became unstable or in whom excessive ventricular ectopy occurred steady pacing was resumed with a slower drive train (500 or 600 ms) with an initial decrementation by 40 ms intervals down to 400 ms and further reduction as explained. Virtual UEs were constructed using the Ensite system at 16 points chosen according to an adapted polar image (Figure 12) used normally for echocardiographic assessment of the LV. Offline data collection and analyses were carried out using software provided by the above system where the ARIs, ATs and DIs were measured by the alternative method described originally by Chen et al and modified for this purpose by Yue et al (Chen, Moser, Dembitsky, Auger, Daily, Calisi, Jamieson, & Feld 1991;Yue, Paisey, Robinson, Betts, Roberts, & Morgan 2004;Yue, Franz, Roberts, & Morgan 2005b).

Patients with structurally normal hearts

These included individuals with idiopathic VF, unobstructed epicardial coronary arteries, normal cardiac structure and function on transthoracic echocardiography and cardiac magnetic resonance (CMR) scans. These patients had either an aborted SCD syndrome, repeated ventricular arrhythmias or channelopathy including LQTs and a family history of sudden or aborted cardiac death.

In these patients, I assessed restitution characteristics, dispersion of activation and repolarisation in addition to ERPs both at baseline and following flecainide challenge; that consisted of 2 mg/kg flecainide with a maximum total dosage of 150 mg, infused intravenously over a period of 10 minutes with continuous ECG monitoring for the subsequent 45 minutes. Standard 12 lead ECGs were made at 2 minute intervals or sooner if any alteration was noted on the monitor during infusion of the flecainide, then at 5 minute intervals for the first 15 minutes after completion of the infusion and then at 10 minute intervals for another 30 minutes. No high ECG lead placements (2^{nd} and 3^{rd} rib spaces) were used. Pacing for restitution curves was carried out from the RV apex at basic drive train cycle lengths of 600 and 400 ms initially for 2 minutes to establish steady state and then for 10 beat drive train with the introduction of a ventricular extra-stimulation S2 with similar decrementation to the baseline protocol described until ventricular refractoriness. The induction of any arrhythmia terminated the restitution studies.

See Appendix A and B for the final version of the study protocol and patient information sheet.

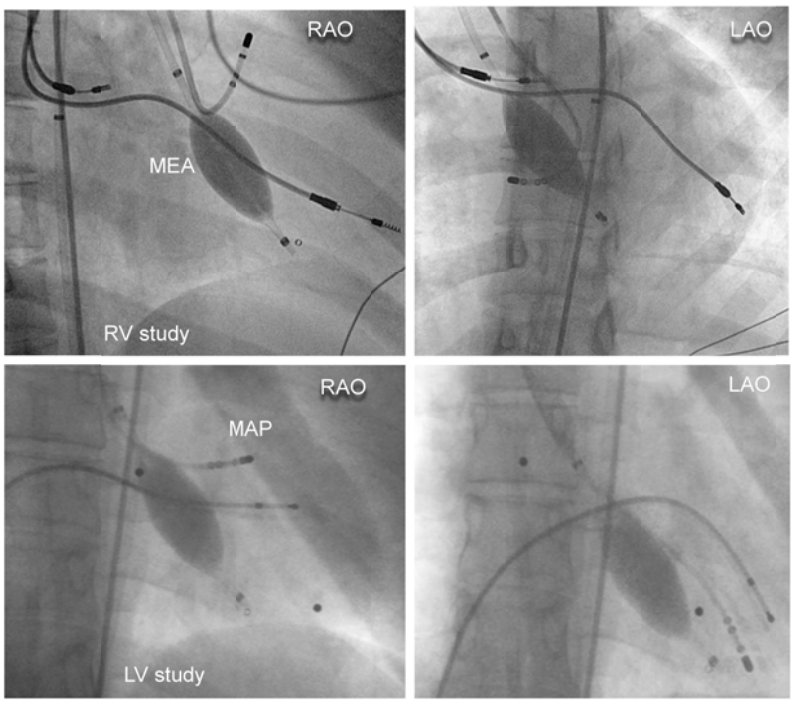

Figure 11 Fluoroscopic images of the Ensite multielectrode array, quadripolar ablation catheter and bipolar pacing catheter

Right anterior oblique (RAO) and left anterior oblique (LAO) views; note the balloon is radiopaque from half strength contrast and the presence of pacing leads in the upper panel. These were from two separate patients, from right ventricular study (upper panel) and left ventricular study (lower panel). MEA; multielectrode array, MAP; ablation catheter.

2.3.2 Reconstruction of electrograms

Far-field endocardial electrical activity measured by the MEA is based on the inverse solution to Laplace's equation utilising the boundary element method whereby a signal detected at a remote point (blood-endocardial boundary) appears at the source. Virtual UEs were selectively displayed on the workstation during offline analysis and review using manual placement of a cursor on the endocardial geometry at the required sites. Filter settings were adjusted to optimise visualisation of the electrograms. The spatial and adaptive filters were off. The filter bandwidth for the Ensite system (for dV/dt) was set at 0.1- 25 Hz and ECG recording bandwidth of 0.1-300 Hz. Measurements were carried out at sweep speeds of 200 mm/s. The UE T wave morphology was central to the repolarisation assessments and measurements of the ARI. The T waves were classed as positive, biphasic and negative. A custom designed template was saved and

utilised to display simultaneously the surface ECG and 2 pairs of UE and their first derivative from 2 sites at a given time.

2.4 Restitution curves

Electrical restitution curves were constructed by plotting the ARIs against their preceding DIs following decremental pacing from the RV apex at basic drive CLs of 400, 500 and 600 ms down to refractoriness at 16 predefined global sites in the ventricle studied. Conduction velocity restitution curves were constructed by plotting the CV at the same sites against the corresponding DI.

2.4.1 Pacing protocols and premature stimulation

Standard non-dynamic restitution protocols were used as described by Koller et al (Koller, Riccio, & Gilmour, Jr. 1998). Pacing was carried out at basic drive CLs of 400 ms at outset (S1) from RV apex at twice-diastolic threshold and stimulus duration of 2ms using a non-steerable bipolar catheter (Bard EP Inc.) for 2 minutes to achieve steady state. Patients who experienced excessive VEs or those who became haemodynamically unstable with drive train pacing at 400 ms were paced at slower rates with drive CLs of 500 or 600 ms. An extrastimulus (S2) was introduced after a train of 10 stimuli (S1) during the DI with a one-second pause between the consecutive drive trains. The S1-S2 coupling interval was progressively shortened in steps of 40 ms from basic CLs of 600 and 500 ms until 400 ms was reached then from 400 ms it was decremented in steps of 20 ms to 300 ms and in steps of 10 ms onwards down until ventricular refractoriness. Refractoriness was defined as the longest S1-S2 coupling interval that failed to evoke a ventricular response.

2.4.2 Construction of restitution curves

ARIs measured at sixteen pre-specified ventricular sites according to an adapted polar image and plotted against their preceding DIs from the basic drive CL until ventricular refractoriness produced the ERC. CV restitution curves at the same sites were determined by plotting CV from the site of earliest activation in the ventricle against the preceding DIs. Where tolerated a second restitution curve was performed with a drive train of 400 ms. In case of haemodynamic instability with faster rate pacing the second drive train was carried out at 500 ms.

Offline analysis of the anatomical endocardial and isochronal maps was performed using precision software versions 4.2 until 6.0 (Verisimo) on the Silicon graphics workstation or computer with the specially designed system software. Activation time (AT), ARI and DI were measured at sweep speed of 200 mm/s using electronic drop down calipers that permitted measurement to the nearest 1ms. ARIs were measured by the alternative method described by Chen et al similar to that performed by Yue et al (Chen, Moser, Dembitsky, Auger, Daily, Calisi, Jamieson, & Feld 1991;Yue, Paisey, Robinson, Betts, Roberts, & Morgan 2004).

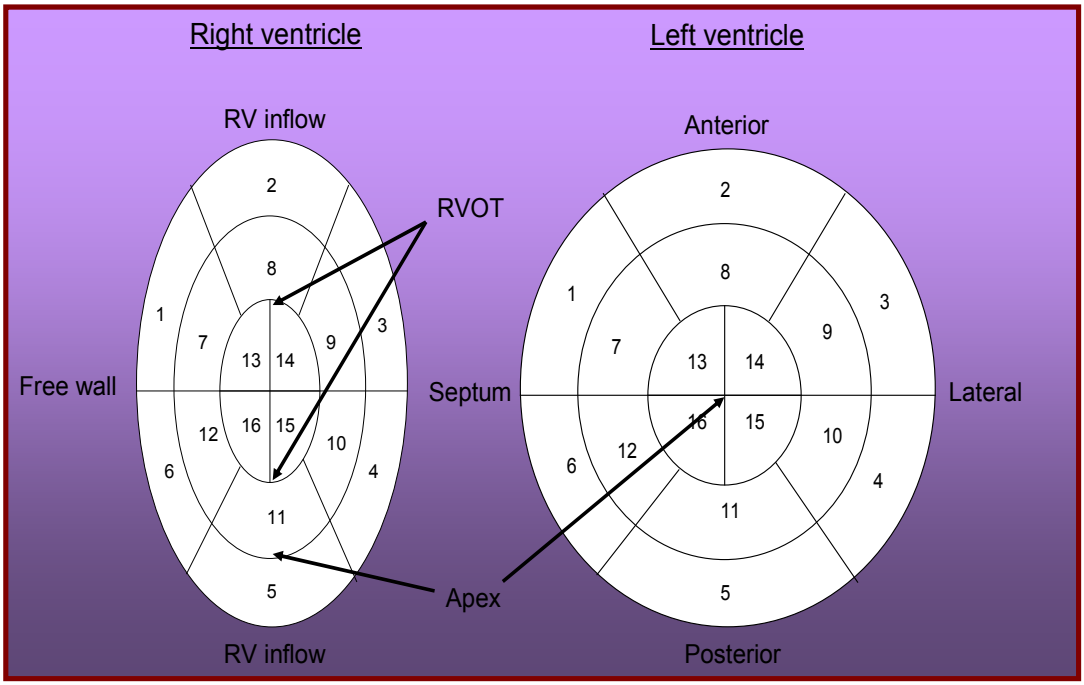

Figure 12 Schematic diagram of the polar representation of 16 segments of the right and left ventricles.

These 16 predetermined segments at which AT, ARI, DI, CV were measured and restitution curves were constructed. RVOT indicates the right ventricular outflow tract.

2.5 Activation Recovery Intervals

2.5.1 Local ARIs

Estimation of repolarisation timings from reconstructed UEs has previously been validated . Local AT was measured from onset of activation to the time of dV/dt_{min} of the local QRS complex. ARI was defined as the interval between AT and repolarisation time (RT) and measured in milliseconds. RT was measured at the dV/dt_{max} for the negative T wave, the dV/dt_{min} for the positive T wave, and at the mean time between dV/dt_{max} and dV/dt_{min} for the biphasic T wave (Figure 13). T waves with an interrupted descending or ascending phase were occasionally seen, and were thought to be related to the effect of the M cell region and contribution of repolarisation from the transmural myocardium (Yan & Antzelevitch 1998) resulting in double peak derivatives. Local RT at these sites was estimated as the mean time between two peak derivatives. UEs with flat T waves and ST segment elevation without discernible T wave up or down strokes were excluded from measurement. AT was defined as the interval from the onset of the QRS or pacing artefact from surface ECG to the onset of ARI. Repolarisation or recovery time was taken as the sum of the local AT and ARI intervals. DI was measured from the end of repolarisation from the preceding beat to the AT of the following beat. At very short S1-S2 coupling intervals when the RT of the last S1 beat was not clearly visible due to encroachment of the S2, the last S1 RT was estimated as the average of 3 preceding S1 RTs during steady state pacing.

A. Positive T wave: Measurement of AT (114 ms) & ARI (206 ms) during restitution pacing. Recordings from top to bottom: surface ECG, UE and dV/dt.

B. Negative T - AT (150 ms), ARI (138 ms), DI (33) ms measurements

C. Biphasic T wave. There is drive train pacing at 400 ms with introduction of an extra stimulus S2 at 240 ms.

Figure 13 Reconstructed unipolar electrograms with positive, negative and biphasic T waves during ventricular pacing

In the above images A,B and C, the top recordings in white are the surface ECG from lead II at 200 mm/s sweep speed. The middle recordings in yellow represent the local virtual unipolar electrograms and the lower recordings displayed in green are the first derivative (dV/dt). Calipers are used to measure the various timing intervals as explained.

2.5.2 Global ARIs

A custom designed template was used to display the paired UE and its first derivative (dV/dt) from two endocardial sites at a time. At each S1-S2 coupling interval, a total of 16 sites were analysed from each ventricle. Each site was randomly selected from each of 16 predefined segments in the left or right ventricular geometry. Sites were sampled evenly and selected from the entire ventricle prior to electrogram analysis. (Figure 14) Two reconstructed endocardial UEs from different segments of the geometry were simultaneously displayed on the workstation for analysis at a given time. Global dispersion of repolarisation was determined by the range of repolarisation times within a map (maximum RT- minimum RT).

Adjacent dispersion of repolarisation was defined as the difference between timings of two randomly selected adjacent sites 1 cm apart within the same segment of the ventricle. Variability measurements were made during constant basic cycle length pacing and at the shortest S1-S2 coupling interval of each restitution curve.

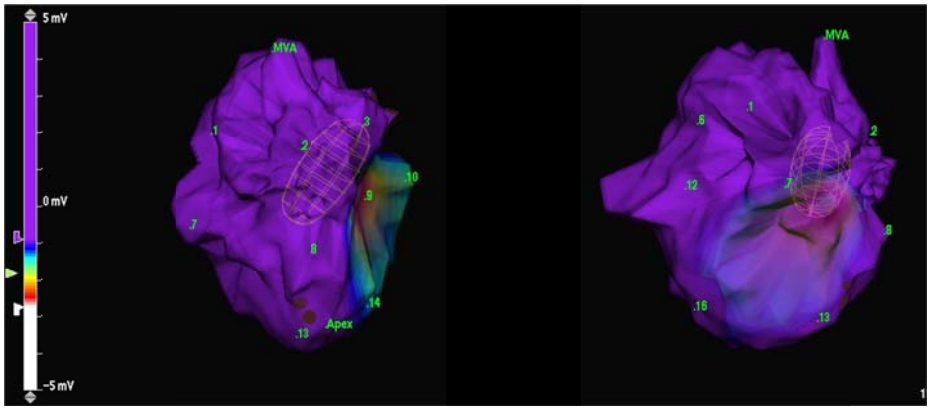

Figure 14 Three dimensional LV endocardial showing the 16 global sites for data acquisition

2.5.3 ARI restitution slopes

The maximum slope for each electrical restitution curve was fitted using the overlapping least-squares linear segments as described in (Taggart, Sutton, Chalabi, Boyett, Simon, Elliott, & Gill 2003). Restitution slopes were analysed from 40 ms DI segments in steps of 10 ms with the maximum slope used for comparison with other curves in the chamber. Global measurements for the ventricle were based on the mean

maximum slopes (S_{max}) obtained from multiple globally distributed sites within the studied ventricle. Heterogeneity was demonstrated by variation in the value of the restitution slopes and their shapes. The morphology of the restitution curve was also assessed by measuring the slopes of a curve at 5 segments of the total range of S_1-S_2 diastolic intervals from S_2 refractoriness to baseline pacing. Standardisation of ARIs to percentages of baseline values was performed, to allow global comparison, given the possible discrepancy of baseline ARI values in the different ventricular segments.

2.6 Conduction velocity

CV restitution curves were produced by plotting the CV against the preceding DI. CV was calculated by dividing the distance from the site of earliest activation to the recording site of interest by the activation time between the two sites (CV m/s=D mm/AT ms) (Wu, Lin, Weiss, Ting, & Chen 2002) . The point of earliest activation was determined by activation isochronal maps. Straight lines on the surface of the 3D map and perpendicular to the isochrones were drawn to measure the distance between the earliest activation point and the location being analysed. The distance between these sites was taken as an average of three consecutive measurements. The range between the CV at baseline and that at shortest coupling interval is known as the maximum CV and it is a measure of the steepness of the CV restitution slope. (Wu, Lin, Weiss, Ting, & Chen 2002). Magnitude of CV restitution was calculated as a percentage of the baseline value (Yue, Franz, Roberts, & Morgan 2005b). Both the maximum CV and the CV magnitude % were used as measures of the steepness of the CV restitution slope.

2.7 Dispersion studies

Local and global dispersion during activation and repolarisation in the right and left ventricles was assessed during RV pacing, sinus rhythm (Figure 15), ventricular ectopy and induction of VT. Local (adjacent) dispersion was defined as the absolute difference in timing intervals between two sites 10 mm apart and within the same segment. Global ventricular dispersion of repolarisation was defined as the time taken for ventricular recovery and was calculated by the range of the RTs (RT maximum - RT minimum) within the ventricular endocardial map from 16 points taken globally within the ventricle. Sinus beat measurements were taken on the fifth consecutive sinus beat and 2 minutes after pacing cessation. Constant RV pacing was taken at baseline cycle lengths at steady state and at short coupling intervals just prior to refractoriness and analysis was performed for spontaneous ventricular ectopy. Patients in whom VT was induced

activation and repolarisation measurements were obtained. During VT induction, measurements of AT,ARI and DI were taken from the last beat within the coupling interval that initiated the clinical VT and the first VT beat. Subsequent beats within the VT were difficult to analyse because of the extreme difficulty in deciphering the T wave onset from the end of the QRS from the preceding beat. All measurements were performed offline in the review mode at sweep speeds of 200 mm/s on the workstation using the precision software. Dispersion of activation within the ventricle was similarly taken during the same beats and defined as the difference between the earliest and latest activation time during the specific beat.

Figure 15 Reconstructed unipolar electrograms displaying T wave morphology during sinus rhythm

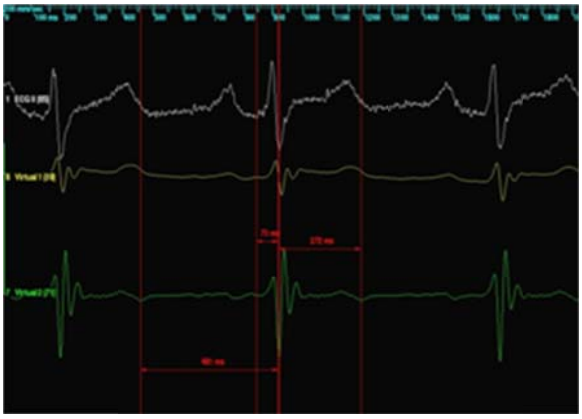

A Biphasic T wave ; measurements of AT, ARI, DI

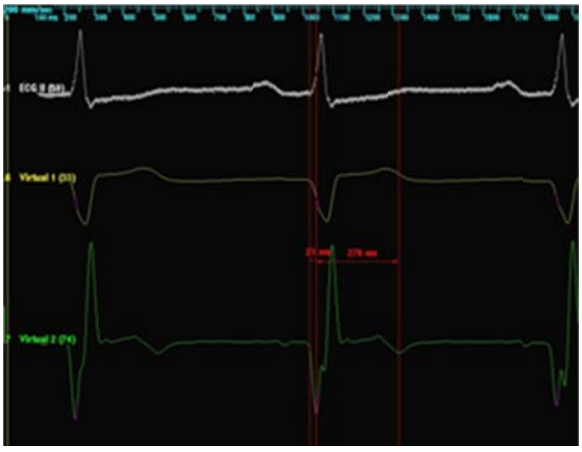

B. Positive T wave

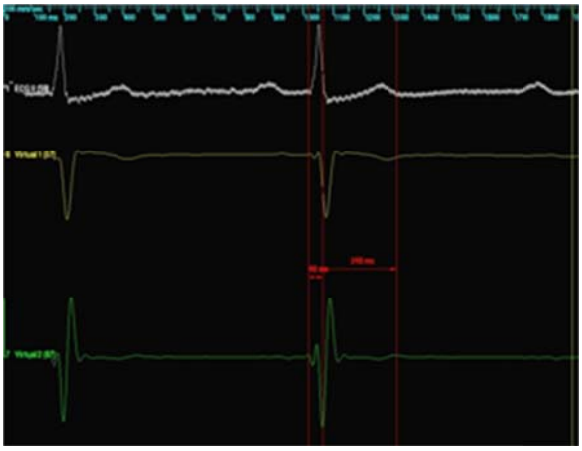

C. Negative T wave.

2.8 T wave maps

These were formulated by displaying isochronal maps of the endocardial geometry with detection sensitivity set at maximum and filter bandwidth set at 0.1- 300 Hz. Following the selection of the static map function on the Ensite system, calipers were placed at the onset and at the end of T on the surface ECG. ARI maps were constructed from virtual UEs corresponding to points on the endocardial geometry. These were determined by placing the calipers to measure the ARI as defined (end of activation to the end of repolarisation depending on the T wave morphology as described in section 2.5.1- page 102) using the filter bandwidth 0.1-25 Hz. Different T wave maps were created during RV pacing, sinus rhythm, ventricular ectopics or VT (Figure 16).

Figure 16 Isochronal repolarisation map using the Ensite system during ventricular pacing, VT and sinus rhythm.

A. Repolarisation map of the LV during RV pacing

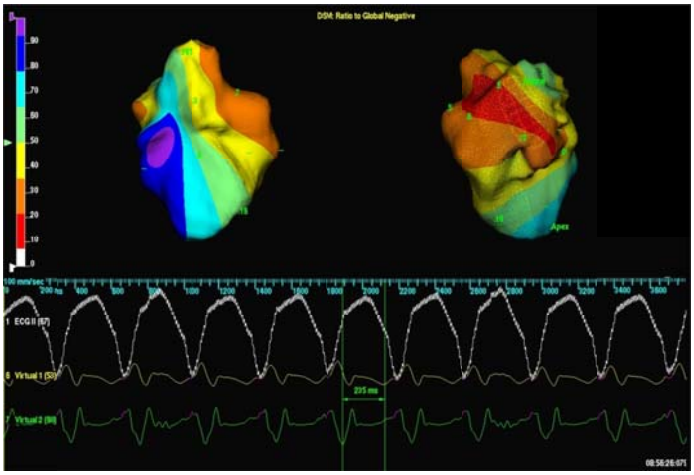

B. Isochronal Ensite repolarisation map during VT with ARI 235 ms

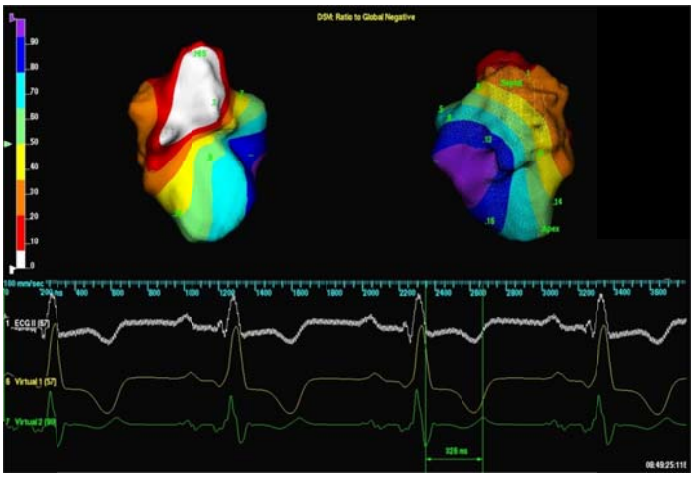

C. Isochronal Ensite repolarisation map during sinus rhythm.

2.8.1 Basic computed T wave maps

Data in the form of T wave morphology, activation and repolarisation maps have been formulated to allow basic visual comparisons using primary colours (red, green and blue) plotted onto the 16 segment polar image of the LV and RV schematic diagrams.

Heat Map Generator version 1.0 is a purpose designed Windows application software that was specifically written for my project to allow varying data sets obtained from 16 left or right ventricle sites to be displayed in colour on the polar image template. This custom designed software programme allowed data obtained from the virtual UEs to be assigned primary colours; red, blue and green. The data were defined either as text to display T wave morphology where red was allocated to positive T waves, green to biphasic T waves and blue to negative T waves or as numerical values. The data sets of T wave morphologies for each endocardial map were imported from an Excel spread sheet (Microsoft® XP) and were translated and displayed as a colour coded polar image of the corresponding ventricle. The final colour of the ventricular segment depended on the density and percentage of the T wave morphologies obtained from the virtual UEs in that given segment (Figure 17). The primary colours were arbitrarily allocated to represent the different T wave morphologies. The constructed LV and RV maps were saved as bitmap images on Microsoft computers.

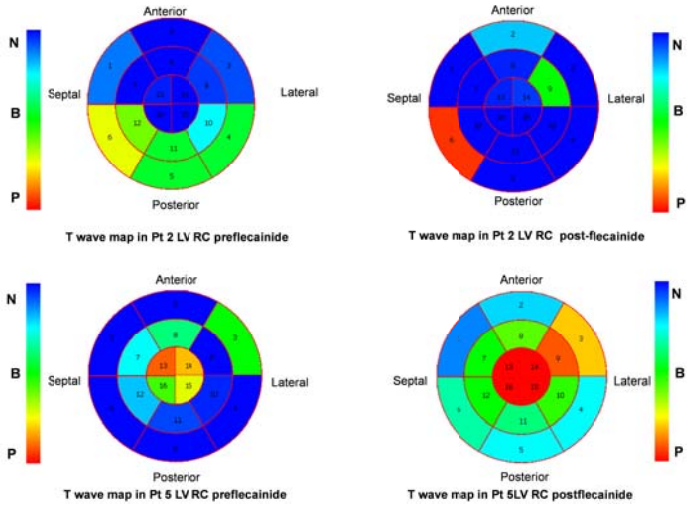

Figure 17 T wave mapping displayed on polar image template

Polar image of the LV in 2 patients with idiopathic VF demonstrating a T wave map during restitution study with a drive train cycle length of 400ms preflecainide and postflecainide. Red indicates positive T waves, blue is for negative T waves and green for biphasic T waves.

2.9 Data analysis

Data were analysed offline in review mode with the Silicon Graphics workstation using the standard Precision TM software (versions 4.2- 6). A custom designed template was used to display simultaneously the following waveforms on the screen from the same selected endocardial site: surface ECG and UE and its first derivative (dV/dt). Measurements were made manually from electrograms displayed on a Silicon Graphics colour monitor at 200mm/s resolution. The use of horizontal (timing) and vertical (amplitude) electronic calipers from the workstation allowed timings of activation and repolarisation to be determined to within 1 ms. The distance of each sampling site of the geometry from the centre of the MEA was documented using a pre-set workstation algorithm with the radial measure function. In addition, 2 paired recordings on average were randomly selected at widely spaced intervals from each site for comparison. Recording bandwidth was set at 0.1-300 Hz for UE recordings. No adaptive, notch or spatial filters were used. For measurement of the minimum derivative (dV/dt_{min}) of QRS and maximum derivative (dV/dt_{max}) of UE T wave, the filter bandwidth was selected at 0.1-25 Hz to reduce noise in the dV/dt channel. The custom designed template with 2

surface ECGs (II and aVF) and 2 pairs of reconstructed UEs and their first derivative (dV/dt) were displayed simultaneously on screen.

Linear measurements of distances were taken as an average of 3. Distance between sites was taken on the surface of the geometry perpendicular to the isochrones of the interval in question using the straight measure function. Chamber size was measured as the longest diameter in 2 orthogonal planes, not necessarily traversing the centre of the MEA using the straight line function. However, radial measurements and distances of allocated sites were made in reference to the centre of the MEA balloon.

2.10 Statistical analysis

Continuous data were presented as means ± SD unless otherwise mentioned. Dispersion was measured from the range and SD. Comparisons made between two groups pre and post flecainide were analysed using the paired Student's t test as were those between ARI and CV data from the same ventricle at identical sites. Left and right ventricular data were compared by unpaired t testing. One way ANOVA was utilised for multiple comparisons particularly for comparison of interval data between the different pathological subgroups of patients and Kruskal-Wallis' test and Dunn's multiple comparisons test were utilised and highlighted in the relevant chapters. In the presence of unequal variances a Mann Whitney test was performed for nonparametric data. Prospective follow up data were obtained from clinic visits, device interrogation logs and hospitalisation records and used for Kaplan Meier survival analysis. A p value of <0.05 was considered statistically significant.

2.11 Validation of measurement reproducibility

I will here establish the reproducibility of manual measurements using the Ensite system particularly for the restitution studies between and within observers with emphasis on the description of T wave morphology.

Inter and intra observer accuracy and reproducibility of manual measurements using the ESI system

The reliability of the scientific data obtained from NCM depends on the accuracy and reproducibility of the manual measurements between the same and different individuals, which has never been assessed. I aimed to assess the degree of inter and intra

observer variability during manual measurements for restitution dynamics using NCM technology.

Activation times, activation recovery intervals, diastolic intervals and T wave morphology determined from reconstructed UE and their first derivative (dV/dt) taken during RV apical pacing for restitution studies using the offline analysis function of the Ensite 3000 NCM system from 8 sites distributed globally around the LV (Figure 18) in 2 different patients; one with structural heart disease and the other with a normal heart, after reaching steady state and at shortest coupling interval. Measurements were carried out by four blinded observers (3 fellows in electrophysiology and 1 electrophysiology technician) with varying experience in using the Ensite 3000 system ranging from no experience to competent user, from the same points on 2 different occasions 1 week apart. The ventricular sites from which the measurements were taken were saved on the endocardial geometry in four different views in two orthogonal planes at a time using the notebook function. The radial distances of the sites from the MEA centre were also measured to ensure accurate positioning of the sites on the second measurement sitting a week later. Observers who were unfamiliar with making the measurements and the general function of the Ensite system were given at least two hour sessions of appropriate training. Restitution curves were constructed by all of the observers by plotting the measured ARIs against the measured DIs from the preceding beat.

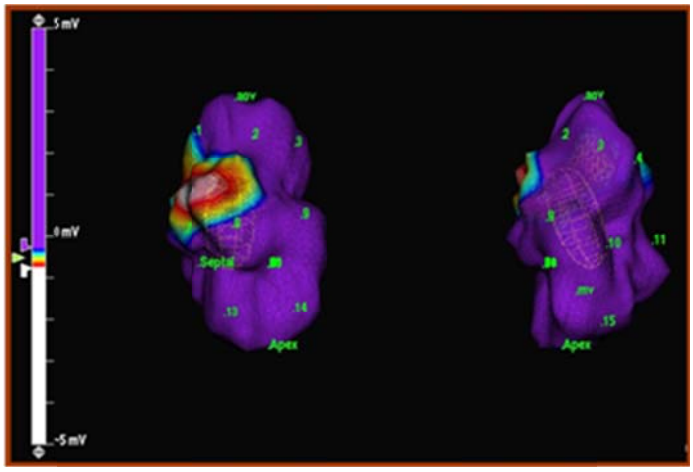

Figure 18 Three dimensional reconstruction of LV endocardium, isopotential map.

Measurements taken at odd points:1,3,5,7,9,11,13 & 15 for variability validation.

Results

A total of 424 measurements (AT, ARI, DI) and 46 T wave morphologies were repeatedly analysed at 8 left ventricular sites. Each observer provided 106 measurements and described the morphology of the 46 T waves. The total interobserver variability for AT,ARI and DI was 3.1 ± 3.5 ms (SD, 95 % CI 2.72 to 3.28) (Table 3). AT and ARI variability were much lower (2.0 ± 1.2 ms and 3.3 ± 5.7 ms respectively) compared to DI. DI measurements showed the highest interobserver variability of 6.7 ± 3.3 ms (95 % CI 4.78-8.58). The variability of the maximum slope of ARI restitution (S_{max}) was 0.1 ± 0.06. This may be accounted for by the greater variability of DI. The overall agreement in T wave morphology analysis was 89.7%. The overall intraobserver variability for AT,ARI and DI was 1.2±1.9 ms (AT 0.96 ± 0.89 ms, ARI 1.33 ± 2.51 ms and DI 1.81 ± 1.66 ms) which was significantly less than interobserver data (p< 0.001). Intraobserver variability of S_{max} was 0.03± 0.05 and agreement of T wave morphology was 92.4%.

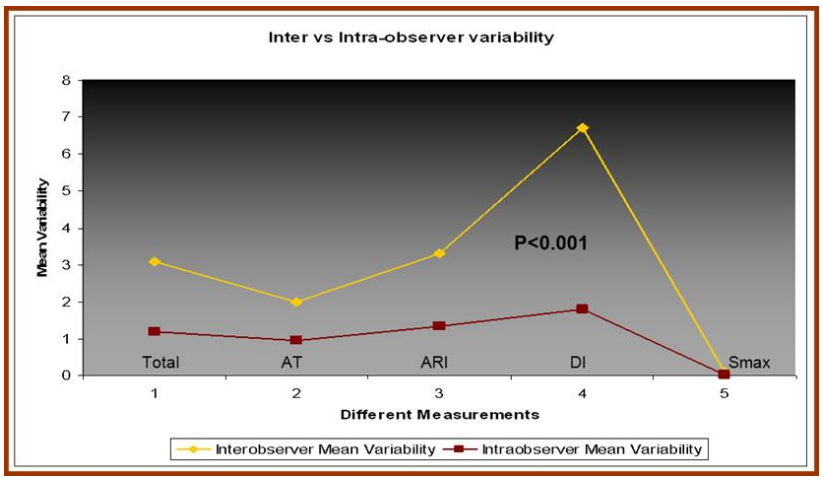

Figure 19 Variability graph between and within observers.

Table 3 Variability within and between observers.

Variability Measurements	Inter-observer	Intraobserver
Total (AT, ARI, DI)	3.1 ± 3.5 ms*	1.2 ± 1.9 ms*
Activation Time (AT)	2.0 ± 1.2 ms*	0.96 ± 0.89*
Activation Recovery Interval (ARI)	3.3 ± 5.7 ms‡	1.33 ± 2.51‡
Diastolic Interval (DI)	6.7 ± 3.0 ms †	1.81 ± 1.66†
Maximum Restitution Slope (Smax)	0.1 ± 0.06	0.03 ± 0.05
T wave concordance	89.7 %	92.4 %
* p<0.001, ‡ p< 0.05,† p<0.01		

Table demonstrating the variability between and within observers during the measurement of activation times, activation recovery intervals, diastolic intervals, T wave morphology and restitution data from 2 different patients a week apart.

Discussion and conclusion

These results show that measurements of cardiac electrical restitution in the intact human heart using the Ensite system are repeatable and reproducible as shown by an agreement scale between observers of 0.98 (Cronbach' s α) and correlations that were highly significant (intraclass correlation 0.96) (Figure 20- 22). This was feasible because the work station allows measurements of timing intervals to be determined to the nearest 1 ms using electronic calipers at different sweep speeds (200 mm/s used). Our short- and intermediate term variability measurements were in agreement with those obtained by *Kautzner et al (Kautzner, Yi, Camm, & Malik 1994)*.

The differences in the restitution curve slopes (Figure 23) were attributed to the differences in DI measurements which are closely linked to the determined configuration of the T wave and this was particularly evident with biphasic T waves.

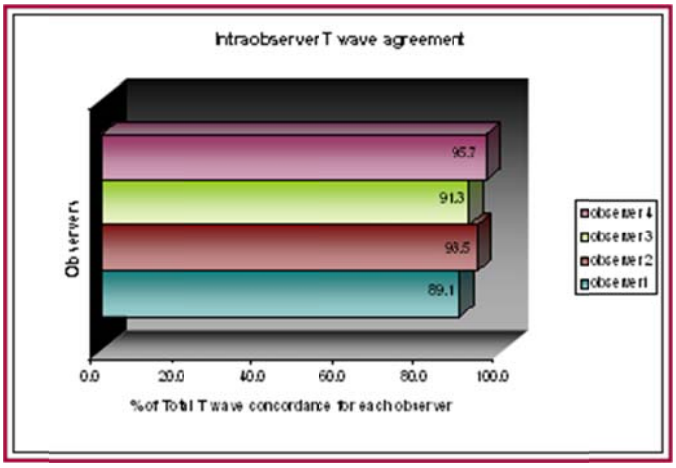

Figure 20 Stacked bar chart showing intraobserver variability in defining the T wave morphology

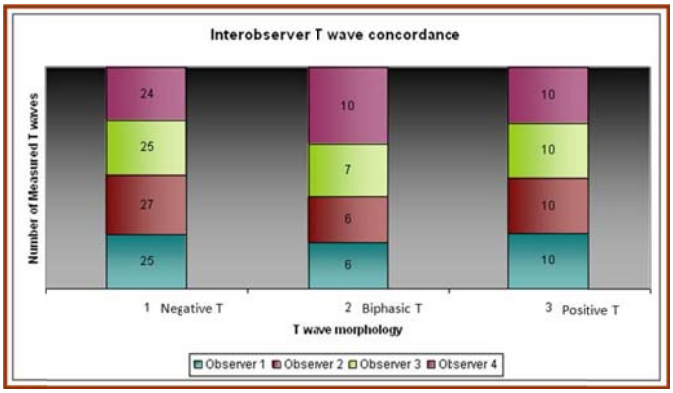

Figure 21 Bar chart showing T wave concordance within observers

Figure 22 Scatter plot showing correlation between observer measurements ARI, DI and AT during a restitution study

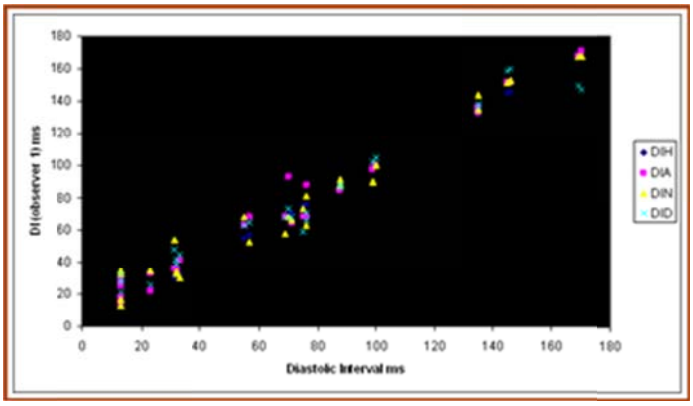

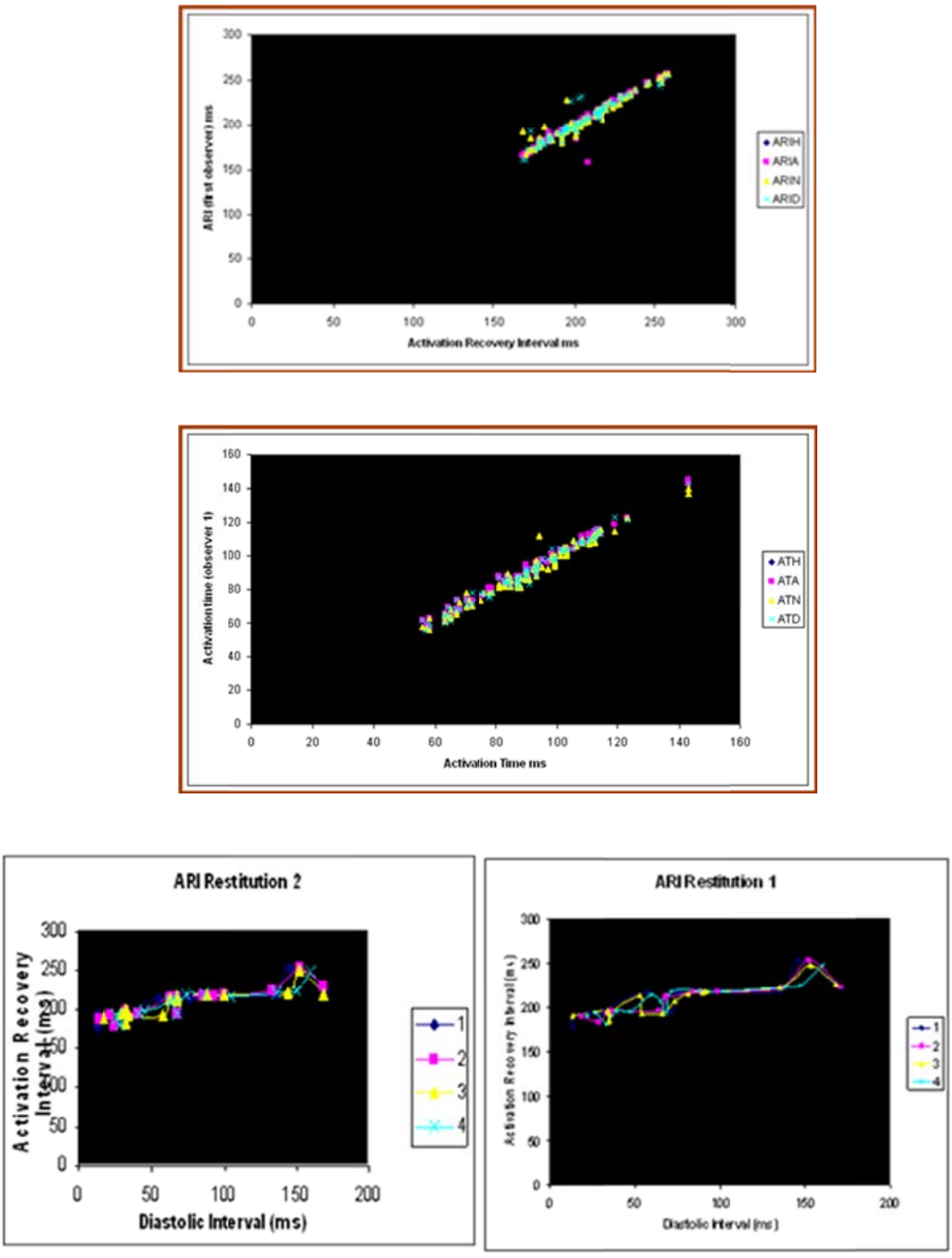

Figure 23 Electrical restitution curves from two patients produced independently by each observer.

Thus I concluded that manual measurements using Ensite's NCM technology appear to be reproducible and display low inter and intra observer variability.

2.12 Discussion and Conclusion

The debate relating to the correct method of measuring the end of repolarisation from the T wave of UEs particularly the positive T wave continues. In the present study I adopted the alternative method that was proposed by Chen et al and was validated against MAPs using NCM in swine and structurally normal hearts in man by Gepstein and Yue et al (Chen, Moser, Dembitsky, Auger, Daily, Calisi, Jamieson, & Feld 1991;Gepstein, Hayam, & Ben-Haim 1997b;Yue, Paisey, Robinson, Betts, Roberts, & Morgan 2004). This is because the conventional (Wyatt) method of measurement (Wyatt, Burgess, Evans, Lux, Abildskov, & Tsutsumi 1981) has been shown to underestimate the ARIs in complexes with positive T waves by up to 40 ms (Chen 1991, Yue 2004). Although various experimental and computer simulation studies including those based on propagation in a uniform cable confirmed the validity of the Wyatt method of measuring the ARI from the instant of steepest upstroke of the T wave regardless of the T wave morphology (Millar, Kralios, & Lux 1985;Steinhaus 1989;Haws & Lux 1990;Coronel, de Bakker, Wilms-Schopman, Opthof, Linnenbank, Belterman, & Janse 2006) and this was revisited in a 3D computerised simple model by Poste et al who argued that there was a weak correlation between the instant of the T wave down stroke from UEs measurements in positive T waves and total repolarisation and they advocated the use of the instant of maximum upstroke of the T wave regardless of its morphology and that the minimum dV/dt should be avoided. They found that the repolarisation time in positive T waves occurs 40 ms earlier than in negative T waves (Potse, Vinet, Opthof, & Coronel 2009). However, these most recent computerised findings were obtained in models of normal isotropic myocardium and did not incorporate anisotropy and tissue heterogeneity in the model. Additionally, its reliability to simulate fully UEs in cases of localised or regional fibrosis has not been demonstrated and it has not been validated in the clinical setting. The discrepancy in results from the literature may be related to the lack of direct comparison of measurements using the two techniques at the same sites and the difference in the definition of repolarisation using MAPs (Coronel, de Bakker, Wilms-Schopman, Opthof, Linnenbank, Belterman, & Janse 2006;Yue 2007).

This study validated use of the Ensite NCM system as a reliable tool for the fundamental definition of the T wave morphology of the virtual UE and its use in measuring the different timing intervals of AT,ARI and DI between and within observers by adequate training of the observers. The system was reliable and reproducible with

low and statistically insignificant inter and intraobserver variability. And although agreement between observers was high and the variability of measurements within and between observers was low, a discrepancy related to difference in the measured DI and the configuration of biphasic T waves did occur. Increased fractionation of the UE and the recording of complexes with double peaked activation and repolarisation waves may exacerbate these discrepancies but that is yet to be demonstrated. However from my results, formulation of an algorithm that allows instant automated global measurements via the Ensite system can be achieved.

Chapter 3 Global electrical restitution in human right and left ventricles in patients at high risk of arrhythmic cardiac death

3.1 General demographics

A total of 26 consecutive high arrhythmic risk patients (Figure 24) consented to participate in the restitution study. Twenty two patients (13 male, median age of 55.5 years, range of 18-85 years) with the females on average being 7 years younger (mean 47), underwent VT ablation or PES due to high risk of SCD, using the Ensite system. Seven patients, median age 37, had structurally normal hearts (SNH) (Table 5) of which four had idiopathic VF (IVF) and 1 had LQTs with a significant family history of SCD. Fifteen patients had structural heart disease (SHD) their details are displayed in Table 4. Both groups had predominately males with 3:2 ratio. All patients with SHD had a manifest abnormality on their resting 12 lead ECG whereas 2 of the 7 patients with SNH had completely normal looking ECGs.

Four patients were excluded from the study for reasons listed below. Thus, 15 patients with SHD were studied (mean age 60.5 years). In all patients but one, it was a univentricular study.

Fifteen patients had SHD (Table 4) and seven SNH (Table 5). 16 left ventricular and 7 right ventricular endocardial NCMs were constructed. One patient (15, 16) with IHD had sequential mapping of both ventricles.

The average QRS duration between the two groups was highly significant as was the overall function of their systemic ventricle; with median QRS duration of 95 ms and EF of 65 ± 4% in the normal hearts group compared to mean QRS of 148 ms and EF 33 ± 15% in the SHD group ($p<0.0001$). The LV or systemic ventricle was of normal size and morphology in the SNH group (LVD 49 mm) but was significantly dilated in the SHD group with mean LVD of 63 mm ($p=0.0005$).

Both groups were high-risk for fatal ventricular arrhythmias and SCD, thus the similarity in prevalence of ICDs implanted.

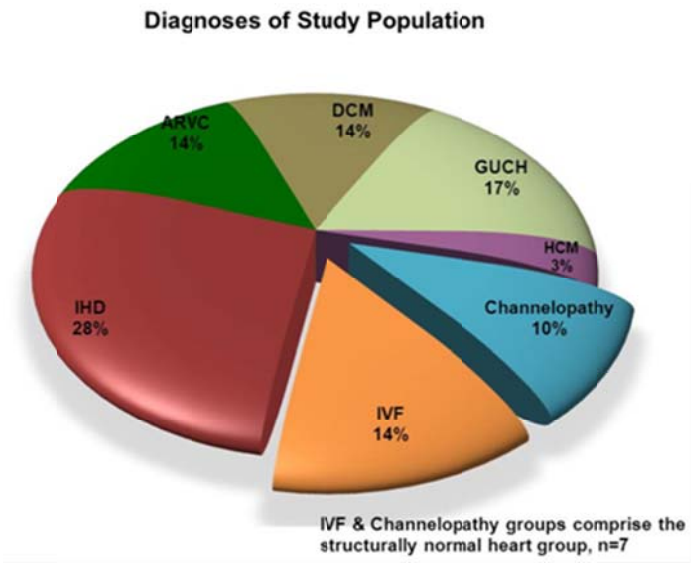

Figure 24 Pie chart demonstrating the diagnoses of the restitution study population

Table 4 Characteristics of patients in the structural heart disease group

Pt= patient, LV EF= left ventricular ejection fraction, M=male, F= female, sVT: sustained ventricular tachycardia, ARVC= arrhythmogenic right ventricular cardiomyopathy, IHD= ischaemic heart disease, DCM= non-ischaemic dilated cardiomyopathy, HCM= hypertrophic cardiomyopathy, cTOF= corrected tetralogy of Fallot, rTGA= surgically repaired transposition of great arteries (Mustard),dex= dextrocardia, BB= beta blockers, Amio= amiodarone, Lig= lignocaine, LVD: Left ventricular size in diastole on transthoracic echocardiography in millimetres, (s) systemic, AA= atrial arrhythmias, PR= severe pulmonary regurgitation, AVR= aortic valve replacement- in this patient a Bjork-Shiley mechanical valve, TVR= tricuspid valve prosthesis.*This patient (number 15 ,16) had sequential mapping of right and left ventricles- both were studied.

Pt No.	Sex	Age	Diagnosis	Ventricle studied	LV EF%	NYHA Class	Studied chamber function	LVD (mm)	Radial distance (mm)	Ensite chamber (mm)	QRS (ms)	Drugs	Cardiac arrest/ syncope	sVT	Comorbidities
1	M	57	ARVC	Right	55	I	Moderate	53	64	121x71	80	BB	No	No	ICD
2	M	76	IHD	Left	30	I	poor	74	38	94x80	120	BB,amio	Yes	Yes	MI,CABG,ICD
3	F	69	cTOF	Right	53	I	Mod 40%	52	32	82x75	160	BB,amio	No	Yes	HTN,RBBB
4	F	52	DCM	Left	<10	III	Ext poor	66	32	91x45	166	BB,amio	Yes	Yes	CRTD, AA
5	M	61	IHD	Left	30	III	Poor	59	38	102x71	150	BB,amio	No	Yes	3VD, ICD
6	M	42	f-DCM	Left	45	I	Mild	54	46	78x67	100	Nil	No	No	Nil
7	F	72	HCM	Left	40	II	Moderate	52	47	65x57	120	BB,amio	Yes	Yes	AA, ICD
8	F	26	rTGA	(s) Right	23	III	Poor	56	38	77x84	140	BB	No	Yes	CRT-D,AA,baffle leak
9	M	73	IHD	Left	30	IV	Poor	74	69	95x89	180	BB	Yes	Yes	MI,CRT-D,AA
10	F	76	DCM	Left	15	III	Ext poor	61	38	88x74	140	BB	Yes	Yes	ICD, AA
11	M	73	IHD	Left	35	I	Moderate	67	70	95x88	120	BB	No	Yes	ICD,HTN, MI, CABG
12	M	57	DCM	Left	20	IV	Poor	60	55	98x77	166	BB, amio, mexiltine	Yes	Yes	ICD
13	F	35	cTOF	Right	57	I	Good	47	47	89x63	125	Nil	No	No	PR, RBBB
14	M	32	rTGA dex	(s) Right	20	III	Poor	68	49	77x73	190	BB,digoxin	No	Yes	CRT-D, AVR, PR, TVR,CKD
15	M	63	IHD	Left	20	III	Poor	83	60	93x66	204	BB,amio, lig	Yes	Yes	MI,CABG,CRTD
16	M	63	IHD	Right	20	III	moderate	83	69	127x111	204	As above	As above	Yes	As above

Table 5 Patient characteristics of the structurally normal hearts group

Pt No.	Sex	Age	Dx	Cardiac Arrest/ Syncope	FHx	ECG	QRSms	QTc ms	EF%	LVD (mm)	Flecainide challenge/ EPS	Ventricle studied	Ensite chamber size (mm)	Radial (mm)	Drug Therapy	Device
1	M	31	OHVF	Yes	Yes	ST-T V1-V6	100	420	69	56	-	Left	92x54	43	Flecainide, amiloride	ICD
2	M	37	Channelopathy	No	Yes	ST-T V1-V6	98	390	66	56	-	Left	88x64	42	Nil	ICD
3	M	42	OHVF	Yes	No	Normal	90	400	55	42	-	Right	89x59	39	Disopyramide, carvedilol	ICD*
4	F	54	OHVF	Yes	No	IVCD	110	392	70	45	-	Left	70x54	39	Atenolol	ICD
5	F	18	OHVF	Yes	No	Normal	87	411	60	43	-	Left	81x67	30	Bisoprolol	ICD
6	M	45	cLQT	No	Yes	LQT	80	500	65	50	N/A	Left	88x65	46	Nil (intolerant)	Reveal
7	F	24	SSN/ Channelopathy	No	Yes	ST-T, brady, bigemny	100	480	60	48	-	Left	91x71	49	Nil	PPM

All patients were NYHA class I, had normal coronary arteries, negative EP study and structurally normal heart on trans-thoracic echocardiography and on CMR

3.2 Overview of combined results

The median radial distance from the centre of the MEA and surface of the ventricle perpendicular to the MEA equator in these patients was 41 mm thus allowing acceptable virtual UE reconstruction. The majority of patients in both groups underwent LV mapping (62.5% in SHD, 86% in normal hearts) with one patient in the SHD having additional sequential mapping of the RV.

Measurements of AT, ARI, DI, RT and CV were taken from a total of 546 ventricular sites distributed in 16 predefined segments of the ventricle. ARI (Figure 25) and CV restitution curves were simultaneously constructed from these sites and ARI restitution slopes were determined using the overlapping least-squares linear segments method described by Taggart et al (2003).

8712 beats were analysed using the virtual UEs and their first derivative (dV/dt) constructed from the Ensite 3000 NCM system. In total; 563 beats were excluded (6.5%) from analysis because of flat or ambiguous T waves particularly at short coupling intervals.

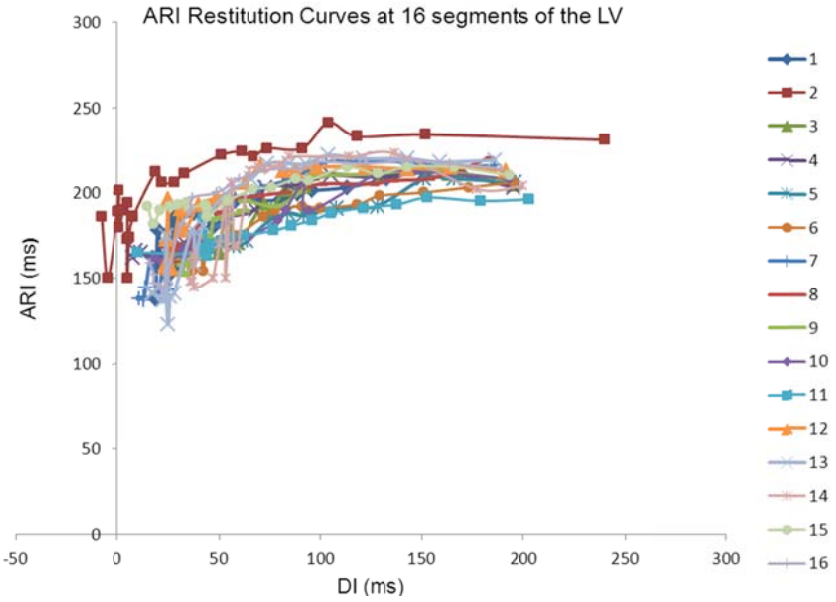

Figure 25 Global ARI restitution curves in a single ventricle

Figure showing 16 electrical restitution curves in patient 16 (see demographic table for SHD patients- Table 4)

3.2.1 Ventricular effective refractory period

Mean global ventricular effective refractory period at baseline was 211 ms, (range 170-290 ms) with a mean of 209 ms on average in the LV and similar overall VERP in the RV (216 ms).

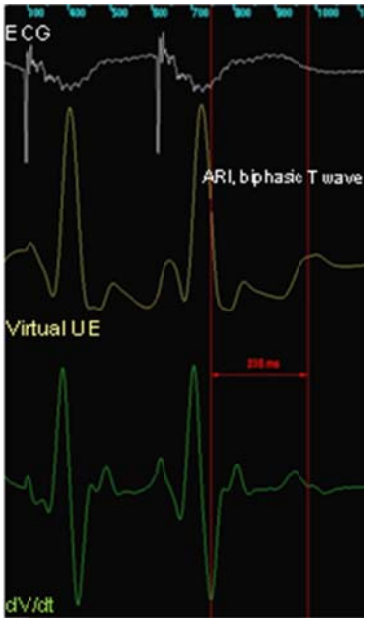

Figure 26 Local ARI of biphasic T wave during restitution study

3.2.2 ARI restitution slopes

546 paired electrical (ARI and CV) restitution curves were constructed, of which 90 were post flecainide provocation in the idiopathic VF group.

55% had 400 ms, 25%; 500 ms and 20%; 600 ms drive trains. Although we attempted to perform restitution curves with drive trains of 600 and 400 ms in all patients, this was not tolerated in some patients because of haemodynamic instability particularly in those with poor ventricular function or recurrent VEs. Thus, where necessary the basic drive train CL was adjusted from 400 - 600 ms guided by the response of the individual patient. Average number of restitution curves per patient was 1.6 and 20 % of the study group had more than 1 restitution curve mainly in the group with structurally normal hearts where multiple curves were constructed in 57% of patients at baseline.

3.2.3 Global ARI slopes

The mean global (S_{max}) for the study population was 0.97± 0.35 (range 0.5- 2.43) with similar findings in the LV and RV (Figure 27). The LV mean S_{max} values of 0.99 ± 0.2 (0.51- 1.32) and RV values of 0.93 ± 0.62 (0.5 -2.43) (p= 0.7 ns). The highest mean global S_{max} was in patient (3) from the SNH group who had repeated ablations for VE triggered VF with high arrhythmia burden.

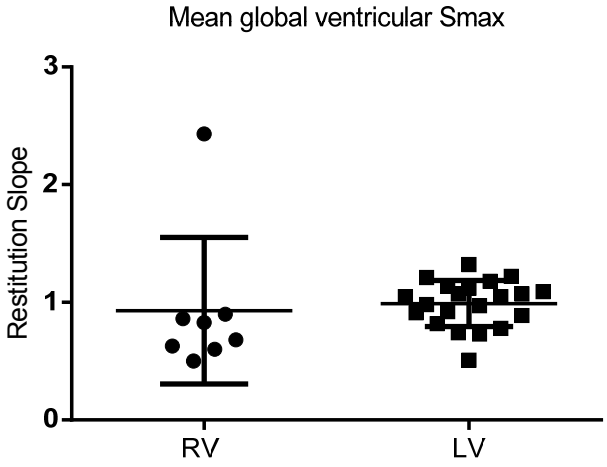

Figure 27 Scatter plot of the mean Smax value per ventricle studied

In the 23 ventricles studied, 214 sites had S_{max} values> 1 amounting to 39.2% of the sites studied with an average of 6 sites per ventricle (range 0-18). 116 of these sites were in the SHD group (25.4 % of total and 36% of all SHD sites) whilst 98 sites in SNH had S_{max} greater than 1, 56 at baseline (43% of all sites in this group) and 42 postflecainide sites, thus overall 44 % of S_{max} values in SNH were >1.

80% of all sites with maximum restitution slopes exceeding 1 were in the LV (173).

Average maximum S_{max} from the entire study group was 2.24 ± 1.09 with similar findings in both right (2.20 ± 1.7) and left ventricular studies (2.26± 0.79).

The shape of the ERC was triphasic (Figure 29) in 47% of the patients; with an initial short steep phase at short DIs followed by a rapid short descent and rapid ascent to the hump or shoulder of the curve(the super normal phase) which transcended into a long plateau phase that was very flat. The remainder of the curves were more complex and did not follow a consistent pattern. In approximately 11% of the curves there was lack of decrementation of the ARI as the DI shortened and in 6% the ARI inversely lengthened at short DIs.

Further assessment of the shape of the ERC was carried out by dividing the curve into 5 main segments (0-10%, 10-30%, 30-50%, 50-75%, 75-100%) (Figure 28) based on the percentage of DI of the extrastimulus (S2) to the baseline value. This was done in an attempt to standardise the DIs to baseline given their different geographical values. The ERC was steepest between 10-30% of baseline DIs in 50% of the curves both in the LV and the RV. The S_{max} was located at 10% of baseline DI or less in only 11% of the curves; however, 93 % of maximum slopes of the ERC occurred at DIs shorter than 50% of the baseline pacing value and no S_{max} values occurred at DIs above 75%. The steep initial portion of the ERC was found at a mean DI of 36 ± 40 ms.

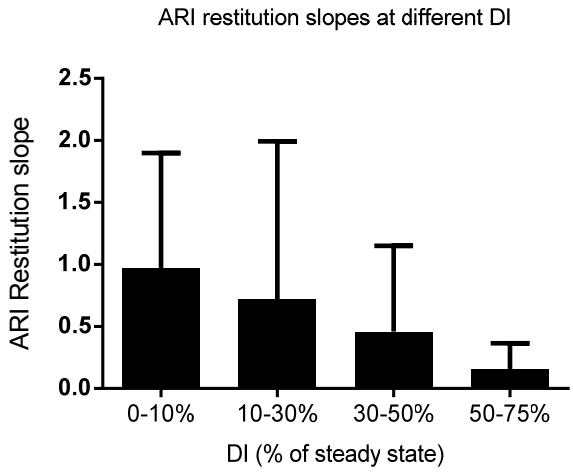

Figure 28 Distribution of the ARI restitution slopes at different diastolic intervals

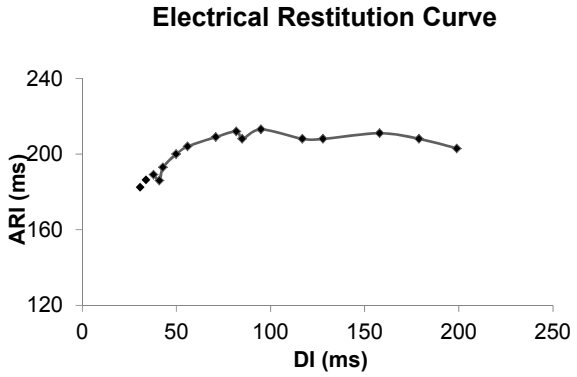

Figure 29 Example of triphasic electrical restitution curve with a slope less than 1.

Mean S_{max} of 0.35 in this LV study.

3.2.4 Local ARI slopes

The mean of the absolute maximum restitution slopes in the ventricle studied was 2.27 ± 1.08 (range 0.97- 6) with mean LV absolute values of 2.26 ± 0.79 and RV mean values of 2.2 ± 1.72.The sites of S_{max} corresponded identically to the ablation segment that terminated the VT in 6/13 patients (46%) (Table 6) and adjacent to it (within a distance of 20 mm) in 3/13 (23%) patients suggesting a possible relationship between the site of maximum restitution slope and areas targeted for ablation in 69% of studies (Figure 30). There was no apparent relationship between the segment in which RF was delivered and that containing the S_{max} in 4 of the ablated ventricles. The 10 remaining patients did not receive ablation therapy.

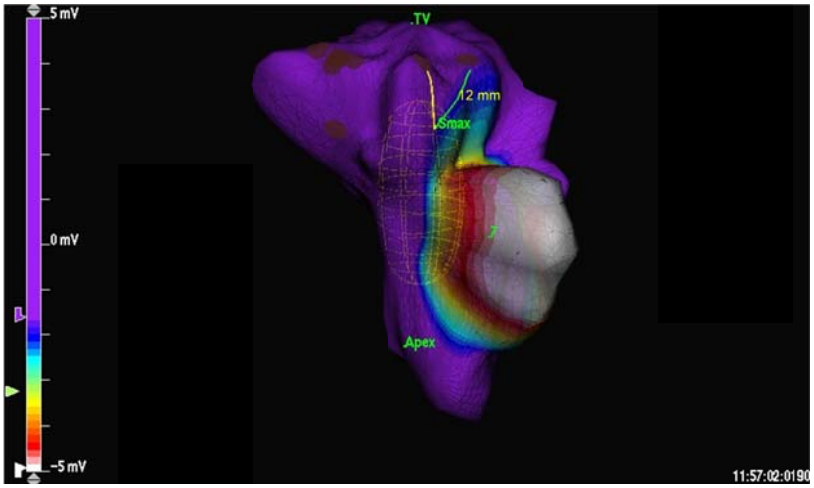

Figure 30 Ensite isopotential map of RV showing correspondence of S_{max} to segments of RF ablation near RV inflow

Local assessment of the ventricle at the individual sites revealed that global analysis diluted and obscured the effect of geographical dispersion, which is a manifestation of regional and local tissue heterogeneity. Thus, local assessment is paramount in the detection of and unmasking of inhomogeneous results, which may account for arrhythmia mechanisms from discrepancies in local activation, repolarisation and CV of impulse transmission and propagation. The mean overall S_{max} in the six segments in which the RF ablation was delivered was 1.5 ± 0.41 and when incorporating those segments where RF was delivered within a distance of 20 mm, the total sum amounted to nine of the thirteen patients. Their mean overall S_{max} was 2.12 ± 1.5.

Table 6 Restitution characteristic including maximum slopes matched to ablated segments

Pt No	Age	Gender	Dx	Ventricle Studied	EF % of studied Venticle	Mean global Smax	No. Smax>1	Dispersion of Smax (range)	Dispersion of Smax (SD)	Maximum Smax	Segment of Smax	No. of RF lesions	Segment of RF
1	M	57	ARVC	RV	55	0.5	0	0.59	0.15	0.97	10	3	10,4,5
2	M	76	IHD	LV	30	0.91	5	2.58	0.62	2.83	16	17	5 &4
3	F	69	cTOF	sRV	40	0.68	3	1.22	0.34	1.33	3	7	2,3,4
4	F	52	DCM	LV	<10	0.98	6	1.99	0.47	2.17	7	5	10
5	M	81	IHD	LV	32	0.89	5	1.24	0.44	1.45	8	4	8
6	F	72	HCM	LV	40	1.14	11	2.07	0.5	2.33	2	8	5 &13
7	M	73	IHD	LV	30	0.78	2	1.29	0.39	1.64	3	13	9
8	M	74	IHD	LV	35	1.32	8	4.89	1.17	2.2	11	3	11
9	M	57	DCM	LV	20	1.05	7	1.45	0.39	1.83	8	37	7
10	F	35	cTOF	sRV	50	0.6	2	0.67	0.21	1.06	5	1	14
11	M	63	IHD	RV	40	0.63	4	1.52	0.52	1.7	3	22	3
12	M	63	IHD	LV	20	0.74	1	0.98	0.31	1.37	6	11	1 & 6
13	M	42	IVF	RV	55	2.43	18	5.71	1.56	6.27	7	12	5,8,11

Alteration of the pacing CL concomitantly affected the global and local S_{max} value and the spatial dispersion of the maximum slopes by altering the segments in which the S_{max} is located. Suggesting a dynamic response of repolarisation to different basic drive train CL (400 and 500 ms). This phenomenon was seen in 7 patients from both SHD and SNH groups (Table 7).

All ventricles studied except one (patient number 1 in SHD group) had at least one local S_{max} value of >1 with an overall average of 6 per ventricle.

The dispersion of S_{max} in both LV and RV studies was similar (p=0.7, ns) (2.11 ± 0.54 in LV) and (1.91 ± 0.55 in RV) respectively.

Table 7 The effect of pacing cycle length alteration on ARI restitution slope characteristics and the site of maximum slope

Patient	Dx	Ventricle	EF %	Basic CL	No. Smax> 1	Mean Global Smax	Maximum Smax	Dispersion of Smax (Range)	Dispersion of Smax (SD)	Site of Smax	Site of RF
1	IHD	RV	40	400	4	0.63	1.7	1.52	0.52	3	3
	IHD	RV	40	500	4	0.83	2.46	2.3	0.54	10	3
2	IHD	LV	20	400	2	0.51	1.45	1.31	0.33	11	1 & 6
	IHD	LV	20	500	1	0.74	1.37	0.98	0.31	6	1 & 6
3	IHD	LV	34	400	8	1.32	2.2	4.89	1.17	11	11
	IHD	LV	34	500	9	1.21	2.9	1.76	0.51	11	11
4	IHD	LV	30	400	9	1.05	2.83	2.48	0.62	13	9
	IHD	LV	30	500	2	0.78	1.64	1.29	0.39	3	9
5	DCM	LV	15	400	11	1.07	1.54	1.22	0.39	6	…
	DCM	LV	15	500	7	1.07	2.17	1.93	0.56	7	…
6	IVF	LV	69	400	5	0.97	2.39	1.9	0.58	2	…
	IVF	LV	69	500	4	1.09	2.56	1.92	0.58	2	…
7	IVF	LV	60	400	5	0.82	2.15	1.88	0.54	2	…
	IVF	LV	60	500	3	0.97	1.9	1.62	0.51	7	…

3.2.5 Average ARI and regional variability in right and left ventricles

The mean ARI during steady state RV apical pacing in the entire study group was 243 ± 24 ms and at shortest S1-S2 coupling intervals 218 ± 28 ms. This was very similar in both right and left ventricles at steady state and during the shortest S1-S2 coupling intervals prior to ventricular ERP albeit with increased variability in the recordings of the RV. In the RV, mean ARI at basic CL RV pacing after steady state was 248 ± 41 ms and 221 ± 33 ms at shortest coupling interval, whilst in the LV mean ARI at baseline CL was 241± 16 ms and pre ventricular ERP was 217± 27ms.

3.2.6 Conduction velocity restitution

The mean global peak CV was 0.17 ± 0.1 m/s with a mean overall peak magnitude of 27 ± 8.6% of baseline value. On average this was more pronounced in RV studies (CV Mg % of 32 ± 9%, CV of 0.22 ± 0.12 m/s) than in LV studies (CV Mg% of 25 ± 8%, CV of 0.15 ± 0.09 m/s) but not significantly so (p=0.1) (Figure 31).

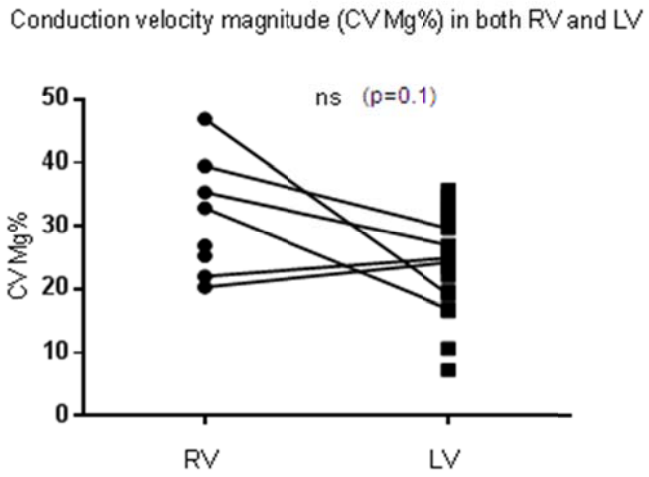

Figure 31 Comparison of conduction velocity magnitude between studies of the right and left ventricles

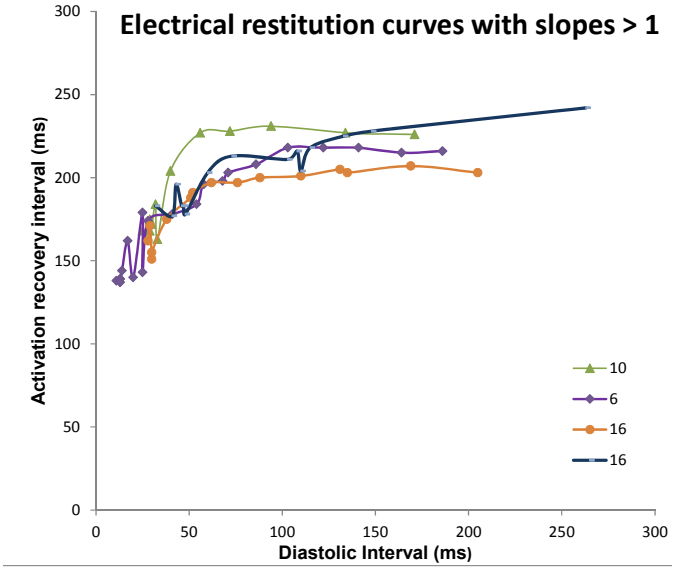

Figure 32 Steep electrical restitution slopes

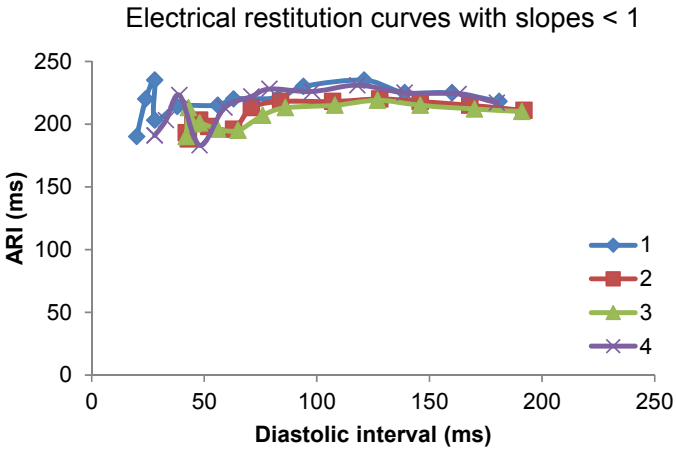

Figure 33 Shallow electrical restitution slopes

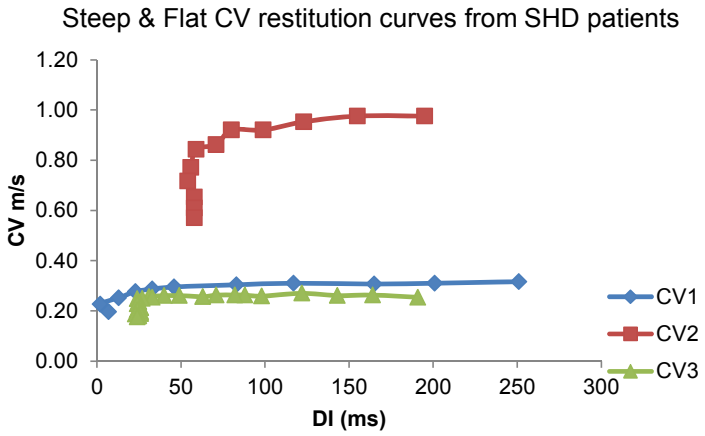

Figure 34 Conduction velocity restitution curves with different magnitudes

The ARI restitution slopes at identical endocardial locations operated across a wider range of DIs compared to CV thus resulting in a shallower restitution curve magnitude and flatter curve (Figure 33 and 34). In all but two patients (93.5%), the magnitude of the CV restitution curves were steeper than the ARI restitution curves (Table 8, Figure 35).

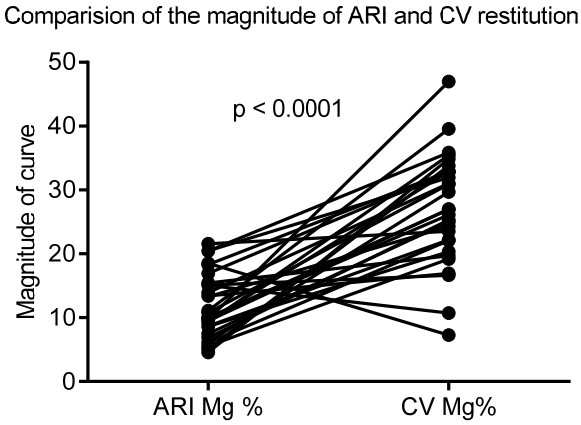

Figure 35 Comparison between magnitude of activation recovery interval and conduction velocity restitution slopes

Table 8 Results of global ARI restitution slopes, magnitude of ARI and CV restitution curves

Patient	Diagnosis	Ventricle studied	Maximum ARI Slope (mean ±SD)	Magnitude of ARI restitution (mean ± SD%)	Magnitude of CV restituiton (mean ± SD%)
1	IMF	RV	2.43 ± 1.56	11 ± 7.5	40 ± 7
2	TOF	sRV	0.68± 0.34	6 ± 7	22 ± 7
3	cTP,Dex	sRV	0.86± 0.63	9 ± 5	35 ± 6
4	TOF rep	sRV	0.6 ± 0.21	18 ± 6	33 ±5
5	dTGA	sRV	0.90 ± 0.44	9 ± 8	47 ±9
6	ARVC	RV	0.5 ± 0.15	8 ± 4	20 ±7
7	IHD	RV	0.63 ± 0.52	10 ± 8	27 ±10
	IHD	RV	0.83 ± 0.54	7 ± 6	25. ±7
	IHD	LV	0.51 ± 0.33	6 ± 6	30 ±3
	IHD	LV	0.74 ± 0.31	7 ± 4	25 ±7
8	IHD	LV	0.91 ± 0.62	9 ± 11	27 ±8.5
9	IHD	LV	0.89 ± 0.44	13 ± 15	17 ±14
10	IHD	LV	1.32 ± 1.17	5 ± 6	19 ±9
	IHD	LV	1.21 ± 0.51	13 ± 9	24 ± 5
11	IHD	LV	0.78 ± 0.39	20 ± 6	36 ± 17
	IHD	LV	1.05 ± 0.62	17 ± 12	33 ± 22
12	DCM	LV	0.98 ± 0.47	14 ± 10	31 ± 5
13	DCM	LV	1.18 ± 0.56	5 ± 7	34 ± 6
14	DCM	LV	1.07 ± 0.39	22 ± 19	24 ± 16
		LV	1.07 ± 0.56	20 ± 19	32 ± 16
15	DCM	LV	1.05 ± 0.39	15 ± 8	17 ± 13
16	HCM	LV	1.14 ± 0.5	18 ± 13	7 ± 10
17	IMF	LV	0.97 ± 0.58	15 ± 15	20 ± 30
		LV	1.09 ± 0.58	9 ± 9	33 ± 15
18	Channelopathy	LV	0.92 ± 0.73	15 ± 8	11 ± 19
19	IMF	LV	1.12 ± 0.63	10 ± 13	26 ± 17
20	IMF	LV	0.82 ± 0.54	4 ± 3	35 ±3
21	LQTS	LV	0.73 ± 0.57	8 ± 11	22 ± 6
22	Channelopathy	LV	1.22 ± 1.06	11 ± 14	31 ± 3
Mean			0.97± 0.35	12 ± 5*	27± 9*

ARI= activation recovery interval, CV= conduction velocity, * p<0.0001

3.3 Structural heart disease group

Nineteen patients with structural heart disease were enrolled into the study. These were a mixture of IHD (7), non-ischaemic DCM (5), ARVC (2), HCM (1) and adults with congenitally corrected cardiac abnormalities (4). Four patients were excluded for reasons, which included lack of suitable retrograde arterial access for MEA placement, occurrence of VT storm with multiple VT morphologies and occurrence of complete heart block during ablation.

All patients (Table 4 page 125) except number 6 & 13 were on beta blocker therapy. This was bisoprolol except in two patients (numbers 7, 11) who were on carvedilol and sotalol respectively, however all patients had multiple previous trials of various beta-blockers. ACE inhibitors or ARBs were used in all patients with impaired LV or systemic RV function and diuretics including spironolactone were used in all NYHA class III patients. Eight patients were on chronic amiodarone therapy.

3.3.1 Ischaemic heart disease

Seven patients with IHD were enrolled into the study to assess their restitution characteristics, however two were withdrawn early due to lack of appropriate data resulting from either inability to place the MEA in the LV because of difficult retrograde vascular approach in one patient or the occurrence of VT storm with a single extra stimulus (S2) early in the restitution protocol (S1,S2 600, 560 ms and 500, 480ms) with the occurrence of multiple VT morphologies.

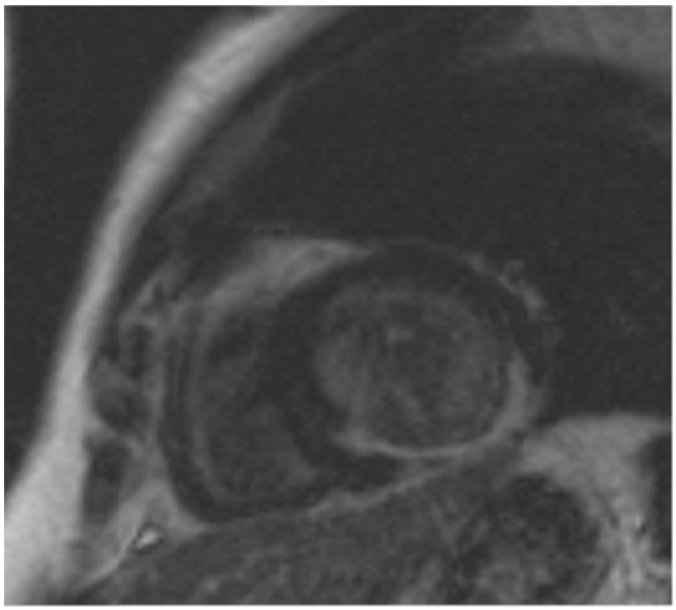

Figure 36 Short axis of cardiac MRI showing full thickness inferolateral scar

These were exclusively male patients with a median age of 76 years (63-81) and all had ischaemic cardiomyopathy with impaired EF (median 30%, range 20- 35 %) and dilated LV (median LVD 74 mm, range 59- 83 mm) from long standing previous myocardial infarction with scar and adverse ventricular remodelling. All patients had previous revascularization; 3 with coronary artery bypass grafting over a decade prior to presentation and 2 with previous multivessel angioplasty. All patients had defibrillators implanted- 3 biventricular ICDs and 2 ICDs- and were all admitted with ICD storms due to repeated drug refractory monomorphic VT and all received at least 5 device discharges. One patient had 119 treated arrhythmia episodes, mainly ATP. Average VT CL was 330 ms although slow VTs did occur (460 ms CL) and one patient had 2 prior VT ablations (patient number 2). Coronary angiography showed no targets for revascularization with well collateralised 3 vessel native coronary artery disease and patent grafts in the post bypass patients. There were no features of acute ischaemic trigger for the events or any reversible metabolic or infective conditions. All patients were on beta blocker therapy and although all received intravenous amiodarone in the acute phase, while four were on long term amiodarone in addition to beta blockers and one required a period of intravenous therapy with a class Ib antiarrhythmic (lignocaine) which was discontinued on the morning of the VT ablation. Restitution studies were conducted after VT ablation was performed.

NCM

The procedure was performed under conscious sedation in the post absorptive state. The MEA was introduced under fluoroscopy guidance via the retrograde trans-femoral approach from the common femoral artery and placed in the LV of all 5 patients. A separate arterial vascular access was utilised for haemodynamic pressure monitoring. Full heparinisation was required to maintain an ACT> 300 seconds throughout the study. One patient (15,16) had sequential mapping of both ventricles for a septal originating VT and thus the MEA was repositioned via the common right femoral vein into the RV after the LV study was concluded. A separate bipolar woven catheter was used for RV pacing and a standard 4 or 8 mm deflectable (nonirrigated) ablation catheter. Data were obtained for off line analysis which was performed at a later time on the computer work station.

Endocardial ERC

Steady state was achieved after continuous pacing for 2 minutes at the tested basic CL (400 ms). Four patients had restitution studies assessed at 2 different drive trains: 400, 500 ms. One patient became haemodynamically unstable with increased basic pacing rate thus his restitution studies were assessed only at 600 ms drive train. A train of 10 S1 paced beats followed by an extrastimulus S2 with repeated decrementation as previously described. Virtual UE and their first derivative (dV/dt) were displayed as a custom designed template from two points at a time on the Silicon graphics work station. Global AT, ARI and DIs were measured from at least 16 evenly distributed sites in the ventricle. Up to 5 randomly allocated sites were tested for adjacent dispersion (Chapter 4).

In one patient VT was induced with an S2 coupling interval of 260 ms allowing the analysis of the induced VT beats which are discussed later (Chapters 4 and 5).

Local and global ARIs

2273 beats were assessed for suitable determination of local AT, ARIs and DIs using the NCM system and alternative validated method for the assessment of the end of repolarisation by T wave morphology (Taggart, Sutton, Chalabi, Boyett, Simon, Elliott, & Gill 2003;Yue, Paisey, Robinson, Betts, Roberts, & Morgan 2004). Paired electrical and CV restitution curves were constructed. 200 beats were excluded from analysis because of indiscernible T waves and thus impossible interval measurements.

Mean ventricular ERP was 223 ± 21 ms. The mean global restitution slope was 0.89 ± 0.25 (range 0.51-1.32). A total of 49 slopes exceeded 1, occurring at 34% of the analysed sites with an average of 8 per studied ventricle.

Alteration of the pacing CL affected the spatial distribution of the sites with steep restitution slopes. These were not static or constant but appeared rather dynamic and at two different basic drive train CL except for 2 reproducible and constant common points that maintained the steep slope however, the majority showed newly developed steep slopes at distant points in other ventricular segments. This phenomenon was noticed in 4 of the 5 IHD ventricles studied including the RV studies. Of interest, the segment of the ventricle containing the peak local recorded S_{max} corresponded to the segment targeted for RF ablation. The 2 reproducible points with S_{max}> 1 at these sites were constant and included the site that portrayed the maximum S_{max} value. In these two ventricles, the segments containing the maximum slopes were not altered with change in the pacing dynamics by increasing or decreasing the basic drive pacing CL.

The recorded peak S_{max} in the IHD patients ranged from 1.37- 2.83. The patient with the absolute maximum slope had a mean maximum S_{max} of 1.05 and range of 0.34-2.83; however, his ventricle displayed steep slopes in 9 of the 16 globally analysed ventricular points. The S_{max} location did not alter with alteration in the drive train pacing CL and it corresponded to the segment in which RF delivery was given to terminate VT. The S_{max} at the sites of remote RF lesions to the arrhythmia circuits when assessed were consistently less than 1 and in this particular ventricle was 0.81.

The morphology of the ERCs in this group was in keeping with that explained in the cumulative pooled data description (section 3.2.3, pages 129-130). However, the ERCs appeared flat overall and the steepness of the ERC as assessed from the magnitude of the ARI curve (as a percentage) was 11 ± 5 % and was shallower in the RV studies i.e. mean of 8 ± 2% (LV 12 ± 5%).

Conduction Velocity

CV restitution operated over a narrower range of DIs compared to the ARI ERC, thus the CV slowed significantly and rather abruptly at short DIs prior to ERP resembling an inflection point. The CV remained very stable and almost constant despite significant shortening of the DIs until a threshold was reached when the endocardium could no longer propagate the impulse at a certain DI. As a consequence the resultant CV restitution curves were biphasic with a long plateau phase during long paced coupling intervals with sudden considerable slowing of the CV. The average magnitude of the CV restitution (%) in the IHD group was 26 ± 5% (range 17-36%) and an average maximum CV restitution was 0.18 ± 0.11 m/s ranging from 0.08-0.2 m/s with faster conduction velocities measured in the RV study (0.2 m/s, 26 ± 1.15%).

The effect of baseline-pacing drives on restitution curves

Electrical and conduction velocity restitution curves at the same 48 sites in 3 paired ventricular studies were constructed with drive trains of 400 and 500 ms until ventricular refractoriness. Increase in drive rate pacing did not alter the general shape and outline of the restitution curves however faster pacing shifted the hump or shoulder of the curve (supernormal portion) marginally downward and towards the right. There was a significant reduction in the ventricular ERP (p=0.02), ARI values at baseline (p=0.03) and pacing at short coupling intervals (p=0.03) (Table 9). Although both the ARI and CV restitution curves showed a downward and marginal rightward shift, this did not reach statistical significance (Figures 37 & 38). The altered baseline pacing drive had no significant effect on the steepness of the curves or their slopes both locally and globally (S_{max} p=0.05, CV Mg % p= 0.4, ARI Mg% p= 0.5). These findings concur with data from single RV sites (Morgan, Cunningham, & Rowland 1992b).

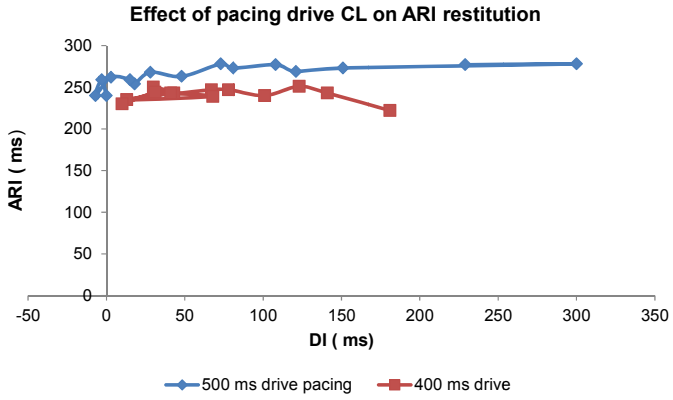

Figure 37 Effect of pacing cycle lengths on the ERC

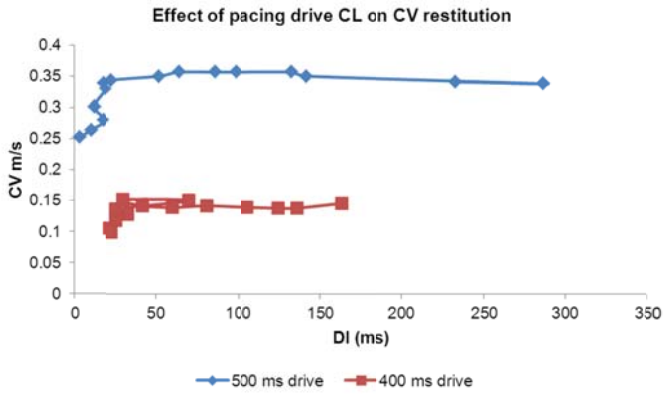

Figure 38 The effect of pacing cycle length on conduction velocity restitution

Table 9 Effect of drive train cycle length on electrical and conduction velocity restitution

Faster drive (400 ms)									
ERP*	Mean Smax	Max Smax	Site of max slope	RF site	No Smax> 1	ARI long†	ARI short‡	CV Mg %	ARI Mg %
210	0.63	1.7	3	3	4	233	227	27	10
210	1.32	2.2	11	11	8	233	198	19	5.5
190	1.05	2.83	13	9	9	236	238	33	17
203	1.00 (0.63-1.05)	2.24 (1.7-2.83)			21	234 (233- 260)	221 (198- 238)	27± 6	10.5 ± 5
Slower drive (500 ms)									
ERP*	Mean Smax	Max Smax	Site of max slope	RF site	No Smax > 1	ARI long†	ARI short‡	CV Mg %	ARI Mg%
230	0.83	2.46	10	3	4	264	244	25	7
230	1.21	2.29	11	11	9	250	227	24	13
220	0.78	1.64	3	9	2	255	258	36	20.5
227	0.94 (0.78- 0.89)	2.13 (1.45-2.46)			15	256.333 (235-264)	243 (227-258)	25.5 ± 8	13± 5

Table showing the characteristics between paired data from 50 sites studied in 3 ventricles. Paired t test utilised for data analysis. Statistical significance was indicated by $p<0.05$. *, †, ‡ were significant. (* $p=0.02$, † $p=0.03$, ‡$p=0.03$). Data are displayed as means ± SD with ranges in parentheses.

3.3.2 Nonischaemic dilated cardiomyopathy (DCM)

Four patients, (2 male), with a median age of 53 years, LV EF 17% (range of ≤10-45%) and LVD of 60 mm were studied. All patients but one had severe LV functional impairment and moderate dilatation, electrical dyssynchrony with QRS ≥ 140 ms and had suffered previous cardiac arrest or compromising ventricular arrhythmias. Three patients had ICDs, one incorporated into a cardiac resynchronization device. Functional class ranged from I- IV although three were severely limited with heart failure despite optimal drug therapy and antiarrhythmics. Their demographics are displayed in Table 4 (page 125). The fourth patient with asymptomatic mild LV dysfunction was being screened for a familial form of autosomal dominant DCM with strong family history of premature cardiac death (arrhythmic and pump failure).

All of these patients underwent LV mapping by the retrograde trans-aortic approach under full heparinisation and sedation in the post-absorptive state. Three of these studies were performed as urgent in-patient procedures in conjunction with ablation of

drug refractory VT with coronary angiography excluding atherosclerosis as the cause of LV impairment and VT storms. All reversible causes were excluded and any recognised metabolic derangements were rectified.

All four patients underwent restitution studies at 400 ms basic pacing CL. However, one had an additional study at 500 ms. VT was induced during one of the studies at CL of 260-280 ms. Restitution curves were constructed from 82 LV sites. Of the 1350 beats that were analysed, 79 (5%) were excluded because of lack of clarity of the UE from complex fractionated signals or T wave ambiguity.

The mean ventricular ERP was 220ms (range 175-240 ms). The average maximum restitution slope was 1.07 ranging from 0.98-1.18. All ventricles studied had regional restitution slopes in excess of 1. The number of S_{max}>1 was 41 (median seven per ventricle), corresponding to 50% of the assessed ventricular sites. The maximum restitution slope average was 2.02, range 1.83- 2.40. The absolute maximum segmental (local) S_{max} value overall of 2.40 and the maximum averaged S_{max} reading of 1.18 (±0.56) occurred in the LV of the patient with the inherited DCM, who also displayed an abundance of local low amplitude complex fractionated electrograms. Thus, 10 of 16 ventricular sites analysed in this patient exceeded 1 (S_{max} range of 0.35-2.4) with relative sparing of the posterior and lateral LV walls.

The average magnitude percentage of the ERC (ARI Mg %) was 15 (range 5 to 22). Three patients underwent VT ablation, in their ventricles the site of the maximum S_{max} did not correspond to the ablated segment, except in one where the segment with the steepest ARI slope was adjacent to the ablated segment. VT was induced during PES for the restitution curve in one study while pacing at CL of S_1,S_2: 400, 380 ms. The tachycardia CL was 300 ms and it originated from the inferoseptal wall. This was terminated during ablation but reinitiated with a different morphology. Offline analysis of the first VT beat revealed marked dispersion of local activation of 114 ms and dispersion of repolarisation of 149 ms between the apical and septal segments of the ventricle with regional (30%) heterogeneity of T wave morphology.

Only 47% of the ERCs in this DCM population were triphasic or biphasic in their appearance. The remainder had complex patterns.

Mean global ARI during steady state pacing was 242ms and during RV pacing following the introduction of an S_2 at short coupling intervals was 220 ms.

The magnitude of CV restitution was consistently steeper than ARI restitution in all patients; CV Mg % of 27 (range of 17-34%)- Table 8 page 138.

3.3.3 Grown up congenital heart disease (GUCH)

Four patients, median age 33 years, 3 females and 1 male (Table 4 and 10). All had moderate to severe defects that had been repaired. Two had TOF and the other two had dTGA corrected with a Mustard operation, of whom one had dextrocardia and metallic prosthetic valve replacements of the aortic and tricuspid valves. The latter two patients, required ventricular pacing. Median systemic ventricular function in the 4 patients was 36%, but the patients with TOF had good LV function (mean EF 54%), normal LV diastolic dimension, NYHA functional class I and no implanted devices. One of whom had sustained monomorphic VT without haemodynamic compromise but required cardioversion for termination and the other, high VE burden with one episode of NSVT of 23 beats duration. These patients (TOF group) had moderately dilated RVs.

The second group with the surgical corrected TGA were significantly younger, had severely impaired systemic ventricles (sRV, EF 21% on average), worse functional class (NYHA III), repeated hospitalisations, sustained atrial and nonsustained ventricular arrhythmias (one had slow VT 130 b/min) and both had dual chamber permanent pacemakers implanted at a young age, with recent upgrades to cardiac resynchronisation devices (CRT-Ds) and additional subcutaneous leads for failed defibrillation at implant. They received optimum medical therapy with a beta blocker, ACE inhibitor, spironolactone including long term anticoagulation in the impaired ventricular function group.

Electrical restitution was assessed following steady state pacing according to the previously described study protocol. 400 ms drive trains were used in all patients but one, where a slower (600 ms) drive was required due to conduction disease and haemodynamic effects.

Table 10 Characteristics of patients with grown up congenital heart disease

Sex	Age	Dx	Ventricle studied	systemic EF%	NYHA Class	Studied chamber function	Systemic ventricle (mm)	Radial distance (mm)	Ensite chamber (mm)	QRS (ms)	Drugs	Cardiac arrest/ syncope	sVT	Comorbidities
F	69	cTOF	Right	53	I	Mod 40%	52	52	82x75	160	BB,amio	No	Yes	HTN,RBBB
F	35	cTOF	Right	57	I	Good	47	47	89x63	125	Nil	No	No	PR, RBBB
F	26	rTGA	(s) Right	23	III	Poor	56	56	77x84	140	BB	No	Yes	CRT-D,AA,baffle leak
M	32	rTGA dex	(s) Right	20	III	Poor	68	49	77x73	190	BB,digoxin	No	Yes	CRT-D, AVR, PR, TVR,CKD

Age in years. BB= beta blockers, HTN= hypertension, AA= atrial arrhythmias. The Ensite system was utilised to study the RV in this patient group which was the systemic ventricle in 2 patients.

In these 4 GUCH patients 850 beats were analysed of which 8 beats were discarded because of ambiguity and unclear UE morphology. 65 restitution curves were produced. The mean ventricular ERP was 220 ms but 240 ms in the TGA subgroup and 200 ms in the TOF subgroup. The parameters and results obtained are displayed in Table 11 (results are displayed as means ± SD with ranges in parentheses). Note the steepness of the ARI restitution slopes but overall low magnitude ARI curve and steep average CV curve suggestive of slow conduction. Statistical testing with a two tails t Test assuming unequal means and correction for unequal variance.

There were highly significant differences in steepness of the ARI and CV restitution curves and marked differences in ARIs between basic steady state pacing and short pre-refractory coupling interval between the subgroups, but no detectable difference in the ventricular refractory intervals and the magnitude of the restitution curves. This may indicate that both subgroups have shallow flat curves with abrupt limited change that occurs at short DIs. However, one patient's ARI restitution curves were constructed with a slower basic drive train than the others and this may have affected the overall results.

In the TOF subgroup: one had ablation of a VT focus on the anterolateral tricuspid annulus (RV inflow) and near the junction with a ventriculotomy scar a site that corresponded to the segment with the peak regional S_{max} value, while the other had very little ventricular ectopy and no VT on the day of ablation her peak regional S_{max} did not correspond to the ablated segment. No ablation was required in the TGA subgroup due to lack of clinical and inducible arrhythmias. Measurements are displayed in Table 11.

Table 11 Electrical and conduction velocity restitution curve slopes in the GUCH subgroup

Parameter	TOF Group	tGA group	p value	Total
VERP ms	200	240	ns	220
Mean (global) Smax	0.64 (0.6-0.68)	0.89 (0.86-0.9)	p= 0.02 (CI 0.03-0.4)	0.76 (0.6-0.9)
Mean peak local Smax	1.2 (1.06-1.53)	1.9(1.76-2.05)		1.55 (1.06-2.05)
Number Smax>1	5 (3,2)	10 (5,5)		15
Max slope site	RV inflow	RV inflow& adjacent		
RF site	1/2 corresponding	No RFA		
Mean ARI basic pacing	225	285	p<0.0001	255 (211-335)
Mean ARI at short CI	189	242	p<0.0001	216 (183-279)
Mean ARI Mg %	12± 8	9.5 ± 0.3	ns, p=0.18	11± 5
Mean Mx CV restitution	0.2 ± 0.06	0.3 ± 0.25	p<0.0001 (CI 8.6-18.5)	0.3 ±0.2
Mean CV Mg %	27.5± 8	41 ± 8		34 ±10

CI indicates 95% confidence interval; statistical significance is indicated by a p< 0.05

Shape of the ERC

The overall shape of the ERC remained constant but there was clear grouping of the patient population. The difference seen in the ARI readings of patient 4 and the other patients and shifting of the ERC downward and leftward may result from the difference in the basic pacing drive between the patients (Figure 39). This patient could not tolerate faster pacing drive trains than 600 ms and he had a maximum regional S_{max} of 2.05 (mean global S_{max} of 0.86). These results combined with the appearance and shape of his ERCs may support that we cannot totally exclude the role of inherent anatomical and tissue properties related to his poor ventricular function and underlying substrate as contributors to prolonged recovery times and not merely a function of the slower pacing cycle length. 70% of all S_{max} values occurred between 10-30% normalized segment of the adjusted DI.

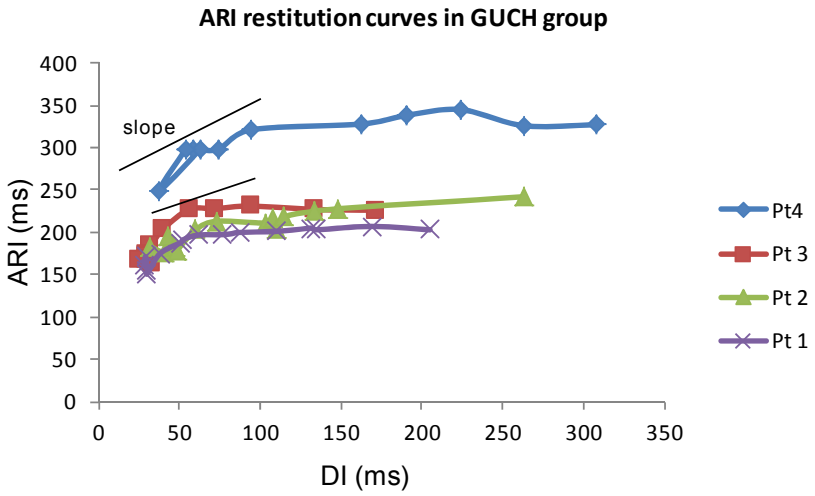

Figure 39 ARI restitution curves in the GUCH subgroup

Shape of CV restitution curves

The appearance of the CV restitution curves in the GUCH patients was generally biphasic (Figure 40) with a minimal alteration in the CV despite significant decrementation of the DI for the first 60% of the CV restitution curve until the DI reached a critical level followed by a small surge and then marked reduction of the CV. The CV operated over shorter DIs compared to ARIs.

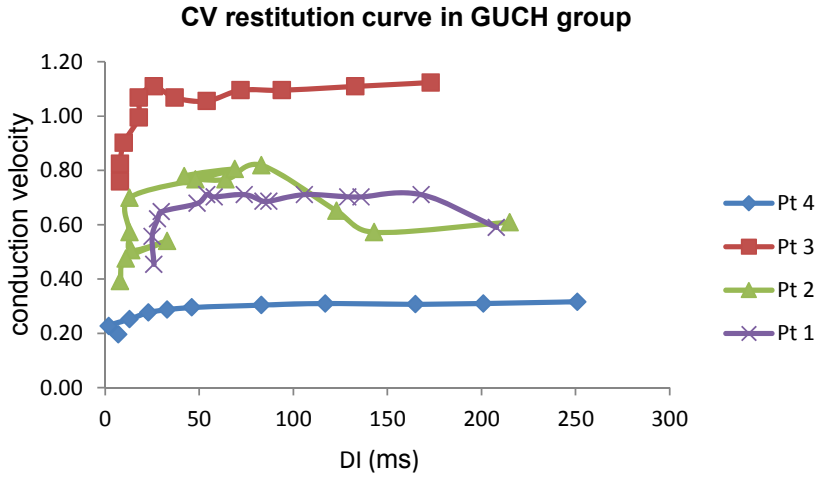

Figure 40 Conduction velocity restitution curves in the GUCH subgroup

3.3.4 Other cardiomyopathies

Two patients with other cardiomyopathies underwent full restitution protocols and are included together for combined analysis. Details of their conditions are outlined in Table 4, page 123. One was a 48 year old male with ARVC, previous syncope and VT, no prior history of cardiac arrest, good LV function but moderately impaired and dilated RV, functional NYHA class I and CMR features of ARVC. The other was 72 female with mild non-obstructive hypertrophic cardiomyopathy of indeterminate origin with an aneurysmal posterobasal LV wall (suspected of LV ARVC) , moderate LV dysfunction (EF 40%), moderate mitral regurgitation, unobstructed coronary arteries, atrial arrhythmias including atrial flutter ablation and previous VT ablation for VT storm. Both patients have an ICD and were enrolled for VT ablation. The MEA was placed in the RV for the ARVC study and in the LV for the indeterminate HCM study. In the LV study, VT could not be abolished and remained easily inducible with a single extrastimulus (S2 260 ms) during 500 and 600 ms drive trains, thus ERP was not reached. 492 beats were analysed in these two patients from 34 ventricular sites (Table 12). Mean overall S_{max} was 0.82 ± 0.33. However, the maximum local S_{max} was 0.97 in the ARVC study and 2.33 in the HCM study. The S_{max} corresponded to the targeted ablation region in the ARVC patient, although the S_{max} measurements in this ventricle did not exceed 1. However, 61% of the points studied in the HCM LV study were > 1.

Table 12 Characteristics of the 2 patients in the miscellaneous cardiomyopathy group

Parameter	ARVC	HCM	Combined
Ventricle studied	RV	LV	
Number of sites	16	18	34
Number of beats	240	252	492
ERP	220	VT @260	
Mean Smax*	0.5	1.14	0.82
Disp of Smax	0.15	0.5	0.33
Maximum Smax	0.97	2.33	1.65
Site Smax	10	2	
RF segment	10,4,5 RVOT	5, (posterobasal)13	
No. Smax>1	0	11	
ARI at long RVP	205	255	230
ARI at short CI	191	202	196.5
ARI Mg%†	8±4	18 ± 13	14 ± 11
CV Max‡	0.13 ± 0.06	0.03± 0.04	0.08± 0.07
CV magnitude %¶	20± 7	7± 10	13 ± 12

Analysis using non-paired t Test (assuming unequal variance) indicates statistical significance *p<0.0001 (95% CI 0.4-0.9), † p= 0.005 (95% CI 3.2-16.6), ‡ p< 0.0001, ¶ p=0.0002.

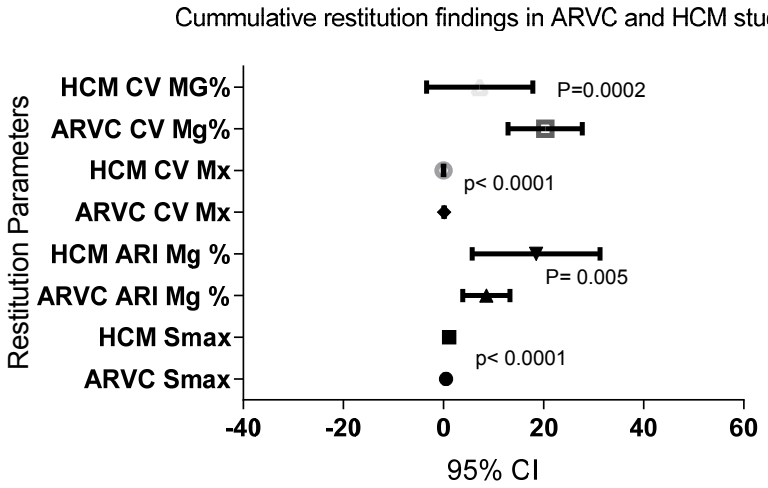

Figure 41 Box and whisker plot of the electrical and conduction velocity restitution parametrs in the miscellanous cardiomyopathy subgroup

Note that the studies were conducted in different cardiac chambers. And that in the RV study all S_{max} values were below 1 (albeit maximum S_{max} was 0.97) despite the history of VT in this patient.

While in the LV study, 11 out of 18 ventricular sites had S_{max}> 1 (range 0.26 to 2.33). Ventricular ERP could not be established because of the repeated induction of VT with minimal stimulation -single extra stimulus (S_2) - with different basic drive train CL from 260 ms onwards despite RF ablation. There were multiple exit sites to the VT that was arising from an aneurysmal posterobasal segment. The VT had multiple morphologies and CL 360-300 ms. There were documented mid-diastolic potentials (Figure 42 A) during VT which were targeted with ablation and complex fractionated late signals (Figure 42 B) and systolic potentials in sinus rhythm. It is however noticeable that her CV restitution curves were unusually flatter and of lower magnitude than the ARI restitution curve (Table 8 patient number 16).

A. Induction of re-entry VT in pt 7 (LV study) during restitution assessment- note diastolic potentials.

B. Fractionated late potentials, low amplitude complex fractionated electrograms in the same patient on the ablation catheter channel.

Figure 42 Two images of induced VT with visible diastolic and late potentials (structural heart disease patient)

3.4 Structurally normal hearts

3.4.1 Patient Characteristics

Seven patients (3 females, 4 males) of median age 37 years, range of 18-54 of whom four had an index presentation of out of hospital VF arrest (OHVF). Two of the remaining three patients were referred as part of the Inherited Cardiac Conditions Service because of a strong family history of unexplained premature SCD. The group included LQTs, a Brugada like channelopathy and an autosomal dominant pattern of profound sinus bradycardia and intermittent bigeminal rhythm (the latter, patient number 7). She had repolarisation abnormalities with T wave inversion throughout the precordial leads on resting ECG and mild QTc prolongation of 480 ms but no reversible and metabolic causes. She displayed features of autosomal inherited sick sinus node disease from a channelopathy despite negative genetic tests for *SNC5A* and *LQT* genes.

All were (Table 5, page 126) functionally NYHA class I, had smooth unobstructed coronary arteries (in patient 7 the right coronary artery had an anomalous anterior origin from the right sinus of valsava), negative EPS, structurally normal heart on trans-thoracic echocardiography and CMR and negative toxicology screens. Six patients were new presentations. All patients except patient 6 who had confirmed LQTs underwent flecainide challenge with 1.5- 2 mg/kg of flecainide, with negative results. In patient 5 at the time of EPS and restitution studies flecainide suppressed ventricular ectopy. Patient 3 had earlier experienced OHVF arrest of unexplained aetiology with negative result on flecainide challenge and no demonstrable structural heart disease, and had undergone previous RV VE ablations, which eliminated the culprit ectopic, triggering the VT storm, thus repeat flecainide challenge was not undertaken on this occasion. Similarly, patient number 4 underwent flecainide challenge on a separate occasion, so this was not repeated. Patient number 6 had cLQT phenotype and genetic confirmation with a mutation in KCNQ1 gene (tyrosine to guanine substitution at nucleotide position 742 in exon 5) but no arrhythmias or syncope.

The patient characteristics of this group are displayed in Table 5 (page 126).

3.4.2 Risk stratification and investigations

Patients 1-5 (71%) were at high risk of life threatening arrhythmic events and SCD because of high relative risk of recurrence of VF and received an automatic implantable defibrillator (ICD). In four implantation was for secondary prevention and in patient 2 for primary prevention grounds because of a strong family history of premature cardiac death from a channelopathy and abnormal repolarisation on resting ECGs.

Two patients (number 6 and 7) by comparison had relatively lower risk and did not receive ICDs. Patient 6; a 45 year old male with phenotype of cLQTS (QTc interval intermittently ranging from 400-600 ms) with confirmed genetic mutation in the KCNQ1gene. He had no history of syncope or documented cardiac arrhythmias apart from isolated atrial extra systoles. He was intolerant to beta blockers and because of palpitations had an implanted internal loop recorder (Reveal, Medtronic Inc). Patient 7, a 24 year old lady with symptomatic sinus bradycardia, intermittent bigeminal rhythm and repolarisation abnormality with global T wave inversion on resting ECG. She had extensive history from her maternal side of relatively premature pacemaker implantation but no SCD. Her QTc ranged from 480-500ms and U waves were apparent. She and her family did not reveal mutations in *SCN5A, KCNQ1 and KCNH2* genes and she had a dual chamber permanent pacemaker implanted for profound symptomatic bradycardia late in the second trimester of pregnancy.

All had macroscopically normal hearts on various imaging modalities as explained with median LV EF 65% and median LV end diastolic dimension of 48 ± 5.8mm. Patients 3 and 5 who had suffered incessant VF had totally normal resting ECGs.

Flecainide challenge, was performed in all but patient 6, (cLQTs) and all patients underwent a VT stimulation study which was negative for the induction of ventricular arrhythmias.

3.4.3 Endocardial ARI restitution curves

3D electroanatomical mapping was performed using the Ensite system. Ten restitution curves were constructed at baseline after steady state pacing from the RVA at pulse width duration of 2 ms and stimulus strength at twice diastolic threshold for 2 minutes. After steady state was achieved an extrastimulus, S_2, was introduced repeatedly after a 10 beat train (S_1). Details have been explained in chapter 2. A total of 2258 beats were analysed from 131 sites and 14 to 20 sites per ventricle, arranged according to the predefined polar template, with the analysis of additional adjacent sites in 4 patients. 108 beats were excluded (4.5%) either because of ambiguity of the T wave or the

occurrence of a VE (repetitive ventricular response) at the time of S_2 that precluded accurate measurement of ARI, AT and DIs.

After baseline data were observed, 2 mg/kg flecainide (maximum 150 mg) was infused intravenously into the patient over 10 minutes in the cardiac catheter lab and the same restitution protocol was once again repeated and data recorded for offline analysis. ECG monitoring continued for a further 45 minutes from the end of the flecainide infusion following which the procedure ended and the patient would leave the lab. Three patients (1,4 and 7) had repeated restitution studies at more than one drive cycle length.

The EPS including the restitution protocol were carried out in a conscious, post absorptive state apart from in patient number 3 who had sedation for ventricular ectopy ablation.

Local vs global ARIs

All but patient number 3 had studies of the LV using the Ensite intraccardiac MEA (Figure 43). In all but patient number 3, this was introduced into the LV via the retrograde transaortic approach. In one patient (3) the Ensite balloon was introduced via the right femoral vein through a 9F sheath and advanced into the RV.

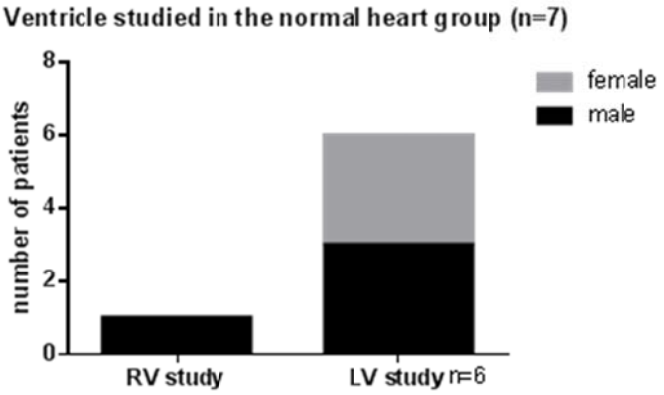

Figure 43 Distribution of chamber studied in the normal heart group

The predefined 16 segment ventricular model based on the polar image was similarly adopted for these patients and UE and their first derivative (dV/dt) were displayed in pairs on the computer workstation for offline analysis.

Median VERP was 190 ms throughout and similar for both the left and right ventricular studies.

Local ARIs

Repolarisation timings were assessed from the reconstructed virtual UE and their first derivative as previously explained. The local AT was measured from the onset of the pacing spike to the dV/dt_{min} of the local QRS. The ARI depended on the morphology of the T wave and was measured from the end of activation to the dV/dt_{min} of a positive T wave, dV/dt_{max} of a negative T wave and to midway between dV/dt_{max} and dV/dt_{min} of a biphasic T wave. Beats with indiscernible T waves could not be used for assessment of the ARI or repolarisation time (the sum of AT and ARI) and so were excluded. This occurred due to ambiguity of the T wave from the presence of low amplitude complex electrograms which prevented interpretation of the local T wave signal or the occurrence of a VE which masked the S_2 induced response. Despite the macroscopically normal appearance of these hearts, 4.7 % of the beats analysed were excluded mainly because of the presence of complex fractionated electrograms (Figure 44, Figure 46) .These are grossly abnormal signals and observed in areas of scar and are electrical substrates for arrhythmias because they are usually a marker of delayed activation, asynchronous depolarisation and slow conduction; all of which can lead to reentry and VT. They occurred during ventricular pacing and during sinus rhythm in three patients- who had abnormalities on their resting ECGs and which could not be correlated to a specific common segment of the endocardium. Patient 2 (Table 5) had fractionation of the virtual UE in sinus rhythm which became grossly coved in the UEs and its first derivative during the flecainide challenge, however the surface ECG remained unchanged Figure 47.

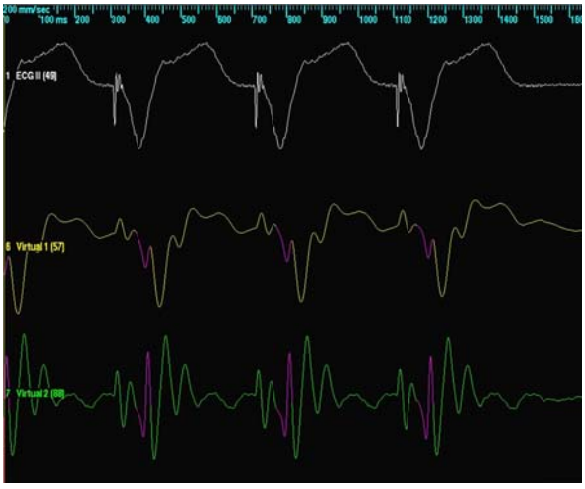

Figure 44 Complex fractionated electrograms during ventricular pacing, normal heart

Complex fractionated low amplitude electrograms in the virtual unipolar electrogram recording (yellow) with corresponding fractionation in the associated dV/dt (green), in a patient with familial sick sinus node, previous documented bigeminal rhythm and repolarisation abnormalities on her ECG all due to an unidentified channeloptahy.

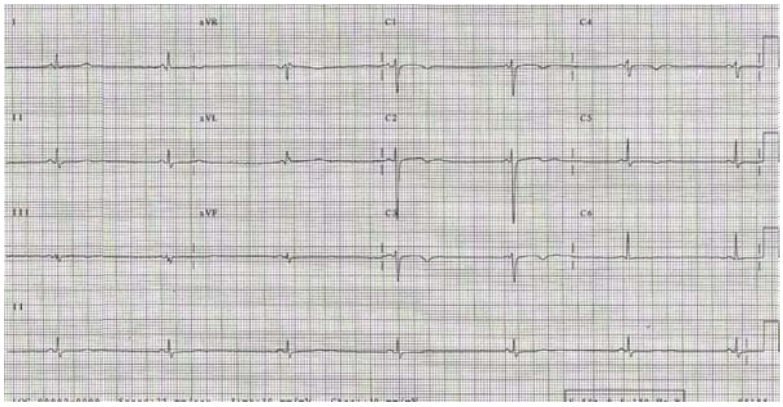

A.

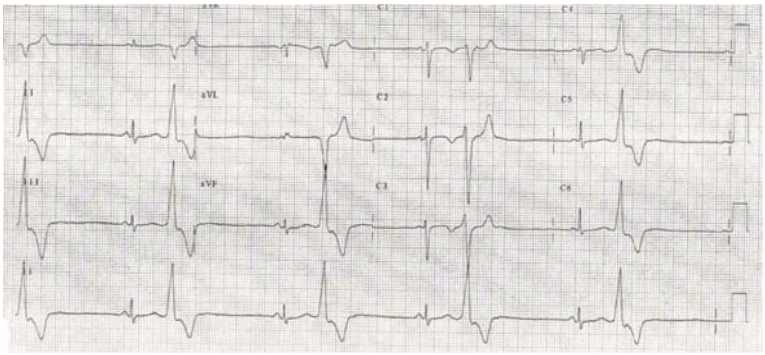

B.

Figure 45 Surface ECG of patient 7 during sinus and bigeminal rhythm

Surface ECGs of the patient with the complex fractionated low amplitude electrograms and the structurally normal heart. (A) sinus bradycardia with widespread repolarisation abnormalities (B) ECG on a separate occasion bigeminal rhythm without interpolation.

Figure 46 Complex local electrograms during sinus rhythm (normal heart patient)

Figure 47 Virtual reconstructed unipolar electrogram showing coved ST segment elevation postflecainide with ST sagging on surface ECG

Complex low amplitude virtual electrogram during sinus rhythm. In patient (2). Figure 47 was taken during the flecainide challenge and shows convex coving of the virtual UE T wave which is mirrored in the trace of the first derivative. Notice at the time the surface ECG shows no similar change- the flecainide challenge was deemed negative.

2150 beats were analysed from 131 sites at baseline from the six LV and one RV electroanatomical maps. Following the achievement of steady state and initiation of the restitution studies, average the maximum ventricular ARI was 329 ± 88 ms and the mean minimum recorded ARI was 130 ±24 ms. In the RV maximum ARI was 311 ± 42 ms. Average ARI at long pacing coupling intervals was 234 ±19 ms which became 212

±17 ms at intermediate pacing CL and down to 207± 25 ms at short pre refractory period pacing CL. The effect of decrementation of the ARI with introduction of an earlier extrastimulus was statistically significant at p= 0.01 using the paired t Test statistic.

Electrical restitution curves

These were produced after right ventricular pacing at 400 ms for 2 minutes to achieve steady state, then decrementing with the introduction of an extrastimlus (S_2) after a 10 impulse drive - train in keeping with the protocol described in chapter 2- until ventricular refractoriness.

Between 14 and 20 restitution maps were produced per ventricle at baseline conditions. Four patients had additional studies at faster pacing rates and four patients had recordings following flecainide challenge. The shape of curve was much more complex than that in the previously described group of patients (structural heart disease). Only about one third of these curves had an obvious triphasic or biphasic morphology. The curves appeared very complex and multiphasic in 100% of the curves obtained from two patients (1 & 3- Table 5). Although there was a trend towards shortening of the ARI with shortening of the DI, the ARI could remain constant or even increase despite shortening of the DI which is not the usual expected relationship described for repolarisation.

43% of all assessed ventricular sites at baseline had maximum restitution slopes above 1. Mean global S_{max} was 1.16 ± 0.54 (range 0.73-2.43) with an average peak of 3.3 ± 1.5 (average peak local S_{max}). The highest averaged S_{max} was from the RV study in which 18 of 20 points analysed had a maximum ERC slope value above 1 and the S_{max} of the 19^{th} point was 0.98 and only one point had a slope of 0.56 near the anterior portion of the RV free wall. This patient (number 3 in Table 5) had very high arrhythmia burden with an index presentation at 34 years of age and over the next 7 years had repeat VT and VF storms that required ablation of a VF inducing ventricular ectopic beat.

The average magnitude % of the ARI curves was 11± 3.5%.

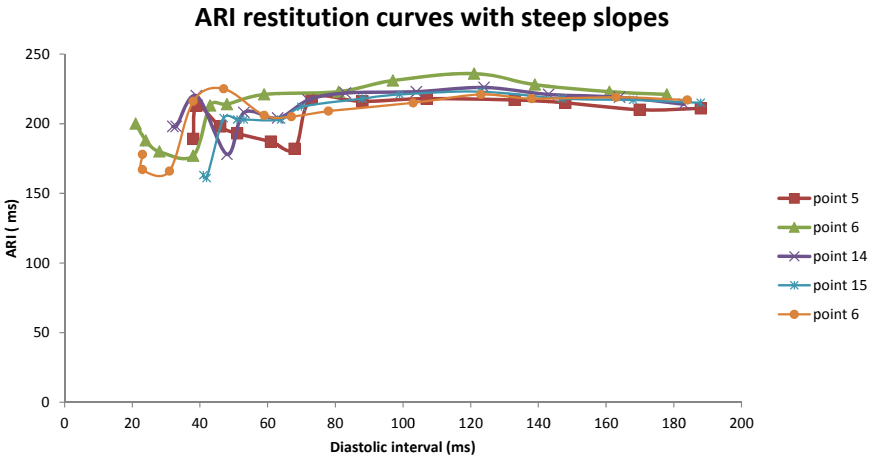

Figure 48 ARI restitution slopes in normal heart cohort

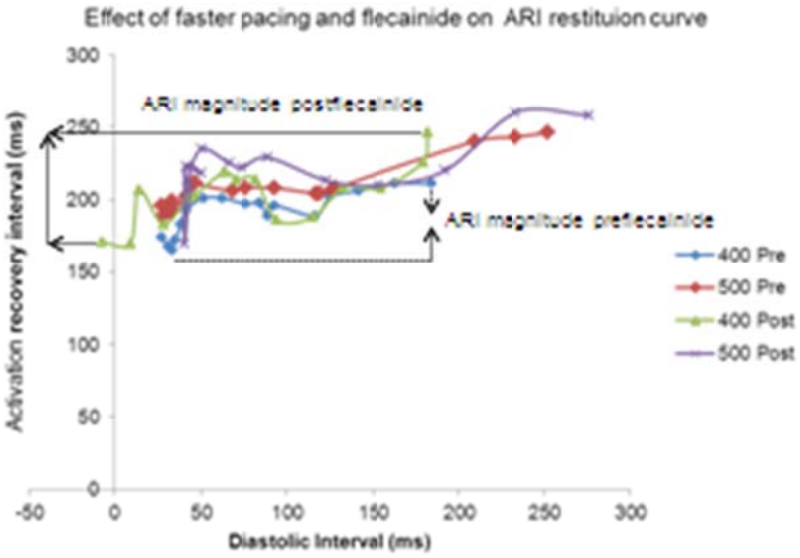

Figure 49 Restitution curves showing the effect of pacing cycle length post flecainide challenge

Four restitution curves from the same point in the same patient showing the effects of increased rate pacing: 400 ms, 500 ms at baseline, followed by pacing at the same CL post flecainide challenge.

Faster pacing drive trains did not significantly alter the dynamics of the ERC at baseline (Figure 49). However flecainide significantly enhanced the magnitude of the ARI

restitution slope (19.5 ± 8 % vs 11 ± 3.5% preflecainide p= 0.0007, 95% CI 3.5- 12.9) mainly at the supernormal portion of the slope with very little change in the plateau region (Figure 49). Thus the curve is shifted upward and leftward.

As in the SHD group (Figure 28) the slope of the ERC was steepest between 10-30% of the baseline DI in 59% of points, between 30-50% of baseline DI in 24% of points and below 10% of baseline DI value in 17% of points. The steepest regional slopes in the ventricle occurred in the 10% value of the diastolic interval. No steep slopes occurred after the DI reached 50% of the baseline value. There was no correlation between the site of the maximum ARI restitution slope and the maximum or minimum activation and recovery times in the ventricle.

Table 13 Conduction velocity and ARI restitution parameters in the normal heart group, pre and post flecainide

Parameter	Preflecainide	Postflecainide	Analysis
Number of sites	131	91	222
Number of included beats	2150	989	3139
VERP	190	200	195
Mean Smax (Global)	1.16±0.54	1.2 ± 0.25	ns (p=0.9)
Mean Maximum(regional) Smax	3.3 ± 1.5	2.4 ± 0.63	ns (p=0.19)
Range of global ventricular Smax	0.73- 2.43	0.67- 1.32	ns (p=0.45)
No. Smax>1	56 sites (43%)	42 sites (46 %)	
ARI at steady state (ms)	234 ± 19	234 ± 16	ns (p=0.15)
ARI at short CL	207 ± 25	229 ± 32	ns (p=0.15)
ARI Mg %†	11± 3.5	19.5 ± 8	p=0.0007
CV Max*	0.16 ± 0.04	0.11 ± 0.02	p=0.01
CV magnitude %	27 ± 9	26 ± 4	ns (p= 0.9)

Table showing the results of the basic restitution studies and the effect of flecainide. Statistical significance was calculated as $p<0.05$.*, † indicates a significant difference on the magnitude of the ERC and the CV (see text).

Conduction velocity

The CV generally operated over narrower DIs compared to ARI restitution curves. The CV restitution curves appeared usually biphasic with a steep initial phase that ascended into the flat or plateau phase. The average magnitude of CV curve (CVMg%) was 27± 9%. As in the isolated incident in the SHD group (patient number 7 Table 4) one patient in the normal hearts group (patient number 2 Table 5) had the unusual feature of an ARI curve, which was larger in magnitude than the flatter CV restitution curve (displayed as patients 16 and 18 in Table 8). Flecainide resulted in a downward and rightward shift of the CV restitution curve (Figure 52) that reduced the overall maximum CV (0.11± 0.02) significantly without affecting the magnitude of the curve (p=0.01).

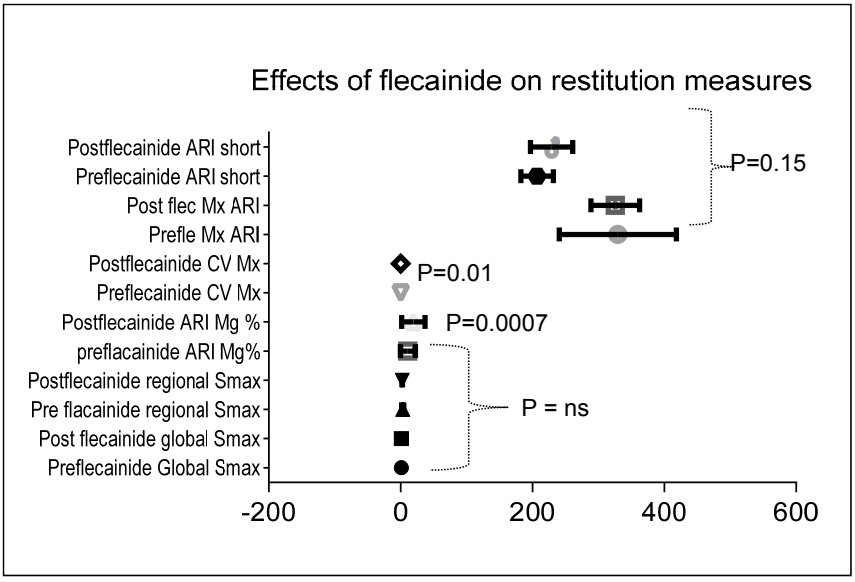

Figure 50 Box and whisker plot showing restitution parameters pre and post flecainide in the normal heart cohort

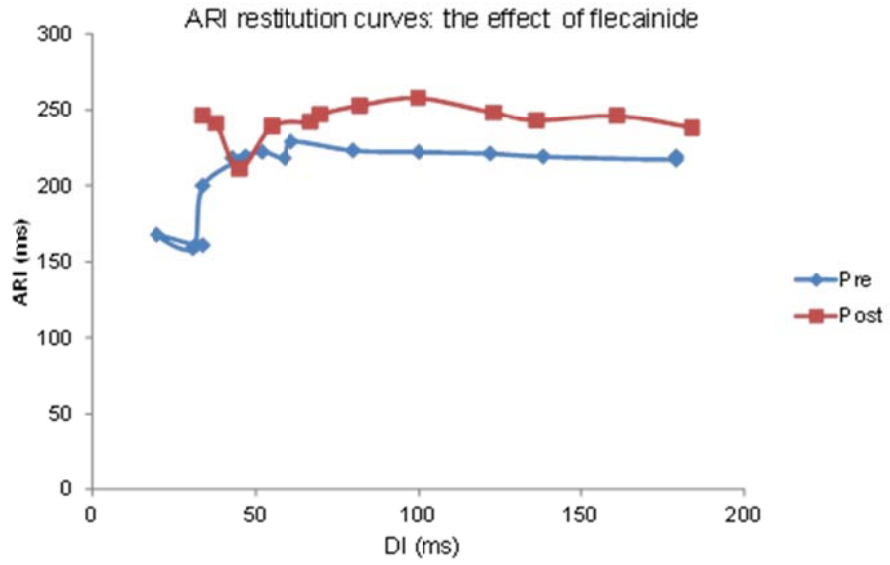

Figure 51 Flecainide effect on ARI restitution slope

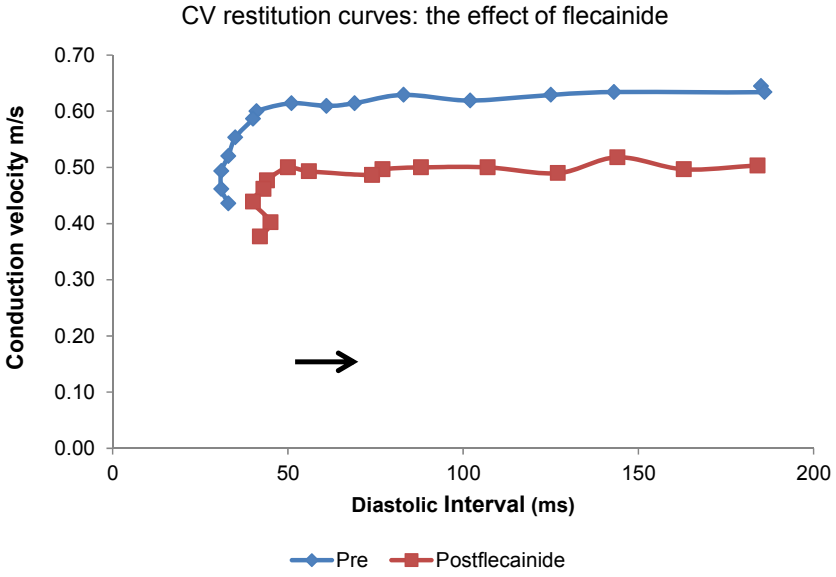

Figure 52 Flecainide effect on conduction velocity in the normal heart cohort

3.4.4 Flecainide effect

In high-risk structurally normal hearts, flecainide did not affect the slope of the ERC (Figure 51) but increased the ventricular ERP by 15% and in one half of postflecainide maps altered the site of the maximum S_{max}. There was no significant difference between

values before and following flecainide in relation to ARI duration (maximum and minimum values) and the effect of long and short coupling interval RV pacing on ARI duration. Flecainide significantly (p=0.0007) enhanced the magnitude of ARI ERC particularly near the shoulder or the supernormal phase of the curve (from 11 ± 3.5% to 19.5 ± 8, 95% CI 3.5-12.9) but it lifted the ARI ERC upward limiting the range of DIs that spanned activation and recovery.

Flecainide reduced the overall CV maximum significantly (0.11 ± 0.02, p=0.01) without reducing the magnitude of the CV restitution curve (Figure 52).

3.5 Amiodarone effect

Chronic amiodarone therapy was used in 35% of the patients, all of whom had structural heart disease. This patient population was significantly older (p=0.001) with poorer left ventricular function (EF 30% vs 48%, p=0.02) and had ECG features of more profound electrical dyssynchrony, with significantly wider QRS complexes (p=0.006) (Table 14). Although the patients treated with amiodarone did not differ in their AT, ARI and RT dispersion characters during long and short coupling interval RV pacing from those who did not receive chronic amiodarone therapy (p ranged from 0.1- 0.8, ns), with similar mean global S_{max} dispersion calculations. A trend suggestive of higher regional and local maximum slope values (p=0.06), higher global dispersion of S_{max} (p=0.09) and quicker conduction velocities (p=0.07) was observed in those ventricles not treated with amiodarone. This noticeable trend of conduction slowing in the amiodarone group was mainly observed at short DIs and resulted in a reduction of CV magnitude compared to the non-treated group (22 ± 8% in amiodarone treated hearts vs 29 ± 9% in the non-treated group, p=0.09, ns)- Table 14.

Table 14 Differences in the restitution, activation and repolarisation parameters between patients treated with chronic amiodarone compared to no amiodarone.

Parameters	Amiodarone Treated (n=8)	No Amiodarone (n=15)	*P* value
Sex,% M	63%	60%	
Age	67 ± 10	44.5 ± 19	0.001
EF % of systemic ventricle	30 ± 14	48 ± 19	0.02
QRS duration (ms)	161 ± 32	116 ± 34	0.006
VERP	229 ± 27	205 ±29	0.08 (ns)
Global Smax	0.8 ± 0.2	1.05 ± 0.44	0.17 (ns)
Local Smax	1.9 ± 0.5	2.8 ± 1.56	0.06 (ns)
Smax dispersion	1.7 ± 0.5	2.4 ± 1.5	0.09 (ns)
ARI Mg%	11.6 ± 4	11.5 ± 5	0.9 (ns)
CV maximum	0.1 ± 0.1	0.19 ± 0.12	0.07 (ns)
CV Mg %	22 ± 8	29 ± 9	0.09 (ns)
AT dispersion (RVP)	67 ± 26	65 ± 24	0.8 (ns)
ARI dispersion (RVP)	94 ± 39	140 ± 99	0.1 (ns)
RT dispersion (RVP)	89 ± 34	82 ± 46	0.6 (ns)
ARI Long CL	247 ± 18	240 ± 31	0.5 (ns)
Max ARI Long CL	306 ± 41	317 ± 75	0.7 (ns)
ARI short CL	224 ± 25	213 ± 31	0.36 (ns)

3.6 Summary

There was a significant difference in the ERP of the ventricles studied between the patients with grossly normal hearts and those with structural abnormality, with refractoriness occurring significantly earlier in the SHD group 220 ± 27 ms and the normal hearts being stimulated till 193 ± 11 ms (p=0.0007). However, the two groups despite their marked difference in cardiac function and gross structural appearance had otherwise similar characteristics in their response to decremental extrastimulus pacing and electrical restitution (Table 15). Although the SNH group appeared to have shorter recovery times, during long coupling interval pacing at baseline and during short coupling interval pacing pre-refractoriness, these were not significant. The global S_{max} values were slightly higher, but not significantly so, in the normal hearts. However, the degree of local S_{max} values between the two groups did differ significantly, with the structurally normal hearts having comparatively higher regional maximum restitution

slopes (p=0.04). Similarly, the two groups did not differ in the magnitude of the ARI or the number of sites per ventricle where there were maximum slopes that exceeded one. CV which was measured identically in both groups by the distance from the site in question divided by the activation time. The data suggest that despite the difference in macroscopic structure between the two groups there was no significant difference in the CV measured between the SHD group (0.17 ± 0.12 m/s) and the normal heart group (0.16 ± 0.04 m/s). The steepness of the CV curves was nearly identical (p=0.95, ns).

Table 15 Characteristics and restitution parameters in the structural heart disease and no structural heart disease patients

Parameter	SHD	No SHD	Analysis
Age (median)	66	37	p= 0.002
Male gender, n (%)	9 (60%)	4 (57%)	
Abnormal ECG (%)	100%	71%	
QRS, ms	148	95	< 0.0001
LV EF, %	33 ± 15	65 ± 4	p< 0.0001
LVD , mm	63	49	p= 0.0005
Defibrillator n (%)	12 (80%)	5 (71%) (1 PPM)	
No. of RV studies, (%)	6 (37.5%)	1 (14%)	
No of LV studies, (%)	10 (62.5%)	6 (86%)	
VERP	220 ± 27	193 ± 11	p= 0.0007
ARI at basic CL	246 ± 27	234± 19	ns, p= 0.2
ARI at short CL	223 ± 29	207± 25	ns, p=0.1
No. of Smax >1, (%)	116 (36%)	56 (43%)	
Global Smax	0.9 ± 0.2	1.16 ± 0.5	ns, p= 0.2
Local Smax	1.9 ± 0.5	3.3 ± 1.5	p= 0.04
ARI magnitude %	12 ± 5	11 ± 3.5	ns, p=0.4
CV maximum	0.17 ± 0.12	0.16 ± 0.04	ns, p=0.56
CV magnitude % (Mg)	27 ± 9	27 ± 9	ns, p=0.95

EF%= ejection fraction, LVD= left ventricular diameter in diastole, RV= right ventricle, LV =left ventricle, VERP= ventricular effective refractory period, ARI activation recovery interval, PPM= permanent pacemaker, S_{max}= maximum restitution slope, ns= non-significant

Table 16 Clinical characteristics and electrophysiological results between the different patient subgroups

Group	No of pt	Age	LV EF% (median)	LVD mm	V ERP ms	mean Smax ± SD (global)	Mx local slope(averaged)	Range of global Smax	ARI @ basic paced CL	ARI @ short CL	No. Smax >1 (%)	Mg of ARI %	CV mx	CV Mg %
IHD	5	74	30 ± 6	74 ± 9	223 ± 21	0.89 ± 0.25	1.05	0.51- 1.32	247 ± 12	234 ± 16	49 (34%)	11± 5	0.18 ±0.12	26 ± 5
DCM	4	53	17 ± 16	60 ± 5	220 ± 27	1.07± 0.07	2.02	0.98- 1.18	242 ± 23	220 ± 38	41 (50%)	15± 6.5	0.14 ± 0.03	27± 7
other CMO	2	64.5	47 ± 10	52 ± 1	…….	0.82 ± 0.5	1.65 ± 0.96	0.5- 1.14	230 ± 35	197 ± 8	11 (32%)	14 ± 7	0.08 ±0.07	14 ± 9
GUCH	4	40.5	38 ± 19	56 ± 5	220 ± 47	0.76± 0.14	1.55± 0.44	0.6- 0.9	255 ± 55	215 ± 43	15 (23%)	11± 5	0.3 ± 0.17	34 ±10
SNH	7	37	65 ± 4	49 ± 6	193± 11	1.16± 0.04	3.3 ± 1.5	0.73- 2.43	234± 19	207± 25	56 (43%)	11 ± 3.5	0.16 ± 0.04	27 ± 9

IHD= ischaemic heart disease, DCM= dilated cardiomyopathy, CMO= cardiomyopathy, GUCH= grown up congenital heart disease, SNH, structurally normal heart, LV EF= left ventricular ejection fraction, LVD: left ventricular end diastolic diameter, Smax= maximum slope of activation recovery restitution curve, ARI = activation recovery interval, CL= cycle length, No.= number, Mg= magnitude, CV= conduction velocity.

3.7 Discussion

The electrical restitution curve demonstrates rate dependent shortening of action potential duration with incomplete recovery of membrane conductance between the beats. Under physiological conditions, the APD (ARI) shortens with increased heart rate and reduced DI. The ERC has been reported to assume either a biphasic or triphasic shape in various cardiac models (Bass 1975;Chialvo et al. 1990;Morgan, Cunningham, & Rowland 1992a;Watanabe et al. 1995;Franz 2003;Yue, Franz, Roberts, & Morgan 2005b). Thus after extra-stimulation there is an initial shortening phase of APD, followed by an increase in APD over a narrow range of extrastimulus coupling intervals (and DIs) followed by further shortening of APD with increasingly premature extra-stimulation resulting in a transient decline of the ERC before it straightens out and plateaus at steady state DIs. This steep initial phase that represents an early maximum APD, is usually reached at DIs of 50 ms or less (Franz 2003). This early portion of the minority of the curves is a reflection of rapid recovery of APD with extrastimulus pacing from recovery of inactivation of the fast Na^+ channels, from widely open $I_{Ca+2\text{-}L}$ (L-type) channels that result from reduction of the negative feedback effect on these channels following the earliest premature stimulation or from increased conductance of inward K^+ channels (Iinuma and Kato 1979;Franz 2003). However, most ERCs in this study (53%) were complex and did not follow a consistent pattern; linear, exponential, monotonic or otherwise. Unlike Franz et al the ERCs produced in this study were determined at 10 ms decrements with ARIs, that have been related to APD_{90} rather than MAPs (Franz 2003). In the present study failure of the ARIs to shorten at reduced DIs may reflect blockade of multiple ion currents particularly I_{Na}^+ and L-type I_{ca}^{+2} (phases 1 and 2 of repolarisation) with resultant prolongation of APD. In the SHD group the use of a combination of amiodarone and class I antiarrhythmic drugs in 3 patients (mexilitine and lignocaine in separate patients- table 4) may explain this finding in conjunction with the occurrence of PRR (Kirchhof, Degen, Franz, Eckardt, Fabritz, Milberg, Laer, Neumann, Breithardt, & Haverkamp 2003a). Although in the SNH this effect was greater suggesting a more convincing role for inherent tissue heterogeneity and defects in ion channels, notably L-type Ca^{+2} inward current and the loss of the normal inverse relationship between it and Ca^{+2} ion release from sarcoplasmic reticulum, given the negative flecainide challenge in the SNH patients. Additionally, the consideration that the distance between the pacing site and the recording sites strongly influences the degree of APD shortening which would have affected the data obtained from those sites that were further from the RV apex. However in 6% of the curves the ARI inversely

lengthened with shortening of the DI. This is an exaggeration of the aforesaid mechanism and may also reflect prolonged AT which if marked, the functional refractory period may never shorten sufficiently for the ARI/ APD to shorten over what should be the steep portion of the ERC. Likewise the effect of slowed conduction would be more at sites that are distant from the stimulus site where the absolute increase in AT would be marked especially in the presence of antiarrhythmic therapy (Kirchhof, Fabritz, & Franz 1998). The greater the conduction delay of an impulse the greater the range of DIs to which the myocardium is exposed thus the greater range of ERCs in the chamber. This wide disparity of CV in different regions of the ventricle also contributes towards arrhythmogenesis. The combination of anatomical (Derksen et al. 2003) and functional block related to tissue heterogeneity and ion channel dysfunction perpetuates conduction delay and this was particularly noted in the chronically treated amiodarone patients with SHD who demonstrated a trend towards having slower CV by comparison to the SNHs.

The near flat ERCs that were observed in a minority of the SHD group are non-physiologic and reflect extensive tissue damage from underlying pathology with marked ion channel dysfunction (mainly Na^+ channels). This supposition is supported by the findings of Kurz et al from experiments on the intact rabbit heart following irreversible ischaemia that showed APD alternans failed to occur and APD remained constant regardless of pacing CL. The ERC had flattened approaching a straight line reflecting severe disruption in ion channel function (Kurz, Mohabir, Ren, & Franz 1993).

The similar overall mean and maximum S_{max} values in ventricles from both groups (SHD and SNH) of this high-risk patient population supports the effect of the underlying disease process and its progression and the exaggeration of tissue inhomogeneity and thus dispersion of repolarisation. This concurs with evidence reported by Morgan et al of exaggerated adjacent dispersion and shifting of the ERC with premature extra-stimulation at some paired sites in patients with right ventricular or right and left ventricular disease and complicating VT (Morgan, Cunningham, & Rowland 1992a). Those pathologies have wide spread myocardial involvement -albeit patchy in some conditions-, which contributes to dispersion of repolarisation within and between the ventricles. Yet these findings differ from those reported by Kurz et al in rabbit heart experiments and Yue et al in humans (Kurz, Ren, & Franz 1994;Yue, Franz, Roberts, & Morgan 2005b). The former investigated varying degrees of global ischaemia on the rabbit heart by measuring epicardial MAP recordings from 1 RV and 2 LV sites. They

reported that the sequence of changes that occurred in the RV differed to those that occurred in the LV and were proportionally delayed. This however examined the effect on one ventricle. Yue et al (2005) in keeping with the findings of Franz (2003) reported a significantly greater restitution slope in the LV compared to the RV endocardium in low risk structurally normal heart patients (0.94± 0.49 vs. 0.66 ± 0.25, $p<0.001$). This discrepancy may be related to the contrast in the underlying disease processes and differing pathologies between our patient cohorts.

All patients, but one, in this high risk arrhythmic group had at least one regional electrical restitution slope greater than 1. One patient whose maximum electrical restitution slope was 0.97 had syncopal VT but no VF or cardiac arrest and had an ICD implanted for ARVC. The remainder of his regional restitution slopes ranged from 0.38-0.66 with a mean of 0.47 if we were to exclude the high reading of 0.97. The magnitude and features of his ARI and CV restitution slopes all complied with what has been reported in normal subjects (17.6 ± 8% and 20 ± 7% respectively). The dispersion of S_{max} in his ventricle may have triggered discordant alternans but perhaps interacted in a way to stabilise wavebreak thus resulting in an organised arrhythmia- monomorphic VT rather than VF as demonstrated in simulated ischaemic studies during elective cardiac surgery (Clayton 2005) or the experimental usage of pharmacotherapy to prevent VF (Garfinkel, Kim, Voroshilovsky, Qu, Kil, Lee, Karagueuzian, Weiss, & Chen 2000;Weiss, Chen, Qu, Karagueuzian, & Garfinkel 2000). It is also proposed that conduction delay leading to wavebreak and fragmentation act as precipitants for VT/VF. The combination of slowed conduction- anatomical or functional-, unidirectional block and inhomogeneous ARI restitution slopes result in ideal conditions that precipitate re-entry. Other explanations include the effect of cardiac memory in establishing and maintaining APD alternans (Huang et al. 2004) or on the contrary the effect of a flat restitution slope in promoting arrhythmogenesis by preventing the occurring APD to reach the ERC plateau as quickly as it should and thus if alternans develops it will continue and ion channel function particularly Ca^{+2} , as intracellular Ca^{+2} recycling, appears to be responsible for electrical alternans especially at faster rates. (Franz 2003).

GUCH patients are a well-known group to develop a vast array of cardiac arrhythmias. I have studied the restitution kinetics in a group of adult's with surgically treated congenital heart defects with a range of complex pathologies including repaired TOF and Mustard operations for transpositions of the great arteries in addition to dextrocardia. As these populations are living longer, the majority will present with re-entry arrhythmias both atrial and ventricular during the course of their lives. Emphasis

on risk stratifying these patients is based mainly on surface ECG for QRS duration and microvolt T wave alternans, (Gatzoulis et al. 1995) , exercise testing (Alexander et al. 2006;Lui et al. 2011), on functional ventricular assessment using transthoracic echocardiography (Ramos et al. 2010;Diller et al. 2012)and assessment of pulmonary vascular resistance and serum biomarkers (Giannakoulas et al. 2010;Norozi et al. 2011). However they are high risk patients for SCD mainly from ventricular arrhythmias (30%) rather than asystole or PEA precipitated by vascular events particularly pulmonary (13%). (Deanfield et al. 1985) investigated the mechanism of ventricular arrhythmias in repaired TOF patients with conventional endocardial mapping of RV and some LV recordings. They concluded the mechanism to be abnormal depolarisation rather than repolarisation although they documented low frequency signals after the T wave in 77% of their patients. Risk stratification has been attempted based on combined haemodynamic and functional assessments (Silka and Bar-Cohen 2012) allowed with defibrillator follow up data (Yap et al. 2011;Lam and Friedman 2011;Koyak et al. 2012a). Invasive electrophysiology studies have a limited role in risk stratification given their high false negative rates (Alexander et al. 1999). This is the first series to date which characterises electrical restitution in this population subset. My data have shown a tendency for the GUCH patients to have steeper restitution slopes at two main sites: namely the RVOT (as shown in 2 patients), the RV inflow or both (as shown in 2 patients) which are similar to the arrhythmogenic triad in ARVC patients. They are also noted to have marked dispersion of repolarisation and impairment of activation repolarisation coupling (chapter 5). These may occur from adverse ventricular remodeling from valvular heart disease and their sequelae of anatomical stretch and subsequent localised fibrosis occurring in dispersed areas of the ventricle. These are prerequisites for reentry from the localised effects of conduction delay and loss of activation repolarisation coupling. My studies support the presence of inter and intra-ventricular heterogeneity of restitution.

In the present study, overall mean S_{max} was significantly higher than that of patients with structurally normal hearts, low risk and no family history of SCD reported by Yue et al (0.97 ± 0.35 vs 0.79 ± 0.49) (Yue, Franz, Roberts, & Morgan 2005b). These S_{max} results agreed with the static APD restitution slope properties of patients with SHD reported by Koller et al (0.91 ± 0.06) (Koller, Maier, Gelzer, Bauer, Meesmann, & Gilmour, Jr. 2005) . However, unlike Koller et al we did not perform dynamic pacing protocols in our patient population mainly because the majority of the patients became haemodynamically compromised with rapid pacing and reduced coupling intervals.

Unlike our study, Koller et al investigated the restitution characteristics obtained from a single ventricular site (RV septum), regardless of the cardiac structure and underlying pathology.

There appeared to be a correlation between the site of the absolute maximum S_{max} in the ventricle and re-entrant arrhythmias. I have demonstrated in the studied patients who underwent RF energy ablation (12 SHD patients and 1 SNH patient) that 46% of peak S_{max} for that chamber, be it RV or LV corresponded exactly to the segment where RF energy was delivered to terminate the arrhythmia. In another 23% the segments with the maximum slopes were at the border of the adjacent segment where RF was delivered and within a 20 mm distance. I believe this is related to the factors of local tissue heterogeneity and underlying substrate causing heterogenous dispersions of repolarisation, rather than being caused by the induced tissue change with RF ablation, particularly as calculation of the S_{max} on random distant ablation points in other segments was always < 1 and because in the remaining 30% of patients who had ablation therapy, their S_{max} sites were not related to the sites of the ablation lesions. This suggests that steep ARI restitution slopes are regionalised in pathological human hearts and that critical pathways of VT circuits may be linked to steep ERC slopes in keeping with the assertions of Pak et al (Pak, Hong, Hwang, Lee, Park, Ahn, Moo, & Kim 2004). This concurred with finding steeper ARI restitution slopes in the positively induced VF group of ischaemic dogs in studies of Yukki et al (Yuuki, Hosoya, Kubota, & Yamaki 2004). Similarly Yue et al reported this in 3 patients with structurally normal hearts and fascicular VT (Yue, Betts, Roberts, & Morgan 2005a). However, the possibility exists that regional differences in electrical restitution may be masked by global analysis as demonstrated previously by (Morgan, Cunningham, & Rowland 1992a). Four of the 13 patients who received RF ablation did not demonstrate this finding, but in one patient (TOF repair) the arrhythmia mechanism was increased automaticity from a focal VE/VT rather than re-entrant. Whereas in the other 3 ablated patients with no correspondence between S_{max} and RF segment, this could have been related to a mid-myocardial circuit in the HCM patient with dampening of the virtual signals obtained from the MEA especially in relation to a posterobasal pouch (aneurysm) that was present in her ventricle and thought to be the source of the VT. While the remaining 2 patients (IHD, DCM) had markedly dilated and severely impaired LVs with early recurrent VT despite acutely successful ablations, which may support presence of an epicardial circuit and thus the dampened signals obtained via the MEA (Thiagalingam 2004a).

Intravenous flecainide is one of the standard pharmacologic agents used in provocative tests to identify individuals with concealed forms of Brugada syndrome or *SCN5A* mutation, who may present with IVF (Brugada et al. 2000). Experimental studies on canine Purkinje fibres ex vivo showed that flecainide slowed electrical restitution by prolonging APD_{90} by 26 ± 4%. However these effects were thought to be derived from flecainide's action on currents other than the Na^+ as similar studies with propafenone did not produce the same effect (Malfatto et al. 1994). Therefore the flecainide challenge served the purpose of excluding concealed Brugada syndrome and sodium channelopathy in this group of IVF patients and the study of their restitution properties at baseline and postflecainide allowed the in vivo assessment of modulation of electrical restitution in this patient group. Yet unlike the findings of Malfatto et al where flecainide slowed APD_{90} by 26% from 245 to 310 ms in dog Purkinje fibres our results show slowing of ARI by only 10.6% (from 207 to 229 ms) during short coupling intervals. Given the lack of slowing demonstrated by propafenone in their studies, they attributed this effect to flecainide's action on the I_k current suggesting that reduction in CV with minimal slowing of the recovery from refractoriness may in a re-entry circuit result in slowing of the circuit wave length. In the present study, at baseline during PES and construction of the restitution curves repeated ventricular ectopic beats occurred with shortening of the coupling intervals (250 ms and less) and faster pacing in the SNH which may be attributed to local reexcitation of the tissue from electrical heterogeneity resulting in the occurrence of phase 2 reentry however this did not to progress to full circus movement re-entry and sustained arrhythmias were not induced in this group. Flecainide did not affect ARI duration during steady state and long CL pacing which concurred with the minimal changes in sheets of canine endocardium demonstrated by (Krishnan and Antzelevitch 1993) but unlike their findings in I_{To} rich epicardial sheets with resultant truncation of APD, flecainide suppressed VEs in the studied SNH rather than precipitate further arrhythmias.

In three of the SNH patients- two of whom have abnormal resting ECGs with wide spread repolarisation abnormalities but were not themselves sufferers of SCD- who underwent LV studies, were noted to have areas of low amplitude fractionated electrograms during ventricular pacing (construction the of ERC) and during SR. These low amplitude fractionated EGMs or late potentials reflect the presence of abnormal areas in the endo/mid/ or epicardium, but most likely the endocardium. These serve as markers of asynchronous depolarization and slow conduction and thus a substrate for functional re-entrant arrhythmias. These abnormal electrograms are not seen in ventricles of truly structurally normal hearts (Cassidy, Vassallo, Marchlinski, Buxton,

Untereker, & Josephson 1984). These patients could be in the early stages of their conditions and had not yet experienced an arrhythmic event particularly as these are not widespread and were only detected upon detailed offline analysis when assessing the ventricle in its entirety. There are similarities between these findings and the fractionated EGMs of the Brugada patients which were linked to the arrhythmia inducing substrate. Martini et al in 1989 described the ECG pattern of what later was named Brugada syndrome (Martini et al. 1989;Brugada & Brugada 1992). He questioned the presence of underlying structural heart disease as part of the phenotype following detailed histologic examination. These findings were upheld by Frustaci and (Coronel et al. 2005)et al who demonstrated histological changes on endomyocardial biopsy suggestive of a localized myocarditis, micro-aneurysms and the presence of viral genome and increased apoptosis in a cohort of Brugada syndrome patients (Frustaci et al. 2005).Thus a therapy strategy of abolishing the phenotype by ablating these targets and treating the arrhythmia has been proposed by (Nademanee, Veerakul, Chandanamattha, Chaothawee, Ariyachaipanich, Jirasirirojanakorn, Likittanasombat, Bhuripanyo, & Ngarmukos 2011). More information is needed to elucidate whether the asymptomatic stage demonstrated in my SNH patients is a preclinical phase in the natural history of the disease and whether they progress to a manifest and arrhythmic phase.

Two features surfaced from the flecainide challenge, the first was suppression of spontaneous ventricular ectopy in all postflecainide studies but one (the RV study of the patient with idiopathic VF), which may represent the effect of flecainide of Na^+ ion channel blockade and prolongation of APD/ARI which similar to the Brugada, early repolarisation and LQT3 syndromes may resultantly enhance the occurrence of ventricular arrhythmias. Secondly, flecainide did not reduce the dispersion of repolarisation that was present at baseline studies following SR and steady state RV apical pacing (91 ± 37 ms to 195 ± 41 ms respectively, p= 0.03) although there was no significant discrepancy between the activation and repolarisation times per se. But as appreciated the dispersion of ARI following constant RV apical pacing increased significantly when compared to sinus rhythm (p=0.03) and this relationship was not altered or affected in any way following the flecainide challenge, resulting in the persistence of the same dispersion of ARI measurements post flecainide. The effects of flecainide on delayed Na^+ channel reactivation concur with those reported by (Kirchhof et al 2003a) of amiodarone and propafenone and with Garfinkel et al (2000) on bretylium, however unlike amiodarone flecainide reduced CV.

The sudden drop in the CV after a small surge in CV restitution curves may be related to ion channel saturation or dysfunction. Hearts that are low risk for fatal or unstable ventricular arrhythmias tend to have steeper CV restitution curves compared to ARI restitution curves manifested by a greater CV to ARI magnitude for a given site. CV restitution has been reported to be steeper and to function over shorter DIs. During rapid pacing or VT that results in diastolic intervals of <10 ms, ARI restitution is likely to engage CV restitution because of the greater magnitude and steepness of the latter, which may lead to discordant alternans and VT or VF. However, the S_{max} values of the ARI slopes suggest a large degree of dispersion in the ventricular recovery.

Restitution undoubtedly plays a major role in arrhythmogenesis however this role is not absolute as dispersion of repolarisation even in normal myocardium may predispose to VT and VF from transventricular and transmural gradients (Misier et al. 1995). Most arrhythmias are due to functional re-entry. Unidirectional block, a prerequisite for re-entry of any type, results from heterogeneity of tissue or dispersion of repolarisation. Thus, delivery of a premature stimulus or the occurrence of a VE sufficiently early in an area of dispersion of repolarisation results in failure of impulse propagation and the formation of a line of conduction block. The impulse eventually propagates to areas where the tissue is fully repolarised resulting in circus continuation of the impulse and resultant re-entry arrhythmia.

Although the antiarrhythmic effect of amiodarone is thought to be explicable by homogenous prolongation of repolarisation, PRR without conduction slowing or dispersion of ARI (Kirchhof, Degen, Franz, Eckardt, Fabritz, Milberg, Laer, Neumann, Breithardt, & Haverkamp 2003a). Chronic amiodarone therapy reduces recurrent ventricular arrhythmias without increasing mortality (Connolly 1999;Wyse et al. 2001). However, its tendency to proarrhythmia is well known but the mechanism of this effect is disputed especially as abnormal dispersion of repolarisation was initially thought to be the mechanism of TdP in LQTs. The proarrhythmic effect of amiodarone has been attributed to heterogeneous dispersion of repolarisation especially in LQTs or via after depolarisations that act as a trigger for ectopy and arrhythmia induction (Sclarovsky et al. 1983;Bonatti et al. 1985;Morgan, Lopes, & Rowland 1991). The depolarisation hypothesis is related to the trigger of after depolarisations from Ca^{+2} loading or abnormal handling which may arise in phase 3 of the action potential and result in ectopic activity or ventricular arrhythmia including TdP. Mapping of after depolarisations in humans is usually performed by contact electrodes during MAP recordings and would be considered very challenging with NCM technology. Amiodarone prolongs phases 2

and 3 of the action potential of repolarisation on steady-state ventricular pacing and acts by blocking multiple ion currents in the heart including I_{TO} channels. Amiodarone must have contributed to the reduced magnitude of the ERC in the IHD ventricles.

3.8 Conclusion

The results on electrical and conduction velocity restitution showed no significant difference between high -risk patients with normal hearts and those with a variety of pathological, functional and morphological abnormalities.

This similarity could arise (a) because of changes at the cellular level in those with normal hearts that result from areas of inhomogeneous molecular structure such as from channelopathies of tissue anisotropy and provoke functional re-entry or (b) because the sample studied was too small to reveal significant differences.

Arrhythmic risk appears to be a continuum and cannot be dichotomized because of its multifactorial nature and the contribution of coinciding influencing parameters. There appears to be a correlation between the site of peak S_{max} in the ventricle and re-entrant arrhythmias given the correlation between these sites and VT circuits.

Chapter 4 Spatial dispersion of ventricular activation and repolarisation in pathological human hearts

4.1 Dispersion of repolarisation

Nonuniformity of spatial activation, repolarisation and temporal dispersion in the recovery of excitation has been linked to wavebreaks and the induction of fibrillation (Han & Moe G 1964) This has been studied in limited ventricular sites in the RV and sequentially at multiple LV sites using contact mapping with MAP recordings in patients with previous myocardial infarction and LQTs survivors of VF, compared to normal controls (Vassallo, Cassidy, Kindwall, Marchlinski, & Josephson 1988) and predisposes to re-entry (Kuo, Munakata, Reddy, & Surawicz 1983). However, knowledge of simultaneous global activation and repolarisation dispersion in ventricular arrhythmic high-risk patients with heterogeneity of structural heart diseases compared to equally high arrhythmic risk patients with structurally normal hearts is lacking. I set out to assess the global and local characteristics of activation, repolarisation and recovery in these patients using noncontact mapping technology.

This was conducted in two groups of patients with cardiac pathology; those with structurally normal hearts but sufferers of aborted cardiac death or at high risk from significant family history and those with anatomical substrates for ventricular arrhythmias related to structural heart disease.

4.1.1 Patient demographics

Twenty eight patients were included in this study (13 females, 15 males) with mean age of 54 years. All were eligible for the study as they had clinical need for VT ablation or VT stimulation studies for risk stratification purposes (Figure 53).

Twenty nine *maps* were constructed; 22 from patients with SHD of whom 8 had IHD (one patient had biventricular maps), 4 had DCM, 5 had adult congenital heart disease, 4 had ARVC and 1 had HCM with mean EF 49%, were enrolled into one arm of this study (Figure 54) and compared with 7 patients with SNHs with previous idiopathic VF or channelopathies and high arrhythmic risk, (information presented in Table 6) in the other arm. All patients underwent evaluation with history, clinical examination, resting 12 lead ECG, transthoracic echocardiography and cardiac catheterisation, which included coronary angiography and ventriculography. CMR was only conducted in those patients

presenting for the first time and did not have implanted devices. Coronary angiography excluded acute ischaemia in all patients including those with CAD.

The mean age for this study group was 54 ± 19 years, but a median of 60 years in the SHD subjects and 37 years in those with normal hearts. 16 male patients and 12 females were assessed –7 of who had normal hearts. Measurements of global AT, ARI and RT were obtained during 18 left ventricular and 11 right ventricular studies. Global ventricular activation, repolarisation and recovery time dispersion were calculated during right ventricular extrastimulus testing. Further assessments were conducted during sinus rhythm, spontaneous ventricular ectopy and during the induction of VT. Adjacent dispersion was measured within the same segment but 10 mm away from the original measurement site.

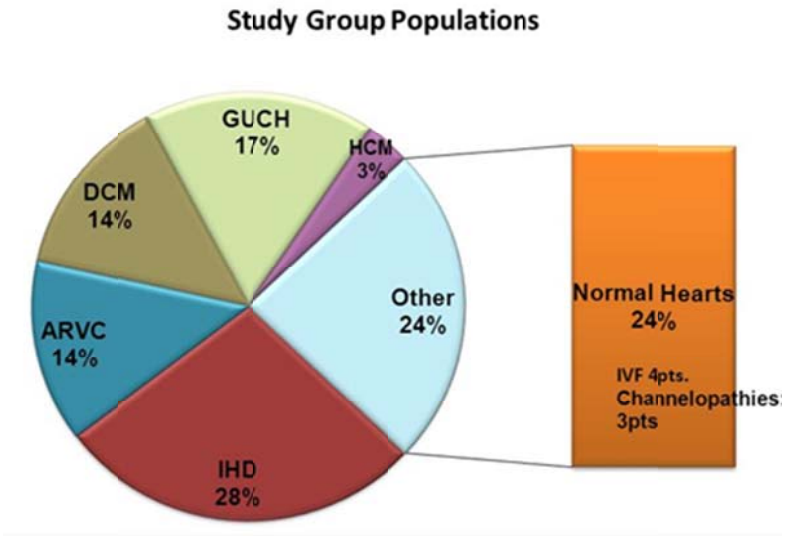

Figure 53 Pie chart of study group diagnoses

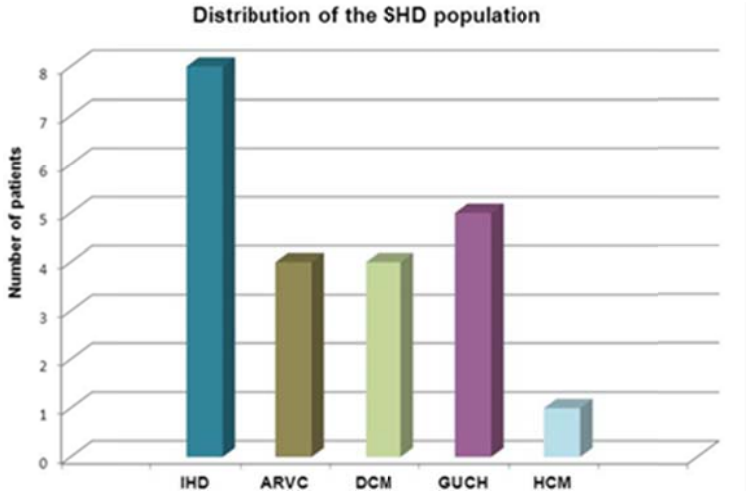

Figure 54 Bar chart of the structural heart disease group

4.1.2 NCM

The technique of using the Ensite system has previously been detailed in chapter 2. The balloon mounted MEA was introduced into the relevant ventricle to be studied. One patient with surgical corrected TGA required placement of the MEA from the superior approach given anomalous venous drainage from the lower limbs. Three-dimensional electroanatomical mapping including the production of isochronal and isopotential maps was performed. Reconstructed virtual UEs and their first derivatives were displayed in pairs in a pre-set template for offline analysis on the workstation. Filter bandwidths were set at 0.1-300Hz for the NCM system for activation and QRS measurements but for timing measurements of the T waves and derivatives of the QRS the filter bandwidth was set at 0.1-25 Hz. Local AT, ARI and RT were taken as previously described with measurements of repolarisation dependent on the T wave morphology (chapter 2).

4.1.3 Global dispersion

Global dispersion, defined as the difference between the longest and shortest repolarisation time in the given chamber related to a specific beat or impulse. Calculated as the range and displayed as means ± SD for AT, ARI and RT for the different impulses.

Dispersion of repolarisation was assessed in SR, at baseline during steady state RV pacing and at short coupling intervals immediately prior to ventricular refractoriness, at the induction of VT and its preceding beat and during spontaneous VEs in 60 maps in the SHD group and 45 baseline maps in the SNH group.

Following flecainide challenge a further 25 maps were assessed for postflecainide evaluation.

4.1.4 Local dispersion

Five selected pairs of points 10 mm apart were analysed in the ventricle at sites with the greatest RT to assess for adjacent dispersion. Local dispersion was defined as the maximum timing difference between these two adjacent sites and was considered significant if > 30 ms difference.

Assessments in the structurally normal heart group occurred at baseline and following flecainide provocation challenge in 4 patients.

4.2 Statistical analysis and results

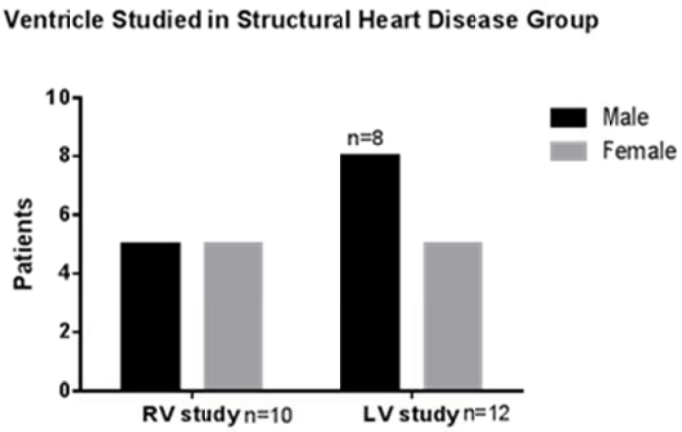

Figure 55 Distribution by ventricle studied

4.2.1 Structural heart disease group

Twenty one patients with an average age of 60 years and ventricular function (EF%) of 36 ± 16%, were assessed from 60 formulated maps: 22 during constant RV pacing at long basic cycle lengths, 17 during SR, 12 during VT, 4 during the preceding VT beat and 5 during spontaneous VE.

In 12 studies the MEA was placed in the LV and in 10 studies it was placed in the RV (Figure 55).

All patients were assessed during constant RV pacing, conducted at basic drive train cycle lengths while establishing steady state. Pacing was at 400 ms coupling interval except in 4 patients when haemodynamic intolerance required pacing at 600 ms. In the 352 investigated beats; the mean AT during RV pacing in the SHD group was 106 ± 26 ms, mean ARI 259 ± 37 ms (range 193 to 353ms) and mean RT 361 ± 46 ms. Global mean AT dispersion was 70 ± 24 ms, whereas mean global ARI dispersion was 99 ± 51 ms and that of RT was 86 ± 43 ms (Table 17).

Assessment of sinus beats was done prior to pacing in 17 patients. In 3 patients there was no SR from pacing dependency (in 2) or permanent AF (in 1). The sinus beat utilised was the fifth consecutive beat. In 272 beats studied mean global AT during SR was 83 ± 62 ms, ARI was 289 ± 63 ms and RT was 388 ± 69 ms. Mean global dispersion of activation during SR in the ventricle was 64 ± 26 ms, with global dispersion of ARI 86 ± 60 ms and RT 79 ± 79 ms. The sites of maximum and minimum ARI recordings in the ventricle were not constant and had no particular pattern.

Although VT was induced in 12 studies it was not possible to assess the timing intervals of the pre-VT beat except in 5 studies because of encroachment of the first VT beat on the preceding T wave. The 21 different VT morphologies induced in 12 ventricles averaged 2 VTs per ventricle, range 1 to 4, with different VT morphologies and average CL of 370 ms (range 270 to 600 ms). Five VTs were induced in the RV studies and 7 in the LV and occasionly with visible evidence of conduction delay (Figure 56- drive train pacing, S_1, of 400 ms and VT is induced after introducing S_2 at 250 ms).

Table 17 Measured AT, ARI, RT and their global dispersions in ventricular endocardium of the structural heart disease group following different beats.

Structural Heart Disease Patients			
Beat	Interval (ms)	Mean ± SD	Dispersion
RVP	AT	106 ± 26	70 ± 24
	ARI	259 ± 37	99 ± 51
	RT	361 ± 46	86 ± 43†
SR	AT	83 ± 62	64 ± 26
	ARI	289 ± 63	86 ± 60
	RT	388 ± 69	79 ± 79†
VT	AT	76 ± 20	72 ± 24
	ARI	259 ± 47	113 ± 47*
	RT	337 ± 47	96 ± 49†
Pre VT	AT	124 ± 62	79 ± 29
	ARI	227 ± 32	134 ± 26
	RT	351 ± 71	119 ± 44†
VE	AT	62 ± 8	59 ± 14
	ARI	278 ± 47	63 ± 21*
	RT	348 ± 58	51 ± 19†

*P= 0.03 † p= 0.026

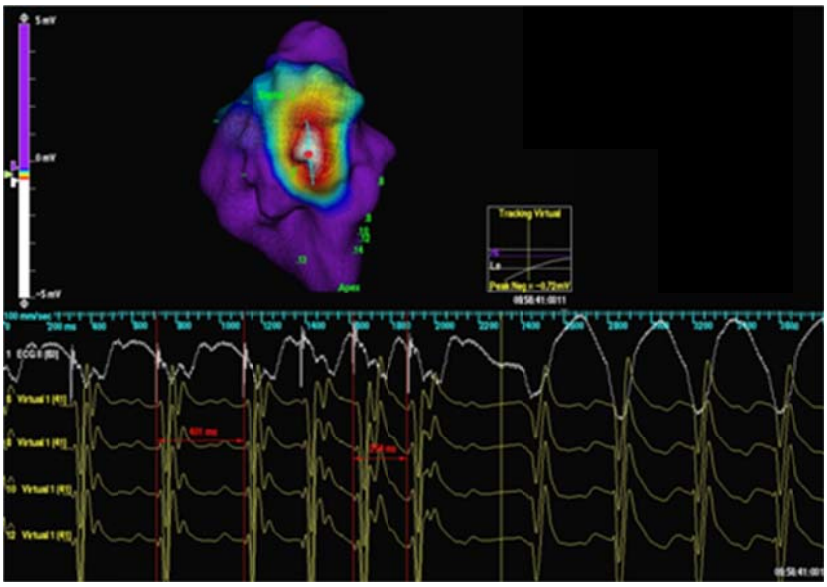

Figure 56 Isopotential 3D map showing VT induction

Mean global AT of the first VT beat 76 ± 20 ms. Mean global dispersion of activation was 72 ± 24 ms whereas global dispersion of ARI and RT were 113 ± 47 ms and 96 ± 49 ms respectively. The sites of origin of the studied VT corresponded to those with the shortest ARI in that ventricle on 42% of occasions, independent of whether the ventricle studied was the LV or RV. And usually from VTs that arose from the septal, inferior and posterior wall of the LV or adjacent to the TV annulus in the RV. It was not possible to correlate the apical LV VTs with particular ARI measurements.

The beat that preceded the induced VT beat- a paced beat- (similar to VT induction with intermediate paced CLs) had a median CL of 270 ms. This was assessed in 80 beats in 16 predefined global ventricular locations. Mean global AT of this beat was 124 ± 62 ms. Mean global ARI was 227 ± 32 ms and RT 351 ± 71 ms. The average global ventricular dispersion of AT in these maps was 79 ± 29 ms, with ARI disperison of 134 ± 26 ms and RT dispersion of 119 ± 44 ms.

Spontaneous ventricular ectopy was assessed in 5 ventricles. They showed considerably prolonged repolarisation with overall mean RT 348 ± 58 ms and mean global ARI of 278 ± 47 ms and mean AT was 62 ± 8 ms. Dispersion of AT, ARI and RT was more homogeneous with interval dispersions of 59 ± 14 ms, 63 ± 21 ms and 51± 19 ms respectively. The AT- repolarisation relationship was coupled and showed an inverse linear relationship, which will be discussed in the following chapter.

Statistical analysis

Analysis of the dispersion for each of the AT, ARI and RT during each of the different beats was conducted using one way ANOVA catered for samples with differing means using the Kruskal Wallis test. P value was considered significant if <0.05.

There was no statistical difference between AT during constant RV pacing, SR, VT, intermediate- short coupled RV pacing (pre-VT beat) and following spontaneous VEs (p= 0.065). Likewise global ARI dispersion across the various beats did not reach statistical signifcance (p= 0.055) (Figure 57 and 58) but there was significant discrepancy between global dispersion of ARI during VT and spontaneous VEs (p=0.03). Additionally global dispersion of RT between the five different beats varied significantly (p= 0.026) mainly because of variation between RT in SR and the first VT beat.

RV vs LV measurements

During constant RV pacing the mean global AT, ARI and RT were very similar in both ventricles; RV measurements: 100 ± 92 ms, 261 ± 38 ms and 362 ± 61 ms respectively, whereas in the LV; 111 ± 21 ms, 257 ± 38 ms and 359 ± 33 ms respectively. Similarly global AT, ARI and RT dispersion was not significantly different between both ventricles. AT dispersion was 64 ± 18 ms in RV compared to 75 ± 28 ms in LV. ARI dispersion of 96 ± 50 ms in RV studies compared to 101 ± 54 ms in the LV and comparatively mean global RT dispersion of 83 ± 53 ms in the RV with 91± 36 ms in the LV.

During SR; global mean AT dispersion 63 ± 24 ms in the RV and 65 ± 29 ms in the LV. The global mean ARI was 269 ± 70 ms in the RV with mean global ARI RV dispersion of 68 ± 21 ms, whereas mean LV ARI was 298 ± 60 ms and LV ARI dispersion of 100 ± 80 ms. The global RT averaged 399 ± 82 ms in the RV and 380 ± 62 ms in the LV with mean RT dispersion in the RV of 59 ± 31 ms compared to mean global LV RT dispersion of 91 ± 105 ms- all of the differences not being statiscally significant (p =0.4 and 0.9).

5 VTs were induced in the RV and 7 in the LV with global AT dispersion of 66 ± 20 ms, ARI dispersion of 125 ± 38 ms and RT dispersion of 89 ± 31 ms in the RV and global LV dispersion of AT; 77 ± 28 ms, ARI 102 ± 54 ms and RT 107 ± 64 ms which were of no statistical significance (p= 0.14 and 0.19).

Thus, there was no significant difference between RV and LV mean AT, ARI, RT or their dispersion measurements in this SHD group.

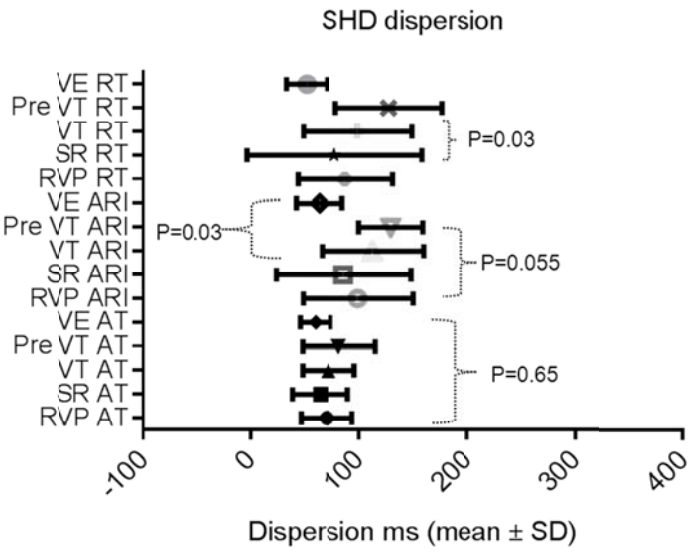

Figure 57 Box and whisker plot of activation and repolarisation during different beats in structurally abnormal hearts

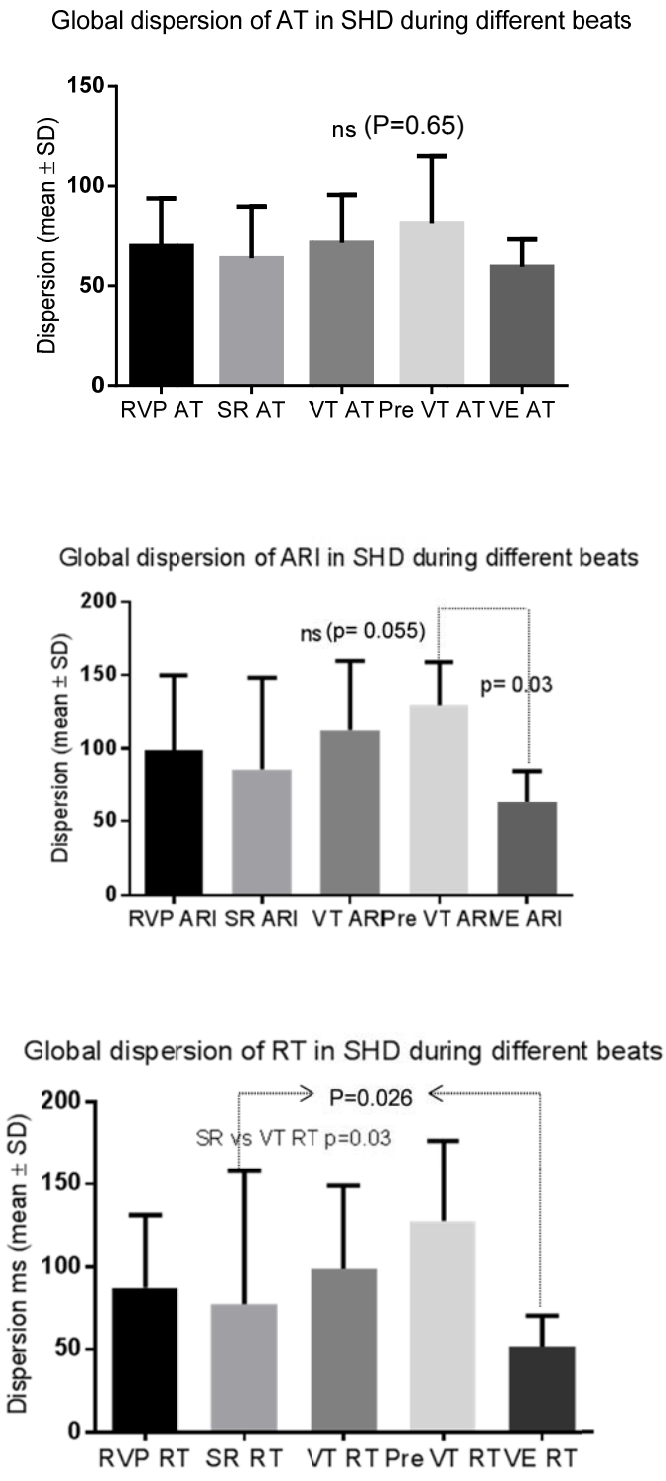

Figure 58 Global dispersion of AT, ARI and RT during different beats in structural heart disease.

Local (adjacent) dispersion

Local dispersion was calculated as the absolute difference between values within the same segment and 10 mm apart. This was assessed during constant RV pacing and SR.

Adjacent dispersion during SR was uniform with AT adjacent dispersion of 12 ± 21 ms, ARI dispersion was 16 ± 23 ms and RT local dispersion was 12 ± 16 ms. Adjacent dispersion in SR was not significant as only 5% of AT, 9% of ARI and 7% of RT adjacent dispersion measurements exceeded 30 ms (p= 0.5, 0.8, 0.4 respectively, ns). However during constant RV pacing, adjacent dispersion was markedly significant with local RT dispersion (p=0.0005) and local AT dispersion (p=0.01). 18% of AT, 22% of ARI and 27% of RT adjacent dispersion measurements during constant RV pacing exceeded 30 ms. Additionally, regional analysis showed sites of local AT and ARI dispersion of 140 ms at the base of the heart and 167 ms at the apex, but the overall effect of these local dispersions were masked with global assessment.

During RV pacing mean local dispersion of AT (25 ± 40 ms), of ARI (24 ± 32 ms) and RT (24 ± 26 ms). Assessment of mean AT, ARI and RT dispersion did not differ significantly between apical and basal segments of the ventricles studied. In basal segments; dispersion of AT was 34 ± 48 ms, ARI was 28 ± 38 ms and RT dispersion was 16 ± 16 ms and in the apical segments; dispersion of AT was 26 ± 49 ms, of ARI was 23 ± 29 ms and RT was 17 ± 21 ms.

Change of pacing site from the RV apex to RV base with fixed pacing CL of 400 ms was performed in 2 studies. This demonstrated that the average same site dispersion of the 16 predefined sites was 37 ± 26 ms for AT, 21 ± 20 ms for ARI and 39 ± 28 ms for RT.

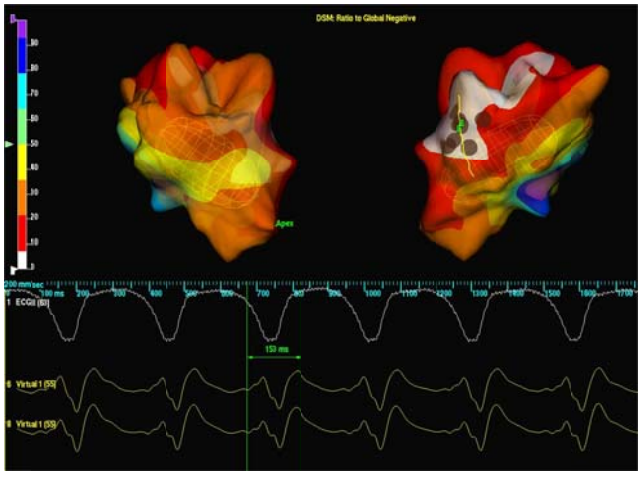

Figure 59 Isochronal endocardial Ensite map during VT (ARI 153 ms)

4.2.2 Structurally normal hearts

Preflecainide1489 points analysed in this group with measurements from 1325 points included in analysis.

Global dispersion at baseline was assessed during constant RV pacing, SR and following a spontaneous VE. Prior to flecainide challenge and during constant RV pacing; mean global AT was 96 ± 16 ms, mean ARI was 236 ± 19 ms and mean RT was 329 ± 25 ms. Global dispersion of AT during RV pacing was 61 ± 17 ms, mean global ARI dispersion of 200 ± 100 ms and RT of 103 ± 54 ms.

Global dispersion of AT during SR was 46 ± 11 ms, with ARI dispersion of 116 ± 80 ms and RT dispersion of 105 ± 96 ms.

However global dispersion following a spontaneous VE was more homogeneous during activation and repolarisation with AT 73 ± 30 ms, ARI 77 ± 20 ms and RT dispersion of 78 ± 23 ms.

Mean local (adjacent) dispersion when assessed at a distance of 10 mm away from the predefined site at baseline conditions prior to flecainide challenge was 16 ± 22 ms for AT, 26 ± 36 ms for ARI and 19 ± 24 ms for RT during constant RV pacing. While regional dispersion within the basal and apical segments of the ventricle during RV apical pacing in the basal region was; AT dispersion of 15 ± 24 ms, ARI dispersion of 26 ± 23 ms and RT dispersion of 18 ± 15 ms and in the apical region; AT dispersion of 7 ± 18 ms, ARI 15 ± 16 ms and RT 13 ± 14 ms. However, geographical dispersion between the apex and base of the ventricle studied in SNH preflecainide showed AT dispersion was 20 ± 8 ms, ARI dispersion 21 ± 18 ms and RT dispersion 21 ± 27 ms.

Post flecainide

After flecainide challenge the global dispersion in the ventricle during constant steady state RV pacing was 60 ± 15 ms for AT, ARI dispersion was 195 ± 41 ms and RT dispersion was 97 ± 31ms (Table 18). This was less heterogeneous during SR where global AT dispersion was 68 ± 25 ms, ARI dispersion was 91 ± 37 ms and RT was 56 ± 32 ms. Only one of the 5 patients who underwent flecainide challenge showed spontaneous VEs following flecainide infusion with marked reduction in global dispersion measurements to AT 49 ms, ARI 66 ms and RT 60 ms. Although flecainide significantly prolonged AT and RT in SNH, dispersion was not affected.

Table 18 The effect of flecainide on AT, ARI, RT intervals and their global dispersions in ventricular endocardium of structurally normal hearts

Structurally Normal Hearts					
Beat	Interval (ms)	Preflecainide		Postflecainide	
		Mean ± SD	Dispersion	Mean ± SD	Dispersion
RVP	AT	96 ± 16	61 ± 17	138 ± 17	60 ± 15
	ARI	236 ± 19	200 ± 100*	234 ± 16†	195 ± 41
	RT	329 ± 25	103 ± 54	370 ± 27	97 ± 31
SR	AT	55 ± 19	46 ± 11	61 ± 25	68 ± 25
	ARI	286 ± 64	116 ± 80*	281 ± 60†	91 ± 37
	RT	341 ± 69	105 ± 96	403 ± 98	56 ± 32
VE	AT	82 ± 29	73 ± 30	...	...
	ARI	274 ± 32	77 ± 20*	...	...
	RT	350 ± 36	78 ± 23	...	...

* p=0.03 † p=0.03

Statistical analysis

Adjacent dispersion of AT, ARI and RT during RVP was not statistically significant with p value of 0.15, 0.7 and 0.9 respectively. Assessment of the effect of global dispersion on each of the timing parameters preflecainide was conducted with one way ANOVA corrected for non-normal distribution using Kruskal Wallis test, this showed that the global dispersion in AT between RV pacing, SR and spontaneous ventricular ectopy and the difference in RT dispersion were not significantly different (p=0.07 and 0.7 respectively). However the dispersion of ARI varied significantly following the different beats (p=0.03) (Figure 60 B, Table 18). Flecainide did not seem to have any major effect on global AT, ARI or RT dispersion as AT and RT dispersion postflecainide did not vary between the different beats, constant RVP to SR (p= 0.3 and 0.1 respectively- Figure 60 A) but ARI dispersion was different between RV pacing and SR (p =0.03).

The value of global dispersion in the macroscopically normal hearts pre and post flecainide of AT during SR or during RV pacing did not differ (p= 0.15 and 0.88 respectively). Global dispersion of ARI pre and post flecainide did not differ during SR (p=0.7) or constant RV pacing (p= 0.7), neither did the global dispersion of RT pre and post flecainide show any significant difference during SR and RVP with p values of 0.2 and 0.99 respectively. However, the dispersion of ARI following constant RV apical pacing increased significantly when compared to SR (p=0.03) and this relationship was not altered or affected in any way by the flecainide challenge (Figure 60 B, Table 18).

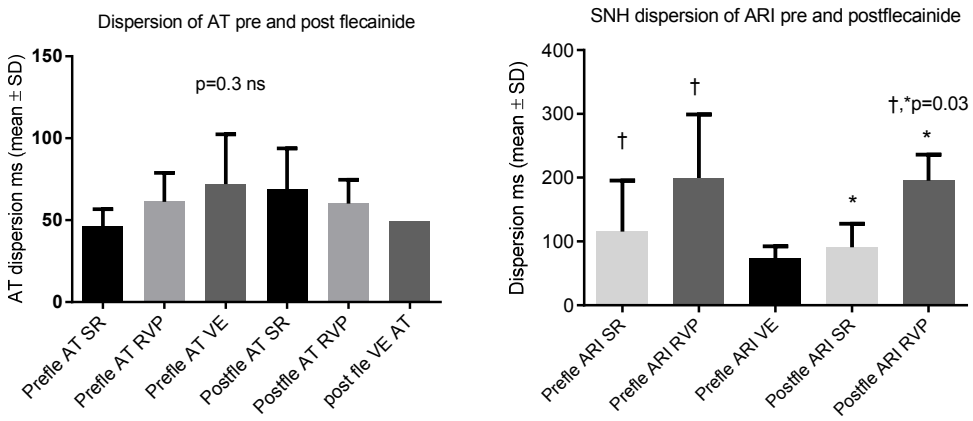

A. **B**.

†, * p=0.03 statistically significant.

Figure 60 Global dispersion of AT (A) and ARI (B) pre and postflecainide during different beats in normal hearts

4.2.3 Dispersion in SHD and SNH

ANOVA was used to assess the significance of dispersion between the structural heart disease group and those with macroscopically normal hearts using the Kruskal- Wallis test and Dunn's multiple comparison test. Global dispersion of AT between the two groups of patients during constant RV pacing, SR and spontaneous VEs did not differ significantly (p= 0.2) (Figure 61). Similarly global dispersions of RT within the studied ventricle during the same beats between the two groups was not significantly different (p=0.58) and this did not differ when comparing the two groups with each individual beat using a two tailed T test. Mann Whitney testing of RT dispersion in the ventricle between the two groups during SR p=0.12, during a VE p=0.19 and during constant RV pacing p=0.47- all non-significant. However, the overall global ARI dispersion encompassing the different beats; constant RV pacing, SR and VE, between the two groups differed significantly (p=0.0025) and this was mainly attributed to the difference in ARI dispersion during constant RV pacing between the SHD and SNH groups (p=0.002) whereas the global dispersion between the two pathological groups did not differ significantly in their ARIs during SR and following a VE (p= 0.14, p=0.68 respectively).

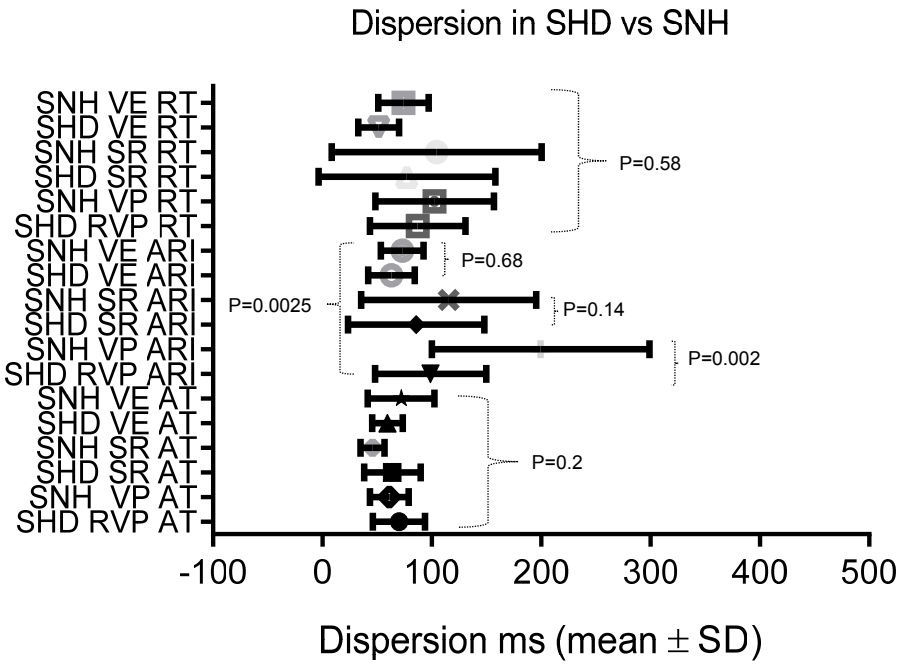

Figure 61 Box and whisker plot comparing global dispersion of AT, ARI and RT during different beats, between structurally normal and abnormal hearts

4.3 Discussion

Universally in the present study compared to known values from the literature, there was delay in activation during SR, spontaneous VEs or RV constant and extrastimulus pacing (Durrer, van Dam, Freud, Janse, Meijler, & Arzbaecher 1970;Vassallo, Cassidy, Kindwall, Marchlinski, & Josephson 1988;Yue, Paisey, Robinson, Betts, Roberts, & Morgan 2004). This delay exceeded that reported by Vassallo et al in their group 2 patients with previous MI and VT, where 12 LV endocardial sites were studied in 6 patients (75 ± 23 ms). Contrary to their findings, the current study demonstrates an exaggeration of dispersion of activation, in addition to the dispersion of repolarisation in the SHD group during steady (ARI dispersion 99 ± 51 ms- Table 17) which is similar to dispersion of refractoriness in their group 3 patients; LQT survivors of SCD (87 ± 27 ms).The results of the current study were in keeping with those from patients with dilated and ischaemic cardiomyopathy reported by (Subramanian et al. 2011). The difference in the dispersion of repolarisation between our studies may reflect the difference in drive train pacing rate on repolarisation (600 ms vs 400 ms) combined with the effects of concomitant antiarrhythmic drug therapy and delayed conduction from anatomical and functional block. Not to mention that activation times rely on tissue heterogeneity, the distance between the site of extra-stimulation and the recording site. Contrary to ATs in normal swine and human ventricles (Gepstein, Hayam, & Ben-Haim 1997b;Yue, Betts, Roberts, & Morgan 2005a) there was an increase in the dispersion of activation which was statistically similar regardless of the type of activated beat, the ventricle or group studied (normal or diseased).

Increase heterogeneity in repolarisation was observed in SHD. Spatial dispersion of repolarisation was particularly manifest with increased prematurity of extrastimulus testing especially at intermediate to short coupling intervals which initiated VT and in recovery times between a sinus beat and a VE. Heterogeneity of refractoriness has been demonstrated to initiate conduction block and facilitate re-entry (Han & Moe G 1964;Kuo, Munakata, Reddy, & Surawicz 1983;el-Sherif, Caref, Yin, & Restivo 1996;Gepstein, Hayam, & Ben-Haim 1997b;Shimizu & Antzelevitch 1998;Yue, Betts, Roberts, & Morgan 2005a). These authors have shown that delivery of an extrastimulus at areas of shortest repolarisation in preconditioned myocardium of open chest dogs or at the time of marked repolarisation gradient resulted in the induction of ventricular arrhythmia from univentricular block and phase 2 re-entry. The exaggeration of global dispersion of repolarisation seen in ventricles of the SHD group was significantly evident during the extrastimulus beat that initiated VT or between SR and VT. This is explicable by the achievement of a certain critical degree of dispersion of repolarisation after which

a single stimulus alone can initiate a ventricular arrhythmia as reported by Kuo et al in their animal model (Kuo, Munakata, Reddy, & Surawicz 1983). Unidirectional block of conduction can result from an introduced extrastimulus beat or VE in the presence of anatomical tissue substrate with inhomogeneous distribution of refractoriness. Heterogeneity of refractoriness by increased, dispersion of repolarisation, dynamic anisotropy and change in conduction velocity all may contribute to the occurrence of unidirectional block. Dispersion was mainly local and regional between nearby segments, paradoxically there was loss of reported geographic apico-basal dispersion which has been noted mainly from animal studies (Autenrieth, Surawicz, & Kuo 1975;Cohen, Giles, & Noble 1976;Potse, Vinet, Opthof, & Coronel 2009). However, local activation and repolarisation were significantly altered in our SHD group even during constant steady state RV pacing. The differences in activation and repolarisation at juxtapositioned sites may allow an excitatory current of significant magnitude to reexcite the fibre or cell with the shorter APD/ARI and thus initiate local re-entry.

Spatial variations in ARI response to RVP in SNH compared to SHD was clearly demonstrated. This was manifested as a significantly prolonged dispersion of repolarisation in SNH post RVP compared to SHD. With tighter coupling intervals during RV pacing, an emergence of ectopic beats occurred, particularly from 250 ms onwards until ERP was reached. Spatial variations in response to ventricular pacing resulted in zones of nonuniform APD gradients with an emphasis on increased ARI dispersion. Tightly coupled VEs that arose in SNH and the VTs that were induced by intermediate to short coupling interval extrastimulation in SHD were probably a product of transmural action potential gradients and phase 2 re-entry (SNH) and figure of 8 re-entry (SHD). Alterations in the action of ion channel currents; namely Na^{+}, Ca^{+2} and the outward K^{+} rectifier (I_{TO}) and their distribution within the myocardial wall may explain the cellular mechanisms of arrhythmogenesis and the ECG manifestations in these SNH patients. However, this is only speculation as these studies were not designed to establish cellular mechanisms.

Although it was anticipated that marked dispersion of repolarisation would be seen in the SHD group, whereby their underlying anatomical and electrical remodelling substrate, namely from localised fibrosis and scar with disruption of gap junction function, would promote tissue heterogeneity, slow conduction and dispersion of refractoriness. The marked delay of repolarisation in the SNH and the significantly increased dispersion of repolarisation in this group compared to the SHD group could be explained by delayed conduction resulting in unidirectional block, which may precipitate re-entry. Additionally, the occurrence of local and adjacent phase 2 re-entry

from transmural ARI gradients resembling the mechanism of APD dispersion in LQTs and Brugada syndrome may also be valid. However, the lack of a significant alteration in activation and repolarisation findings following flecainide challenge in these studies discounts the sole implication of Na^+ channels in their condition but may be related to the significant slowing of conduction post-flecainide which was explained in an earlier section (3.4.4 page 164).

Global dispersion of activation and repolarisation in both study groups was increased with ventricular pacing compared to SR although not significantly so. This resembled the findings of (Yuan et al. 1995) who performed MAP measurements at 2 distant RV sites. Also, I found dispersion of repolarisation increased prior to VT induction (Kuo, Munakata, Reddy, & Surawicz 1983) termed the critical magnitude of dispersion. However, ventricular ectopy shortened activation and repolarisation times and their global dispersion within the ventricle regardless of it being right or left ventricle. My findings differ from those of Yue (2006) where in normal hearts with intact conduction systems and no scar, ventricular pacing reduced dispersion of repolarisation compared to SR. In normal hearts the AT should be less than 82 ms, and 95% of activation has occurred in the LV at intervals less than 70 ms with a mean AT of 54 ± 13 ms (Cassidy, Vassallo, Marchlinski, Buxton, Untereker, & Josephson 1984).

Delayed global activation during RV steady state pacing at 400 ms, was demonstrable in both SHD and SNH ventricles, particularly the latter. The observation of marked alteration in the adjacent dispersion of the total recovery time was primarily a reflection of AT dispersion, explicable by regional variability of activation and the presence of activation gradients persuasively resulting from slowed conduction which concur with findings in Brugada Syndrome, IHD and DCM (Vassallo, Cassidy, Kindwall, Marchlinski, & Josephson 1988;Lambiase, Ahmed, Ciaccio, Brugada, Lizotte, Chaubey, Ben-Simon, Chow, Lowe, & McKenna 2009;Subramanian, Suszko, Selvaraj, Nanthakumar, Ivanov, & Chauhan 2011). Similarly, the increased dispersion of repolarisation in the SHDs may reflect localised tissue heterogeneity, the formation and expansion of progressively expanding arcs of functional and unidirectional block, especially in late activation areas. These may precipitate wave breaks resulting in re-entry VT or VF (Chow, Segal, Davies, & Peters 2004). The effect of acute amiodarone therapy could sufficiently explain the marked dispersion of repolarisation in this group in addition to the contributory effects of other antiarrhythmics, which may exaggerate conduction slowing and enhance uncoupling of activation and repolarisation (chapter 5).

Increased pacing rate and tightening of coupling intervals may result in oscillations from multiple wave breaks precipitating discordant alternans with subsequent arrhythmogenesis this might explain the discrepancy in ARI dispersion during steady state RVP with that of shortened coupling intervals pre- VT induction.

Average ARI and regional variability in right and left ventricles in these high risk patients were similar to those reported by Yue et al (2005b) in patients with normal heart VT. Similar APD_{90} results were described using contact techniques with MAP recordings in patients with IHD and VT induced during pacing at 400 ms drive train (238.1 ± 19.7 ms), with a reduction to 203 ms with S_1-S_2 stimulation 5ms prior to ERP (Koller, Karasik, Solomon, & Franz 1995).

In the present study, the sites of origin of the studied VT corresponded to the sites with shortest ARI timing in the ventricle in 42% of the cases independent of the ventricle studied and this was generally noticed from VTs that arose from the septal, inferior and posterior wall of the LV or adjacent to the TV annulus in the RV. It was not possible to correlate the apical LV VTs with particular ARI measurements unlike the findings of Chauhan et al (2006). However, their study lacked spatial resolution as they only sampled the anterolateral wall of the LV epicardium. Similarly Chow et al demonstrated that areas of abnormal activation linked to the initiation of VF were spatially related to pathways of VT circuits. Their findings linked areas of increased refractoriness to the development of arcs of functional block, late local activation and wavefront fragmentation in patients with previous full thickness myocardial infarctions (Chow, Segal, Davies, & Peters 2004). Rotors, which have been recently implemented in the maintenance of VF, and are found in areas of the myocardium that display the shortest refractoriness and the fastest activation during VF. The emergence of the view that the occurrence of VT or VF depends on a single mechanism whereby the organisation of the electrical waves into rotors; stationary or drifting and the frequency of their rotation will dictate whether the arrhythmia produced is VT or VF (Jalife 2000;Samie & Jalife 2001). The slowing of conduction in the present study from tissue heterogeneity and the effect of antiarrhythmics may well have resulted in a stationary single sustained rotor with an organised rotation frequency that allowed 1:1 activation of both ventricles thereby producing monomorphic VT rather than disorganised VF. Additionally, rapid pacing must have produced oscillations that were spatially out of phase resulting in discordant alternans (Weiss, Chen, Qu, Karagueuzian, & Garfinkel 2000;Weiss et al. 2006).Given the inherent inhomogeneous nature of the tissue in the ventricles studied, spontaneous arrhythmia occurred even without a triggering VE and dynamic heterogeneity could arise from spatial variations in CV restitution (Watanabe, Fenton,

Evans, Hastings, & Karma 2001). Discordant alternans causes alteration in the pattern and sequence of impulse propagation and affects cardiac repolarisation by producing conditions necessary for unidirectional block, resulting in re-entry. The occurrence of a VE or a premature extrastimulation causes conduction block in the region with the most delayed repolarisation, resulting in a line of functional block of which the beat wraps around creating the first beat of re-entry. This may transform physiologic repolarisation gradients into critical pathophysiologic gradients.

Likewise, the effects of cardiac memory (Mironov et al. 2008) and APD accommodation may have limited the effects of the steepness of ARI restitution slopes (S_{max}> 1) in predicting the onset of alternans and producing VF in these patients(Weiss, Karma, Shiferaw, Chen, Garfinkel, & Qu 2006). As restitution is affected by cardiac memory, the ERC may differ during alternans in response to long or short beats demonstrating both temporal and spatial heterogeneity.

4.4 Conclusion

Pathophysiologic dispersion of repolarisation forms a basis for functional re-entry in cardiac tissue. One of the mechanisms for this is spatial heterogeneity of repolarisation. As demonstrated in both groups being similar in their high arrhythmia burden and risk of SCD but differing in the presence of or the lack of a variety of anatomical structural abnormalities. This may act as an arrhythmia mechanism even when cardiac structure is normal probably because of abnormal cell to cell coupling. There was little difference in the electrophysiological characteristics of activation, repolarisation and recovery between the structurally abnormal hearts and the normal hearts in their global dispersion of AT, RT generally and ARI, specifically in SR or following a VE. This supports the theory that macroscopic cardiac structure and anatomical block due to scarring is not the prime determinant of arrhythmia and that microscopic or cellular abnormalities in the high-risk arrhythmogenic groups occurring because of alteration in the function of the ion channels equally matches the risk of dangerous and fatal re-entrant ventricular arrhythmias to those with gross macroscopic anatomical arrhythmia substrate. This suggests a prominent role for functional re-entry and a commonality for the pathophysiology for arrhythmogenesis regardless of underlying structure.

Chapter 5 Activation repolarisation coupling in pathological human hearts

5.1 Introduction

It is believed that the coupling between activation and repolarisation provides stability and serves as a mechanism to preserve homogeneity within the normal heart (Franz, Bargheer, Rafflenbeul, Haverich, & Lichtlen 1987;Gepstein, Hayam, & Ben-Haim 1997b). Tissue heterogeneity and anisotropy has been linked to the occurrence of unidirectional block from an activation sequence eliciting functional re-entry from inhomogeneity of refractoriness resulting in arrhythmias (Osaka et al. 1987) and disturbances in the coupling of activation and repolarisation have been shown to allow the induction and maintenance of arrhythmias in predisposed conditions (1981;el-Sherif, Caref, Yin, & Restivo 1996).

Given the arrhythmia burden in this high-risk group and the obvious tissue heterogeneity and anatomical substrate in the SHD patients, I compared the relationship between activation and repolarisation in them to those with SNH who equally are high-risk patients. This study was conducted on the same 28 patients on whom dispersion data were obtained and analysed as described in the previous chapter (page178).

NCM using the Ensite system allowed global assessment of activation and repolarisation in these patients to investigate activation-repolarisation coupling during RV pacing- steady state and short coupling intervals, SR, spontaneous ventricular ectopy and induced VT.

5.2 Methods

AT, ARI and RT were assessed from 16 predefined sites in the ventricle during RV pacing, sinus rhythm, spontaneous VEs and VT. The method for measuring AT, ARI and RT has been explained in detail in the general methodology and in previous chapters and is dependent on the morphology of the T wave and use of the first derivative of the virtual UE. Constant RV pacing was performed with a woven bipolar catheter at 400 ms and steady state confirmed after continuous pacing for 2 minutes. Data for continuous pacing were obtained after the fifth beat of a drive. Short coupling intervals for S_1-S_2 were defined as the shortest interval that provoked a ventricular response and usually found to be 10 ms prior to ventricular ERP. Intermediate coupling intervals were taken at the 75% interval between basic steady state pacing and refractoriness. SR measurements were obtained from the fifth consecutive sinus beat

prior to any pacing or at least 2 minutes after pacing had fully ceased. Sustained monomorphic VT was induced either during PES for VT ablation (Wellens' Protocol) (Wellens et al. 1985) or during restitution studies. This occurred in 12 studies in which the last extra-stimulus beat prior to the VT induction and the first VT beat were assessed. Spontaneous VEs occurred in 23% of the structural heart disease population and in 71% of the macroscopically normal heart group and were studied. In the SNH group measurements were made at baseline and after flecainide challenge.

5.3 Statistical analysis

Timing and interval data are presented as means ± SD unless otherwise specified. The relationship between activation and repolarisation was assessed using Pearson's correlation coefficient and simple linear regression analysis. Data that were not normal were compared using the Wilcoxon analysis. Two tail t tests were used for pre and postflecainide measurements and non-uniform t tests were used to compare SHD group with SNH. One way ANOVA was used to assess the correlation in the different beats.

5.3.1 Activation repolarisation coupling in structural heart disease

A total of 60 maps were constructed for the 21 patients in this group: 22 for constant RV pacing, 17 SR, 12 for VT, 4 for preVT and 5 for spontaneous VEs. 976 paired AT and ARI measurements were performed. The RT was calculated as the sum of the AT and ARI in ms. The AT was inversely related to the repolarisation and recovery times.
The mean AT during RV pacing 106 ± 26 ms, in SR 83 ± 62 ms, during VT induction 76 ± 20 ms and during VE 62 ± 8 ms. The AT was longer during the pre-VT beat 124 ± 62ms. Whilst the ARI was 259 ± 37 ms during RV pacing at basic drive train CL (400 ms), 289 ± 63 ms during SR, 259 ± 47 ms during VT, 227± 32 at the pre-VT beat but lengthened to 278 ± 47 ms during a spontaneous VE. The mean RT during RV pacing in this group was 361 ± 46 ms, 388 ± 69 ms during sinus beats, 337± 47 at the first VT beat, 351 ± 71ms in the pre-VT beat and 348 ± 58 ms following a VE (See table 17 page 182).

Following constant RV pacing at long cycle lengths the mean pooled correlation coefficient in this group overall was -0.52 (ranging from -0.09 to -0.93) with noticeable least correlation between AT and ARI in patients with IHD and DCM. The inverse linear relationship between AT and ARI was more apparent in the RV compared to the LV studies (-0.59 compared to -0.41 respectively) but not statistically different (p=0.4).

ANOVA showed no difference in the activation repolarisation relationships with the different beats (RV pacing, SR, VT induction, spontaneous VE and pre VT, p=0.46) (Figure 62).

During SR the relationship between AT and ARI was inverse and linear (-0.64) and equivalent in the LV and RV (-0.66 vs -0.62). However the least correlation was found in a GUCH patient with previous TOF repair and VT ablation who had a near flat regression slope (-0.05).

Although the overall correlation in the VT induced beat remained inverse and linear the slope was increasingly flat. This was less so in the LV studies and the correlation was poor and associated with flat regression slopes (-0.15) (Figure 64). This was especially seen in a patient with IHD who experienced VT storm with the induction of 4 different morphologies. This patient also had marked global dispersion of repolarisation with ARI dispersion of 191 ms and RT dispersion of 227 ms.

In the extrastimulus beat preceding the first VT beat, the coupled activation repolarisation relationship is diminished with slight flattening of the regression slope with an overall median value of -0.47 ranging from -0.33 to -0.66. There is marked dispersion in activation, repolarisation and recovery times. However, in the spontaneous VE there appeared to be a relatively tight correlation between AT and ARI with a steep inverse regression slope which on average was -0.68 (-0.58 to -0.89).

The box and whisker plot (Figure 62) shows the mean, maximum and minimum values of the regression slopes for overall ventricular activation repolarisation correlation following different beats. The difference in the regression slopes was not significant. The variation is clear during RV pacing, SR and VT where there is a wide range of discrepancy between the slopes.

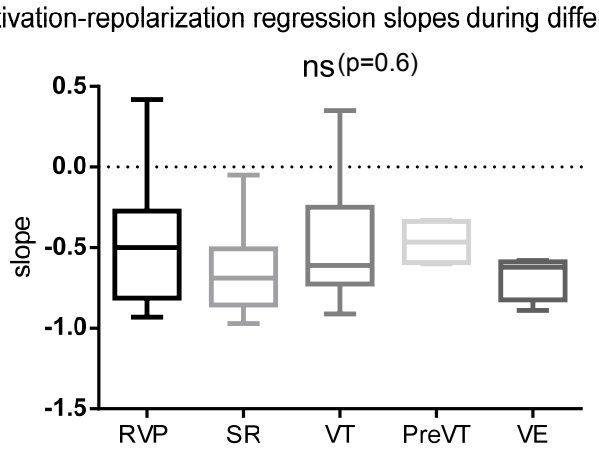

Figure 62 Box and whisker plot showing activation repolarisation regression slopes during different beats in SHD

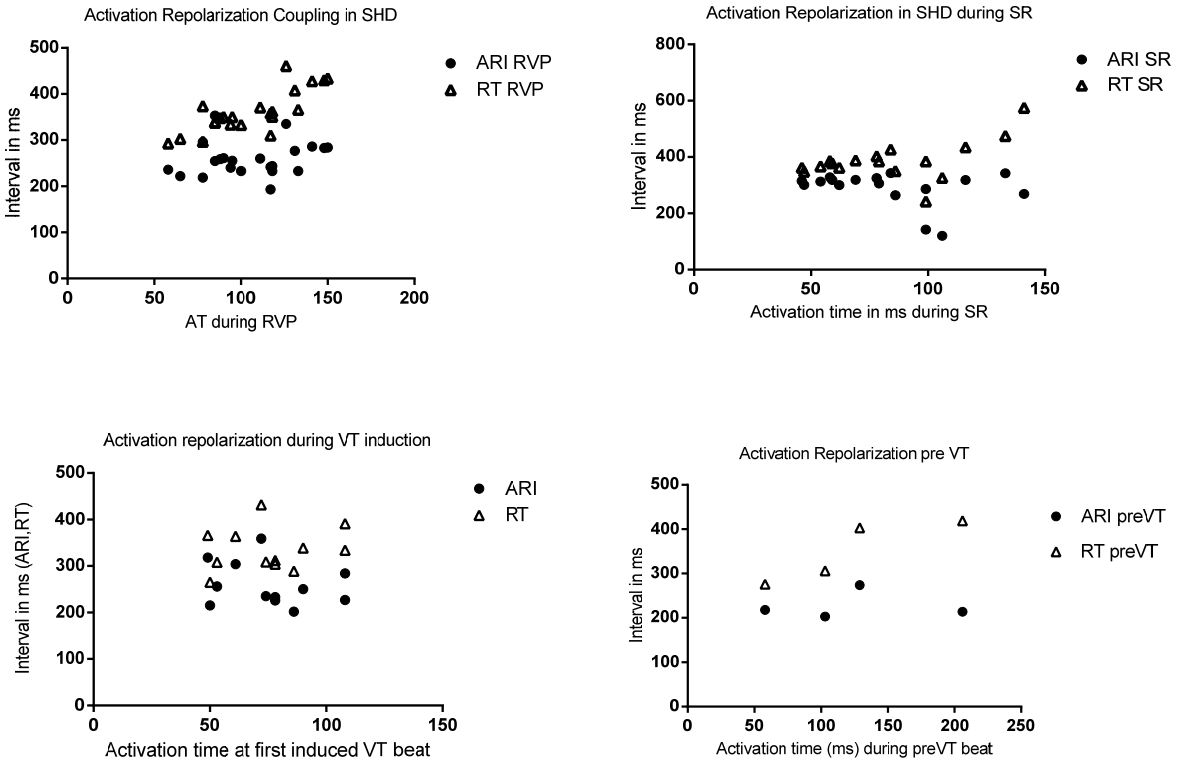

Figure 63 Scatter plot showing activation- repolarisation relationship during RVP, SR, VT, preVT in SHD

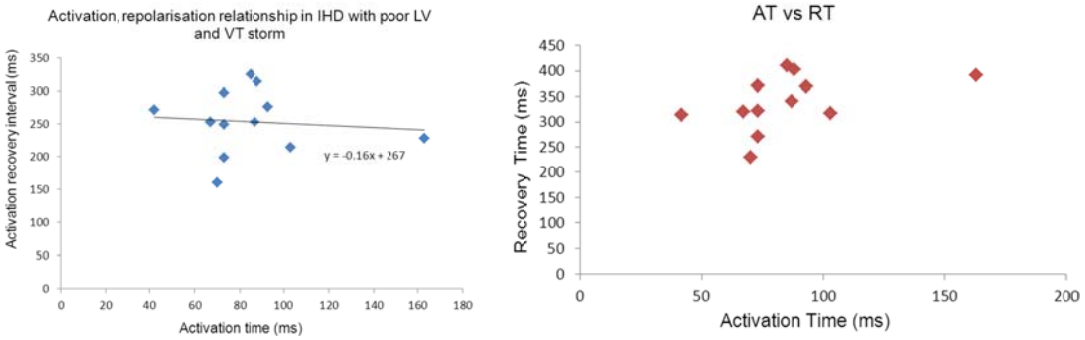

Figure 64 Scatter plot showing the relationship between activation and repolarisation with loss of activation repolarisation coupling, flattening of the regression slope showing poor correlation.

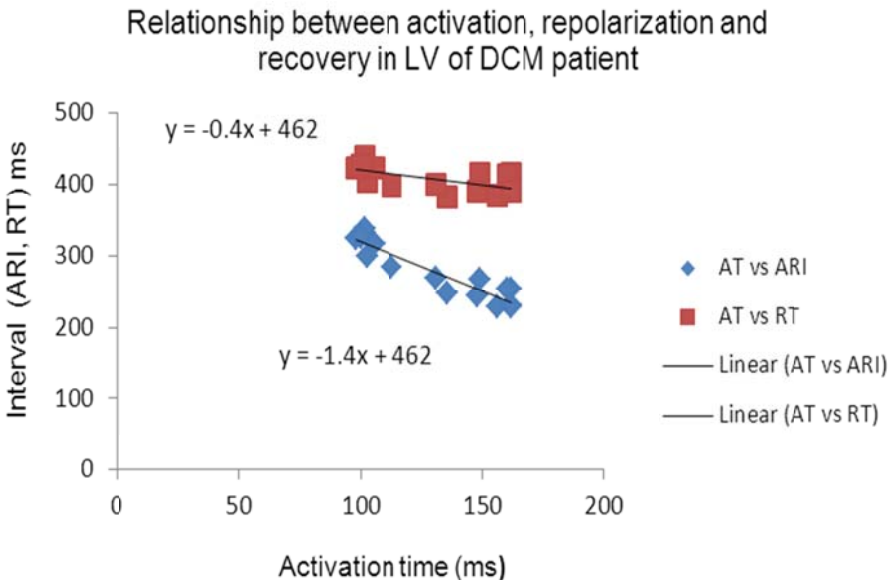

Figure 65 Linear relationship between AT, ARI and RT

Figure 65- showing linear inverse correlation with a straight linear regression line and steep slope of the AT/ARI. There is a direct linear relationship between AT and recovery time.

With the use of the Ensite 3000 NCM system, I was able to demonstrate the coupling of activation and repolarisation in addition to the differing polarities and morphologies of the T wave. This was seen in the LV, RV and during pacing, SR and VT as demonstrated from the diagrams below (Figure 66).

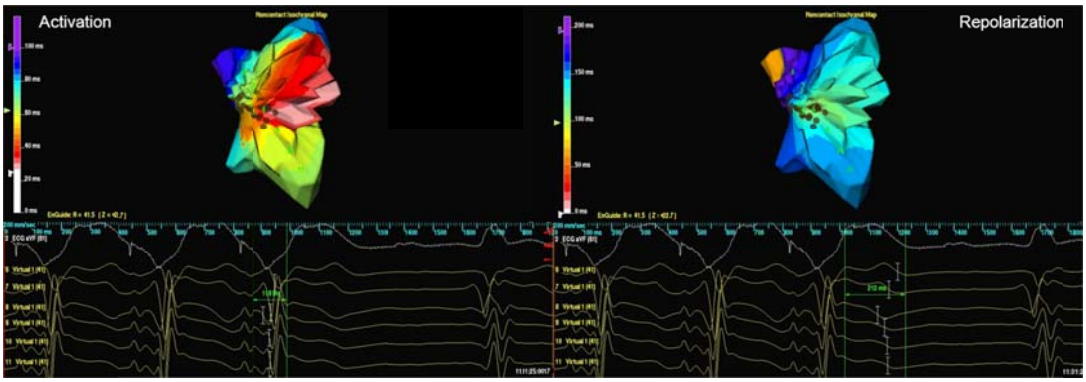

A. RV activation and repolarisation isochronal map during RV pacing

Isochronal map of the LV during RV pacing showing earliest activation point in white followed by red with the reverse occurring during mapping the T wave or repolarisation phase where the earliest repolarisation is in blue and this is shown by the virtual UE with the positive T waves with an alteration in colours depending on T wave morphology.

B. LV activation and repolarisation map during RV pacing

Here on the left panel: I have utilised the filter band widths suitable for the UE and first derivative 0.1-25Hz to demonstrate on the electroanatomic map the activation time during RV pacing for restitution studies. The AT is measured from the beginning of activation until the minimum dV/dt of the QRS. On the right panel the opposite occurs whilst performing repolarisation mapping using the ARI. Note that the activation and repolarisation are linked.

This is also featured during sinus rhythm and VT (Figure 66 C and D). This signifies that although there is flattening of the regression slope in the markedly abnormal arrhythmogenic ventricles, but it is not possible to say that there is a global loss of activation, repolarisation coupling. However, there are the segmental and regional variations where this loss occurs but unfortunately, global analysis of the chamber in totality dilutes and masks the effects of heterogeneous regional areas.

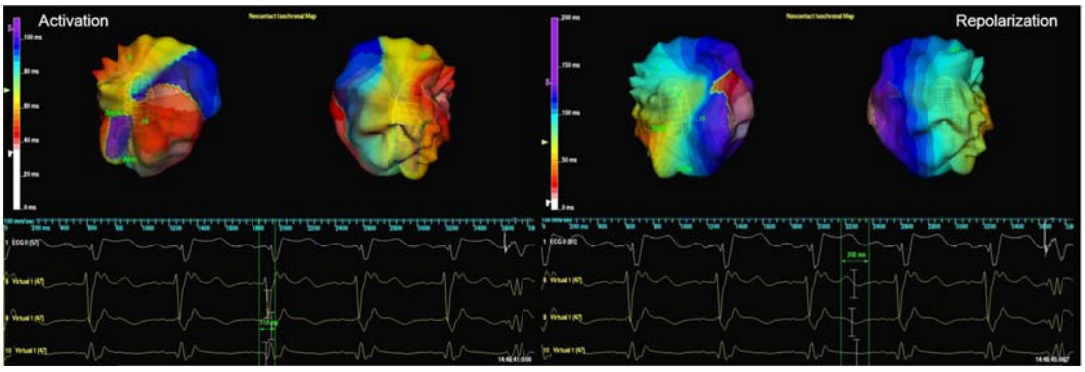

C. Activation and repolarisation map of LV during sinus rhythm

Activation, repolarisation coupling in SR in the LV of a patient with cardiomyopathy and hypertrophied ventricle.

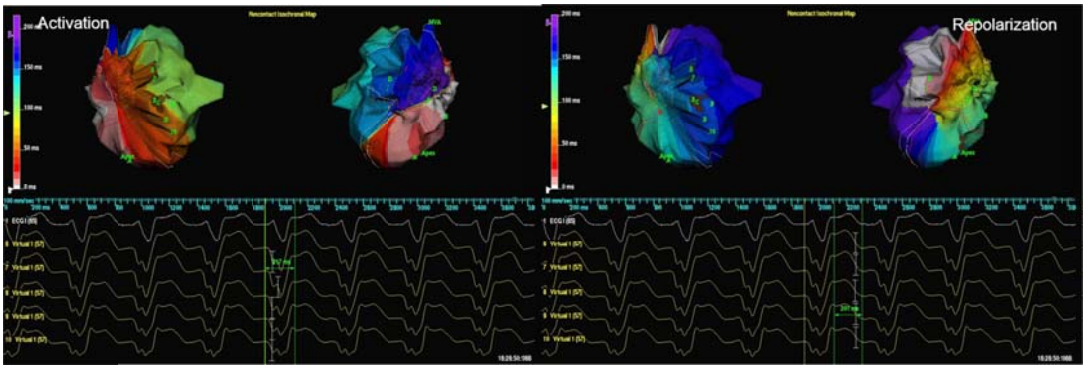

D. Activation and repolarisation maps of LV during monomorphic VT.

Figure 66 Paired isochronal maps during activation and repolarisation (A,B, C, D)

5.3.2 Activation- repolarisation coupling in structurally normal hearts

In the structurally normal heart population, 67 maps were created, of which 42 were at baseline preflecainide. Of the latter 10 were at basic cycle length RV pacing (long), 10 at intermediate coupling intervals (260 ± 34 ms), 10 at short-pre-ventricular refractory period pacing cycle length, 7 during SR and 5 during spontaneous ventricular ectopy. The remaining 25 maps were carried out postflecainide in 5 patients. Only one map was formulated for ventricular ectopy post flecainide challenge because of paucity of ectopic beats following provocation testing in this population.

In SNH the mean AT preflecainide was 96 ± 16 ms during RV pacing at long CL the RT was 329 ± 25 ms. The ARI during steady state following RV pacing at 400 ms was 236 ± 19 ms, at intermediate CL pacing 212 ± 18 ms, with further shortening to prerefractory pacing CL it was 207 ± 25 ms (Table 18 page 189).

The inverse activation repolarisation relationship was maintained during SR at baseline with a median correlation coefficient of -0.65 and straight steep regression line. However; the slope was reduced following the administration of flecainide (Table 19).

During RV pacing at 400 ms, activation remained inversely related to repolarisation in 6 of the 7 patients (85% of the ventricles). In the isolated ventricle that showed loss of activation-repolarisation coupling at a drive train of 400 ms, reduction of the pacing rate restored the coupling. There was also loss of the normal inverse relationship between activation and repolarisation with the increase in prematurity of the extra-stimulus in 2 studies.

During one SR study, the AT was directly related to the ARI with a positive linear correlation (0.58).

VEs also had flatter regression slopes in SNH group similarly supporting their proarrhythmic predisposition with the loss of the protective coupling of activation and repolarisation when they occur at vulnerable periods with short coupling intervals.

Flecainide effect

Following flecainide provocation there was significant prolongation of the AT with mean AT during RV pacing measuring 138 ± 17ms, mean RT 370 ± 27 ms and mean ARI at long pacing CL of 234 ± 16 ms and during short pacing CL to 229 ± 32 ms.

In these patients flecainide showed a tendency to flatten the regression slopes in the RV-paced beats with average correlation between AT and ARI decreasing but not significantly post flecainide (Table 19). Although flecainide did not have a significant effect on the activation repolarisation relationship per se during SR and steady state pacing (Figure 67), it did result in a significant flattening of the regression slope following tightly coupled premature beats (p=0.038). Flecainide also prolonged the AT during basic CL 400 ms RV pacing (p=0.0006) but had no significant effect on the ARI at long, intermediate or short pacing cycle lengths. However because of its effect on the AT it significantly prolonged RT (p=0.03). This and the slowing of activation may contribute to its proarrhythmic effect.

Flecainide abolished the ventricular ectopy in 4 of the 5 patients who underwent flecainide challenge and none of these 5 patients had inducible VT.

Table 19 Activation repolarisation relationship during sinus rhythm, pacing at different cycle lengths and following a ventricular ectopic pre and post flecainide

Beat	Preflecainide	Postflecainide
SR	-0.65 (-0.92 to 0.58)	-0.57 (-0.47 to -0.81)
RVP long	-0.63 (-0.83 to 0.01)	-0.32 (-0.25 to 0.53)
RVP intermediate	-0.53 (0.0006 to -0.81)	-0.44 (-0.17 to -0.57)
RVP short	-0.5* (-0.13 to -0.74)	-0.04*(-0.002 to -0.34)
VE	-0.63 (-0.19 to -0.86)	……..

*p =0.038

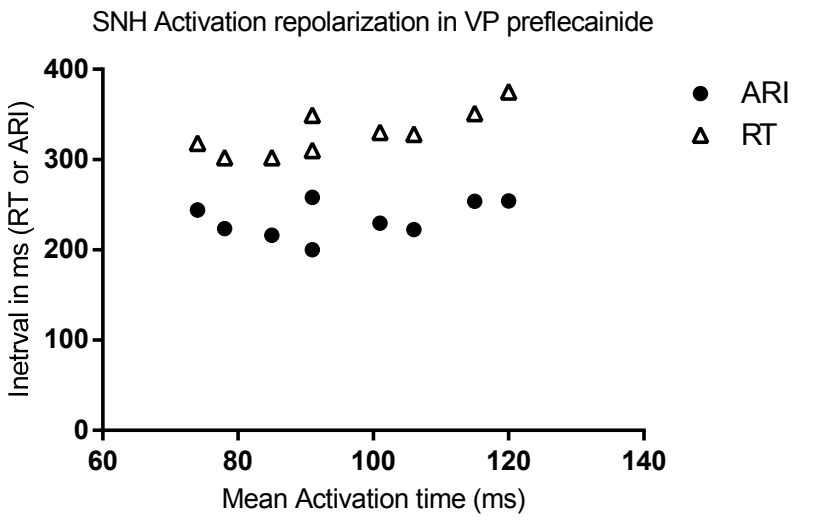

A.

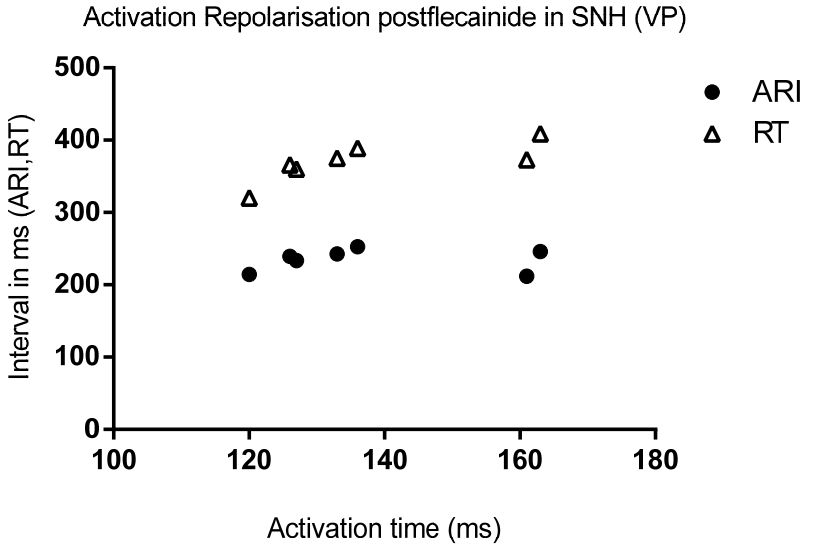

B.

Figure 67 Scatter plot showing effect of flecainide on activation repolarisation relationship during RV pacing pre and post flecainide (A,B)

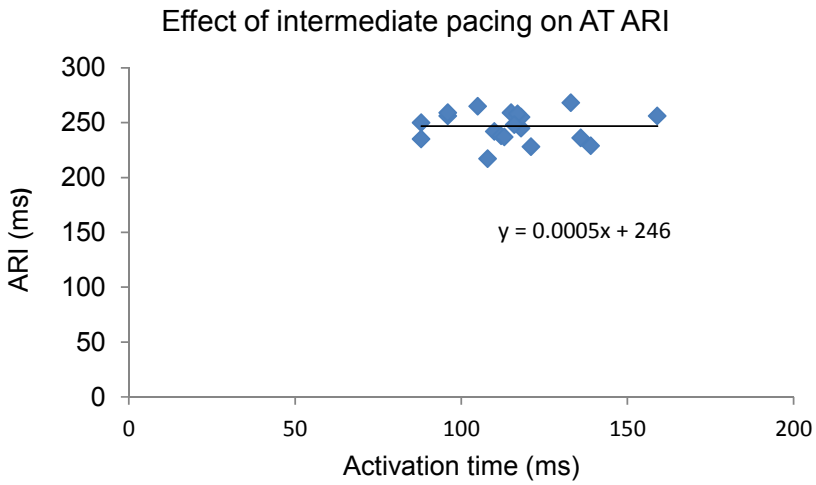

Figure 68 Scatter plot showing relationship between AT and ARI during intermediate pacing cycle length in a structurally normal heart study

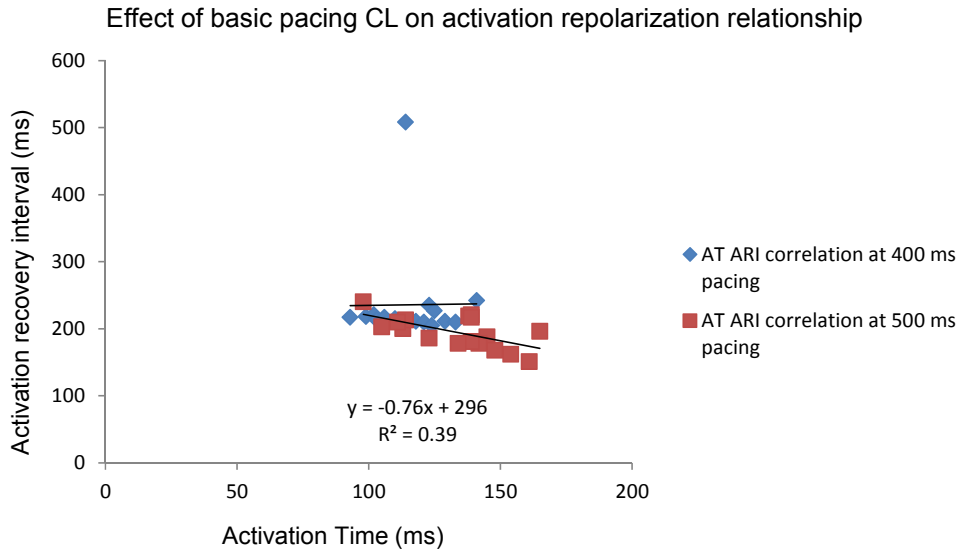

Figure 69 Scatter plot showing the effect of long RV pacing at 400 and 500 ms on AT and ARI in normal heart patient

In figure 69, the scatter plot demonstrates that in the same patient; pacing with a faster basic cycle length flattened the regression slope, as opposed to the maintenance of the inverse relationship between activation and repolarisation that is seen with the faster pacing drive train.

.

5.4 Discussion

The data presented in this study suggest that the relationship between activation and repolarisation in the endocardium of highly arrhythmogenic ventricles was not simple. Although there was an apparently inverse linear relationship between activation and repolarisation this was not a predictive relationship and in an isolated incident it was heart rate dependent. Tightly coupled extra stimuli may facilitate the induction of ventricular arrhythmias, mainly by impairing the normal activation, repolarisation relationship and flattening of their regression slope.

The activation- repolarisation coupling observed during RV apical pacing at baseline (long CI) was more obvious in the RV than the LV compared to that in SR. This relates primarily to the proximity of the pacing site, its distance from the recording site and propagation of activation from the RV to the LV. With increased heart rates, there is decreased conduction velocity restitution magnitude especially at short DIs. In agreement with the findings of Subramanian et al, RV pacing with tight coupling intervals at the preVT induced beat demonstrated an overall disturbance of the activation-repolarisation coupling in these ventricle, probably related to an increase in RT (Gough et al. 1985;Hanson et al. 2009;Subramanian, Suszko, Selvaraj, Nanthakumar, Ivanov, & Chauhan 2011). This was particularly evident in the SNHs following flecainide challenge, due to the conduction slowing properties of the latter. These changes result in global and regional transmural and interventricular gradients that may result in functional conduction block and provide a substrate for functional re-entry arrhythmias.

An exaggeration of this was seen following flecainide provocation in the SNHs. These findings concurred with those demonstrated in nonischaemic guinea pig hearts where flecainide caused a prolongation of endocardial ERP and uncoupling of activation-repolarisation precipitating short lived nonsustained VT in 45% of their studies. This may attribute to the proarrhythmic effect of flecainide (Osadchii 2012). Mechanistically, this may relate from electrotonic modulation and intermyocyte conduction predominately via gap junctions rather than via specialised Purkinjie fibers following premature extra-stimulation or ventricular ectopy, especially with tight coupling (Peters 1996;Peters, Coromilas, Severs, & Wit 1997).

Loss of this inverse relationship was seen in 2 patients with SHD and repeated ventricular arrhythmias. Inhomogeneous impulse decrementation and lack of activation repolarisation coupling in the ventricles has been associated with spatially discordant alternans and increased wavebreak and a propensity to arrhythmogenesis particularly ventricular fibrillation from figure-eight re-entry and amplification of dispersion of

refractoriness (Chow, Segal, Davies, & Peters 2004) (Weiss, Karma, Shiferaw, Chen, Garfinkel, & Qu 2006) . Whilst in the majority of my patients there was maintenance of the inverse activation-repolarisation coupling during different beats including constant ventricular pacing and SR. Flattening of the activation repolarisation regression slope with loss of correlation between them occurred in the patients with SHD when VT was induced which supports the nonlinear relationship between AT and ARI in vulnerable patients to VT and T wave alternans described by (Chauhan et al. 2006). Similar nonlinear relationship between AT and APD was reported by Cowan et al (1988) in 4 patients with aortic stenosis and LVH although not correlated to VT induction. However, the activation- repolarisation coupling persisted during spontaneous ventricular ectopy in the SHD patients. And in SNH group two patients demonstrated loss of activation-repolarisation coupling with increased prematurity of the extrastimulus beat during ventricular pacing and one showed complete uncoupling of activation and repolarisation during spontaneous ventricular ectopy. These resemble the findings described by (Subramanian, Suszko, Selvaraj, Nanthakumar, Ivanov, & Chauhan 2011). This may suggest a supportive role of the close activation repolarisation correlation relationship to be protective against arrhythmias (Franz, Bargheer, Rafflenbeul, Haverich, & Lichtlen 1987;Gepstein, Hayam, & Ben-Haim 1997b).The loss of the inverse linear relationship between activation and repolarisation in morphologically normal hearts may be explained by loss of ion channel function or gap junction remodeling, which may have some influence on the corrected linking of activation and repolarisation. Especially as in pacing models the APD/ARI affects the subsequent DI inversely but is directly affected by the preceding DI and thus there is an effect of memory function with the caveat that APD restitution from pacing protocols may not be truly representative of inherent restitution function.

5.5 Conclusion

In high-risk ventricles, structurally normal and abnormal, repolarisation heterogeneity increases in response to closely coupled RV extrastimuli, which may provide the substrate for re-entrant arrhythmias. This is primarily because of augmented AT dispersion in proximity to the pacing site in combination with markedly reduced activation-repolarisation coupling.

Chapter 6 Repolarisation and T wave maps

Rudolf van Dam and Dirk Durrer in their paper of 1964 suggested that the T wave is caused by electrical fields generated by the spatial and temporal sequence of rapid repolarisation in phase 3 of the MAP and further more they hypothesised that repolarisation is not a uniformly propagated phenomenon even in normal conditions (van Dam & Durrer 1964). Although electrical field mapping in intact dog hearts with transmural electrodes suggested that during SR the transmural gradients are responsible for genesis of the T wave, transventricular gradients are thought to be the culprit following VEs (Spach & Barr 1975) . And when assessing repolarisation sequences using intramural electrodes they found that the T wave at the epicardium was slightly negative in keeping with their postulated antagonism between repolarisation and depolarisation (van & Durrer 1961) whilst it was “diphasic” in the transmural recordings. However, they could not assess or predict the temporal sequence of repolarisation across the LV given their point by point measurements using transmural needle electrodes.

We are still striving to identify accurate non-invasive methods to risk stratify patients at increased risk for fatal ventricular arrhythmias and SCD. Various groups have utilised different techniques including QT interval dispersion as a simple marker for spatial dispersion of ventricular repolarisation but its utility was limited by measurement inaccuracies (Kautzner, Yi, Camm, & Malik 1994;Savelieva, Yi, Guo, Hnatkova, & Malik 1998;Malik and Batchvarov 2000;Batchvarov and Malik 2000). The T wave residuum was assessed and established as a prognostic marker for heterogeneity of ventricular repolarisation in a follow-up study in US veterans by (Zabel et al. 2002).

This chapter deals with patterns of T wave morphology in the two groups of patients presented in chapter 3. Here I assessed the T wave morphology during constant ventricular stimulation during construction of the restitution curves ranging from basic CL pacing (long CLs) which was 400 ms except – as described in the methods chapter- for those who did not tolerate pacing at fast CLs or responded with repeated ventricular ectopy which made interpretation and interval measurements impossible and inaccurate. T wave morphology was assessed from at least 16 global predefined ventricular sites and at decremental CL from baseline steady state pacing down to ventricular refractoriness. The morphology of the T wave was classified into positive, biphasic and negative during offline data analysis on the silicon graphics workstation. These were then manually uploaded directly or from another program eg Excel into a custom written Microsoft software programme (Heat Map Generator version 1.0) which generated a coloured schematic polar image of the ventricle using an arbitrary primary colour scheme dependent on the percentage and density of T waves at the specific point with positive T waves displayed as red, biphasic T waves as green and negative T waves as blue. They were also assessed in sinus rhythm in 13 patients, following a spontaneous VE in 5 patients and after the induction of VT, during the first VT beat in 6 patients.

6.1 T waves in SHD

T wave morphology was interpretable in 4882 beats during the restitution curves of 16 patients with SHD; 45% were positive in morphology, 40% were negative and 15% were biphasic (Table 20). The predominant morphology of the T wave in any given study was either positive or negative but not biphasic. The distribution of the positive and negative T waves were split equally between the population of the SHD patients with the majority of the IHD studies displaying predominantly positive T waves (4 out of 6 patients, 67%). All the DCM patients had predominantly negative T waves. In the IHD population, it was noted that the positive T waves during the restitution studies were always found to be positive at the scar border and around the RF ablation sites. In the ARVC patient the overall positive T waves occurred at sites of shorter ATs compared to the negative T waves, these were found to be similar in SR but drastically differed in T wave morphology following spontaneous VE although the AT did not change significantly but the ARI lengthened. The T wave morphology was compared between the different beats using non-parametric testing (Mann- Whitney test) with unpaired t- testing. 221 T waves were assessed in SR, 84 following a spontaneous ectopic beat and 96 following the induction of VT. The change in T wave morphology compared to RV pacing and SR was highly significant following a spontaneous VE where the predominate T waves changed

to positive, 79 %,(p=0.005). Additionally following the induction of VT 67% of the beats had positive T waves which differed significantly with the T wave morphology during SR and RVP (p=0.04). 71% of the RV studies had a marked predominance of positive T waves globally.

The morphology of the T waves did not differ significantly by altering the basic CL of pacing during restitution studies as demonstrated in the two panels of the polar diagram of the LV during 400 and 500 ms restitution curves (Figure 71).

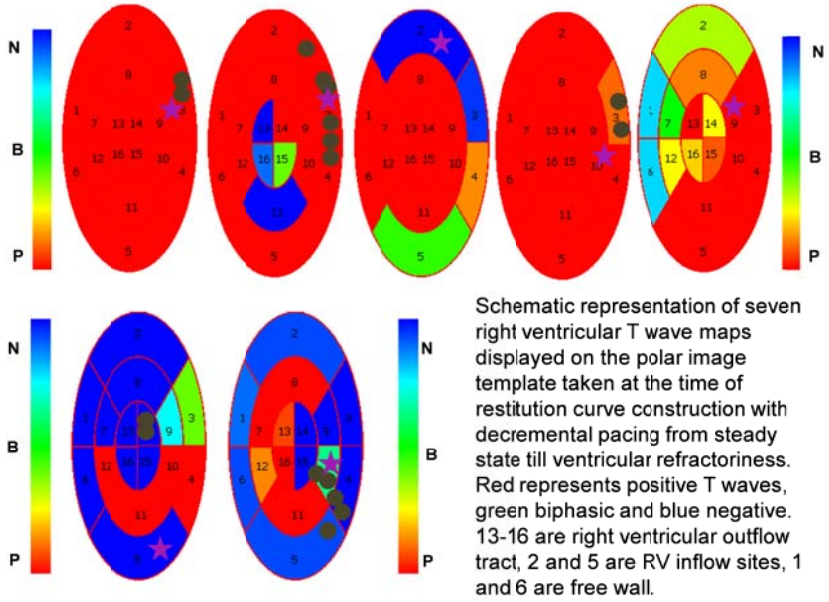

Figure 70 Polar diagram of T wave distribution map during restitution curve of the right ventricle.

The brown dots represent ablation points and the purple star represents the site of S_{max}.

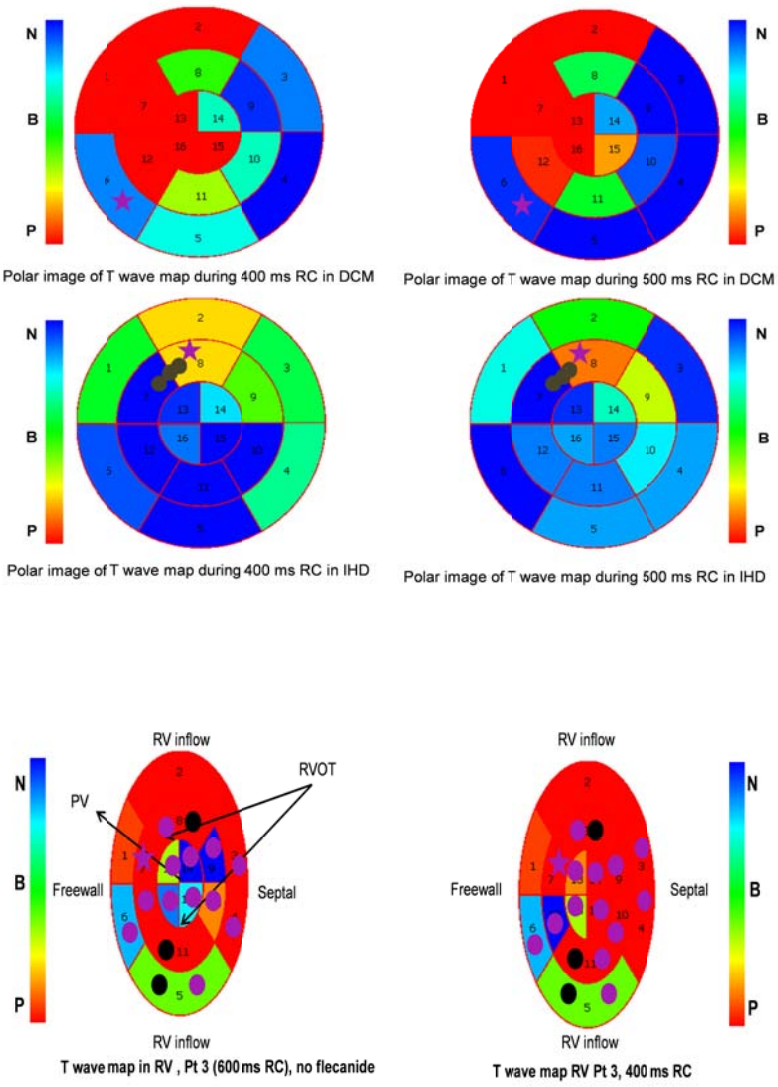

Figure 71 Polar diagram displaying the effect of change in basic cycle length of restitution pacing on T wave maps in the LV and RV

The demonstrated colour scale where N indicates negative (blue), B is biphasic (green) and P is positive (red).

Table 20 Density and percentage distributions of T wave morphology in patients with structural heart disease

Pt No	Ventricle	Dx	Negative	Biphasic	Positive	Total
1	RV	ARVC	144	53	62	259
2	LV	IHD	98	63	33	194
3	RV	GUCH	42	15	182	239
4	LV	DCM	118	28	108	254
5	LV	IHD	89	30	79	198
6	LV	DCM	357	43	1	401
7	LV	CMO/HCM	182	34	6	222
8	RV	GUCH	14	52	126	192
9	LV	IHD	176	86	227	489
10	LV	DCM	67	42	109	218
	LV	DCM	91	36	79	206
11	LV	IHD	120	48	69	237
	LV	IHD	120	56	35	211
12	LV	DCM	84	24	74	182
13	RV	GUCH	177	8	66	251
14	RV	GUCH	20	14	141	175
15	LV	IHD	0	33	207	240
	RV	IHD	0	0	224	224
	LV	IHD	6	27	88	121
	RV	IHD	0	3	252	255
16	LV	IHD	63	15	36	114
Total	LV= 14 RV= 7		1968	710	2204	4882
Percentage			40	15	45	

Table showing the patients with SHD, their diagnostic subgroup (Dx) and the T wave morphology for every beat during the construction of the electrical restitution curve from 16 predefined global ventricular sites. LV= left ventricle, RV= right ventricle. Pt No= patient number.

6.2 T waves in SNH

6.2.1 Baseline T wave morphology in SNH

From the 1367 T waves that were assessed in this group at baseline prior to any provocation studies, 56% have negative morphology and 22% were biphasic. The positive T waves were a minority representing only 16%. During these analyses it was necessary to exclude 6% of the beats from analysis because of ambiguity it was impossible to correctly describe their morphologies.

6.2.2 The effect of flecainide on T wave maps during restitution studies

Seven patients were part of the structurally normal heart group of which four had suffered a previous cardiac arrest as their index presentation. During construction of ERCs for these patients by decremental RV pacing following steady state till ventricular refractoriness 1367 T waves were assessed globally from six LVs and one RV and a further 1291 T waves were assessed globally following flecainide challenge (Table 21, Figure 72). 6.6% of T waves were not suitable for analysis and thus excluded because of their ambiguous appearance. 56% of T waves during construction of the restitution curves were negative, 22% were biphasic with either an initial positive deflection and subsequent negative part or vice versa and only 16% of T waves were truly positive during restitution curve pacing prior to flecainide provocation. Flecainide provocation was performed in five patients, and there was no significant difference between the morphology of the T waves before and after flecainide with the predominate morphology being negative (46%).

Table 21 Percentage distribution of T wave morphology in patients with structurally normal hearts pre and post flecainide

T wave morphology	Preflecainide	Postflecainide	Total
Positive	220 (16.1%)	250 (19.4%)	470 (17.7%)
Negative	763 (55.8%)	595 (46.1%)	1358 (51.2%)
Biphasic	301 (22%)	352 (27.3%)	653 (24.5%)
Ambiguous-Excluded	83 (6.1%)	94 (7.3%)	177 (6.6%)
Total	1367	1291	2658

Figure 72 Polar images of T wave maps of the LV endocardium pre and post flecainide

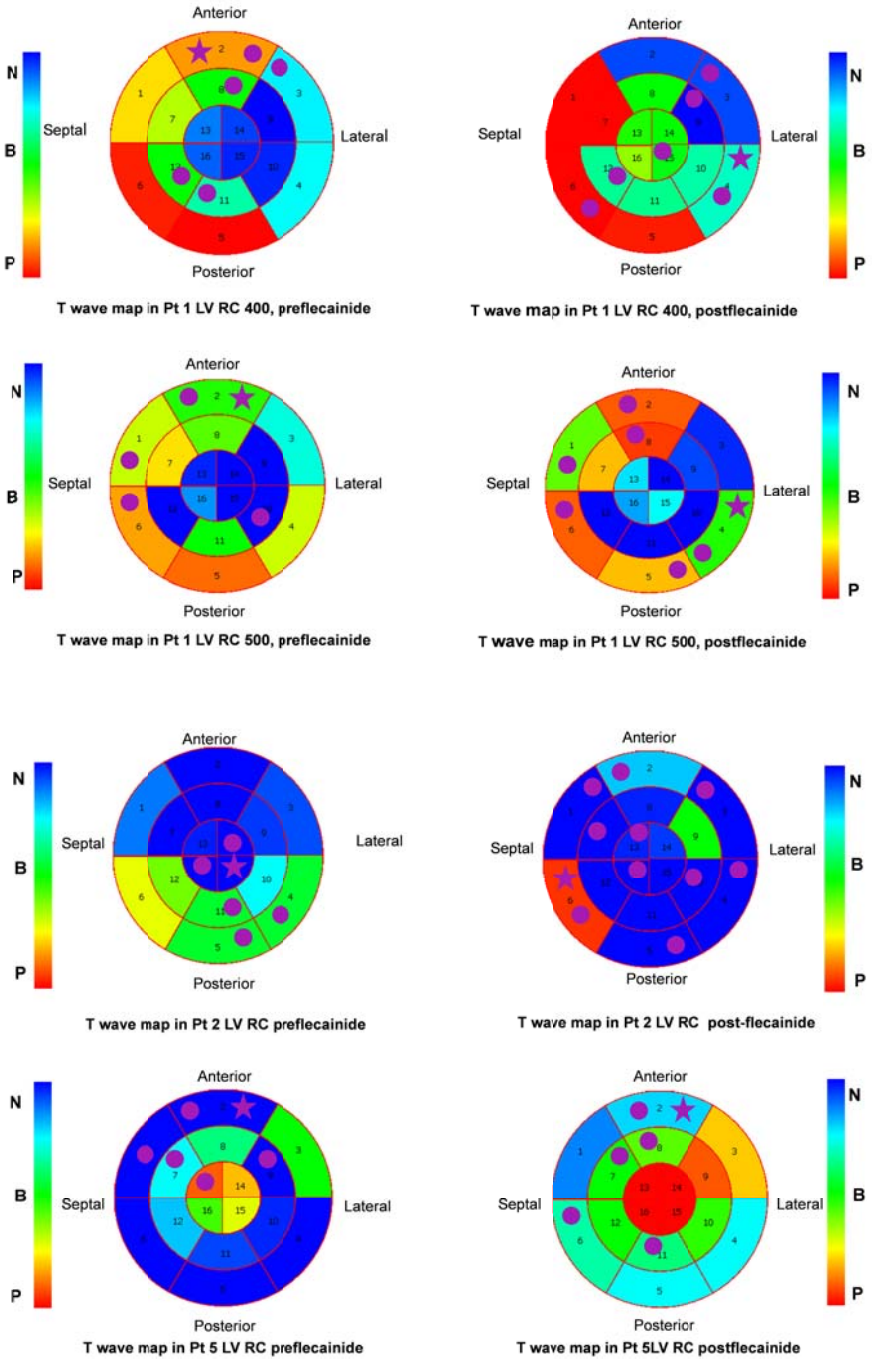

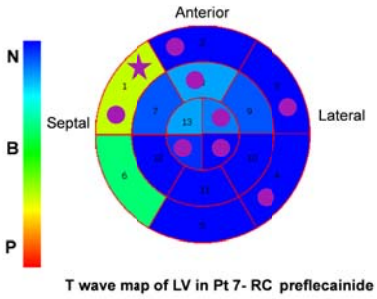

T wave map of LV in Pt 7- RC preflecainide

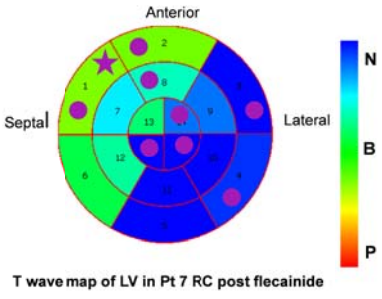

T wave map of LV in Pt 7 RC post flecainide

RC= restitution curve, purple stars are sites of S_{max} , purple dots indicate S_{max} > 1.

6.2.3 T wave mapping during SR and VE

During preflecainide assessments in SR 113 T waves were assessed globally from seven ventricular studies and 48.7% of these were positive and the rest were equally distributed between of negative and biphasic (25.7%). However, following spontaneous ventricular ectopy, as seen in the SHD group, alteration in T wave morphology to negative occurred in 46% of 83 analysed beats while 41% remained positive. Following flecainide provocation no further spontaneous VEs were seen but 54% of the T waves during SR were positive, 33% were negative and 13% were biphasic.

The difference in T wave morphology between SR and VE and between SR pre and post-flecainide had p values of more than 0.1.

6.3 Limitations

I could not compare activation and repolarisation patterns in the RV to those in the LV in structurally normal hearts as I had only one patient in whom the RV was studied. Although he had a structurally normal heart and normal resting ECG he had VF storms triggered by RV VEs. These were mapped successfully and in sequence from the basal RV free wall and inferior apex. This patient continued to experience VF and ICD storms over the years with at least an annual ablation and thus eventually required surgical disarticulation of the RV.

6.4 Discussion

The present study assessed the global distribution of T waves in the studied ventricle during constant steady state right ventricular pacing, restitution curve construction with long, short and intermediate paced beats, SR, following a spontaneous ectopic beat and

during VT induction. The overall distribution of the T waves in the present study resembled findings from (Chen, Moser, Dembitsky, Auger, Daily, Calisi, Jamieson, & Feld 1991) in their epicardial assessment of patients with pulmonary hypertension. Predominantly the T waves in structurally damaged hearts were positive in morphology and this was noticeably so at the edge of the scar border, following VEs and with the induction of VT in the LV studies and in the majority of the RV studies occurring overall in 67-79% of beats. However, of interest the DCM group on the contrary had mainly negative T waves and this was reflected in the distribution of the T wave morphologies in the SNH patients which similarly showed mainly negative and followed closely by biphasic T waves. These results did not alter with flecainide provocation. The aforementioned findings may support the proposal by some groups (Lambiase, Ahmed, Ciaccio, Brugada, Lizotte, Chaubey, Ben-Simon, Chow, Lowe, & McKenna 2009;Nademanee, Veerakul, Chandanamattha, Chaothawee, Ariyachaipanich, Jirasirirojanakorn, Likittanasombat, Bhuripanyo, & Ngarmukos 2011) that the channelopathies and their occurrence result in a localised molecular cardiomyopathy with the progression of the condition as described. However, T wave polarity may progressively alter with progression of the disease state, as a response to cardiac memory and in response to drugs and severe electrolyte changes. Haws and Lux described their biphasic T waves as only ever having an early negative followed by a later positive deflection. They showed from their experiments on dog hearts that T wave polarity may alter with alteration of the pacing site and with sympathetic stimulation (Haws & Lux 1990). However, the ARIs they recorded remained unaltered as they used the Wyatt method to determine the end of repolarisation and they did not assess restitution dynamics. Arguably, Kuo and Suwaricz showed alteration in T wave polarity in canine studies where the stellate ganglia were stimulated. Changes in MAP duration in their study correlated with changes in T wave polarity. They concluded that T wave is a sensitive indicator of relatively small changes (<20 msec) in the sequence of ventricular repolarisation (Kuo and Surawicz 1976). Recovery waves, unlike activation waves, are thought to be the passive of slow velocity and have opposite polarity to activation.

6.5 Conclusion

T wave mapping allows an easy visual assessment of the global distribution of T wave polarities in the ventricle studied. When incorporated onto a single map, detailed information regarding the sites of maximum restitution slopes, S_{max} dispersion and

ablation sites may aid to establish a link between the behaviour and distribution of T wave polarity adjacent and distant from areas of tissue heterogeneity and slowed conduction. Repolarisation maps may be tied to activation maps, which may corroborate the characteristics of abnormal areas of slow conduction and assist in mechanistic differentiation of substrates where dispersion of recovery is primarily due to activation delay, from those conditions that arise from pure repolarisation delay.

Chapter 7 Repolarisation parameters- potential markers for risk stratification

7.1 Background

To assess the effect of steepness of the restitution slope and dispersion of repolarisation on the prognosis of the twenty two patients who underwent a combination of restitution and dispersion studies (Table 4, Table 5) they were followed up on average for 26 ± 15 months (range 3 weeks to 5.5 years). The end point was sustained ventricular arrhythmia that required therapy be it anti-tachycardia pacing or internal defibrillation from their device in patients with ICDs, external defibrillation, antiarrhythmic drug therapy or over drive pacing in the few patients without ICDs or death. Most of the follow up data were retrieved retrospectively from their hospital records, from device clinic follow-ups and interrogations, clinic attendances, hospitalisations and GP correspondence. Only 8 patients reached the primary end point (36%). There were 4 deaths (18%) and 4 patients (18%) had therapy for sustained ventricular arrhythmias. Two patients were lost to follow up one after 3 weeks and the other after a year. Both patients were from the SHD group and one had familial DCM with mild LV dysfunction and no implanted device as no previous documented ventricular arrhythmias whereas the other had an ICD for secondary prevention from IHD. Survival was defined as time to first event or end of follow-up.

Eight patients had events after a median of 19 ± 10 months. The 4 deaths occurred in the SHD group with a median duration of 23 months following VT ablation, one death was arrhythmic in nature and the remaining 3 had pump failure. The four patients who required therapy were distributed equally between the SHD and SNH groups and needed therapy at a median of 17 months after they were studied. One patient had over drive pacing without shocks but the remaining 3 (75%) had appropriate ICD shocks. One patient had appropriate therapy for VF 20 months after her first presentation, and suffered subsequently from inappropriate shocks from noise related to a faulty lead, which was on an advisory recall (Sprint Fidelis lead, Medtronic Inc).

Table 22 Demographic and restitution parameters in the events group versus the nonevents group

Parameters	Died/VT/Shocks, n=10	No events, n=12
Age	61 ± 14*	44 ± 21*
Gender (M %)	70%	50%
EF % of systemic ventricle	33 ± 19†	50 ± 17†
VERP	205 ± 18	218 ± 37
Global Smax	1.13 ± 0.49	0.85 ± 0.21
Local Smax	2.6 ± 1.37	2.15 ± 1.07
Smax dispersion	2.26 ± 1.3	1.85 ± 1.04
ARI Mg%	12 ± 5	12 ± 5
CV maximum	0.17 ± 0.1	0.16 ± 0.12
CV Mg %	28 ± 7	25 ± 11
AT dispersion (RVP)	70 ± 24	65 ± 23
ARI dispersion (RVP)	111 ± 83	136 ± 92
RT dispersion (RVP)	80 ± 26	86 ± 53

* p= 0.03, † p=0.04

The electrical characteristics including restitution kinetics and demographics of these patients using univariate analysis (Table 22) showed that impairment of the systemic ventricular function (usually LV) was predictive of events whereas measures of dispersion of activation and repolarisation including global and local S_{max}, dispersion of S_{max}, ARI and RT dispersion did not correlate well with the occurrence of events (p ns, values 0.1- 0.7). There were no significant differences between the groups except in their age and the degree of LV dysfunction. In two of the patients from the event group there was almost total loss of the inverse relationship between activation and repolarisation. This was not observed in any patient from the no event group. In patients with SNH who had recurrent arrhythmias one required four ablations over five years of a VF precipitating VE that was mapped to different locations in the RV and eventually required surgical disarticulation of the RV from LV with resultant RV dilatation and dysfunction to prevent further arrhythmias that could induce shock therapy.

The SHD group had an event rate of 40% that became 53% with added consideration of 2 patients who were lost to follow-up. The SNH group had an event free survival of 72% over an average duration of 5 years. Thus, 37% of the sample had events from 4 months to 3 years after their presentation with an average of 19 months, resulting on average in 1 out of 5 deaths (20%) within 2 years.

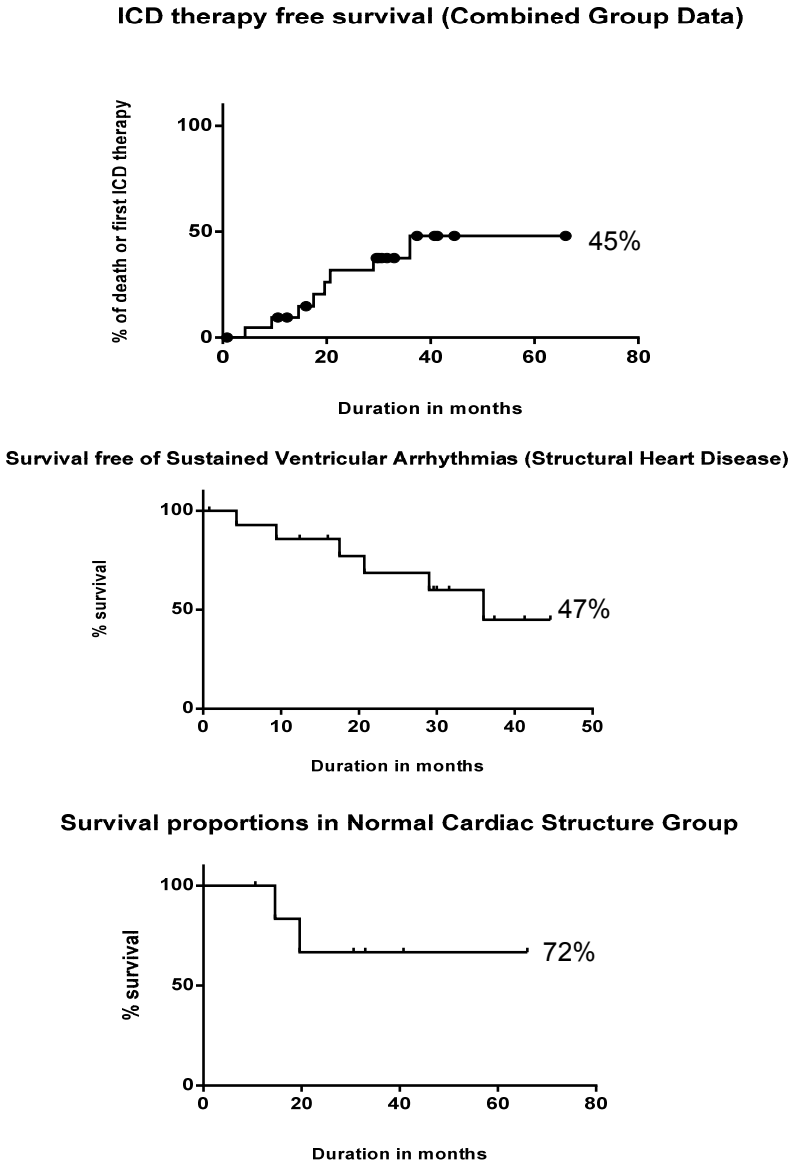

Figure 73 Event free survival in the study groups combined and segregated

7.2 Discussion

Our follow up data suggested that over a median follow up of 2 years, 20% of the pooled patient population had suffered ventricular arrhythmia or death. This occurred in both the structurally normal and abnormal hearts groups. Although overall survival was worse in the morphologically abnormal hearts which may be directly related to their older age and poorer ventricles. Our follow-up results are in keeping with the results of

MADIT trials and those shown in the pilot study from Leicester, as 23% of their patients had a ventricular arrhythmia or died. These similar findings occurred despite the difference in pathology of our patient populations (Moss, Hall, Cannom, Daubert, Higgins, Klein, Levine, Saksena, Waldo, Wilber, Brown, & Heo 1996;Moss, Zareba, Hall, Klein, Wilber, Cannom, Daubert, Higgins, Brown, & Andrews 2002;Nicolson et al. 2011a;Nicolson et al. 2011b). A probable explanation of arrhythmias in the high risk SNH group is that slowing of conduction occurs from the development of lines of functional block. This results in dynamic dispersion of repolarisation in non-scared myocardium (Misier, Opthof, van Hemel, Vermeulen, de Bakker, Defauw, van Capelle, & Janse 1995). Anisotropy and inhomogeneity of tissue architecture from electrical and anatomic remodeling (of tissue and ion channels) and the occurrence of functional conduction slowing (Peters & Wit 1998). These circumstances may precipitate phase 2 re-entry with the occurrence of a VE that becomes the first reentry beat of an arrhythmia. Or a randomly occurring VE may find a suitable substrate with unidirectional block, to perpetuate a circus reentry resulting in VT. The mechanism of which I have already explained in detail in the discussion of earlier chapters; 3-5.

7.3 Limitations

This small sample could not provide data useful for prognostic purposes. It relied on data collection, mainly retrospective from case notes and device follow-up clinics similar to registry data. The 2 patients lost to follow-up had a significant effect on the interpretation of the data.

7.4 Conclusion

The data displayed are in keeping with well-known facts that LV systolic function has a significant impact on patient prognosis with an inverse relation between the two. However, given the limitations outlined above I am unable to utilise the data further to aid in prognostic predictions. Nonetheless, by conventional risk predictors we already know that this patient group is high-risk. Whether global and local dispersion of repolarisation or S_{max} dispersion can aid in prognostication remains to be assessed and will require larger sample sizes and prospective study design with a control group. One very disturbing conclusion is that despite ICDs and advances in arrhythmia ablation we are still unable to prevent these sudden deaths.

Chapter 8 Conclusions

8.1 Thesis Conclusions

SCD continues to be a leading cause of death in the adult population. Although many efforts and advances have been made over the last 20 years at identifying vulnerable populations mainly those with CAD and impaired EF, however because of the numerous factors that come into play and the probabilistic nature of SCD it remains a very complex subject and its prediction by risk stratification techniques remains sub-optimal especially in patients with structurally normal hearts.

This thesis examined the characteristics of repolarisation and the T wave in two groups of patients with high arrhythmia burden and increased risk of sudden cardiac death. The aim of this work was to characterise repolarisation, restitution and conduction velocity parameters in these two groups who are at high risk of fatal ventricular arrhythmias and SCD but with completely different cardiac structure.
This is the largest collection of data from patients with highly arrhythmic pathological hearts examining electrical and conduction velocity invasively in a global manner using NCM. The characteristics of activation and repolarisation in these dissimilar groups of patients support a common pathophysiologic pathway for arrhythmia induction.

Activation recovery interval and conduction velocity restitution were examined globally and regionally in the right and left ventricles of these patients using virtual unipolar electrograms from reconstructed three dimensional endocardial maps produced by the Ensite noncontact mapping system. The electrical and CV restitution properties were similar in both high arrhythmic risk groups regardless of variations in their pathological, morphological and functional characteristics suggesting a commonality in the pathophysiology of arrhythmogenesis perhaps related to changes- in their ventricular myocardium- at the cellular and molecular levels with local fibrosis or myocyte uncoupling. This was supported by the observation of complex fractionated electrograms in the ventricles of patients with structurally normal hearts during programmed electrical stimulation and sinus rhythm suggesting areas of slow conduction even during resting conditions regardless of whether they had normal or abnormal 12 lead ECGs. Their ventricles also displayed frequent and markedly steep ARI restitution slopes similar to the results of the structural heart disease group.

Additionally, alteration in pacing cycle lengths during construction of restitution curves changed the ventricular segment in which the maximum restitution slope occurred. This also supports the likelihood of a functional substrate developing in response to altered restitution dynamics with shortened diastolic intervals rather than a mere anatomical substrate acting as the basis for arrhythmia precursors.

It is paramount to perform both global and regional assessment of the ventricle to truly characterise the effects of electrical and conduction velocity restitution. Global assessments alone dilute and mask activation and repolarisation dispersion which is a feature of regional and local tissue heterogeneity and is exacerbated by conduction slowing. Moreover, my results showed that in these pathological human hearts, steep ARI restitution slopes were regionalised to the segments where ablation terminated the VT. Hence, suggesting their association with critical pathways of ventricular arrhythmia circuits. And similarly the predilection seen of the origins of VT in patients with structural heart disease to sites with the shortest repolarisation timings which corresponded to the septal, inferior and posterior walls of the left ventricle and to the right ventricular inflow sites also illustrates the importance of local tissue heterogeneity seen in structural remodelling.

The electrical restitution curve in high risk arrhythmogenic ventricles is complex in its appearance and influenced by many factors associated with multi-ion channel recovery and deactivation that cannot be explained by simple linear or mono-exponential curves.

The uncoupling of activation and repolarisation was seen in these highly arrhythmogenic human ventricles, both in the structurally abnormal and structurally normal hearts. Both subgroups, particularly the SNHs, demonstrated delayed activation compared to control values from the literature in low arrhythmic risk ventricles. The loss of the inverse relationship between activation and repolarisation timings occurred during the induction of ventricular tachycardia in the structurally abnormal hearts and following spontaneous ventricular ectopy and with tightly coupled paced extrastimuli in structurally normal hearts. This acts as another factor increasing the vulnerable window for the occurrence of ventricular arrhythmias, perhaps related to electrotonic currents resulting from loss of an inherent myocardial stabilizer.

These findings have enhanced our understanding of the commonality of the pathophysiologic basis for arrhythmogenesis in high-risk human ventricles regardless of their aetiology.

NCM can determine the dynamic change and dispersion of repolarisation between global and closely opposed endocardial sites. It could potentially be a powerful risk stratification tool if it had an algorithm that permitted quick real time analysis particularly in patients with a readily identifiable repolarisation pattern.

Given that manual measurements using the Ensite NCM technology appear to be reproducible and display low inter and intra observer variability. The reliability and concordance of measurements is important for future development of a software package, which would allow instant global repolarisation measurements, construction of electrical restitution curves and T wave morphology identification using this system.

8.2 Limitations

NCM technology has been validated for repolarisation assessments using ARIs against APD_{90} MAPs in structurally normal hearts (Yue, Paisey, Robinson, Betts, Roberts, & Morgan 2004) and its usage in activation mapping in pathological hearts across different beats (Schilling, Peters, & Davies 1998;Schilling, Peters, & Davies 1999a;Strickberger, Knight, Michaud, Pelosi, & Morady 2000) along with scar identification using the dynamic substrate function (Jacobson, Afonso, X, Eisenman, Schultz, Lazar, Michele, Josephson, & Callans 2006) has been scrutinised successfully against contact mapping. Given the system's accurate identification of even low voltage fractionated EGMs including diastolic, presystolic potentials and areas of slow conduction of VT exit sites I extrapolated its utility in the assessment of repolarisation studies in the SHD group from findings of previous activation studies. However direct comparison and validation of NCM's virtual UEs in scar tissue against MAPs in repolarisation studies is lacking. The correlation between scar mapping by incorporating images from previous CMR scans using the Verisimo segmentation tool (Ensite version 6.0 software) was not available during the enrolment phase of this study.

There are inherent technical difficulties with the NCM methodology in correctly identifying the morphology of some electrograms and its impact thereafter on the accurate measurement of the DIs. This is particularly evident in progressive disease states, during short coupling intervals and rapid heart rates and following pharmacologic provocation, which can hinder the correct assessment of the end of repolarisation using the technology hereof and hence may contribute to the on-going controversies surrounding the precise method of measuring ARIs particularly in positive T waves (Wyatt, Burgess, Evans, Lux, Abildskov, & Tsutsumi 1981;Chen, Moser, Dembitsky, Auger, Daily, Calisi, Jamieson, & Feld 1991;Yue, Paisey, Robinson, Betts, Roberts, & Morgan 2004;Coronel, de Bakker, Wilms-Schopman, Opthof, Linnenbank, Belterman, & Janse 2006;Potse, Vinet, Opthof, & Coronel 2009).

I excluded an average of 5% of the recorded beats from analysis of the structurally normal and grossly abnormal hearts because of ambiguity of the T wave morphology, because local repolarisation could not be reliably determined from those beats. This was 5-fold higher than that described by Yue et al (2006) but less than the 8.5% of beats excluded by Thiagalingam et al (2004a). The difference illustrates the complex electrograms that are seen in patients with extensively damaged hearts and more tissue heterogeneity from anatomical obstacles but also from local cardiomyopathic and functional changes in the SNH patients (Martini, Nava, Thiene, Buja, Canciani, Scognamiglio, Daliento, & Dalla 1989;Coronel, Casini, Koopmann, Wilms-Schopman,

Verkerk, de Groot, Bhuiyan, Bezzina, Veldkamp, Linnenbank, van der Wal, Tan, Brugada, Wilde, & de Bakker 2005;Frustaci, Priori, Pieroni, Chimenti, Napolitano, Rivolta, Sanna, Bellocci, & Russo 2005)Lambiase 2009 and Nademanee 2011). However, I do not believe that the excluded data would have had a major impact on the results since the global assessment of the ventricles with predefined sites of measurements and greater detail on the spatial heterogeneity by adjacent point assessments within a 10 mm distance would have compensated for the excluded beats.

Inability to compare activation and repolarisation characteristics between the LV and the RV in high risk patients with structurally normal hearts given the limited data available from only one RV study in that group of patients.

My patient populations were relatively small and of heterogeneous pathology and the follow-up period was too short for definitive risk profile and prognostic assessments. These findings need to be evaluated in larger studies especially for the prognostication, as similarly previous retrospective data from 12 lead ECG QT dispersion were initially promising as a marker for repolarisation heterogeneity in the 1990's, where subsequent prospective trials did not confirm its clinical benefit (Zabel et al. 2000).

8.3 Future directions

The 3D mapping system has become essential in the electrophysiology laboratory, praticularly for ventricular arrythmias and the Ensite system is an established diagnostic tool that facilitates delivery of therapy via ablation epsecially in patients with haemodynically compromising arrhythmias. Although emphasis so far has been on facilitating activation mapping, the identifcation of complex repolarisation syndromes particularly in the younger populations makes the development of a facility to conduct real time repolarisation mapping a goal to achieve. Nonetheless, the data produced in this thesis were very labourous and relied on many hours of offline analysis.

We have seen from the GUCH disease cohort that high risk patients could be potentially differentiated from those of lower risk and although this population have underlying structural heart disease as their substrate for ventricular arrhythmias, the relative reassurance obtained from the assessment of the restitution slopes and the curative role of ablation in the lower risk groups that correspond to the sites of maximum slopes could be incorporated into an algorithm that targets these areas during ablation. This may facilitate further risk stratification and avoid unnecessary defibrillator implanation for primary pevention in these young patients who are likely over their life time to succumb to serious chronic complications from device implantation.

Further investigation is needed in high risk normal heart conditions particularly related to areas of local fractionation. Perhaps future research in similar inherited conditions would aid to answer whether these are precursors to fatal arrhythmic conditions in these populations and would there be any gain in treating them prophylactically in family members of sudden cardiac death survivors or whether they can be used as markers for risk stratification purposes.

Knowledge from a more homogeneous study group e.g the LQT, Brugada or early repolarisation syndrome population and development of risk stratification methods to differentiate survivors of SCD in those with structurally normal hearts and abnormal ECGs as opposed to those who have a normal hearts and normal ECG recordings.

The future requires a partnership between clinical electrophysiologists, industry and biomedical engineers or physicists to incorporate these labour intense concepts of electrical and conduction velocity restitution into a rapid functioning algorith that will allow real time analysis directly in the cardiac catheter lab.

Appendix A Patient information sheet version 5.1

Southampton NHS
University Hospitals NHS Trust

Wessex Cardiothoracic Centre
Mailpoint 46
Southampton General Hospital
Tremona Road
Southampton SO 16 6 YD
Tel : 02380798676

A study of the heart repolarization process with noncontact mapping technique

Patient information sheet (study group)

You are being invited to take part in a research study. Before you decide it is important for you to understand why the research is being done and what it will involve. Please take time to read the following information carefully and discuss it with friends, relatives and your GP if you wish. Please ask us if there is anything that is not clear or if you would like more information. Please take time to decide whether or not you wish to take part in this study.

Consumers for Ethics in Research (CERES) publish a leaflet entitled 'Medical Research and You'. This leaflet gives more information about medical research and looks at the questions you may have. A copy may be obtained from CERES, PO Box 1365, London N16 0BW.
Thank you for reading this.

What is the purpose of the study?

Patients with abnormal cardiac repolarization and some structural heart disease conditions are at risk of sudden death due to dangerous fast heart rhythms. Cardiac repolarization refers to the process by which the electricity of the heart recovers following a contraction cycle. Normally this process happens simultaneously within the whole heart chamber. Some individuals are born with a tendency to have abnormal cardiac repolarization, where the electrical recovery process occurs at different rates in different regions of the heart. The result is a predisposition to dangerous fast heart rhythms. Other people become prone to develop dangerous heart rhythms following conditions that damage the heart muscle which results in some degree of weakness for example heart attacks, viral inflammations of the heart muscle (myocarditis) or due to certain hereditary conditions affecting the heart muscle (certain cardiomyopathies).
Some individuals are at high risk of developing dangerous heart rhythms and will require treatment with an implantable cardioverter defibrillator (ICD), a device that treats dangerous heart rhythms by administering an electric shock. However, some are at low risk, and may not require any specific treatment at all.
At present, there is no test that allows us to distinguish between these two groups of patients reliably. Noncontact mapping is a technology that allows the study of electrical activities within the heart chamber and determines changes in many regions of the heart very quickly. We believe that noncontact mapping will help us to understand which patients have high risk of developing dangerous fast heart rhythms and thus may have increased risk of sudden cardiac death. This study will provide valuable information to guide appropriate treatment in the future. The duration of this study is estimated to be 30

to 45 minutes. The study will take place at the Southampton General Hospital, between March 2003 and December 2007.

Why have I been chosen?

You have been chosen to take part in the study for one of these reasons:
1- Because heart tracings (electrocardiogram, or ECG) from your relatives or yourself have shown some changes that may be caused by abnormal cardiac repolarization.

2-You have had a dangerous heart rhythm (ventricular tachycardia) in the past and you may be at increased risk of sudden cardiac death as compared to the general public or have a strong family history of sudden cardiac death.

3- You have had a previous cardiac arrest caused by a heart condition.

4- You have a hereditary progressive heart condition which has been associated with a higher risk of developing dangerous heart rhythms along with a strong family history of cardiac arrest or sudden cardiac death.

5-You have been scheduled on clinical grounds to have the focus precipitating the dangerous heart rhythm ablated using the noncontact system.

Your doctor believes that a study of the heart electrical activity with noncontact mapping technology may help to work out the risk of developing dangerous fast rhythms in the future. If you agree to participate in this study, you will be one of *20-30 patients* who will be evaluated.

Do I have to take part?

Your participation in the study is voluntary, will cost you nothing, and you will not be paid. If you decide not to take part in the study, this will neither affect the quality of your medical treatment nor your relationship with your doctor.

If you choose not to be involved, you will undergo a routine coronary angiogram and heart electrical study (electrophysiological study) as planned and be followed up in the usual way by your doctor.

What will happen to me if I take part?

If you agree to take part, the study will be carried out at the same time as your heart electrical study (electrophysiological study). You would normally have undergone a coronary angiogram before this study although this procedure is not required in special circumstances (as in certain types of repolarization syndromes and if your doctor has decided that you require ablation of the focus of dangerous heart rhythm -ventricular tachycardia- using the noncontact mapping technique). As part of the normal procedure, we would already have access to the artery and vein to your right groin. In the study we will need additional access to your left groin artery under local anaesthetic so that we could place the noncontact mapping catheter into the correct position inside the left heart chamber (except in certain heart conditions when access to the right ventricle is needed). The heart electrical study (electrophysiological study) will proceed as planned. Information will be collected from the heart during the duration of the electrical study and

it will be reviewed and analysed after its completion. After the tests, all catheters will be removed.
The noncontact mapping catheter is a thin tube slightly thicker than the angiogram catheters. It is now commonly used to help treatment of complicated heart rhythm problems worldwide. Once the catheter is placed into the left or right heart chamber (ventricle) under X-ray control, a small balloon at its tip is inflated to allow measurements to be made. It measures electrical signals within the space of the heart chamber without the need for physical contact with the inside of the heart.

What do I have to do?

The preparation and follow up of the procedure will be the same as that following a coronary angiogram. Your doctor will give you detailed advice about this, including driving a car.

What are the possible disadvantages and risks of taking part?

By taking part in this study, the duration of the investigation will take approximately 15 to 30 minutes longer. The small risk of complications relating to artery access to the left groin will apply (as in the right side used for coronary angiograms): mild bruising (10%) or haematoma (2-3%), rebleeding (1-2%), false artery pocket formation (pseudoaneurysms) (0.5%). All these complications are treatable, and our department has extensive experience in dealing with these potential problems.

What are the possible benefits of taking part?

The information we get from this study may help us in the future to assess the risk of fast dangerous heart rhythms in patients with abnormal cardiac repolarization.

What if new information becomes available?

Sometimes during the course of a research project, new information becomes available about the treatment that is being studied. If this happens, your doctor will tell you about it and discuss with you whether you should decide to continue in the study. If you decide to withdraw, your care will continue as usual. If you decide to continue in the study, you may be asked to sign an updated consent form.

What happens when the research study stops?

The research study is a one stop procedure where all the data will be collected at the time of the electrophysiology test. The data analysis will proceed thereafter. After the research stops your care will continue as usual. This means that there will be no required follow up visits for the purpose of the research study but you will be reviewed and given medical treatment based on your consultant's advice according to your clinical needs. The results of this study will not alter the treatment offered to you at this stage.

What if something goes wrong?

If you suffer injury directly as a result of being in the study there are no special compensation arrangements. If you are harmed due to someone's negligence, then you may have grounds for a legal action but you have to pay for it. Regardless of this, if you wish to complain about any aspect of the way you have been approached or treated during the course of this study, the normal National Health Service complains mechanisms may be available to you. Your right to claim compensation for injury where you can prove negligence is not affected.

Will my taking part in this study be kept confidential?

If you consent to take part in the research, your medical notes may be looked at by representatives from national or foreign regulatory authorities to check that the study is being carried out correctly. Your identity will at no point be disclosed to any other people. For computerised data processing, your identity will be coded to preserve your anonymity. In accordance with the laws related to data protection, you will be able to exercise your rights to access and to rectify this data at any time.
In participating in the study, you authorize the cardiac electrophysiology research team to use the information obtained during the study for scientific communications or publications. If you agree, your GP may be informed of your participation in this study.

What will happen to the results of the research study?

The results will be analysed and published in scientific journals.

Who is organising and funding the research?

It is a non-commercial research currently organised by the cardiac electrophysiology unit at Southampton General Hospital.

Who has reviewed the study?

The Southampton & S. W. Hants Joint Research Ethics Committee has reviewed this study.

Contact for further information

If you have any problems, concerns or other questions about this study you should preferably contact the investigator (Dr John Morgan, Wessex Cardiothoracic Unit, Mail point 46, Southampton General Hospital, Tel 023 80798676 or 023 80798646). If you have any complaints about the way the investigator has carried out the study, you may contact the Trust complaints department (Complaints Coordinator, Wessex Cardiothoracic Unit, Southampton General Hospital, SO16 6YD).
You will be given one copy of this information sheet as well as a signed consent form to keep.
Thank you for taking the time to think about taking part in this study.

Southampton NHS
University Hospitals NHS Trust
Wessex Cardiothoracic Centre
Mailpoint 46
Southampton General Hospital
Tremona Road
Southampton SO 16 6 YD
Tel : 02380798676

CONSENT FORM

Study Title: Study of cardiac repolarization with noncontact mapping

Name of Principal Investigator: Dr John Morgan

Please initial box

1. I confirm that I have read and understand the information sheet dated 09 October 2006 (Version 5.1) for the above study and have had the opportunity to ask questions. ☐
2. I understand that my participation is voluntary and that I am free to withdraw at any time, without giving any reason, without my medical care or legal rights being affected. ☐
3. I understand that sections of any of my medical notes may be looked at by responsible individuals from regulatory authorities where it is relevant to my taking part in research. I give permission for these individuals to have access to my records ☐
4. I agree to take part in the above study ☐

Name of Patient	Date	Signature
Name of person taking consent (if different from researcher)	Date	Signature
Researcher	Date	Signature

1 for patient, 1 for researcher, 1 to be kept with hospital notes

Appedix B Study protocol version 4.0

An examination of cardiac repolarization with noncontact mapping

Study protocol Version 4 (23 August 2005)

1) **The study aims and objectives**
   - To study the cardiac repolarization characteristics with non-contact mapping technology in patients with: abnormal ECG repolarization, history of ventricular arrhythmias or cardiomyopathies and family history of premature sudden cardiac death. To assess the effect of pacing and premature pacing stimuli on changes of cardiac repolarization within a cardiac chamber.

- **Study design**
  - A pilot, qualitative, observational study.
  - There will be two arms: A study group and control group. The study group is further subdivided into 3 subgroups: 1) study group 1, in patients with repolarization syndromes, 2) study group 2, in patients with documented ventricular tachycardia and 3) study group 3 patients with hereditary cardiomyopathies. 4) The control group, in patients with structurally normal hearts and without repolarization abnormalities but are scheduled to undergo noncontact mapping for ablation procedures.
  - Global endocardial repolarization measurements of the left ventricle will be made, at rest, with programmed extrastimuli, and pharmacological challenge. Colour maps will also be constructed with computer software to aid analysis and comparisons between the two groups.
- **Patients**
  - Approximately 20 to 30 patients, age 18 to 80, with abnormal (or suspected abnormal) cardiac repolarization will be recruited into the study over a 4 year period. Approximately 10 patients who are scheduled to undergo noncontact mapping for catheter ablation procedures but without repolarization abnormalities will be recruited as controls.
- **General approach**
  - Patients will be recruited into the study group 1 if they had repolarization abnormalities on the ECG which may be associated with sudden cardiac death or a strong family history of sudden death associated with repolarization abnormalities
  - Patients will be recruited into study group 2 if they had documented ventricular tachycardia and were regarded on clinical grounds to be at risk of sudden cardiac death

- Patients will be recruited into study group 3 if they have a hereditary cardiomyopathy which may be associated with sudden cardiac death and a strong family history of sudden death or aborted sudden cardiac death associated with the cardiomyopathy.
- Patients will be recruited into the control arm if they were to undergo cardiac catheterization or catheter ablation on clinical grounds.
- This study will be carried out in the same setting as these procedures in the Southampton General Hospital cardiac catheterization laboratories.
- They will be approached in the outpatient clinics or hospital wards when they are admitted for these procedures.

- **Inclusion criteria for study patients (group 1)**
  - Patients with ECG abnormalites of repolarization (ECG abnormalities include long QT syndrome, Brugada syndrome, and other abnormal ST-T changes not fulfilling existing diagnostic criteria.)
  - Structurally normal heart
  - Patients with a previous history or strong family history of aborted sudden death associated with repolarization abnormalities
- **Exclusion criteria for study patients (group 1)**
  - Structural heart disease
  - Normal cardiac repolarization on ECG without a previous or family history of repolarization abnormalities and sudden death
  - Inability to sign informed consent
  - Pregnancy
  - Currently enrolled in another study including drug investigations

- **Inclusion criteria for study patients (group 2)**
  - Patients with documented ventricular tachycardia on ECG
  - Patients clinically indicated to undergo electrophysiological study for risk stratification **OR**
  - Patients who are to undergo ventricular tachycardia ablation with the noncontact mapping system on clinical grounds
- **Exclusion criteria for study patients (group 2)**
  - Patients who have contraindications to electrophysiological studies on clinical grounds
  - Inability to sign informed consent
  - Pregnancy
  - Currently enrolled in another study including drug investigations

- **Inclusion criteria for study patients (group 3)**

  - Patients with hereditary cardiomyopathies e.g. HCOM or hereditary dilated cardiomyopathies or arrhythmogenic right ventricular dysplasia (ARVD).
  - Patients with a strong family history of sudden cardiac death or aborted sudden cardiac death.
- Exclusion criteria for study patients (group 3)
  - Patients who have contraindications to electrophysiological studies on clinical grounds
  - Inability to sign informed consent
  - Pregnancy
  - Currently enrolled in another study including drug investigations.

- **Inclusion criteria for control patients**
  - Patients scheduled to undergo catheter ablation using noncontact mapping on clinical grounds.
  - Patients scheduled for left heart procedures i.e. left atrial or left ventricular ablations.
  - No abnormalities of cardiac repolarization identifiable on the ECG.
  - Patients have a structurally normal heart
- **Exclusion criteria for control patients**
  - Abnormal cardiac repolarization on ECG
  - Inability to sign informed consent
  - Pregnancy
  - Currently enrolled in another study including drug investigations

- **Outline of procedures for study patients**
  - Before the study, patients will have undergone diagnostic coronary angiography via the right femoral artery. Except for special groups who wouldn't need a coronay angiogram including special repolarisation groups who have nearly normal ECGs and those who have indications to have VT ablation using the noncontact mapping system on clinical grounds.
  - In the same session, the non-contact mapping catheter will be introduced via the left femoral artery site into the left ventricular chamber.
  - A conventional catheter is introduced via the right femoral artery into the left ventricle to help construction of chamber geometry. This catheter will be removed before pacing.
  - A conventional catheter is introduced via a femoral vein into the right ventriclular apex for pacing and routine electrophysilogical studies
  - Cardiac pacing will be performed as in a conventional electrophysiological study.
  - Measurements are performed automatically in real time by the non-contact mapping catheter.
  - All catheters are removed following the study.

- **Outline of procedures for control patients**
  - Patients will have femoral venous and/or arterial access as indicated for catheter ablations.
  - If patients were to undergo left ventricular ablations, the noncontact mapping catheter will be introduced and prepared as usual. The study measurements will be carried out immediately before the ablation procedures.
  - If patients are to undergo left atrial ablations, the noncontact mapping catheter will first be introduced into the chamber via the transseptal technique as usual. Before the ablation procedures, the catheter will be advanced into the left ventricle first for study measurements to be carried out. Following the study, the catheter will be replaced back into the left atrium to guide ablations.

- **Configuration of workstation software and hardware to allow efficient processing of repolarization data**
  - Determination of local activation times (LAT), using the Ensite isochrone algorithm
  - Determination of local repolarization times (LRT), based on above criteria to define end of repolarization from virtual unipolar electrograms
  - Determination of activation recovery intervals (ARI = LRT - LAT)
  - Establish new algorithm to allow generation of global activation maps (conventional isochronal maps) and global repolarization maps (LRT maps).
  - Program computer to calculate maximum and minimum global and adjacent dispersion of repolarization.

- **Measurements in control study in patients without repolarization abnormalities (including measurements with MAP catheter)**

  - The **MAP catheter** is introduced into the left ventricle following geometry construction with the noncontact mapping catheter. Recordings of endocardial action potential duration (time from onset of activation to 90% repolarization) at 20-30 sites will be made in each patient. MAP signals are recorded at a filtered bandwidth of 0.01 to 400 Hz. The MAP catheter is then removed.

  - By the use of the system's locator, the sites measured by the MAP catheter are localized. Virtual electrograms at these chosen sites are then selected and analyzed. Unipolar recording filters set at 0.1 to 300 Hz
  - Determination of activation-repolarization intervals of the virtual electrograms. From the steepest intrinsic deflection dV/dT min to the end of the local T wave. Definition of end of T waves: for

- Electrical restitution changes measured again during pharmacological challenge
- Recordings from noncontact mapping catheter is constantly made in real time. Analysis of data will be performed off-line following the study. Construction of global repolarization maps at different diastolic intervals will be made.

- For patients with suspected Brugada syndrome: pharmacological challenge
  - Intravenous flecainide 1.5 mg/kg (max 150 mg) or procainamide 1.5 mg/kg will be given as a slow bolus
  - Electrical restitution changes measured again during pharmacological challenge
  - Recordings from noncontact mapping catheter is constantly made in real time. Analysis of data will be performed off-line following the study. Construction of global repolarization maps at different diastolic intervals will be made.

References

1. Adabag, A.S., Luepker, R.V., Roger, V.L., & Gersh, B.J. 2010. Sudden cardiac death: epidemiology and risk factors. *Nat.Rev.Cardiol*, 7, (4) 216-225

2. Ahlberg, S.E., Yue, A.M., Skadsberg, N.D., Roberts, P.R., Iaizzo, P.A., & Morgan, J.M. 2008. Investigation of pacing site-related changes in global restitution dynamics by non-contact mapping. *Europace.*, 10, (1) 40-45

3. Alexander, M.E., Cecchin, F., Huang, K.P., & Berul, C.I. 2006. Microvolt t-wave alternans with exercise in pediatrics and congenital heart disease: limitations and predictive value. *Pacing Clin.Electrophysiol.*, 29, (7) 733-741

4. Alexander, M.E., Walsh, E.P., Saul, J.P., Epstein, M.R., & Triedman, J.K. 1999. Value of programmed ventricular stimulation in patients with congenital heart disease. *J.Cardiovasc.Electrophysiol.*, 10, (8) 1033-1044

5. Allessie, M.A., Bonke, F.I., & Schopman, F.J. 1972. Circus movement in atrial muscle as a mechanism of supraventricular tachycardia. *J.Physiol (Paris)*, 65, Suppl

6. Allessie, M.A., Bonke, F.I., & Schopman, F.J. 1973. Circus movement in rabbit atrial muscle as a mechanism of trachycardia. *Circ.Res.*, 33, (1) 54-62

7. Antzelevitch, C., Sicouri, S., Litovsky, S.H., Lukas, A., Krishnan, S.C., Di Diego, J.M., Gintant, G.A., & Liu, D.W. 1991. Heterogeneity within the ventricular wall. Electrophysiology and pharmacology of epicardial, endocardial, and M cells. *Circ.Res.*, 69, (6) 1427-1449

8. Anyukhovsky, E.P., Sosunov, E.A., Gainullin, R.Z., & Rosen, M.R. 1999. The controversial M cell. *J.Cardiovasc.Electrophysiol.*, 10, (2) 244-260

9. Arntz, H.R., Muller-Nordhorn, J., & Willich, S.N. 2001. Cold Monday mornings prove dangerous: epidemiology of sudden cardiac death. *Curr.Opin.Crit Care*, 7, (3) 139-144

10. Arntz, H.R., Willich, S.N., Schreiber, C., Bruggemann, T., Stern, R., & Schultheiss, H.P. 2000. Diurnal, weekly and seasonal variation of sudden death. Population-based analysis of 24,061 consecutive cases. *Eur.Heart J.*, 21, (4) 315-320

11. Ashino, S., Watanabe, I., Kofune, M., Nagashima, K., Ohkubo, K., Okumura, Y., Mano, H., Nakai, T., Kunimoto, S., Kasamaki, Y., & Hirayama, A. 2011. Effects of quinidine on the action potential duration restitution property in the right ventricular outflow tract in patients with brugada syndrome. *Circ.J.*, 75, (9) 2080-2086

12. Autenrieth, G., Surawicz, B., & Kuo, C.S. 1975. Sequence of repolarization on the ventricular surface in the dog. *Am.Heart J.*, 89, (4) 463-469

13. Baker, L.C., London, B., Choi, B.R., Koren, G., & Salama, G. 2000. Enhanced dispersion of repolarization and refractoriness in transgenic mouse hearts promotes reentrant ventricular tachycardia. *Circ.Res.*, 86, (4) 396-407

14. Banville, I., Chattipakorn, N., & Gray, R.A. 2004. Restitution dynamics during pacing and arrhythmias in isolated pig hearts. *J.Cardiovasc.Electrophysiol.*, 15, (4) 455-463

15. Banville, I. & Gray, R.A. 2002. Effect of action potential duration and conduction velocity restitution and their spatial dispersion on alternans and the stability of arrhythmias. *J.Cardiovasc.Electrophysiol.*, 13, (11) 1141-1149

16. Bardy, G.H., Lee, K.L., Mark, D.B., Poole, J.E., Packer, D.L., Boineau, R., Domanski, M., Troutman, C., Anderson, J., Johnson, G., McNulty, S.E., Clapp-Channing, N., Davidson-Ray, L.D., Fraulo, E.S., Fishbein, D.P., Luceri, R.M., & Ip, J.H. 2005. Amiodarone or an implantable cardioverter-defibrillator for congestive heart failure. *N.Engl.J.Med.*, 352, (3) 225-237

17. Bass, B.G. 1975. Restitution of the action potential in cat papillary muscle. *American journal of physiology*, 228, (6) 1717-1724

18. Batchvarov, V. & Malik, M. 2000. Measurement and interpretation of QT dispersion. *Prog.Cardiovasc.Dis.*, 42, (5) 325-344

19. Behr, E.R., Elliott, P., & McKenna, W.J. 2002. Role of invasive EP testing in the evaluation and management of hypertrophic cardiomyopathy. *Card Electrophysiol.Rev.*, 6, (4) 482-486

20. Belhassen, B., Glick, A., & Viskin, S. 2004. Efficacy of quinidine in high-risk patients with Brugada syndrome. *Circulation*, 110, (13) 1731-1737

21. Belhassen, B., Shapira, I., Pelleg, A., Copperman, I., Kauli, N., & Laniado, S. 1984. Idiopathic recurrent sustained ventricular tachycardia responsive to verapamil: an ECG-electrophysiologic entity. *Am.Heart J.*, 108, (4 Pt 1) 1034-1037

22. Belhassen, B. & Viskin, S. 1993. Idiopathic ventricular tachycardia and fibrillation. *J.Cardiovasc.Electrophysiol.*, 4, (3) 356-368

23. Belhassen, B., Viskin, S., Fish, R., Glick, A., Setbon, I., & Eldar, M. 1999. Effects of electrophysiologic-guided therapy with Class IA antiarrhythmic drugs on the long-term outcome of patients with idiopathic ventricular fibrillation with or without the Brugada syndrome. *J.Cardiovasc.Electrophysiol.*, 10, (10) 1301-1312

24. Bezzina, C., Veldkamp, M.W., van Den Berg, M.P., Postma, A.V., Rook, M.B., Viersma, J.W., van Langen, I.M., Tan-Sindhunata, G., Bink-Boelkens, M.T., van Der Hout, A.H., Mannens, M.M., & Wilde, A.A. 1999. A single Na(+) channel mutation causing both long-QT and Brugada syndromes. *Circ.Res.*, 85, (12) 1206-1213

25. Bhandari, A.K., Shapiro, W.A., Morady, F., Shen, E.N., Mason, J., & Scheinman, M.M. 1985. Electrophysiologic testing in patients with the long QT syndrome. *Circulation*, 71, (1) 63-71

26. Bigger, J.T., Jr., Whang, W., Rottman, J.N., Kleiger, R.E., Gottlieb, C.D., Namerow, P.B., Steinman, R.C., & Estes, N.A., III 1999. Mechanisms of death in the CABG Patch trial: a randomized trial of implantable cardiac defibrillator

prophylaxis in patients at high risk of death after coronary artery bypass graft surgery. *Circulation*, 99, (11) 1416-1421

27. Blanchard, S.M., Damiano, R.J., Jr., Asano, T., Smith, W.M., Ideker, R.E., & Lowe, J.E. 1987. The effects of distant cardiac electrical events on local activation in unipolar epicardial electrograms. *IEEE Trans.Biomed.Eng*, 34, (7) 539-546

28. Bonatti, V., Rolli, A., & Botti, G. 1985. Monophasic action potential studies in human subjects with prolonged ventricular repolarization and long QT syndromes. *Eur.Heart J.*, 6 Suppl D, 131-143

29. Bourgeois, E.B., Reeves, H.D., Walcott, G.P., & Rogers, J.M. 2012. Panoramic optical mapping shows wavebreak at a consistent anatomical site at the onset of ventricular fibrillation. *Cardiovasc.Res.*, 93, (2) 272-279

30. Brilakis, E.S., Friedman, P.A., Maounis, T.N., Rokas, S.G., Shen, W.K., Stamatelopoulos, S.F., & Cokkinos, D.V. 2005. Programmed ventricular stimulation in patients with idiopathic dilated cardiomyopathy and syncope receiving implantable cardioverter-defibrillators: a case series and a systematic review of the literature. *Int.J.Cardiol*, 98, (3) 395-401

31. Brugada, J., Brugada, R., & Brugada, P. 2011. Electrophysiologic testing predicts events in Brugada syndrome patients. *Heart Rhythm.*, 8, (10) 1595-1597

32. Brugada, P. & Brugada, J. 1992. Right bundle branch block, persistent ST segment elevation and sudden cardiac death: a distinct clinical and electrocardiographic syndrome. A multicenter report. *J.Am.Coll.Cardiol*, 20, (6) 1391-1396

33. Brugada, R., Brugada, J., Antzelevitch, C., Kirsch, G.E., Potenza, D., Towbin, J.A., & Brugada, P. 2000. Sodium channel blockers identify risk for sudden death in patients with ST-segment elevation and right bundle branch block but structurally normal hearts. *Circulation*, 101, (5) 510-515

34. Bryant, S.M., Wan, X., Shipsey, S.J., & Hart, G. 1998. Regional differences in the delayed rectifier current (IKr and IKs) contribute to the differences in action potential duration in basal left ventricular myocytes in guinea-pig. *Cardiovasc.Res.*, 40, (2) 322-331

35. Burdon-Sanderson J & Page FJM 1882. On the time-relations of the excitatory process in the ventricle of the heart of the frog. *Journal of Physiology* (2) 385-412

36. Burton, F.L., McPhaden, A.R., & Cobbe, S.M. 2000. Ventricular fibrillation threshold and local dispersion of refractoriness in isolated rabbit hearts with left ventricular dysfunction. *Basic Res.Cardiol*, 95, (5) 359-367

37. Buxton, A.E., Fisher, J.D., Josephson, M.E., Lee, K.L., Pryor, D.B., Prystowsky, E.N., Simson, M.B., DiCarlo, L., Echt, D.S., & Packer, D. 1993. Prevention of sudden death in patients with coronary artery disease: the Multicenter Unsustained Tachycardia Trial (MUSTT). *Prog.Cardiovasc.Dis.*, 36, (3) 215-226

38. Buxton, A.E., Lee, K.L., Hafley, G.E., Pires, L.A., Fisher, J.D., Gold, M.R., Josephson, M.E., Lehmann, M.H., & Prystowsky, E.N. 2007. Limitations of ejection fraction for prediction of sudden death risk in patients with coronary artery disease: lessons from the MUSTT study. *J.Am.Coll.Cardiol*, 50, (12) 1150-1157

39. Buxton, A.E., Lee, K.L., Hafley, G.E., Wyse, D.G., Fisher, J.D., Lehmann, M.H., Pires, L.A., Gold, M.R., Packer, D.L., Josephson, M.E., Prystowsky, E.N., & Talajic, M.R. 2002. Relation of ejection fraction and inducible ventricular tachycardia to mode of death in patients with coronary artery disease: an analysis of patients enrolled in the multicenter unsustained tachycardia trial. *Circulation*, 106, (19) 2466-2472

40. Cao, J.M., Fishbein, M.C., Han, J.B., Lai, W.W., Lai, A.C., Wu, T.J., Czer, L., Wolf, P.L., Denton, T.A., Shintaku, I.P., Chen, P.S., & Chen, L.S. 2000. Relationship between regional cardiac hyperinnervation and ventricular arrhythmia. *Circulation*, 101, (16) 1960-1969

41. Cao, J.M., Qu, Z., Kim, Y.H., Wu, T.J., Garfinkel, A., Weiss, J.N., Karagueuzian, H.S., & Chen, P.S. 1999. Spatiotemporal heterogeneity in the induction of ventricular fibrillation by rapid pacing: importance of cardiac restitution properties. *Circ.Res.*, 84, (11) 1318-1331

42. Cassidy, D.M., Vassallo, J.A., Marchlinski, F.E., Buxton, A.E., Untereker, W.J., & Josephson, M.E. 1984. Endocardial mapping in humans in sinus rhythm with normal left ventricles: activation patterns and characteristics of electrograms. *Circulation*, 70, (1) 37-42

43. Catalano, O., Antonaci, S., Moro, G., Mussida, M., Frascaroli, M., Baldi, M., Cobelli, F., Baiardi, P., Nastoli, J., Bloise, R., Monteforte, N., Napolitano, C., & Priori, S.G. 2009. Magnetic resonance investigations in Brugada syndrome reveal unexpectedly high rate of structural abnormalities. *Eur.Heart J.*, 30, (18) 2241-2248

44. Chauhan, V.S., Downar, E., Nanthakumar, K., Parker, J.D., Ross, H.J., Chan, W., & Picton, P. 2006. Increased ventricular repolarization heterogeneity in patients with ventricular arrhythmia vulnerability and cardiomyopathy: a human in vivo study. *Am J.Physiol Heart Circ.Physiol*, 290, (1) H79-H86

45. Chen, P.S., Chen, L.S., Cao, J.M., Sharifi, B., Karagueuzian, H.S., & Fishbein, M.C. 2001. Sympathetic nerve sprouting, electrical remodeling and the mechanisms of sudden cardiac death. *Cardiovasc.Res.*, 50, (2) 409-416

46. Chen, P.S., Moser, K.M., Dembitsky, W.P., Auger, W.R., Daily, P.O., Calisi, C.M., Jamieson, S.W., & Feld, G.K. 1991. Epicardial activation and repolarization patterns in patients with right ventricular hypertrophy. *Circulation*, 83, (1) 104-118

47. Chen, P.S., Wu, T.J., Ting, C.T., Karagueuzian, H.S., Garfinkel, A., Lin, S.F., & Weiss, J.N. 2003. A tale of two fibrillations. *Circulation*, 108, (19) 2298-2303

48. Cherry, E.M. & Fenton, F.H. 2004. Suppression of alternans and conduction blocks despite steep APD restitution: electrotonic, memory, and conduction

velocity restitution effects. *Am.J.Physiol Heart Circ.Physiol*, 286, (6) H2332-H2341

49. Chialvo, D.R., Michaels, D.C., & Jalife, J. 1990. Supernormal excitability as a mechanism of chaotic dynamics of activation in cardiac Purkinje fibers. *Circ.Res.*, 66, (2) 525-545

50. Choi, B.R., Liu, T., & Salama, G. 2001. The distribution of refractory periods influences the dynamics of ventricular fibrillation. *Circ.Res.*, 88, (5) E49-E58

51. Chow, A.W., Segal, O.R., Davies, D.W., & Peters, N.S. 2004. Mechanism of pacing-induced ventricular fibrillation in the infarcted human heart. *Circulation*, 110, (13) 1725-1730

52. Chudin, E., Goldhaber, J., Garfinkel, A., Weiss, J., & Kogan, B. 1999. Intracellular Ca(2+) dynamics and the stability of ventricular tachycardia. *Biophys.J.*, 77, (6) 2930-2941

53. Clayton, R.H. 2005. Regional differences in APD restitution can initiate wavebreak and re-entry in cardiac tissue: a computational study. *Biomedical engineering online*, 4, 54

54. Cleland, J.G., Chattopadhyay, S., Khand, A., Houghton, T., & Kaye, G.C. 2002. Prevalence and incidence of arrhythmias and sudden death in heart failure. *Heart Fail.Rev.*, 7, (3) 229-242

55. Cohen, I., Giles, W., & Noble, D. 1976. Cellular basis for the T wave of the electrocardiogram. *Nature*, 262, (5570) 657-661

56. Connolly, S.J. 1999. Evidence-based analysis of amiodarone efficacy and safety. *Circulation*, 100, (19) 2025-2034

57. Coronel, R., Casini, S., Koopmann, T.T., Wilms-Schopman, F.J., Verkerk, A.O., de Groot, J.R., Bhuiyan, Z., Bezzina, C.R., Veldkamp, M.W., Linnenbank, A.C., van der Wal, A.C., Tan, H.L., Brugada, P., Wilde, A.A., & de Bakker, J.M. 2005. Right ventricular fibrosis and conduction delay in a patient with clinical signs of Brugada syndrome: a combined electrophysiological, genetic, histopathologic, and computational study. *Circulation*, 112, (18) 2769-2777

58. Coronel, R., de Bakker, J.M., Wilms-Schopman, F.J., Opthof, T., Linnenbank, A.C., Belterman, C.N., & Janse, M.J. 2006. Monophasic action potentials and activation recovery intervals as measures of ventricular action potential duration: experimental evidence to resolve some controversies. *Heart Rhythm.*, 3, (9) 1043-1050

59. Coronel, R., Janse, M.J., Opthof, T., Wilde, A.A., & Taggart, P. 2012. Postrepolarization refractoriness in acute ischemia and after antiarrhythmic drug administration: action potential duration is not always an index of the refractory period. *Heart Rhythm.*, 9, (6) 977-982

60. Corrado, D., Basso, C., Pavei, A., Michieli, P., Schiavon, M., & Thiene, G. 2006. Trends in sudden cardiovascular death in young competitive athletes after implementation of a preparticipation screening program. *JAMA*, 296, (13) 1593-1601

61. Corrado, D., Basso, C., Thiene, G., McKenna, W.J., Davies, M.J., Fontaliran, F., Nava, A., Silvestri, F., Blomstrom-Lundqvist, C., Wlodarska, E.K., Fontaine, G., & Camerini, F. 1997. Spectrum of clinicopathologic manifestations of arrhythmogenic right ventricular cardiomyopathy/dysplasia: a multicenter study. *J Am Coll Cardiol*, 30, (6) 1512-1520

62. Cowan, J.C., Hilton, C.J., Griffiths, C.J., Tansuphaswadikul, S., Bourke, J.P., Murray, A., & Campbell, R.W. 1988. Sequence of epicardial repolarisation and configuration of the T wave. *Br.Heart J.*, 60, (5) 424-433

63. Cranefield, P.F. 1977. Action potentials, afterpotentials, and arrhythmias. *Circ.Res.*, 41, (4) 415-423

64. Daly, M.J., Finlay, D.D., Scott, P.J., Nugent, C.D., Adgey, A.A., & Harbinson, M.T. 2013. Pre-hospital body surface potential mapping improves early diagnosis of acute coronary artery occlusion in patients with ventricular fibrillation and cardiac arrest. *Resuscitation*, 84, (1) 37-41

65. Damiano, B.P. & Rosen, M.R. 1984. Effects of pacing on triggered activity induced by early afterdepolarizations. *Circulation*, 69, (5) 1013-1025

66. Davidenko, J.M. & Antzelevitch, C. 1986. Electrophysiological mechanisms underlying rate-dependent changes of refractoriness in normal and segmentally depressed canine Purkinje fibers. The characteristics of post-repolarization refractoriness. *Circ Res*, 58, (2) 257-268

67. Davidenko, J.M., Pertsov, A.V., Salomonsz, R., Baxter, W., & Jalife, J. 1992. Stationary and drifting spiral waves of excitation in isolated cardiac muscle. *Nature*, 355, (6358) 349-351

68. Davis, L.M., Cooper, M., Johnson, D.C., Uther, J.B., Richards, D.A., & Ross, D.L. 1994. Simultaneous 60-electrode mapping of ventricular tachycardia using percutaneous catheters. *J.Am Coll.Cardiol*, 24, (3) 709-719

69. de Vreede-Swagemakers, J.J., Gorgels, A.P., Dubois-Arbouw, W.I., Dalstra, J., Daemen, M.J., van Ree, J.W., Stijns, R.E., & Wellens, H.J. 1998. Circumstances and causes of out-of-hospital cardiac arrest in sudden death survivors. *Heart*, 79, (4) 356-361

70. Deanfield, J., McKenna, W., & Rowland, E. 1985. Local abnormalities of right ventricular depolarization after repair of tetralogy of Fallot: a basis for ventricular arrhythmia. *Am J.Cardiol*, 55, (5) 522-525

71. Derksen, R., van Rijen, H.V., Wilders, R., Tasseron, S., Hauer, R.N., Rutten, W.L., & de Bakker, J.M. 2003. Tissue discontinuities affect conduction velocity restitution: a mechanism by which structural barriers may promote wave break. *Circulation*, 108, (7) 882-888

72. Diller, G.P., Kempny, A., Liodakis, E., Alonso-Gonzalez, R., Inuzuka, R., Uebing, A., Orwat, S., Dimopoulos, K., Swan, L., Li, W., Gatzoulis, M.A., & Baumgartner, H. 2012. Left Ventricular Longitudinal Function Predicts Life-Threatening Ventricular Arrhythmia and Death in Adults with Repaired Tetralogy of Fallot. *Circulation*

73. Dillon, S.M., Allessie, M.A., Ursell, P.C., & Wit, A.L. 1988. Influences of anisotropic tissue structure on reentrant circuits in the epicardial border zone of subacute canine infarcts. *Circ.Res.*, 63, (1) 182-206

74. Dock W 1929. Transitory ventricular fibrillation as a cause of syncope and its prevention by quinidine sulfate. *American Heart Journal* (4) 709-714

75. Duren, D.R., Becker, A.E., & Dunning, A.J. 1988. Long-term follow-up of idiopathic mitral valve prolapse in 300 patients: a prospective study. *J.Am Coll.Cardiol*, 11, (1) 42-47

76. Durrer, D., Schoo, L., Schuilenburg, R.M., & Wellens, H.J. 1967. The role of premature beats in the initiation and the termination of supraventricular tachycardia in the Wolff-Parkinson-White syndrome. *Circulation*, 36, (5) 644-662

77. Durrer, D., van Dam, R.T., Freud, G.E., Janse, M.J., Meijler, F.L., & Arzbaecher, R.C. 1970. Total excitation of the isolated human heart. *Circulation*, 41, (6) 899-912

78. Echt DS, Liebson PR, Brent Mitchell L, & Peters RW 1989. Preliminary report: effect of encainide and flecainide on mortality in a randomized trial of arrhythmia suppression after myocardial infarction. The Cardiac Arrhythmia Suppression Trial (CAST) Investigators. *N.Engl.J.Med.*, 321, (6) 406-412

79. el-Sherif, N., Caref, E.B., Yin, H., & Restivo, M. 1996. The electrophysiological mechanism of ventricular arrhythmias in the long QT syndrome. Tridimensional mapping of activation and recovery patterns. *Circ.Res.*, 79, (3) 474-492

80. el-Sherif, N., Gough, W.B., Zeiler, R., & Mehra, R. 1981. Endocardial Mapping of Triggered Automaticity in Canine Ischemic Purkinje-Fibers. *American Journal of Cardiology*, 47, (2) 489

81. el-Sherif, N. & Turitto G 2003. Risk stratification and management of sudden cardiac death: a new paradigm. *Journal of cardiovascular electrophysiology*, 14, (10) 1113-1119

82. Eldar, M., Fitzpatrick, A.P., Ohad, D., Smith, M.F., Hsu, S., Whayne, J.G., Vered, Z., Rotstein, Z., Kordis, T., Swanson, D.K., Chin, M., Scheinman, M.M., Lesh, M.D., & Greenspon, A.J. 1996. Percutaneous multielectrode endocardial mapping during ventricular tachycardia in the swine model. *Circulation*, 94, (5) 1125-1130

83. Engelstein ED & Zipes DP 1998, "Sudden Cardiac Death," *In The heart, arteries and veins*, Alexander RW, Schlant RC, & Fuster V, eds., New York: McGraw-Hill, pp. 1081-1112.

84. Everett, T.H., Wilson, E.E., Foreman, S., & Olgin, J.E. 2005. Mechanisms of ventricular fibrillation in canine models of congestive heart failure and ischemia assessed by in vivo noncontact mapping. *Circulation*, 112, (11) 1532-1541

85. Extramiana, F. & Antzelevitch, C. 2004. Amplified transmural dispersion of repolarization as the basis for arrhythmogenesis in a canine ventricular-wedge model of short-QT syndrome. *Circulation*, 110, (24) 3661-3666

86. Flowers, N.C. & Horan, L.G. 1990. Body surface mapping including relationships with endocardial and epicardial mapping. *Ann N.Y.Acad.Sci.*, 601, 148-179

87. Franz, M., Schottler, M., Schaefer, J., & Seed, W.A. 1980. Simultaneous recording of monophasic action potentials and contractile force from the human heart. *Klin.Wochenschr.*, 58, (24) 1357-1359

88. Franz, M.R. 1983. Long-term recording of monophasic action potentials from human endocardium. *The American journal of cardiology*, 51, (10) 1629-1634

89. Franz, M.R. 1999. Current status of monophasic action potential recording: theories, measurements and interpretations. *Cardiovascular research*, 41, (1) 25-40

90. Franz, M.R. 2003. The Electrical Restitution Curve Revisited: Steep or Flat Slope - Which is Better? *Journal of cardiovascular electrophysiology*, 14, (10 SUPPL.) S140-S147

91. Franz, M.R., Bargheer, K., Rafflenbeul, W., Haverich, A., & Lichtlen, P.R. 1987. Monophasic action potential mapping in human subjects with normal electrocardiograms: direct evidence for the genesis of the T wave. *Circulation*, 75, (2) 379-386

92. Franz, M.R., Burkhoff, D., Spurgeon, H., Weisfeldt, M.L., & Lakatta, E.G. 1986. In vitro validation of a new cardiac catheter technique for recording monophasic action potentials. *Eur.Heart J.*, 7, (1) 34-41

93. Franz, M.R. & Costard, A. 1988. Frequency-dependent effects of quinidine on the relationship between action potential duration and refractoriness in the canine heart in situ. *Circulation*, 77, (5) 1177-1184

94. Franz, M.R., Flaherty, J.T., Platia, E.V., Bulkley, B.H., & Weisfeldt, M.L. 1984. Localization of regional myocardial ischemia by recording of monophasic action potentials. *Circulation*, 69, (3) 593-604

95. Franz, M.R., Swerdlow, C.D., Liem, L.B., & Schaefer, J. 1988. Cycle length dependence of human action potential duration in vivo. Effects of single extrastimuli, sudden sustained rate acceleration and deceleration, and different steady-state frequencies. *J.Clin.Invest*, 82, (3) 972-979

96. Frustaci, A., Priori, S.G., Pieroni, M., Chimenti, C., Napolitano, C., Rivolta, I., Sanna, T., Bellocci, F., & Russo, M.A. 2005. Cardiac histological substrate in patients with clinical phenotype of Brugada syndrome. *Circulation*, 112, (24) 3680-3687

97. Fukuyama, M., Ohno, S., Wang, Q., Kimura, H., Makiyama, T., Itoh, H., Ito, M., & Horie, M. 2013. L-Type Calcium Channel Mutations in Japanese Patients With Inherited Arrhythmias. *Circ.J.*

98. Garfinkel, A., Chen, P.S., Walter, D.O., Karagueuzian, H.S., Kogan, B., Evans, S.J., Karpoukhin, M., Hwang, C., Uchida, T., Gotoh, M., Nwasokwa, O., Sager, P., & Weiss, J.N. 1997. Quasiperiodicity and chaos in cardiac fibrillation. *J.Clin.Invest*, 99, (2) 305-314

99. Garfinkel, A., Kim, Y.H., Voroshilovsky, O., Qu, Z., Kil, J.R., Lee, M.H., Karagueuzian, H.S., Weiss, J.N., & Chen, P.S. 2000. Preventing ventricular fibrillation by flattening cardiac restitution. *Proc.Natl.Acad.Sci.U.S.A*, 97, (11) 6061-6066

100. Garrey WE 1914. The nature of fibrillary contraction of the heart- Its relation to tissue mass and form. *American journal of physiology*, 33, 397-414

101. Gatzoulis, M.A., Till, J.A., Somerville, J., & Redington, A.N. 1995. Mechanoelectrical interaction in tetralogy of Fallot. QRS prolongation relates to right ventricular size and predicts malignant ventricular arrhythmias and sudden death. *Circulation*, 92, (2) 231-237

102. Gepstein, L., Hayam, G., & Ben-Haim, S.A. 1997a. A novel method for nonfluoroscopic catheter-based electroanatomical mapping of the heart. In vitro and in vivo accuracy results. *Circulation*, 95, (6) 1611-1622

103. Gepstein, L., Hayam, G., & Ben-Haim, S.A. 1997b. Activation-repolarization coupling in the normal swine endocardium. *Circulation*, 96, (11) 4036-4043

104. Giannakoulas, G., Dimopoulos, K., Bolger, A.P., Tay, E.L., Inuzuka, R., Bedard, E., Davos, C., Swan, L., & Gatzoulis, M.A. 2010. Usefulness of natriuretic Peptide levels to predict mortality in adults with congenital heart disease. *Am.J.Cardiol*, 105, (6) 869-873

105. Goldman, S., Johnson, G., Cohn, J.N., Cintron, G., Smith, R., & Francis, G. 1993. Mechanism of death in heart failure. The Vasodilator-Heart Failure Trials. The V-HeFT VA Cooperative Studies Group. *Circulation*, 87, (6 Suppl) VI24-VI31

106. Gorgels, A.P., Gijsbers, C., de Vreede-Swagemakers, J., Lousberg, A., & Wellens, H.J. 2003. Out-of-hospital cardiac arrest--the relevance of heart failure. The Maastricht Circulatory Arrest Registry. *Eur.Heart J.*, 24, (13) 1204-1209

107. Gornick, C.C., Adler, S.W., Pederson, B., Hauck, J., Budd, J., & Schweitzer, J. 1999. Validation of a new noncontact catheter system for electroanatomic mapping of left ventricular endocardium. *Circulation*, 99, (6) 829-835

108. Gough, W.B., Mehra, R., Restivo, M., Zeiler, R.H., & el-Sherif, N. 1985. Reentrant ventricular arrhythmias in the late myocardial infarction period in the dog. 13. Correlation of activation and refractory maps. *Circ.Res.*, 57, (3) 432-442

109. Grant, A.O. & Katzung, B.G. 1976. The effects of quinidine and verapamil on electrically induced automaticity in the ventricular myocardium of guinea pig. *J.Pharmacol.Exp.Ther.*, 196, (2) 407-419

110. Gray, R.A., Jalife, J., Panfilov, A.V., Baxter, W.T., Cabo, C., Davidenko, J.M., & Pertsov, A.M. 1995. Mechanisms of cardiac fibrillation. *Science*, 270, (5239) 1222-1223

111. Greenspon, A.J., Hsu, S.S., & Datorre, S. 1997. Successful radiofrequency catheter ablation of sustained ventricular tachycardia postmyocardial infarction in man guided by a multielectrode "basket" catheter. *J.Cardiovasc.Electrophysiol.*, 8, (5) 565-570

112. Haissaguerre, M., Derval, N., Sacher, F., Jesel, L., Deisenhofer, I., de, R.L., Pasquie, J.L., Nogami, A., Babuty, D., Yli-Mayry, S., De, C.C., Scanu, P., Mabo, P., Matsuo, S., Probst, V., Le, S.S., Defaye, P., Schlaepfer, J., Rostock, T., Lacroix, D., Lamaison, D., Lavergne, T., Aizawa, Y., Englund, A., Anselme, F., O'Neill, M., Hocini, M., Lim, K.T., Knecht, S., Veenhuyzen, G.D., Bordachar, P., Chauvin, M., Jais, P., Coureau, G., Chene, G., Klein, G.J., & Clementy, J. 2008. Sudden cardiac arrest associated with early repolarization. *N.Engl.J.Med.*, 358, (19) 2016-2023

113. Haissaguerre, M., Extramiana, F., Hocini, M., Cauchemez, B., Jais, P., Cabrera, J.A., Farre, J., Leenhardt, A., Sanders, P., Scavee, C., Hsu, L.F., Weerasooriya, R., Shah, D.C., Frank, R., Maury, P., Delay, M., Garrigue, S., & Clementy, J. 2003. Mapping and ablation of ventricular fibrillation associated with long-QT and Brugada syndromes. *Circulation*, 108, (8) 925-928

114. Haissaguerre, M., Shoda, M., Jais, P., Nogami, A., Shah, D.C., Kautzner, J., Arentz, T., Kalushe, D., Lamaison, D., Griffith, M., Cruz, F., de, P.A., Gaita, F., Hocini, M., Garrigue, S., Macle, L., Weerasooriya, R., & Clementy, J. 2002. Mapping and ablation of idiopathic ventricular fibrillation. *Circulation*, 106, (8) 962-967

115. Han , J., Garcia de Jalon, P.D., ., Moe, & , G.K. 1966. Fibrillation threshold of premature ventricular responses. *Circ.Res.*, 18, (1) 18-25

116. Han , J. & Moe G 1964. Nonuniform recovery of excitabilty in ventricular muscle. *Circulation research*, 14, 44-60

117. Hanson, B., Sutton, P., Elameri, N., Gray, M., Critchley, H., Gill, J.S., & Taggart, P. 2009. Interaction of activation-repolarization coupling and restitution properties in humans. *Circ.Arrhythm.Electrophysiol.*, 2, (2) 162-170

118. Haws, C.W. & Lux, R.L. 1990. Correlation between in vivo transmembrane action potential durations and activation-recovery intervals from electrograms. Effects of interventions that alter repolarization time. *Circulation*, 81, (1) 281-288

119. Hershberger, R.E., Hanson, E.L., Jakobs, P.M., Keegan, H., Coates, K., Bousman, S., & Litt, M. 2002. A novel lamin A/C mutation in a family with dilated cardiomyopathy, prominent conduction system disease, and need for permanent pacemaker implantation. *Am Heart J.*, 144, (6) 1081-1086

120. Hoffman, B.F., Cranefield, P.F., Lepeschkin , E., Surawicz, B., & Herrlich , H.C. 1959. Comparison of cardiac monophasic action potentials recorded by intracellular and suction electrodes. *Am J.Physiol*, 196, (6) 1297-1301

121. Hoffman, B.F., Kao , C.Y., & Suckling E.E. 1957. Refractoriness in cardiac muscle. *Am.J.Physiol*, 190, (3) 473-482

122. Huang, J., Zhou X, Smith WM, & Ideker RE 2004. Restitution properties during ventricular fibrillation in the in situ swine heart. *Circulation*, 110, (20) 3161-3167

123. Huffaker, R., Lamp, S.T., Weiss, J.N., & Kogan, B. 2004. Intracellular calcium cycling, early afterdepolarizations, and reentry in simulated long QT syndrome. *Heart Rhythm.*, 1, (4) 441-448

124. Ideker, R.E., Klein, G.J., Harrison, L., Smith, W.M., Kasell, J., Reimer, K.A., Wallace, A.G., & Gallagher, J.J. 1981. The transition to ventricular fibrillation induced by reperfusion after acute ischemia in the dog: a period of organized epicardial activation. *Circulation*, 63, (6) 1371-1379

125. Iinuma, H. & Kato, K. 1979. Mechanism of augmented premature responses in canine ventricular muscle. *Circ.Res.*, 44, (5) 624-629

126. Imaki, R., Niwano, S., Fukaya, H., Sasaki, S., Yuge, M., Hirasawa, S., Sato, D., Sasaki, T., Moriguchi, M., & Izumi, T. 2006. Predictive impact of the inducibility of ventricular fibrillation in patients with Brugada-type ECG. *Int Heart J.*, 47, (2) 229-236

127. Imanishi, S. & Surawicz, B. 1976. Automatic activity in depolarized guinea pig ventricular myocardium. Characteristics and mechanisms. *Circ.Res.*, 39, (6) 751-759

128. Ino, T., Karagueuzian, H.S., Hong, K., Meesmann, M., Mandel, W.J., & Peter, T. 1988. Relation of monophasic action potential recorded with contact electrode to underlying transmembrane action potential properties in isolated cardiac tissues: a systematic microelectrode validation study. *Cardiovasc.Res.*, 22, (4) 255-264

129. Jacobson, J., Afonso, V., X, Eisenman, G., Schultz, J., Lazar, S., Michele, J., Josephson, M., & Callans, D. 2006. Characterization of the infarct substrate and ventricular tachycardia circuits with noncontact unipolar mapping in a porcine model of myocardial infarction. *Heart rhythm : the official journal of the Heart Rhythm Society*, 3, (2) 189-197

130. Jalife, J. 2000. Ventricular fibrillation: mechanisms of initiation and maintenance. *Annual review of physiology*, 62, 25-50

131. Janse, M.J., van Capelle, F.J., Freud, G.E., & Durrer, D. 1971. Circus movement within the AV node as a basis for supraventricular tachycardia as shown by multiple microelectrode recording in the isolated rabbit heart. *Circ.Res.*, 28, (4) 403-414

132. Jenkins, K.J., Walsh, E.P., Colan, S.D., Bergau, D.M., Saul, J.P., & Lock, J.E. 1993. Multipolar endocardial mapping of the right atrium during cardiac catheterization: description of a new technique. *J.Am.Coll.Cardiol*, 22, (4) 1105-1110

133. Jervell , A. & Lange-Nielsen , F. 1957. Congenital deaf-mutism, functional heart disease with prolongation of the Q-T interval and sudden death. *Am.Heart J.*, 54, (1) 59-68

134. Jimenez, R.A. & Myerburg, R.J. 1993. Sudden cardiac death. Magnitude of the problem, substrate/trigger interaction, and populations at high risk. *Cardiol Clin.*, 11, (1) 1-9

135. Jin, Q., Chen, X., Smith, W.M., Ideker, R.E., & Huang, J. 2008. Effects of procainamide and sotalol on restitution properties, dispersion of refractoriness, and ventricular fibrillation activation patterns in pigs. *J.Cardiovasc.Electrophysiol.*, 19, (10) 1090-1097

136. Johnson, N., Danilo, P., Jr., Wit, A.L., & Rosen, M.R. 1986. Characteristics of initiation and termination of catecholamine-induced triggered activity in atrial fibers of the coronary sinus. *Circulation*, 74, (5) 1168-1179

137. Josephson, M.E., Horowitz, L.N., & Farshidi, A. 1978a. Continuous local electrical activity. A mechanism of recurrent ventricular tachycardia. *Circulation*, 57, (4) 659-665

138. Josephson, M.E., Horowitz, L.N., Farshidi, A., Spear, J.F., Kastor, J.A., & Moore, E.N. 1978b. Recurrent sustained ventricular tachycardia. 2. Endocardial mapping. *Circulation*, 57, (3) 440-447

139. Josephson, M.E., Horowitz, L.N., Spielman, S.R., Waxman, H.L., & Greenspan, A.M. 1982. Role of catheter mapping in the preoperative evaluation of ventricular tachycardia. *Am.J.Cardiol*, 49, (1) 207-220

140. Juilliere, Y., Danchin, N., Briancon, S., Khalife, K., Ethevenot, G., Balaud, A., Gilgenkrantz, J.M., Pernot, C., & Cherrier, F. 1988. Dilated cardiomyopathy: long-term follow-up and predictors of survival. *Int J.Cardiol*, 21, (3) 269-277

141. Kadish, A., Hauck, J., Pederson, B., Beatty, G., & Gornick, C. 1999. Mapping of atrial activation with a noncontact, multielectrode catheter in dogs. *Circulation*, 99, (14) 1906-1913

142. Karma, A. 1994. Electrical alternans and spiral wave breakup in cardiac tissue. *Chaos.*, 4, (3) 461-472

143. Katzung, B.G. 1975. Effects of extracellular calcium and sodium on depolarization-induced automaticity in guinea pig papillary muscle. *Circ.Res.*, 37, (1) 118-127

144. Katzung, B.G. & Morgenstern, J.A. 1977. Effects of extracellular potassium on ventricular automaticity and evidence for a pacemaker current in mammalian ventricular myocardium. *Circ.Res.*, 40, (1) 105-111

145. Kautzner, J., Yi, G., Camm, A.J., & Malik, M. 1994. Short- and long-term reproducibility of QT, QTc, and QT dispersion measurement in healthy subjects. *Pacing Clin Electrophysiol*, 17, (5 Pt 1) 928-937

146. Kay, M.W. & Rogers, J.M. 2006. Epicardial rotors in panoramic optical maps of fibrillating swine ventricles. *Conf.Proc.IEEE Eng Med.Biol.Soc.*, 1, 2268-2271

147. Kay, M.W., Walcott, G.P., Gladden, J.D., Melnick, S.B., & Rogers, J.M. 2006. Lifetimes of epicardial rotors in panoramic optical maps of fibrillating swine ventricles. *Am.J.Physiol Heart Circ.Physiol*, 291, (4) H1935-H1941

148. Khoury, D.S., Berrier, K.L., Badruddin, S.M., & Zoghbi, W.A. 1998. Three-dimensional electrophysiological imaging of the intact canine left ventricle using a noncontact multielectrode cavitary probe: study of sinus, paced, and spontaneous premature beats. *Circulation*, 97, (4) 399-409

149. Khoury, D.S., Taccardi, B., Lux, R.L., Ershler, P.R., & Rudy, Y. 1995. Reconstruction of endocardial potentials and activation sequences from

intracavitary probe measurements. Localization of pacing sites and effects of myocardial structure. *Circulation*, 91, (3) 845-863

150. Kirchhof, P., Degen, H., Franz, M.R., Eckardt, L., Fabritz, L., Milberg, P., Laer, S., Neumann, J., Breithardt, G., & Haverkamp, W. 2003a. Amiodarone-induced postrepolarization refractoriness suppresses induction of ventricular fibrillation. *J.Pharmacol.Exp.Ther.*, 305, (1) 257-263

151. Kirchhof, P., Eckardt, L., Franz, M.R., Monnig, G., Loh, P., Wedekind, H., Schulze-Bahr, E., Breithardt, G., & Haverkamp, W. 2003b. Prolonged atrial action potential durations and polymorphic atrial tachyarrhythmias in patients with long QT syndrome. *J.Cardiovasc.Electrophysiol.*, 14, (10) 1027-1033

152. Kirchhof, P.F., Fabritz, C.L., & Franz, M.R. 1998. Postrepolarization refractoriness versus conduction slowing caused by class I antiarrhythmic drugs: antiarrhythmic and proarrhythmic effects. *Circulation*, 97, (25) 2567-2574

153. Klein, H., Karp, R.B., Kouchoukos, N.T., Zorn, G.L., Jr., James, T.N., & Waldo, A.L. 1982. Intraoperative electrophysiologic mapping of the ventricles during sinus rhythm in patients with a previous myocardial infarction. Identification of the electrophysiologic substrate of ventricular arrhythmias. *Circulation*, 66, (4) 847-853

154. Koller, B.S., Karasik, P.E., Solomon, A.J., & Franz, M.R. 1995. Relation between repolarization and refractoriness during programmed electrical stimulation in the human right ventricle. Implications for ventricular tachycardia induction. *Circulation*, 91, (9) 2378-2384

155. Koller, M.L., Maier, S.K., Gelzer, A.R., Bauer, W.R., Meesmann, M., & Gilmour, R.F., Jr. 2005. Altered dynamics of action potential restitution and alternans in humans with structural heart disease. *Circulation*, 112, (11) 1542-1548

156. Koller, M.L., Riccio, M.L., & Gilmour, R.F., Jr. 1998. Dynamic restitution of action potential duration during electrical alternans and ventricular fibrillation. *Am.J.Physiol*, 275, (5 Pt 2) H1635-H1642

157. Kong, M.H., Fonarow, G.C., Peterson, E.D., Curtis, A.B., Hernandez, A.F., Sanders, G.D., Thomas, K.L., Hayes, D.L., & Al-Khatib, S.M. 2011. Systematic review of the incidence of sudden cardiac death in the United States. *J.Am.Coll.Cardiol*, 57, (7) 794-801

158. Korsgren, M., Leskinen, E., Sjostrand, U., & Varnauskas, E. 1966. Intracardiac recording of monophasic action potentials in the human heart. *Scand.J.Clin.Lab Invest*, 18, (5) 561-564

159. Koyak, Z., de Groot, J.R., Van Gelder, I.C., Bouma, B.J., van Dessel, P.F., Budts, W., van, E.L., van Dijk, A.P., Wilde, A.A., Pieper, P.G., Sieswerda, G.T., & Mulder, B.J. 2012a. Implantable cardioverter defibrillator therapy in adults with congenital heart disease: who is at risk of shocks? *Circ.Arrhythm.Electrophysiol.*, 5, (1) 101-110

160. Koyak, Z., Harris, L., de Groot, J.R., Silversides, C.K., Oechslin, E.N., Bouma, B.J., Budts, W., Zwinderman, A.H., Van Gelder, I.C., & Mulder, B.J. 2012b.

Sudden cardiac death in adult congenital heart disease. *Circulation*, 126, (16) 1944-1954

161. Krishnan, S.C. & Antzelevitch, C. 1993. Flecainide-induced arrhythmia in canine ventricular epicardium. Phase 2 reentry? *Circulation*, 87, (2) 562-572

162. Krittayaphong, R., Veerakul, G., Nademanee, K., & Kangkagate, C. 2003. Heart rate variability in patients with Brugada syndrome in Thailand. *Eur.Heart J.*, 24, (19) 1771-1778

163. Kuo, C.S., Munakata, K., Reddy, C.P., & Surawicz, B. 1983. Characteristics and possible mechanism of ventricular arrhythmia dependent on the dispersion of action potential durations. *Circulation*, 67, (6) 1356-1367

164. Kuo, C.S. & Surawicz, B. 1976. Ventricular monophasic action potential changes associated with neurogenic T wave abnormalities and isoproterenol administration in dogs. *Am J.Cardiol*, 38, (2) 170-177

165. Kurz, R.W., Mohabir, R., Ren, X.L., & Franz, M.R. 1993. Ischaemia induced alternans of action potential duration in the intact-heart: dependence on coronary flow, preload and cycle length. *Eur.Heart J.*, 14, (10) 1410-1420

166. Kurz, R.W., Ren, X.L., & Franz, M.R. 1994. Dispersion and delay of electrical restitution in the globally ischaemic heart. *Eur.Heart J.*, 15, (4) 547-554

167. La Rovere, M.T., Bigger, J.T., Jr., Marcus, F.I., Mortara, A., & Schwartz, P.J. 1998. Baroreflex sensitivity and heart-rate variability in prediction of total cardiac mortality after myocardial infarction. ATRAMI (Autonomic Tone and Reflexes After Myocardial Infarction) Investigators. *Lancet*, 351, (9101) 478-484

168. Lam, W. & Friedman, R.A. 2011. Electrophysiology issues in adult congenital heart disease. *Methodist.Debakey.Cardiovasc.J.*, 7, (2) 13-17

169. Lambiase, P.D., Ahmed, A.K., Ciaccio, E.J., Brugada, R., Lizotte, E., Chaubey, S., Ben-Simon, R., Chow, A.W., Lowe, M.D., & McKenna, W.J. 2009. High-density substrate mapping in Brugada syndrome: combined role of conduction and repolarization heterogeneities in arrhythmogenesis. *Circulation*, 120, (2) 106-4

170. Laurita, K.R., Girouard, S.D., & Rosenbaum, D.S. 1996. Modulation of ventricular repolarization by a premature stimulus. Role of epicardial dispersion of repolarization kinetics demonstrated by optical mapping of the intact guinea pig heart. *Circ.Res.*, 79, (3) 493-503

171. Lee, J.J., Kamjoo, K., Hough, D., Hwang, C., Fan, W., Fishbein, M.C., Bonometti, C., Ikeda, T., Karagueuzian, H.S., & Chen, P.S. 1996. Reentrant wave fronts in Wiggers' stage II ventricular fibrillation. Characteristics and mechanisms of termination and spontaneous regeneration. *Circ.Res.*, 78, (4) 660-675

172. Lee, R.J., Liem, L.B., Cohen, T.J., & Franz, M.R. 1992. Relation between repolarization and refractoriness in the human ventricle: cycle length dependence and effect of procainamide. *J Am Coll Cardiol*, 19, (3) 614-618

173. Lee, S., Sahadevan, J., Khrestian, C.M., Durand, D.M., & Waldo, A.L. 2012. High Density Mapping of Atrial Fibrillation During Vagal Nerve Stimulation in the Canine Heart: Restudying the Moe Hypothesis. *J.Cardiovasc.Electrophysiol.*

174. Letsas, K.P., Efremidis, M., Weber, R., Korantzopoulos, P., Protonotarios, N., Prappa, E., Kounas, S.P., Evagelidou, E.N., Xydonas, S., Kalusche, D., Sideris, A., & Arentz, T. 2011. Epsilon-like waves and ventricular conduction abnormalities in subjects with type 1 ECG pattern of Brugada syndrome. *Heart Rhythm.*, 8, (6) 874-878

175. Li, G.R., Feng, J., Yue, L., Carrier, M., & Nattel, S. 1996. Evidence for two components of delayed rectifier K+ current in human ventricular myocytes. *Circ.Res.*, 78, (4) 689-696

176. Liu, Y.B., Pak, H.N., Lamp, S.T., Okuyama, Y., Hayashi, H., Wu, T.J., Weiss, J.N., Chen, P.S., & Lin, S.F. 2004. Coexistence of two types of ventricular fibrillation during acute regional ischemia in rabbit ventricle. *J.Cardiovasc.Electrophysiol.*, 15, (12) 1433-1440

177. Loire, R. & Tabib, A. 1996. [Unexpected sudden cardiac death. An evaluation of 1000 autopsies]. *Arch Mal Coeur Vaiss.*, 89, (1) 13-18

178. Lui, G.K., Silversides, C.K., Khairy, P., Fernandes, S.M., Valente, A.M., Nickolaus, M.J., Earing, M.G., Aboulhosn, J.A., Rosenbaum, M.S., Cook, S., Kay, J.D., Jin, Z., & Gersony, D.R. 2011. Heart rate response during exercise and pregnancy outcome in women with congenital heart disease. *Circulation*, 123, (3) 242-248

179. MacCurdy E 1954. *The notebooks of Leonard Da Vinci* New York, George Braziller.

180. Maire, R., Hess, O.M., Turina, J., Greminger, P., & Krayenbuhl, H.P. 1985. [Long-term follow-up and prognosis of dilated cardiomyopathy]. *Schweiz.Med.Wochenschr.*, 115, (45) 1609-1612

181. Makimoto, H., Kamakura, S., Aihara, N., Noda, T., Nakajima, I., Yokoyama, T., Doi, A., Kawata, H., Yamada, Y., Okamura, H., Satomi, K., Aiba, T., & Shimizu, W. 2012. Clinical impact of the number of extrastimuli in programmed electrical stimulation in patients with Brugada type 1 electrocardiogram. *Heart Rhythm.*, 9, (2) 242-248

182. Malfatto, G., Zaza, A., & Schwartz, P.J. 1994. Modulation of the electrical restitution of canine Purkinje fibers by local anesthetic drugs: a study with flecainide and propafenone. *Pacing Clin.Electrophysiol.*, 17, (11 Pt 2) 2074-2078

183. Malik, M. & Batchvarov, V.N. 2000. Measurement, interpretation and clinical potential of QT dispersion. *J.Am.Coll.Cardiol*, 36, (6) 1749-1766

184. Marchlinski, F.E., Buxton, A.E., Waxman, H.L., & Josephson, M.E. 1983. Identifying patients at risk of sudden death after myocardial infarction: value of the response to programmed stimulation, degree of ventricular ectopic activity and severity of left ventricular dysfunction. *Am J.Cardiol*, 52, (10) 1190-1196

185. Margey, R., Roy, A., Tobin, S., O'Keane, C.J., McGorrian, C., Morris, V., Jennings, S., & Galvin, J. 2011. Sudden cardiac death in 14- to 35-year olds in Ireland from 2005 to 2007: a retrospective registry. *Europace.*, 13, (10) 1411-1418

186. Maron, B.J. 2002. Hypertrophic cardiomyopathy: a systematic review. *JAMA*, 287, (10) 1308-1320

187. Maron, B.J., Epstein, S.E., & Roberts, W.C. 1986. Causes of sudden death in competitive athletes. *J.Am.Coll.Cardiol*, 7, (1) 204-214

188. Maron, B.J., Gardin, J.M., Flack, J.M., Gidding, S.S., Kurosaki, T.T., & Bild, D.E. 1995. Prevalence of hypertrophic cardiomyopathy in a general population of young adults. Echocardiographic analysis of 4111 subjects in the CARDIA Study. Coronary Artery Risk Development in (Young) Adults. *Circulation*, 92, (4) 785-789

189. Maron, B.J., McKenna, W.J., Danielson, G.K., Kappenberger, L.J., Kuhn, H.J., Seidman, C.E., Shah, P.M., Spencer, W.H., III, Spirito, P., Ten Cate, F.J., & Wigle, E.D. 2003. American College of Cardiology/European Society of Cardiology Clinical Expert Consensus Document on Hypertrophic Cardiomyopathy. A report of the American College of Cardiology Foundation Task Force on Clinical Expert Consensus Documents and the European Society of Cardiology Committee for Practice Guidelines. *Eur.Heart J.*, 24, (21) 1965-1991

190. Martini, B., Nava, A., Thiene, G., Buja, G.F., Canciani, B., Scognamiglio, R., Daliento, L., & Dalla, V.S. 1989. Ventricular fibrillation without apparent heart disease: description of six cases. *Am Heart J.*, 118, (6) 1203-1209

191. Martins, J.B. & Zipes, D.P. 1980. Effects of sympathetic and vagal nerves on recovery properties of the endocardium and epicardium of the canine left ventricle. *Circ.Res.*, 46, (1) 100-110

192. Matsuda, H., Noma, A., Kurachi, Y., & Irisawa, H. 1982. Transient depolarization and spontaneous voltage fluctuations in isolated single cells from guinea pig ventricles. Calcium-mediated membrane potential fluctuations. *Circ.Res.*, 51, (2) 142-151

193. McWilliam, J.A. 1887. Fibrillar Contraction of the Heart. *J.Physiol*, 8, (5) 296-310

194. Meissner, M.D., Lehmann, M.H., Steinman, R.T., Mosteller, R.D., Akhtar, M., Calkins, H., Cannom, D.S., Epstein, A.E., Fogoros, R.N., Liem, L.B., & . 1993. Ventricular fibrillation in patients without significant structural heart disease: a multicenter experience with implantable cardioverter-defibrillator therapy. *J.Am.Coll.Cardiol*, 21, (6) 1406-1412

195. Michels, V.V., Moll, P.P., Miller, F.A., Tajik, A.J., Chu, J.S., Driscoll, D.J., Burnett, J.C., Rodeheffer, R.J., Chesebro, J.H., & Tazelaar, H.D. 1992. The frequency of familial dilated cardiomyopathy in a series of patients with idiopathic dilated cardiomyopathy. *N.Engl.J.Med.*, 326, (2) 77-82

196. Millar, C.K., Kralios, F.A., & Lux, R.L. 1985. Correlation between refractory periods and activation-recovery intervals from electrograms: effects of rate and adrenergic interventions. *Circulation*, 72, (6) 1372-1379

197. Mines, G.R. 1913. On dynamic equilibrium in the heart. *J.Physiol*, 46, (4-5) 349-383

198. Mironov, S., Jalife, J., & Tolkacheva, E.G. 2008. Role of conduction velocity restitution and short-term memory in the development of action potential duration alternans in isolated rabbit hearts. *Circulation*, 118, (1) 17-25

199. Misier, A.R., Opthof, T., van Hemel, N.M., Vermeulen, J.T., de Bakker, J.M., Defauw, J.J., van Capelle, F.J., & Janse, M.J. 1995. Dispersion of 'refractoriness' in noninfarcted myocardium of patients with ventricular tachycardia or ventricular fibrillation after myocardial infarction. *Circulation*, 91, (10) 2566-2572

200. Miyazaki, T., Mitamura, H., Miyoshi, S., Soejima, K., Aizawa, Y., & Ogawa, S. 1996. Autonomic and antiarrhythmic drug modulation of ST segment elevation in patients with Brugada syndrome. *J.Am Coll.Cardiol*, 27, (5) 1061-1070

201. Moe , G.K. 1962. On the multiple wavelet hypothesis of atrial fibrillation. *Arch Int Pharmacodyn Ther.* (140) 183-188

202. Moe , G.K. & Abildskov, J.A. 1964. Observations on the ventricular dysrhythmia associated with atrial fibrillation in the dog heart. *Circ.Res.*, 14, 447-460

203. Moe , G.K., Rheinboldt , W.C., & Abildskov, J.A. 1964. A computer model of atrial fibrillation. *Am.Heart J.*, 67, 200-220

204. Mok, N.S., Chan, N.Y., & Chiu, A.C. 2004. Successful use of quinidine in treatment of electrical storm in Brugada syndrome. *Pacing Clin.Electrophysiol.*, 27, (6 Pt 1) 821-823

205. Morgan, J.M., Cunningham, D., & Rowland, E. 1992a. Dispersion of monophasic action potential duration: demonstrable in humans after premature ventricular extrastimulation but not in steady state. *J.Am Coll.Cardiol*, 19, (6) 1244-1253

206. Morgan, J.M., Cunningham, D., & Rowland, E. 1992b. Electrical restitution in the endocardium of the intact human right ventricle. *Br.Heart J.*, 67, (1) 42-46

207. Morgan, J.M., Lopes, A., & Rowland, E. 1991. Sudden cardiac death while taking amiodarone therapy: the role of abnormal repolarization. *Eur.Heart J.*, 12, (10) 1144-1147

208. Morita, N., Lee, J.H., Xie, Y., Sovari, A., Qu, Z., Weiss, J.N., & Karagueuzian, H.S. 2011. Suppression of re-entrant and multifocal ventricular fibrillation by the late sodium current blocker ranolazine. *J.Am.Coll.Cardiol*, 57, (3) 366-375

209. Moss, A.J., Hall, W.J., Cannom, D.S., Daubert, J.P., Higgins, S.L., Klein, H., Levine, J.H., Saksena, S., Waldo, A.L., Wilber, D., Brown, M.W., & Heo, M. 1996. Improved survival with an implanted defibrillator in patients with coronary disease at high risk for ventricular arrhythmia. Multicenter Automatic Defibrillator Implantation Trial Investigators. *N.Engl.J.Med.*, 335, (26) 1933-1940

210. Moss, A.J., Hall, W.J., Cannom, D.S., Klein, H., Brown, M.W., Daubert, J.P., Estes, N.A., III, Foster, E., Greenberg, H., Higgins, S.L., Pfeffer, M.A., Solomon, S.D., Wilber, D., & Zareba, W. 2009. Cardiac-resynchronization therapy for the prevention of heart-failure events. *N.Engl.J.Med.*, 361, (14) 1329-1338

211. Moss, A.J., Zareba, W., Hall, W.J., Klein, H., Wilber, D.J., Cannom, D.S., Daubert, J.P., Higgins, S.L., Brown, M.W., & Andrews, M.L. 2002. Prophylactic implantation of a defibrillator in patients with myocardial infarction and reduced ejection fraction. *N.Engl.J.Med.*, 346, (12) 877-883

212. Moubarak, J.B., Karasik, P.E., Fletcher, R.D., & Franz, M.R. 2000. High dispersion of ventricular repolarization after an implantable defibrillator shock predicts induction of ventricular fibrillation as well as unsuccessful defibrillation. *J.Am Coll.Cardiol*, 35, (2) 422-427

213. Myerburg RJ & Castellanos A 2008, "Cardiac arrest and sudden cardiac death," *In Braunwald's Heart disease: A textbook of cardiovascular medicine*, eigth ed. Libby et al., eds., Saunders Elsevier, pp. 933-971.

214. Myerburg, R.J. & Junttila, M.J. 2012. Sudden cardiac death caused by coronary heart disease. [Review].

215. Myerburg, R.J., Kessler, K.M., & Castellanos, A. 1993. Sudden cardiac death: epidemiology, transient risk, and intervention assessment. *Ann Intern.Med.*, 119, (12) 1187-1197

216. Nabauer, M. 1998. Electrical heterogeneity in the ventricular wall--and the M cell. *Cardiovasc.Res.*, 40, (2) 248-250

217. Nademanee, K., Veerakul, G., Chandanamattha, P., Chaothawee, L., Ariyachaipanich, A., Jirasirirojanakorn, K., Likittanasombat, K., Bhuripanyo, K., & Ngarmukos, T. 2011. Prevention of ventricular fibrillation episodes in Brugada syndrome by catheter ablation over the anterior right ventricular outflow tract epicardium. *Circulation*, 123, (12) 1270-1279

218. Nanthakumar, K., Walcott, G.P., Melnick, S., Rogers, J.M., Kay, M.W., Smith, W.M., Ideker, R.E., & Holman, W. 2004. Epicardial organization of human ventricular fibrillation. *Heart Rhythm.*, 1, (1) 14-23

219. Nash, M.P., Bradley, C.P., & Paterson, D.J. 2003. Imaging electrocardiographic dispersion of depolarization and repolarization during ischemia: simultaneous body surface and epicardial mapping. *Circulation*, 107, (17) 2257-2263

220. Nash, M.P., Mourad, A., Clayton, R.H., Sutton, P.M., Bradley, C.P., Hayward, M., Paterson, D.J., & Taggart, P. 2006. Evidence for multiple mechanisms in human ventricular fibrillation. *Circulation*, 114, (6) 536-542

221. Ng, G.A., Brack, K.E., Patel, V.H., & Coote, J.H. 2007. Autonomic modulation of electrical restitution, alternans and ventricular fibrillation initiation in the isolated heart. *Cardiovasc.Res.*, 73, (4) 750-760

222. NICE. National Institute for Health and Clinical Excellence (NICE) guidelines:Impalntable cardioverter defibrillators for arrhythmias. Review of technology appraisal 11. 2006.

Ref Type: Online Source

223. Nicolson, W.B., Brown, P., Tuan, J., Sandilands, A.J., Stafford, P.J., Schlindwein, F.S., McCann, G.P., & Ng, G.A. 2011a. Novel restitution gradient-based predictor of ventricular arrhythmia.

224. Nicolson, W.B., McCann, G.P., Brown, P.D., Sandilands, A.J., Stafford, P.J., Schlindwein, F.S., Samani, N.J., & Ng, G.A. 2012. A novel surface electrocardiogram-based marker of ventricular arrhythmia risk in patients with ischemic cardiomyopathy. *J.Am.Heart Assoc.*, 1, (4) e001552

225. Nicolson, W.B., Steadman, C., Brown, P., Jeilan, M., Yusuf, S., Kundu, S., Sandilands, A., Stafford, P., Schlindwein, F., McCann, G., & Ng, G.A. 2011b. Pilot study exploring the regional repolarisation instability index in relation to myocardial heterogeneity and prediction of ventricular arrhythmia and death.

226. Nolasco, J.B. 1968. A graphic method for the study of alternation in cardiac action potentials. *Journal of applied physiology*, 25, (2) 191-196

227. Norozi, K., Buchhorn, R., Yasin, A., Geyer, S., Binder, L., Seabrook, J.A., & Wessel, A. 2011. Growth differentiation factor 15: an additional diagnostic tool for the risk stratification of developing heart failure in patients with operated congenital heart defects? *Am.Heart J.*, 162, (1) 131-135

228. Omichi, C., Zhou, S., Lee, M.H., Naik, A., Chang, C.M., Garfinkel, A., Weiss, J.N., Lin, S.F., Karagueuzian, H.S., & Chen, P.S. 2002. Effects of amiodarone on wave front dynamics during ventricular fibrillation in isolated swine right ventricle. *Am J.Physiol Heart Circ.Physiol*, 282, (3) H1063-H1070

229. Osadchii, O.E. 2012. Flecainide-induced proarrhythmia is attributed to abnormal changes in repolarization and refractoriness in perfused guinea-pig heart. *J.Cardiovasc.Pharmacol.*, 60, (5) 456-466

230. Osaka, T., Kodama, I., Tsuboi, N., Toyama, J., & Yamada, K. 1987. Effects of activation sequence and anisotropic cellular geometry on the repolarization phase of action potential of dog ventricular muscles. *Circulation*, 76, (1) 226-236

231. Oudit, G.Y., Kassiri, Z., Sah, R., Ramirez, R.J., Zobel, C., & Backx, P.H. 2001. The molecular physiology of the cardiac transient outward potassium current (I(to)) in normal and diseased myocardium. *J.Mol.Cell Cardiol*, 33, (5) 851-872

232. Page, R.L., Zipes, D.P., Powell, J.L., Luceri, R.M., Gold, M.R., Peters, R., Russo, A.M., Bigger, J.T., Jr., Sung, R.J., & McBurnie, M.A. 2004. Seasonal variation of mortality in the Antiarrhythmics Versus Implantable Defibrillators (AVID) study registry. *Heart Rhythm.*, 1, (4) 435-440

233. Pak, H.N., Hong, S.J., Hwang, G.S., Lee, H.S., Park, S.W., Ahn, J.C., Moo, R.Y., & Kim, Y.H. 2004. Spatial dispersion of action potential duration restitution kinetics is associated with induction of ventricular tachycardia/fibrillation in humans. *J.Cardiovasc.Electrophysiol.*, 15, (12) 1357-1363

234. Pastore, J.M. & Rosenbaum, D.S. 2000. Role of structural barriers in the mechanism of alternans-induced reentry. *Circ.Res.*, 87, (12) 1157-1163

235. Pertsov, A.M., Davidenko, J.M., Salomonsz, R., Baxter, W.T., & Jalife, J. 1993. Spiral waves of excitation underlie reentrant activity in isolated cardiac muscle. *Circ.Res.*, 72, (3) 631-650

236. Peters, N.S. 1996. New insights into myocardial arrhythmogenesis: distribution of gap-junctional coupling in normal, ischaemic and hypertrophied human hearts. *Clinical science*, 90, (6) 447-452

237. Peters, N.S., Coromilas, J., Severs, N.J., & Wit, A.L. 1997. Disturbed connexin43 gap junction distribution correlates with the location of reentrant circuits in the epicardial border zone of healing canine infarcts that cause ventricular tachycardia. *Circulation*, 95, (4) 988-996

238. Peters, N.S. & Wit, A.L. 1998. Myocardial architecture and ventricular arrhythmogenesis. *Circulation*, 97, (17) 1746-1754

239. Potse, M., Vinet, A., Opthof, T., & Coronel, R. 2009. Validation of a simple model for the morphology of the T wave in unipolar electrograms. *Am J.Physiol Heart Circ.Physiol*, 297, (2) H792-H801

240. Priori, S.G., Aliot, E., Blomstrom-Lundqvist, C., Bossaert, L., Breithardt, G., Brugada, P., Camm, J.A., Cappato, R., Cobbe, S.M., Di, M.C., Maron, B.J., McKenna, W.J., Pedersen, A.K., Ravens, U., Schwartz, P.J., Trusz-Gluza, M., Vardas, P., Wellens, H.J., & Zipes, D.P. 2002. Task Force on Sudden Cardiac Death, European Society of Cardiology. *Europace.*, 4, (1) 3-18

241. Priori, S.G., Aliot, E., Blomstrom-Lundqvist, C., Bossaert, L., Breithardt, G., Brugada, P., Camm, J.A., Cappato, R., Cobbe, S.M., Di, M.C., Maron, B.J., McKenna, W.J., Pedersen, A.K., Ravens, U., Schwartz, P.J., Trusz-Gluza, M., Vardas, P., Wellens, H.J., & Zipes, D.P. 2003a. Update of the guidelines on sudden cardiac death of the European Society of Cardiology. *Eur Heart J*, 24, (1) 13-15

242. Priori, S.G., Gasparini, M., Napolitano, C., Della, B.P., Ottonelli, A.G., Sassone, B., Giordano, U., Pappone, C., Mascioli, G., Rossetti, G., De, N.R., & Colombo, M. 2012. Risk stratification in Brugada syndrome: results of the PRELUDE (PRogrammed ELectrical stimUlation preDictive valuE) registry. *J.Am.Coll.Cardiol*, 59, (1) 37-45

243. Priori, S.G. & Maugeri F S 1997. Survivors of out-of-hospital cardiac arrest with apparently normal heart. Need for definition and standardized clinical evaluation. Consensus Statement of the Joint Steering Committees of the Unexplained Cardiac Arrest Registry of Europe and of the Idiopathic Ventricular Fibrillation Registry of the United States. *Circulation*, 95, (1) 265-272

244. Priori, S.G., Napolitano, C., Schwartz, P.J., Grillo, M., Bloise, R., Ronchetti, E., Moncalvo, C., Tulipani, C., Veia, A., Bottelli, G., & Nastoli, J. 2004. Association of long QT syndrome loci and cardiac events among patients treated with beta-blockers. *JAMA*, 292, (11) 1341-1344

245. Priori, S.G., Napolitano, C., Tiso, N., Memmi, M., Vignati, G., Bloise, R., Sorrentino, V., & Danieli, G.A. 2001. Mutations in the cardiac ryanodine receptor gene (hRyR2) underlie catecholaminergic polymorphic ventricular tachycardia. *Circulation*, 103, (2) 196-200

246. Priori, S.G., Schwartz, P.J., Napolitano, C., Bloise, R., Ronchetti, E., Grillo, M., Vicentini, A., Spazzolini, C., Nastoli, J., Bottelli, G., Folli, R., & Cappelletti, D. 2003b. Risk stratification in the long-QT syndrome. *N.Engl.J.Med.*, 348, (19) 1866-1874

247. Qu, Z., Garfinkel, A., Chen, P.S., & Weiss, J.N. 2000a. Mechanisms of discordant alternans and induction of reentry in simulated cardiac tissue. *Circulation*, 102, (14) 1664-1670

248. Qu, Z., Kil, J., Xie, F., Garfinkel, A., & Weiss, J.N. 2000b. Scroll wave dynamics in a three-dimensional cardiac tissue model: roles of restitution, thickness, and fiber rotation.

249. Qu, Z., Weiss, J.N., & Garfinkel, A. 1999. Cardiac electrical restitution properties and stability of reentrant spiral waves: a simulation study. *Am J.Physiol*, 276, (1 Pt 2) H269-H283

250. Ramos, R., Branco, L., Agapito, A., Oliveira, J.A., Sousa, L., Galrinho, A., Fiarresga, A., Toste, A., Lousinha, A., Oliveira, M., Da Silva, J.N., & Ferreira, R.C. 2010. Usefulness of tissue Doppler imaging to predict arrhythmic events in adults with repaired tetralogy of Fallot. *Rev.Port.Cardiol*, 29, (7-8) 1145-1161

251. Rankovic, V., Patel, N., Jain, S., Robinson, N., Goldberger, J., Horvath, G., & Kadish, A. 1999. Characteristics of ischemic and peri-ischemic regions during ventricular fibrillation in the canine heart. *J.Cardiovasc.Electrophysiol.*, 10, (8) 1090-1100

252. Reek, S., Geller, J.C., Mittag, A., Grothues, F., Hess, A., Kaulisch, T., & Klein, H.U. 2003. Noncontact mapping of ventricular tachycardia in a closed-chest animal model of chronic myocardial infarction. *Pacing Clin.Electrophysiol.*, 26, (12) 2253-2263

253. Rensma, P.L., Allessie, M.A., Lammers, W.J., Bonke, F.I., & Schalij, M.J. 1988. Length of excitation wave and susceptibility to reentrant atrial arrhythmias in normal conscious dogs. *Circ.Res.*, 62, (2) 395-410

254. Roberts, W.C., Kragel, A.H., Gertz, S.D., & Roberts, C.S. 1994. Coronary arteries in unstable angina pectoris, acute myocardial infarction, and sudden coronary death. *Am.Heart J.*, 127, (6) 1588-1593

255. Rogers, J.M., Huang, J., Melnick, S.B., & Ideker, R.E. 2003. Sustained reentry in the left ventricle of fibrillating pig hearts. *Circ.Res.*, 92, (5) 539-545

256. Rosen, M.R., Gelband, H., Merker, C., & Hoffman, B.F. 1973. Mechanisms of digitalis toxicity. Effects of ouabain on phase four of canine Purkinje fiber transmembrane potentials. *Circulation*, 47, (4) 681-689

257. Rosenbaum, M.B., Blanco, H.H., Elizari, M.V., Lazzari, J.O., & Davidenko, J.M. 1982. Electrotonic modulation of the T wave and cardiac memory. *Am J.Cardiol*, 50, (2) 213-222

258. Sabir, I.N., Ma, N., Jones, V.J., Goddard, C.A., Zhang, Y., Kalin, A., Grace, A.A., & Huang, C.L. 2010. Alternans in genetically modified langendorff-perfused

murine hearts modeling catecholaminergic polymorphic ventricular tachycardia. *Front Physiol*, 1, 126

259. Samie, F.H. & Jalife, J. 2001. Mechanisms underlying ventricular tachycardia and its transition to ventricular fibrillation in the structurally normal heart. *Cardiovasc.Res.*, 50, (2) 242-250

260. Sanders, G.D., Al-Khatib, S.M., Berliner, E., Bigger, J.T., Buxton, A.E., Califf, R.M., Carlson, M., Curtis, A.B., Curtis, J.P., Domanski, M., Fain, E., Gersh, B.J., Gold, M.R., Goldberger, J., Haghighi-Mood, A., Hammill, S.C., Harder, J., Healey, J., Hlatky, M.A., Hohnloser, S.H., Lee, K.L., Mark, D.B., Mitchell, B., Phurrough, S., Prystowsky, E., Smith, J.M., Stockbridge, N., & Temple, R. 2007. Preventing tomorrow's sudden cardiac death today: part II: Translating sudden cardiac death risk assessment strategies into practice and policy. *Am.Heart J.*, 153, (6) 951-959

261. Sano, T. & Sawanobori, T. 1972. Abnormal automaticity in canine Purkinje fibers focally subjected to low external concentrations of calcium. *Circ.Res.*, 31, (2) 158-164

262. Savelieva, I., Yi, G., Guo, X., Hnatkova, K., & Malik, M. 1998. Agreement and reproducibility of automatic versus manual measurement of QT interval and QT dispersion. *Am.J.Cardiol*, 81, (4) 471-477

263. Savopoulos, C., Ziakas, A., Hatzitolios, A., Delivoria, C., Kounanis, A., Mylonas, S., Tsougas, M., & Psaroulis, D. 2006. Circadian rhythm in sudden cardiac death: a retrospective study of 2,665 cases. *Angiology*, 57, (2) 197-204

264. Scher , A.M. 1964. The sequence of ventricular excitation. *The American journal of cardiology*, 14, 287-293

265. Scherlag, B.J., Kabell, G., Brachmann, J., Harrison, L., & Lazzara, R. 1983. Mechanisms of spontaneous and induced ventricular arrhythmias in the 24-hour infarcted dog heart. *Am.J.Cardiol*, 51, (1) 207-213

266. Schilling, R.J., Peters, N.S., & Davies, D.W. 1998. Simultaneous endocardial mapping in the human left ventricle using a noncontact catheter: comparison of contact and reconstructed electrograms during sinus rhythm. *Circulation*, 98, (9) 887-898

267. Schilling, R.J., Peters, N.S., & Davies, D.W. 1999a. Feasibility of a noncontact catheter for endocardial mapping of human ventricular tachycardia. *Circulation*, 99, (19) 2543-2552

268. Schilling, R.J., Peters, N.S., & Davies, D.W. 1999b. Mapping and ablation of ventricular tachycardia with the aid of a non-contact mapping system. *Heart*, 81, (6) 570-575

269. Schimpf, R., Borggrefe, M., & Wolpert, C. 2008. Clinical and molecular genetics of the short QT syndrome. *Curr.Opin.Cardiol*, 23, (3) 192-198

270. Schwartz, P.J. 1998. The autonomic nervous system and sudden death. *Eur.Heart J.*, 19 Suppl F, F72-F80

271. Sclarovsky, S., Lewin, R.F., Kracoff, O., Strasberg, B., Arditti, A., & Agmon, J. 1983. Amiodarone-induced polymorphous ventricular tachycardia. *Am Heart J.*, 105, (1) 6-12

272. Serio, A., Narula, N., Kodama, T., Favalli, V., & Arbustini, E. 2012. Familial dilated cardiomyopathy. Clinical and genetic characteristics. *Herz*, 37, (8) 822-829

273. Shimizu, W., Aiba, T., & Antzelevitch, C. 2005. Specific therapy based on the genotype and cellular mechanism in inherited cardiac arrhythmias. Long QT syndrome and Brugada syndrome. *Curr.Pharm.Des*, 11, (12) 1561-1572

274. Shimizu, W. & Antzelevitch, C. 1997. Sodium channel block with mexiletine is effective in reducing dispersion of repolarization and preventing torsade des pointes in LQT2 and LQT3 models of the long-QT syndrome. *Circulation*, 96, (6) 2038-2047

275. Shimizu, W. & Antzelevitch, C. 1998. Cellular basis for the ECG features of the LQT1 form of the long-QT syndrome: effects of beta-adrenergic agonists and antagonists and sodium channel blockers on transmural dispersion of repolarization and torsade de pointes. *Circulation*, 98, (21) 2314-2322

276. Shimizu, W. & Antzelevitch, C. 1999. Cellular and ionic basis for T-wave alternans under long-QT conditions. *Circulation*, 99, (11) 1499-1507

277. Silka, M.J. & Bar-Cohen, Y. 2012. A contemporary assessment of the risk for sudden cardiac death in patients with congenital heart disease. *Pediatr.Cardiol*, 33, (3) 452-460

278. Simpson J & Weiner E 1989. *The Oxford English Dictionary* Clarendon Press Oxford.

279. Smith, M.I., Nicolson, W.B., Brown, P.D., Tuan, J., Sandilands, S.J., Stafford, P.J., Schlindwein, F.S., McCann, G.P., & Ng, G.A. 2012. First application of a novel sudden cardiac death risk marker in a non-ischaemic population.

280. Spach, M.S. & Barr, R.C. 1975. Anaylsis of ventricular activation and repolarization from intramural and epicardial potential distributions for ectopic beats in the intact dog. *Circ.Res.*, 37, (6) 830-843

281. Spragg, D.D., Akar, F.G., Helm, R.H., Tunin, R.S., Tomaselli, G.F., & Kass, D.A. 2005. Abnormal conduction and repolarization in late-activated myocardium of dyssynchronously contracting hearts. *Cardiovasc.Res.*, 67, (1) 77-86

282. Sriram, C.S., Syed, F.F., Ferguson, M.E., Johnson, J.N., Sarano, M.E., Cetta, F., Cannon, B.C., Asirvatham, S.J., & Ackerman, M.J. 2013. Malignant Bileaflet Mitral Valve Prolapse Syndrome in Patients with Otherwise Idiopathic Out of Hospital Cardiac Arrest. *J.Am Coll.Cardiol*

283. Steinhaus, B.M. 1989. Estimating cardiac transmembrane activation and recovery times from unipolar and bipolar extracellular electrograms: a simulation study. *Circ.Res.*, 64, (3) 449-462

284. Stevenson, W.G., Stevenson, L.W., Middlekauff, H.R., & Saxon, L.A. 1993. Sudden death prevention in patients with advanced ventricular dysfunction. *Circulation*, 88, (6) 2953-2961

285. Stockner, T. & Koschak, A. 2012. What can naturally occurring mutations tell us about Ca(v)1.x channel function? *Biochim.Biophys.Acta*

286. Strickberger, S.A., Knight, B.P., Michaud, G.F., Pelosi, F., & Morady, F. 2000. Mapping and ablation of ventricular tachycardia guided by virtual electrograms using a noncontact, computerized mapping system. *J.Am Coll.Cardiol*, 35, (2) 414-421

287. Subramanian, A., Suszko, A., Selvaraj, R.J., Nanthakumar, K., Ivanov, J., & Chauhan, V.S. 2011. Modulated dispersion of activation and repolarization by premature beats in patients with cardiomyopathy at risk of sudden death. *Am.J.Physiol Heart Circ.Physiol*, 300, (6) H2221-H2229

288. Sunsaneewitayakul, B., Yao, Y., Thamaree, S., & Zhang, S. 2012. Endocardial mapping and catheter ablation for ventricular fibrillation prevention in Brugada syndrome. *J.Cardiovasc.Electrophysiol.*, 23 Suppl 1, S10-S16

289. Surawicz, B. 1989. Electrophysiologic substrate of torsade de pointes: dispersion of repolarization or early afterdepolarizations? *J.Am.Coll.Cardiol*, 14, (1) 172-184

290. Taccardi, B., Arisi, G., Macchi, E., Baruffi, S., & Spaggiari, S. 1987. A new intracavitary probe for detecting the site of origin of ectopic ventricular beats during one cardiac cycle. *Circulation*, 75, (1) 272-281

291. Taggart, P., Sutton, P., Chalabi, Z., Boyett, M.R., Simon, R., Elliott, D., & Gill, J. 2003. Effect of adrenergic stimulation on action potential duration restitution in humans. *Circulation*, 107, (2) 285-289

292. Taliercio, C.P., Seward, J.B., Driscoll, D.J., Fisher, L.D., Gersh, B.J., & Tajik, A.J. 1985. Idiopathic dilated cardiomyopathy in the young: clinical profile and natural history. *J.Am Coll.Cardiol*, 6, (5) 1126-1131

293. Tamburro, P. & Wilber, D. 1992. Sudden death in idiopathic dilated cardiomyopathy. *Am.Heart J.*, 124, (4) 1035-1045

294. Thiagalingam, A., Wallace, E.M., Boyd, A.C., Eipper, V.E., Campbell, C.R., Byth, K., Ross, D.L., & Kovoor, P. 2004a. Noncontact mapping of the left ventricle: insights from validation with transmural contact mapping. *Pacing Clin.Electrophysiol.*, 27, (5) 570-578

295. Thiagalingam, A., Wallace, E.M., Campbell, C.R., Boyd, A.C., Eipper, V.E., Byth, K., Ross, D.L., & Kovoor, P. 2004b. Value of noncontact mapping for identifying left ventricular scar in an ovine model. *Circulation*, 110, (20) 3175-3180

296. Tiso, N., Stephan, D.A., Nava, A., Bagattin, A., Devaney, J.M., Stanchi, F., Larderet, G., Brahmbhatt, B., Brown, K., Bauce, B., Muriago, M., Basso, C., Thiene, G., Danieli, G.A., & Rampazzo, A. 2001. Identification of mutations in the cardiac ryanodine receptor gene in families affected with arrhythmogenic right ventricular cardiomyopathy type 2 (ARVD2). *Hum.Mol.Genet.*, 10, (3) 189-194

297. Toyoshima, H., Lux, R.L., Wyatt, R.F., Burgess, M., & Abildskov, J.A. 1981. Sequences of early and late phases of repolarization on dog ventricular epicardium. *J.Electrocardiol.*, 14, (2) 143-152

298. Triedman, J.K., Jenkins, K.J., Colan, S.D., Van, P.R., Lock, J.E., & Walsh, E.P. 1997. Multipolar endocardial mapping of the right heart using a basket catheter: acute and chronic animal studies. *Pacing Clin.Electrophysiol.*, 20, (1 Pt 1) 51-59

299. Valderrabano, M., Lee, M.H., Ohara, T., Lai, A.C., Fishbein, M.C., Lin, S.F., Karagueuzian, H.S., & Chen, P.S. 2001. Dynamics of intramural and transmural reentry during ventricular fibrillation in isolated swine ventricles. *Circ.Res.*, 88, (8) 839-848

300. van Dam, R.T. & Durrer, D. 1964. The T wave and ventricular repolarization. *The American journal of cardiology*, 14, (3) 294-300

301. van, D.R. & Durrer, D. 1961. Experimental study on the intramural distribution of the excitability cycle and on the form of the epicardial T wave in the dog heart in situ. *Am.Heart J.*, 61, 537-542

302. Vassallo, J.A., Cassidy, D.M., Kindwall, K.E., Marchlinski, F.E., & Josephson, M.E. 1988. Nonuniform recovery of excitability in the left ventricle. *Circulation*, 78, (6) 1365-1372

303. Vernooy, K., Verbeek, X.A., Peschar, M., Crijns, H.J., Arts, T., Cornelussen, R.N., & Prinzen, F.W. 2005. Left bundle branch block induces ventricular remodelling and functional septal hypoperfusion. *Eur.Heart J.*, 26, (1) 91-98

304. Walcott, G.P., Kay, G.N., Plumb, V.J., Smith, W.M., Rogers, J.M., Epstein, A.E., & Ideker, R.E. 2002. Endocardial wave front organization during ventricular fibrillation in humans. *J.Am.Coll.Cardiol*, 39, (1) 109-115

305. Waldo, A.L., Camm, A.J., deRuyter, H., Freidman, P.L., MacNeil, D.J., Pitt, B., Pratt, C.M., Rodda, B.E., & Schwartz, P.J. 1995. Survival with oral d-sotalol in patients with left ventricular dysfunction after myocardial infarction: rationale, design, and methods (the SWORD trial). *Am.J.Cardiol*, 75, (15) 1023-1027

306. Waldo, A.L., Camm, A.J., deRuyter, H., Friedman, P.L., MacNeil, D.J., Pauls, J.F., Pitt, B., Pratt, C.M., Schwartz, P.J., & Veltri, E.P. 1996. Effect of d-sotalol on mortality in patients with left ventricular dysfunction after recent and remote myocardial infarction. The SWORD Investigators. Survival With Oral d-Sotalol. *Lancet*, 348, (9019) 7-12

307. Walker, M.L., Wan, X., Kirsch, G.E., & Rosenbaum, D.S. 2003. Hysteresis effect implicates calcium cycling as a mechanism of repolarization alternans. *Circulation*, 108, (21) 2704-2709

308. Waller, A.D. 1888. Introductory Address on the Electromotive Properties of the Human Heart. *Br.Med.J.*, 2, (1449) 751-754

309. Watanabe, M., Otani, N.F., & Gilmour, R.F., Jr. 1995. Biphasic restitution of action potential duration and complex dynamics in ventricular myocardium. *Circ.Res.*, 76, (5) 915-921

310. Watanabe, M.A., Fenton, F.H., Evans, S.J., Hastings, H.M., & Karma, A. 2001. Mechanisms for discordant alternans. *J.Cardiovasc.Electrophysiol.*, 12, (2) 196-206

311. Watkins, H., McKenna, W.J., Thierfelder, L., Suk, H.J., Anan, R., O'Donoghue, A., Spirito, P., Matsumori, A., Moravec, C.S., Seidman, J.G., & . 1995. Mutations in the genes for cardiac troponin T and alpha-tropomyosin in hypertrophic cardiomyopathy. *N.Engl.J.Med.*, 332, (16) 1058-1064

312. Weiss, J.N., Chen, P.S., Qu, Z., Karagueuzian, H.S., & Garfinkel, A. 2000. Ventricular fibrillation: how do we stop the waves from breaking? *Circ.Res.*, 87, (12) 1103-1107

313. Weiss, J.N., Chen, P.S., Qu, Z., Karagueuzian, H.S., Lin, S.F., & Garfinkel, A. 2002. Electrical restitution and cardiac fibrillation. *J.Cardiovasc.Electrophysiol.*, 13, (3) 292-295

314. Weiss, J.N., Chen, P.-S., Wu, T.-J., Siegerman, C., & Garfinkel, A. 2004. Ventricular fibrillation: New insights into mechanisms.

315. Weiss, J.N., Garfinkel, A., Karagueuzian, H.S., Qu, Z., & Chen, P.S. 1999. Chaos and the transition to ventricular fibrillation: a new approach to antiarrhythmic drug evaluation. *Circulation*, 99, (21) 2819-2826

316. Weiss, J.N., Karma, A., Shiferaw, Y., Chen, P.S., Garfinkel, A., & Qu, Z. 2006. From pulsus to pulseless: the saga of cardiac alternans. *Circ.Res.*, 98, (10) 1244-1253

317. Wellens, H.J. 1975. Electral stimulation of the heart in the study of ventricular tachycardias. *Adv.Cardiol*, 14, 65-69

318. Wellens, H.J., Brugada, P., & Stevenson, W.G. 1985. Programmed electrical stimulation of the heart in patients with life-threatening ventricular arrhythmias: what is the significance of induced arrhythmias and what is the correct stimulation protocol? *Circulation*, 72, (1) 1-7

319. Wellens, H.J., Janse, M.J., van Dam, R.T., & Durrer, D. 1971. Epicardial excitation of the atria in a patient with atrial flutter. *Br.Heart J.*, 33, (2) 233-237

320. Wichter, T., Matheja, P., Eckardt, L., Kies, P., Schafers, K., Schulze-Bahr, E., Haverkamp, W., Borggrefe, M., Schober, O., Breithardt, G., & Schafers, M. 2002. Cardiac autonomic dysfunction in Brugada syndrome. *Circulation*, 105, (6) 702-706

321. Wiggers CJ 1940. Fibrillation. *Am.Heart J.*, 20, 399-422

322. Wiggers CJ, Bell JR, & Paine M 1930. Studies of ventricular fibrillation produced by electric shock. II. Cinematographic and electrocardiographic observations of the natural process in the dog's heart. *Am.Heart J.* (5) 351-365

323. Wilson, F., MacLeod, A., & Barker, P. 1931. The T deflection of the electrocardiogram. *Tr A.Am Phys.* (46) 29

324. Winkel, B.G., Holst, A.G., Theilade, J., Kristensen, I.B., Thomsen, J.L., Ottesen, G.L., Bundgaard, H., Svendsen, J.H., Haunso, S., & Tfelt-Hansen, J. 2011. Nationwide study of sudden cardiac death in persons aged 1-35 years. *Eur.Heart J.*, 32, (8) 983-990

325. Wu, T.J., Lin, S.F., Weiss, J.N., Ting, C.T., & Chen, P.S. 2002. Two types of ventricular fibrillation in isolated rabbit hearts: importance of excitability and action potential duration restitution. *Circulation*, 106, (14) 1859-1866

326. Wu, T.J., Ong, J.J., Hwang, C., Lee, J.J., Fishbein, M.C., Czer, L., Trento, A., Blanche, C., Kass, R.M., Mandel, W.J., Karagueuzian, H.S., & Chen, P.S. 1998. Characteristics of wave fronts during ventricular fibrillation in human hearts with dilated cardiomyopathy: role of increased fibrosis in the generation of reentry. *J.Am.Coll.Cardiol*, 32, (1) 187-196

327. Wyatt, R.F., Burgess, M.J., Evans, A.K., Lux, R.L., Abildskov, J.A., & Tsutsumi, T. 1981. Estimation of Ventricular Transmembrane Action-Potential Durations and Repolarization Times from Unipolar Electrograms. *American Journal of Cardiology*, 47, (2) 488

328. Wyse, D.G., Talajic, M., Hafley, G.E., Buxton, A.E., Mitchell, L.B., Kus, T.K., Packer, D.L., Kou, W.H., Lemery, R., Santucci, P., Grimes, D., Hickey, K., Stevens, C., & Singh, S.N. 2001. Antiarrhythmic drug therapy in the Multicenter UnSustained Tachycardia Trial (MUSTT): drug testing and as-treated analysis. *J.Am Coll.Cardiol*, 38, (2) 344-351

329. Yamauchi, S., Yamaki, M., Watanabe, T., Yuuki, K., Kubota, I., & Tomoike, H. 2002. Restitution properties and occurrence of ventricular arrhythmia in LQT2 type of long QT syndrome. *J.Cardiovasc.Electrophysiol.*, 13, (9) 910-914

330. Yan, G.X. & Antzelevitch, C. 1996. Cellular basis for the electrocardiographic J wave. *Circulation*, 93, (2) 372-379

331. Yan, G.X. & Antzelevitch, C. 1998. Cellular basis for the normal T wave and the electrocardiographic manifestations of the long-QT syndrome. *Circulation*, 98, (18) 1928-1936

332. Yan, G.X. & Antzelevitch, C. 1999. Cellular basis for the Brugada syndrome and other mechanisms of arrhythmogenesis associated with ST-segment elevation. *Circulation*, 100, (15) 1660-1666

333. Yap, S.C., Harris, L., Chauhan, V.S., Oechslin, E.N., & Silversides, C.K. 2011. Identifying high risk in adults with congenital heart disease and atrial arrhythmias. *Am.J.Cardiol*, 108, (5) 723-728

334. Yuan, S., Kongstad, O., Hertervig, E., Holm, M., Grins, E., & Olsson, B. 2001. Global repolarization sequence of the ventricular endocardium: monophasic action potential mapping in swine and humans. *Pacing Clin.Electrophysiol.*, 24, (10) 1479-1488

335. Yuan, S., Kongstad, O., Hertervig, E., Holm, M., Pripp, C.M., & Olsson, S.B. 2000. Recording monophasic action potentials using a platinum-electrode ablation catheter. *Europace.*, 2, (4) 312-319

336. Yuan, S., Wohlfart, B., Olsson, S.B., & Blomstrom-Lundqvist, C. 1995. The dispersion of repolarization in patients with ventricular tachycardia. A study using simultaneous monophasic action potential recordings from two sites in the right ventricle. *Eur.Heart J.*, 16, (1) 68-76

337. Yue, A.M. 2006. *An examination of human ventricular repolarization using noncontact mapping.* University of Oxford.

338. Yue, A.M. 2007. Significant correlation between monophasic action potential (MAP) durations and activation-recovery intervals (ARIs) determined at the maximum positive slope of the positive T wave (conventional method). *Heart Rhythm.*, 4, (1) 120-121

339. Yue, A.M., Betts, T.R., Roberts, P.R., & Morgan, J.M. 2005a. Global dynamic coupling of activation and repolarization in the human ventricle. *Circulation*, 112, (17) 2592-2601

340. Yue, A.M., Franz, M.R., Roberts, P.R., & Morgan, J.M. 2005b. Global endocardial electrical restitution in human right and left ventricles determined by noncontact mapping. *J.Am.Coll.Cardiol.*, 46, (6) 1067-1075

341. Yue, A.M., Paisey, J.R., Robinson, S., Betts, T.R., Roberts, P.R., & Morgan, J.M. 2004. Determination of human ventricular repolarization by noncontact mapping: Validation with monophasic action potential recordings. *Circulation*, 110, (11) 1343-1350

342. Yuuki, K., Hosoya, Y., Kubota, I., & Yamaki, M. 2004. Dynamic and not static change in ventricular repolarization is a substrate of ventricular arrhythmia on chronic ischemic myocardium. *Cardiovascular research,* 63, (4) 645-652

343. Zabel, M., Acar, B., Klingenheben, T., Franz, M.R., Hohnloser, S.H., & Malik, M. 2000. Analysis of 12-lead T-wave morphology for risk stratification after myocardial infarction. *Circulation*, 102, (11) 1252-1257

344. Zabel, M., Malik, M., Hnatkova, K., Papademetriou, V., Pittaras, A., Fletcher, R.D., & Franz, M.R. 2002. Analysis of T-wave morphology from the 12-lead electrocardiogram for prediction of long-term prognosis in male US veterans. *Circulation*, 105, (9) 1066-1070

345. Zabel, M., Portnoy, S., & Franz, M.R. 1995. Electrocardiographic indexes of dispersion of ventricular repolarization: an isolated heart validation study. *J.Am Coll.Cardiol*, 25, (3) 746-752

346. Zipes, D.P. 1975. Electrophysiological mechanisms involved in ventricular fibrillation. *Circulation*, 52, (6 Suppl) III120-III130

347. Zipes, D.P. 2005. Epidemiology and mechanisms of sudden cardiac death. *Can.J Cardiol*, 21 Suppl A, 37-40

348. Zipes, D.P., Camm, A.J., Borggrefe, M., Buxton, A.E., Chaitman, B., Fromer, M., Gregoratos, G., Klein, G., Moss, A.J., Myerburg, R.J., Priori, S.G., Quinones, M.A., Roden, D.M., Silka, M.J., Tracy, C., Smith, S.C., Jr., Jacobs, A.K., Adams, C.D., Antman, E.M., Anderson, J.L., Hunt, S.A., Halperin, J.L., Nishimura, R., Ornato, J.P., Page, R.L., Riegel, B., Priori, S.G., Blanc, J.J., Budaj, A., Camm,

A.J., Dean, V., Deckers, J.W., Despres, C., Dickstein, K., Lekakis, J., McGregor, K., Metra, M., Morais, J., Osterspey, A., Tamargo, J.L., & Zamorano, J.L. 2006. ACC/AHA/ESC 2006 guidelines for management of patients with ventricular arrhythmias and the prevention of sudden cardiac death: a report of the American College of Cardiology/American Heart Association Task Force and the European Society of Cardiology Committee for Practice Guidelines (Writing Committee to Develop Guidelines for Management of Patients With Ventricular Arrhythmias and the Prevention of Sudden Cardiac Death). *J.Am.Coll.Cardiol*, 48, (5) e247-e346